

**EVALUATION OF SEISMIC PERFORMANCE OF RC FRAME
STRUCTURES BY PUSHOVER AND TIME HISTORY ANALYSES**

MD. NASIM KHAN

MASTER OF SCIENCE IN CIVIL ENGINEERING (STRUCTURAL)



**DEPARTMENT OF CIVIL ENGINEERING
BANGLADESH UNIVERSITY OF ENGINEERING AND
TECHNOLOGY, DHAKA, BANGLADESH**

JUNE, 2013

The thesis titled “EVALUATION OF SEISMIC PERFORMANCE OF RC FRAME STRUCTURES BY PUSHOVER AND TIME HISTORY ANALYSES” submitted by Md. Nasim Khan, Roll No: 100604336P, Session: October/2006; has been accepted as satisfactory in partial fulfillment of the requirement for the degree of Master of Science in Civil Engineering (Structural) on 29 June, 2013.

BOARD OF EXAMINERS

Dr. Tahsin Reza Hossain
Professor
Department of Civil Engineering
BUET, Dhaka-1000.

Chairman
(Supervisor)

Dr. Md. Mujibur Rahman
Professor and Head
Department of Civil Engineering
BUET, Dhaka-1000.

Member (Ex-Officio)

Dr. Mahbuba Begum
Associate Professor
Department of Civil Engineering
BUET, Dhaka-1000.

Member

Dr. Alamgir Habib
Professor (Retd), Dept. of Civil Engg, BUET
Professor, MIST
Urban Heights, Apartment # 2A, House # 124
Road # 9/A, Dhanmondi, Dhaka.

Member (External)

Declaration

It is hereby declared that except for the contents where specific reference have been made to the work of others, the studies contained in this thesis is the result of investigation carried out by the author. No part of this thesis has been submitted to any other University or other educational establishment for a Degree, Diploma or other qualification (except for publication).

Signature of the Candidate

(Md Nasim Khan)

Dedication

To

My

Mother

Contents

Declaration	iii
Contents	v
List of Tables	ix
List of Figures	x
Acknowledgment	xvi
Abstract	xvii
Chapter 1 Introduction	1-5
1.1 Background and present state of the problem	1
1.2 Objectives with specific aims and possible outcomes	3
1.3 Methodology	3
1.4 Layout of thesis	4
Chapter 2 Literature review	6-45
2.1 Introduction	6
2.2 Provision for earthquake load in BNBC	6
2.2.1 Equivalent static force method	7
2.2.2 Dynamic response method	8
2.2.2.1 Response spectrum method	8
2.3 Selection of lateral force method BNBC, 2006	9
2.4 Pushover Analysis	9
2.4.1 Methods to perform simplified nonlinear analysis	10
2.4.2 Capacity	11
2.4.3 Demand (displacement)	11
2.4.4 Performance	12
2.5.5 Reduced demand spectra	12
2.4.6 Development of elastic site response spectra	14
2.4.7 Seismic zone	14
2.4.8 Seismic source type:	15
2.4.9 Near source factor	16
2.4.10 Seismic coefficients	17
2.4.11 Development of elastic site response spectra	19
2.4.12 Establishing demand spectra	19
2.4.13 Capacity spectrum method	22

2.4.14	Displacement coefficient method	30
2.4.15	Seismic performance evaluation	30
2.4.16	Nonlinear static procedure for capacity evaluation of structures	31
2.4.17	Structural performance levels and ranges	32
2.4.17.1	Immediate occupancy structural performance level (S-1)	33
2.4.17.2	Damage control structural performance range (S-2)	33
2.4.17.3	Life safety structural performance level (S-3)	33
2.4.17.4	Limited safety structural performance range (S-4)	34
2.4.17.5	Collapse prevention structural performance level (S-5)	34
2.4.17.6	Target building performance levels	35
2.4.18	Response limit	35
2.4.18.1	Global building acceptability limits	35
2.4.18.2	Element and component acceptability limit	37
2.4.19	Acceptability limit	39
2.5	Nonlinear time history analysis	40
2.5.1	Nonlinear dynamic analysis for earthquake ground motions	41
2.5.2	Linearly elastic and inelastic systems	41
2.5.3	Equation of motion for seismic vibration	42
2.5.4	Solution by incremental time-step integration	43
2.5.5	The average acceleration method	44
2.9	Conclusion	45
Chapter 3	Pushover Analysis	46-74
3.1	Introduction	46
3.2	Details of pushover analysis in SAP2000 and ETABS	47
3.3	Description of case study frame for validation	51
3.3.1	Two story RC frame	51
3.3.2	Five story RC frame	53
3.3.3	Twelve story RC frame	54
3.4	Analysis and results of validation of pushover curve for 2D frame	56
3.5	Comparison of pushover curve for SAP2000 and SeismoStruct	58
3.5.1	Description of SeismoStruct	58
3.5.2	Description of case study frames	60
3.5.3	Analysis and results	60
3.5.3.1	Two storied 2D frame	61

3.5.3.2 Five storied 2D frame	62
3.6 Different loading pattern for pushover curve	63
3.6.1 Two storied 2D frame	63
3.6.2 Five storied 2D frame	64
3.6.3 Twelve storied 2D frame	64
3.7 Performance evaluation of structure	65
3.7.1 Two story 2D frame	66
3.7.1.1 Local level performance	68
3.7.1.2 Global level performance	69
3.7.2 Five story 2D frame	70
3.7.2.1 Local level performance	72
3.7.2.2 Global level performance	73
3.7 Conclusion	74
Chapter 4 Time History Analysis	75-108
4.1 Introduction	75
4.2 Time history analysis using selected earthquakes	76
4.2.1 El Centro 1940 Earthquake	77
4.2.2 Kobe Earthquake	78
4.3 Validation of linear time history analysis for SDOF system	78
4.3.1 Description of SDOF Model	78
4.3.2 Analysis and Result	79
4.4 Nonlinear Time History Analysis	82
4.4.1 Validation of nonlinear time history analysis for SDOF system with SeismoStruct	83
4.4.1.1 Description of model	83
4.4.1.2 Structural geometry and properties	86
4.4.1.3 Modeling and loading	86
4.4.1.4 Analysis type	87
4.4.1.5 Comparison of analysis results	89
4.5 Nonlinear time history analysis for 2D frame using SAP2000	92
4.5.1 Analysis Technique	93
4.5.2 Analysis and results	94
4.6 Comparison of Linear and Nonlinear Time History Analysis	96

4.7 Comparison of capacity curves of pushover and nonlinear time history analysis	99
4.7.1 Description of case studies model	100
4.7.2 Analysis and Result	100
4.8 Performance Evaluation of the Structure using time history	103
4.8.1 Local level performance	103
4.8.2 Global level performance	105
4.8 Conclusion	108
Chapter 5 Performance based analysis of RC frame building	109-143
5.1 Introduction	109
5.2 Performance requirements	109
5.3 Description of 6-story reinforced concrete frame structure building	110
5.3.1 Performance evaluation of a structure design as per BNBC	112
5.3.1.1 Local level performance	118
5.3.1.2 Global level performance	120
5.4 Performance of 6-story RC narrow building	122
5.4.1 Performance evaluation of a structure design as per BNBC	123
5.4.1.1 Local level performance	128
5.4.1.2 Global level performance	129
5.5 Performance of 12-story RC frame building	131
5.5.1 Performance evaluation of a structure design as per BNBC	133
5.5.1.1 Local level performance	138
5.5.1.2 Global level performance	139
5.6 Performance evaluation of structure for gravity loads only	141
5.7 Conclusion	143
Chapter 6 Conclusions and future recommendations	144-146
6.1 Introduction	144
6.2 Findings of the study	145
6.3 Recommendation of future study	146
References	148-153
Appendix- A	1-4
Appendix- B	5-10
Appendix- C	11-18

List of Tables

Table 2.1	Minimum allowable SR_A and SR_V values (Adopted from ATC 40)	13
Table 2.2	Seismic zone factor Z	14
Table 2.3	Seismic source type as per ATC-40	16
Table 2.4	Seismic source factor	16
Table 2.5	Seismic coefficient C_A	17
Table 2.6	Seismic coefficient C_V	18
Table 2.7	Soil profile types (ATC-40)	18
Table 2.8	Calculation of C_A	19
Table 2.9	Calculation of C_V	20
Table 2.10	Deformation Limits (ATC-40)	36
Table 2.11	Examples of possible deformation controlled and force controlled actions (FEMA-356)	38
Table 3.1	Cross section and loading properties of 2-story RC frame	52
Table 3.2	Dynamic properties of 2-Story RC frame	53
Table 3.3	Cross section and loading properties of 5-story RC frame	54
Table 3.4	Dynamic properties of 5-story RC frame	54
Table 3.5	Cross section and loading properties of 12-story RC frame	55
Table 3.6	Dynamic properties of 12-story RC frame	56
Table 3.7	Calculation of C_A	66
Table 3.8	Calculation of C_V	66
Table 4.1	Comparison time history analysis with ETABS of SDOF system and published result from Chopra	79
Table 5.1	Structural dimension of building	110
Table 5.2	Calculation of C_A	112
Table 5.3	Calculation of C_V	112
Table 5.4	Calculation of Reduction factor	113
Table 5.5	Capacity spectrum of the six story building (Procedure A and B)	117
Table 5.6	Number of hinges formed in the 6-storied frame structure building in x and y-direction	118
Table 5.7	Structural dimension of 6-story (aspect ratio) building	122
Table 5.8	Calculation of Reduction factor	123
Table 5.9	Capacity spectrum of the six story building (Procedure A and B)	128

Table 5.10	Number of hinges formed in the 6-storied frame structure building in x and y-direction	129
Table 5.11	Structural dimension of 12-story building	132
Table 5.12	Calculation of Reduction factor	133
Table 5.13	Capacity spectrum of the 12-story building (Procedure A and B)	138
Table 5.14	Number of hinges formed in the 12-storied frame structure building in x and y-direction	139
Table 5.15	Number of hinges for different level of earthquakes	141

List of figures

Fig. 2.1	Normalized response spectra for 5% damping ratio (Adopted from BNBC)	8
Fig. 2.2	Reduced response spectrum	12
Fig. 2.3	Seismic Zoning map of Bangladesh	15
Fig. 2.4	Typical capacity curve	20
Fig. 2.5	Code specified response spectrum in Spectral acceleration vs. Period	23
Fig. 2.6	Response spectrum in ADRS format	23
Fig. 2.7	A typical capacity curve	24
Fig. 2.8	Capacity spectrum	26
Fig. 2.9	Typical capacity spectrum	27
Fig. 2.10	Determination of performance point (Adopted from ATC 40)	28
Fig. 2.11	Component force versus deformation Curves (FEMA-356)	37
Fig. 2.12	Force-deformation action and acceptance criteria (ATC-40)	39
Fig. 2.13	Nonlinear force-displacement relationship	44
Fig. 3.1	Concrete moment and P-M-M hinge property	48
Fig. 3.2	Concrete Shear hinge property	48
Fig. 3.3	An example to illustrate the option of save positive increments only	50
Fig. 3.4	Two story RC frame	52
Fig. 3.5	Five story RC frame	53
Fig. 3.6	Twelve story RC frame	55
Fig. 3.7	Pushover curves of the 2-story 2D frame	57

Fig. 3.8	Pushover curves of the 5-story 2D frame	57
Fig. 3.9	Pushover curves of the 12-Story 2D frame	57
Fig. 3.10	Pushover curves of the 2-story 2D frame for different loading pattern using SAP2000 and SeismoStruct	61
Fig. 3.11	Pushover curves of the 5-story 2D frame for different loading pattern using SAP2000 and SeismoStruct	62
Fig. 3.12	Pushover curves of the 2-story 2D frame for different loading pattern using SAP2000	64
Fig. 3.13	Pushover curves of the 5-story 2D frame for different loading pattern using SAP2000	64
Fig. 3.14	Pushover curves of the 12-story 2D frame for different loading pattern using SAP2000	65
Fig. 3.15	Capacity spectrum of the 2-story 2D frame (Procedure A)	66
Fig. 3.16	Capacity spectrum of the 2-story frame for SE (Procedure B)	67
Fig. 3.17	Capacity spectrum of the 2-story frame for DE (Procedure B)	67
Fig. 3.18	Capacity spectrum of the 2-story frame for ME (Procedure B)	68
Fig. 3.19	Deformation of the 2-story frame at SE level	68
Fig. 3.20	Deformation of the 2-story frame at DE level	69
Fig. 3.21	Deformation of the 2-story frame at ME level	69
Fig. 4.22	Story drift ratio at performance point of 2-Story 2D frame for different earthquake level	70
Fig. 3.23	Capacity spectrum of the 5-story 2D frame (Procedure A)	70
Fig. 3.24	Capacity spectrum of the 5-story frame for SE (Procedure B)	71
Fig. 3.25	Capacity spectrum of the 5-story frame for DE (Procedure B)	71
Fig. 3.26	Capacity spectrum of the 5-story frame for ME (Procedure B)	72
Fig. 3.27	Deformation of the 5-story frame at SE level	72
Fig. 3.28	Deformation of the 5-story frame at DE level	73
Fig. 3.29	Deformation of the 5-story frame at ME level	73
Fig. 3.30	Story drift ratio at performance point of 5-Story 2D frame for different earthquake level	74
Fig. 4.1	Ground acceleration of El Centro, 1940 earthquake record (N-S), adopted from Chopra [5]	77
Fig. 4.2	Ground acceleration of Kobe Earthquake	78
Fig.4.3	SDOF Model	79

Fig. 4.4(a)	Time history analysis of SDOF system to El Centro ground motion for $T_n= 0.5$ sec, $\xi=2\%$	80
Fig. 4.4(b)	Time history analysis of SDOF system to El Centro ground motion for $T_n= 1$ sec, $\xi=2\%$	80
Fig. 4.4(c)	Time history analysis of SDOF system to El Centro ground motion for $T_n= 2$ sec, $\xi=2\%$	80
Fig. 4.5(a)	Time history analysis of SDOF system to El Centro ground motion for $T_n= 2$ sec, $\xi=0\%$	81
Fig. 4.5(b)	Time history analysis of SDOF system to El Centro ground motion for $T_n= 2$ sec, $\xi=2\%$	81
Fig. 4.5(c)	Time history analysis of SDOF system to El Centro ground motion for $T_n= 2$ sec, $\xi=5\%$	81
Fig. 4.6	Input Ground motion (EQ1)	84
Fig. 4.7	Input Ground motion (EQ2)	84
Fig. 4.8	Input Ground motion (EQ3)	84
Fig. 4.9	Input Ground motion (EQ4)	85
Fig. 4.10	Input Ground motion (EQ5)	85
Fig. 4.11	Input Ground motion (EQ6)	85
Fig. 4.12	Pier cross section and bridge pier specimen configuration	86
Fig. 4.13	FE model of the bridge column	87
Fig. 4.14	Analytical results at top displacement with time (EQ1 to EQ6)	88
Fig. 4.15	Analytical results at base shear with time (EQ1 to EQ6)	88
Fig. 4.16	Analytical results at moment with time (EQ1 to EQ6)	89
Fig. 4.17	Experiment vs. Analytical results at top displacement time (EQ1)	89
Fig. 4.18	Experiment vs. Analytical results at top displacement time (EQ3)	90
Fig. 4.19	Experiment vs. Analytical results at top displacement time (EQ5)	90
Fig. 4.20	Experiment vs. Analytical results at base shear time (EQ1)	91
Fig. 4.21	Experiment vs. Analytical results at base shear time (EQ3)	91
Fig. 4.22	Experiment vs. Analytical results at base shear time (EQ5)	92
Fig. 4.23	Time History Analysis for 5-Story 2D Frame (El Centro earthquake)	95
Fig. 4.24	Time History Analysis for 5-Story 2D Frame (Kobe earthquake)	95
Fig. 4.25	Comparison of linear and nonlinear time history analysis for 2-Story frame (El Centro Earthquake)	96

Fig. 4.26	Comparison of linear and nonlinear time history analysis for 2-Story frame (Kobe Earthquake)	97
Fig. 4.27	Comparison of linear and nonlinear time history analysis for 5-Story frame (El Centro Earthquake)	97
Fig. 4.28	Comparison of linear and nonlinear time history analysis for 5-Story frame (Kobe Earthquake)	98
Fig. 4.29	Comparison of linear and nonlinear time history analysis for 12-Story frame (El Centro Earthquake)	98
Fig. 4.30	Comparison of linear and nonlinear time history analysis for 12-Story frame (Kobe Earthquake)	99
Fig. 4.31	Capacity Curve for 2-Story Frame (El Centro earthquake)	102
Fig. 4.32	Capacity Curve for 5-Story Frame (El Centro earthquake)	102
Fig. 4.33	Capacity Curve for 12-Story Frame (El Centro earthquake)	102
Fig. 4.34	Deformation of the 2-Story 2D frame for ME (El Centro earthquake)	104
Fig. 4.35	Deformation of the 2-Story 2D frame for ME (Kobe earthquake)	104
Fig. 4.36	Deformation of the 5-Story 2D frame for ME (El Centro earthquake)	105
Fig. 4.37	Deformation of the 5-Story 2D frame for ME (Kobe earthquake)	105
Fig. 4.38	Maximum story drift at performance point of 2-Story 2D frame for different earthquake level (El Centro earthquake)	106
Fig. 4.39	Maximum story drift at performance point of 2-Story 2D frame for different earthquake level (Kobe earthquake)	106
Fig. 4.40	Maximum story drift at performance point of 5-Story 2D frame for different earthquake level (El Centro earthquake)	107
Fig. 4.41	Maximum story drift at performance point of 5-Story 2D frame for different earthquake level (Kobe earthquake)	107
Fig. 5.1	Layout of the 6-story building	110
Fig. 5.2	Capacity spectrum of the six-story frame structure building in x-direction (Procedure A)	113
Fig. 5.3	Capacity spectrum of the six-story frame structure building in y-direction (Procedure A)	114
Fig. 5.4	Capacity spectrum of the six-story frame structure building in x-direction (SE) (Procedure B)	114
Fig. 5.5	Capacity spectrum of the six-story frame structure building in x-direction (DE) (Procedure B)	115

Fig. 5.6	Capacity spectrum of the six-story frame structure building in x-direction (ME) (Procedure B)	115
Fig. 5.7	Capacity spectrum of the six-story frame structure building in y-direction (SE) (Procedure B)	116
Fig. 5.8	Capacity spectrum of the six-story frame structure building in y-direction (DE) (Procedure B)	116
Fig. 5.9	Capacity spectrum of the six-story frame structure building in y-direction (ME) (Procedure B)	117
Fig. 5.10	Deformation of the building at performance point in x-direction for SE	119
Fig. 5.11	Deformation of the building at performance point in x-direction for DE	119
Fig. 5.12	Deformation of the building at performance point in x-direction for ME	119
Fig. 5.13	Deformation of the building at performance point in y-direction for SE	120
Fig. 5.14	Deformation of the building at performance point in y-direction DE	120
Fig. 5.15	Maximum story drift ratio at performance point for different earthquake level in X-direction	121
Fig. 5.16	Maximum story drift ratio at performance point for different earthquake level in Y-direction	121
Fig. 5.17	Layout of the 6-story building (aspect ratio)	122
Fig. 5.18	Capacity spectrum of the six-story frame structure building in x-direction (Procedure A)	124
Fig. 5.19	Capacity spectrum of the six-story frame structure building in y-direction (Procedure A)	124
Fig. 5.20	Capacity spectrum of the six-story frame structure building in x-direction (SE) (Procedure B)	125
Fig. 5.21	Capacity spectrum of the six-story frame structure building in x-direction (DE) (Procedure B)	125
Fig. 5.22	Capacity spectrum of the six-story frame structure building in x-direction (ME) (Procedure B)	126
Fig. 5.23	Capacity spectrum of the six-story frame structure building in y-direction (SE) (Procedure B)	126
Fig. 5.24	Capacity spectrum of the six-story frame structure building in y-direction (DE) (Procedure B)	127
Fig. 5.25	Capacity spectrum of the six-story frame structure building in y-direction (ME) (Procedure B)	127

Fig. 5.26	Maximum story drift ratio at performance point for different earthquake level in x-direction	130
Fig. 5.27	Maximum story drift ratio at performance point for different earthquake level in y-direction	130
Fig. 5.28	Layout of the 12-story building	131
Fig. 5.29	Elevation of 12-story building	132
Fig. 5.30	Capacity spectrum of the 12-story frame structure building in x-direction (Procedure A)	134
Fig. 5.31	Capacity spectrum of the 12-story frame structure building in y-direction (Procedure A)	134
Fig. 5.32	Capacity spectrum of the 12-story frame structure building in x-direction (SE) (Procedure B)	135
Fig. 5.33	Capacity spectrum of the 12-story frame structure building in x-direction (DE) (Procedure B)	135
Fig. 5.34	Capacity spectrum of the 12-story frame structure building in x-direction (ME) (Procedure B)	136
Fig. 5.35	Capacity spectrum of the 12-story frame structure building in y-direction (SE) (Procedure B)	136
Fig. 5.36	Capacity spectrum of the 12-story frame structure building in y-direction (DE) (Procedure B)	137
Fig. 5.37	Capacity spectrum of the 12-story frame structure building in y-direction (ME) (Procedure B)	137
Fig. 5.38	Maximum story drift ratio at performance point for different earthquake level in x-direction	140
Fig. 5.39	Maximum story drift ratio at performance point for different earthquake level in y-direction	140
Fig. 5.40	Maximum story drift ratio at performance point for different earthquake level in x-direction	142
Fig. 5.41	Maximum story drift ratio at performance point for different earthquake level in y-direction	142

Acknowledgement

The author wishes to convey his profound gratitude to Almighty Allah for His graciousness, unlimited kindness and blessings, and for allowing him to complete the thesis.

The author wishes to express his sincere appreciation and gratitude to his supervisor, Dr. Tahsin Reza Hossain, Professor, Department of Civil Engineering, BUET, Dhaka, for his continuous guidance, invaluable suggestions and continued encouragement throughout the progress of the research work.

The author is also grateful to Dr. Khan Mohammed Amanat, Professor, Department of Civil Engineering, BUET, Dhaka, for his guidance and inspiration at the initial stage of the study.

A very special debt of deep gratitude is offered to his mother and brothers for their continuous encouragement and cooperation during this study. Last but not the least; the author is deeply indebted to his beloved wife for supporting him all the time with love and inspiration.

Abstract

Bangladesh is situated in a seismically active region. Part of the country extended from Sylhet to Chittagong is in the high seismic zone whereas Dhaka lies in the moderate seismic zone. Major metropolitan cities of our country are under serious threat because of inadequacies in design and construction of structures. A lot of multistoried buildings have already been built in order to fulfill the ever increasing demand of urban population. Bangladesh National Building Code (BNBC) proposes equivalent static load method to design the buildings; however a seismic event will result in damaged structure, performance of which cannot be evaluated from a static analysis. Pushover analysis, a comparatively simplified nonlinear method involving certain approximations and simplifications, is capable of predicting the damage extent due to a seismic event. ATC-40 and FEMA-356 propose the pushover analysis method in detail. In this thesis, an attempt has been made to demonstrate the validity and efficiency of pushover analysis method of ATC-40 as incorporated in ETABS, SAP2000 and SeismoStruct software. Performance of building frames designed as per BNBC has also been evaluated against targeted performance levels for serviceability, design and maximum earthquakes. Nonlinear time history analysis, although complicated and time consuming, is a more rigorous method of modeling seismic response of a structure. Both linear and nonlinear time history analyses have been validated against published results using SAP2000 and SeismoStruct. The work also studied the effectiveness of pushover analysis in comparison to more rigorous nonlinear time history analysis with particular emphasis on the load pattern employed in pushover analysis. Different load patterns have been used in pushover analysis and uniform load pattern has been found to give better capacity curves that compare well with nonlinear time history analysis. Performances have also been evaluated for 2D frames designed according to BNBC using nonlinear time history. Well-known EL Centro and Kobe earthquakes have suitably been scaled as per required Z value for use in the analysis. A comparison of linear and nonlinear time history analyses have been carried out to demonstrate the damage extent caused during an earthquake. Similar pushover analyses carried out on 3-D six and twelve story building designed according to BNBC show that they easily satisfy the ATC-40 local and global seismic requirements. A building which is designed only for gravity load failed to satisfy the requirements for serviceability and maximum earthquakes.

Chapter 1

Introduction

1.1 Background and present state of the problem

Bangladesh is situated in a seismically active region. Part of the country extended from Sylhet to Chittagong is in the high seismic zone whereas Dhaka is in the moderate seismic zone. Major metropolitan cities of our country are under serious threat because of inadequacies in design and construction of structures. Rapid urbanization creates a great demand on human shelter especially in big cities like Dhaka, Chittagong etc. As a result, a lot of multistoried buildings are already built in order to fulfill the demand.

There was no written building code in Bangladesh until 1993. In 1993, Bangladesh National Building Code (BNBC) was published by Housing and Building Research Institute (HBRI) which is commonly known as BNBC [1]. The seismic design provisions of BNBC were based on the UBC [2]. Since then, BNBC has widely been used by engineers. BNBC has different provisions for earthquake load calculation and analysis procedure. For the regular structures, the Code defines a simple method to represent earthquake induced inertia forces by Equivalent Static Force for static analysis. For very tall structure or for irregular structure, the Code provisions require more rigorous analysis, namely, 1) Response Spectrum Analysis and 2) Time History Analysis. All these methods detailed in BNBC are force based methods. As in many other codes, the level of forces prescribed by BNBC for a structure is rather arbitrarily set and aimed at damage control performance objectives i.e. no damage under small earthquake and no collapse under extreme earthquake. The code approach is to design seismic load resisting system on the basis of a pseudo-seismic load obtained by dividing the actual load by response modification factor, R. The R value is specified by the code for each structural system without explicitly defining the level of element (i.e. beam, column, connection etc.) ductility required for each system. The code implicitly assumes that the enhanced ductile detailing would result in seismic energy dissipation and hence a reduced demand would result.

Especially the wide availability of computer technology has made a more realistic simulation of structural behavior possible under seismic loading. The focus of seismic design in current building codes is one of life safety level. Economic losses due to recent earthquakes are estimated to be billions of Taka and the numbers will be higher if the indirect losses are included. This fact lets code committees and decision makers think beyond life safety, which is

essential in design, to alleviate economic losses. This trend creates an increased interest in performance-based design for structure. As a result of which a number of methods are proposed by ATC-40 [3], FEMA-356 [4] for a more rational analysis of the structures under seismic loading. These are simplified nonlinear static analysis capable of simulating the degradation of structure. Nonlinear time history analysis is a more rigorous and correct method but requires huge computing and post-processing effort [5]. One of the main advantages of performance-based designs is its ability to show the performance situation of the structure and its components under different load intensities. The performance situation means that the damage level, if any, can be assessed and a judgment can be made as to which degree this structure can continue to service.

Extensive research studies have already been carried out regarding the performance of concrete structures. Comartin et.al [6] gives a practical overview of the ATC-40 method in seismic evaluation and retrofit of concrete buildings. Fajfar and Fischinger [7] proposed as a simple nonlinear procedure for seismic damage analysis of reinforced concrete buildings. The method uses response spectrum approach and nonlinear static analysis. Krawinkler and Seneviratna [8] conducted a detailed study that discusses the advantages, disadvantages and the applicability of pushover analysis by considering various aspects of the procedure. Ynel et. al. [9] conducted a study to evaluate the accuracy of various lateral load patterns used in current pushover analysis procedures. First mode, inverted triangular, rectangular, adaptive lateral load patterns and multimode pushover analysis were studied. Chopra and Goel [10] developed an improved pushover analysis procedure named as Modal Pushover Analysis (MPA) which is based on structural dynamics theory. Sasaki, et al. [11] proposed Multi-Mode Pushover (MMP) procedure to identify failure mechanisms due to higher modes. The procedure uses independent load patterns based on higher modes besides the one based on fundamental mode. Kalkan and Chopra [12] presented a modal-pushover-based scaling (MPS) procedure to scale ground motions for use in nonlinear RHA of buildings. Oguz [13] carried out pushover analyses along with nonlinear time history analyses to evaluate the accuracy of various lateral load patterns.

Many important works have also been carried out in Bangladesh regarding pushover analysis with focus on seismic deficiencies and remedies [14], stiffness irregularity in vertical direction [15], soft story vulnerability [16]. Nonlinear time history analysis for RC frames with brick masonry infill has also been carried out [17]. Hossen and Anam [18], Abdullah et.al. [19] studied nonlinear moment-curvature ($M-\phi$) relationship of beam and column sections and used

them in a nonlinear dynamic analysis to investigate the performance of different structural systems. However, the accuracy of pushover analysis in comparison to more rigorous nonlinear time history analysis has not yet been studied. Also, it is important to ascertain whether building frames designed by BNBC [1] are capable of fulfilling the targeted performance levels.

1.2. Objectives with specific aims and possible outcomes

The specific objectives of the proposed study are as follows:

- 1) To introduce a simplified nonlinear analysis method, i.e. pushover method, for generation of capacity and demand curves of a structure and determine its performance.
- 2) To validate the simplified nonlinear static analysis i.e. pushover analysis as incorporated in different softwares with published numerical results.
- 3) To perform a comparative study of pushover analysis and time history analysis with a view to study the effectiveness of pushover analysis.
- 4) To determine the performance levels for the design of different concrete frames according to BNBC [1] seismic provisions.
- 5) To validate linear and nonlinear time history analyses for SDOF system using different softwares with published numerical and experimental results.

This work aims to demonstrate the validity and efficiency of pushover analysis method of ATC-40 as incorporated in ETABS [20] and SAP2000 [21]. The work would also study the effectiveness of pushover analysis in comparison to more rigorous nonlinear time history analysis with particular emphasis on the load pattern employed in pushover analysis. Finally performance of building frames designed as per BNBC [1] will be evaluated against targeted performance levels for serviceability, design and maximum earthquakes.

1.3. Methodology

In order to achieve the selected objectives, the research work is initiated by studying seismic provisions of current codes of practices, available literatures on nonlinear static and dynamic analyses methods. The adequacy of the simplified nonlinear analysis i.e. pushover analysis as

given in ETABS/ SAP2000/SeismoStruct will be validated with published numerical and experimental results. The analysis is capable of progressive damage of elements by inserting appropriate hinges as the structure is laterally pushed through. Geometric non-linearity (P- Δ effect) is also included in the analysis. The resulting capacity curve (Base shear vs. displacement) is superimposed on earthquake demand curve in the same domain. The point of intersection of these curves will represent structure's performance level. However, the capacity curve depends on the load-pattern assumed in the simplified nonlinear analysis. By comparing with more rigorous nonlinear time history analyses, accuracy of pushover analysis is studied. Particular emphasis is given on the load pattern employed in pushover analysis.

Typical five to twelve storied buildings representative of low to high-rise buildings which are very common in Bangladesh is designed as per the force level detailed in BNBC and pushover analysis is carried out to evaluate the different performance levels under serviceability, design and maximum earthquakes.

The general purpose finite element program e.g. SAP2000, ETABS and SeismoStruct are the primary tool for modeling the structures and studying its behavior in terms of capacity and performance.

1.4. LAYOUT OF THESIS

The general background and present state of the problem, objectives with specific aims, possible outcomes and scope of the thesis and methodology of the work are discussed in Chapter 1, which give the basic idea of the study and its methodology. Chapter 2 describes pushover analysis, Time history analysis for different types of earthquake loading. This chapter also presents M- Φ relation for pushover analysis. In Chapter 3, nonlinear static analysis procedures in terms of capacity and demand curves have been studied. Modeling parameters and acceptance criteria for nonlinear hinges are also presented in this chapter. A site response spectrum with 5% damping for Dhaka is also developed in this chapter. In this chapter, pushover analysis results have been validated by comparing with published numerical results. Also, procedure of performance based analysis of concrete structure using software SAP2000/ETABS have been described. Chapter 4 mainly deals with nonlinear time history analysis, comparison with pushover analysis and validation of linear and nonlinear time history analysis with published results. In Chapter 5, performance based analysis of 3D RC frame building, designed according to BNBC, has been carried out to determine its

performance under three levels of earthquakes. A building not designed for seismic loads have also been studied to determine its seismic performance. Chapter 6 presents the finding of the research work, conclusion along with the recommendations for future study. The appendices are also included to present the ATC-40 provisions.

Chapter 2

Literature review

2.1 Introduction

Majority of buildings in our country are still designed for gravity loads only with nominal non seismic detailing provisions. The knowledge and application of seismic detailing is very limited among the structural designers of Bangladesh. This is quite unexpected, particularly since the Bangladesh National Building Code BNBC [1] contains a chapter on detailing of reinforced concrete structures (PART 6, Chapter 8). A recently published earthquake resistant design manual by Bangladesh Earthquake Society is a significant addition to this type of literature in Bangladesh, which had been practiced worldwide in earthquake prone areas [e.g., seismic design code provisions of American Concrete Institute ACI 318 (1999), Euro code 8 (2002) and Indian Standards IS 1893 (2002) and IS 13920 (2002)].

Many important works have also been carried out in Bangladesh regarding pushover analysis with focus on seismic deficiencies and remedies [14], stiffness irregularity in vertical direction [15], soft story vulnerability [16]. Nonlinear time history analysis for RC frames with brick masonry infill has also been carried out [17]. Hossen and Anam [18], Abdullah et.al.[19] studied nonlinear moment-curvature ($M-\phi$) relationship of beam and column sections and used them in a nonlinear dynamic analysis to investigate the performance of different structural systems. However, the accuracy of pushover analysis in compare to more rigorous nonlinear time history analysis has not yet been studied. Also, it is important to ascertain whether building frames designed by BNBC [1] are capable of fulfilling the targeted performance levels.

2.2 Provisions for earthquake load in BNBC

Bangladesh National Building Code BNBC [1] has different provisions for calculation of earthquake load and analysis procedures for structures subjected to earthquake. Two methods are available in BNBC for determination of seismic lateral forces on primary framing systems.

2.2.1 Equivalent static force method

In this method the dynamic earthquake effect is represented by an equivalent static load at different levels in proportion to mass at that level. In this process BNBC divided the country into three region of different possible earthquake ground response (0.075g, 0.015g, and 0.25g).

The total design base shear for a seismic zone is given by,

$$V = \frac{ZIC}{R}W \dots\dots\dots (a)$$

Where,

Z= seismic zone co-efficient

I= Structural importance co-efficient

$$C = \text{Numerical co-efficient} = \frac{1.25S}{T^{\frac{2}{3}}}$$

$$T = \text{Time period} = C_t(h_n)^{\frac{3}{4}}$$

Where,

$C_t = 0.083$ for moment resisting frame

$= 0.073$ for reinforced concrete frame and eccentric braced still frame

$= 0.049$ for all other structural analysis

h_n = Height in meter above base level n

S = Site co-efficient

R= Response modification co-efficient

W= Total seismic dead load

Lateral force calculated from the above equation known as base shear V , shall be distributed along the height of the structure in accordance with the following equation

$$V = F_t + \sum_{i=1}^n F_i \dots\dots\dots (b)$$

Where, F_i = Lateral force applied at story level i and

F_t = Concentrated lateral force considered at the top of the building in addition to the force F_n .

2.2.2 Dynamic response method

2.2.2.1 Response spectrum method

BNBC recommends that response spectrum to be used in dynamic analysis shall be either of the following:

- a) **Site specific design spectra:** A site specific design spectra shall be developed base on the geologic, tectonic, seismologic, and soil characteristics associated with the specific site.
- b) **Normalized response spectra:** In absence of a site-specific response spectrum, the normalized response spectra shall be used.

The normalized response spectrum curves provided in the code are prepared for three different soil types and 5% of critical damping Fig. 2.1 below

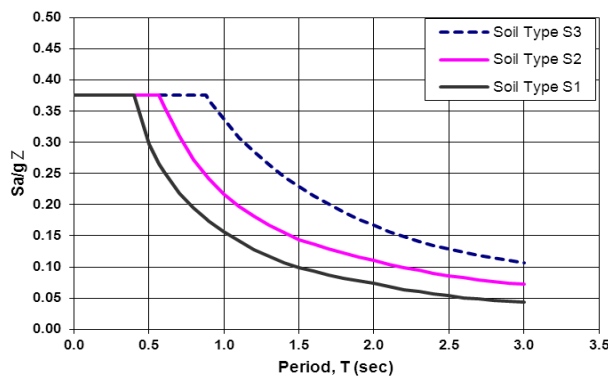


Fig 2.1 Normalized response spectra for 5% damping ratio (Adopted from BNBC)

2.3 Selection of lateral force method in BNBC

Seismic lateral forces on primary framing systems shall be determined by using either the equivalent static force method or the dynamic response method complying with the restrictions given below:

- a) The equivalent static force method may be used for the following structures:
 - i) All Structures, regular or irregular, in Seismic Zone 1 and Structure Importance Category iv in Seismic Zone 2, except case b (iv) below.
 - ii) Regular structures less than 75 meters in height with lateral force resistance provided by structural systems listed in BNBC except case b (iv) below.
 - iii) Irregular structures not more than 20 meters in height.
- b) The dynamic response method may be used for all classes of structure, but shall be used for the structures of the following types.
 - i) Structures 75 meters or more in height except as permitted by case a (i) above.
 - ii) Structures having a stiffness, weight or geometric vertical irregularity of type I, II, III as defined in BNBC.
 - iii) Structures over 20 meters in height in Seismic Zone 3 not having the same structural system throughout their height.
 - iv) Structures regular or irregular, located on soil type S₄ as defined in BNBC.

2.4 Pushover analysis

An elastic analysis gives a good indication of the elastic capacity of structures, but it cannot predict failure mechanisms and account for redistribution of forces during progressive yielding for an earthquake excitation. Inelastic analyses procedures help demonstrate how buildings really work by identifying modes of failure and potential for progressive collapse. The use of inelastic procedures for design and evaluation is attempts to help engineers better understand how structures will behave when subjected to major earthquakes, where it is assumed that the elastic capacity of the structure will be exceeded. Application of this resolves some of uncertainties associated with code and elastic procedures.

Various analysis methods are available, both linear and nonlinear for evaluation of concrete building. The best basic inelastic method is nonlinear time history analysis method. This

method is too complicated and considered impractical for general use. The central focus of this thesis is to introduce the simplified nonlinear procedure for the generation of the “pushover” or capacity curve of a structure. Pushover analysis is a simplified static nonlinear analysis method which use capacity curve and reduced response spectrum to estimate maximum displacement of a building under a given level of earthquake.

2.4.1 Methods to perform simplified nonlinear analysis

As a structure responds to earthquake ground motion, it experiences lateral displacements and, in turn, deformations of its individual elements. At low levels of response, the element deformations will be within their elastic (linear) range and no damage will occur. At higher levels of response, element deformations will exceed their linear elastic capacities and some of structural components will experience damage. In order to provide reliable seismic performance, a structure must have a complete lateral force resisting system, capable of limiting earthquake induced lateral displacements to levels at which the damage sustained by the structural elements will be within acceptable levels for the intended performance objective. The basic factors that affect the lateral force resisting system’s ability to do this include the mass, stiffness, damping and configuration; the deformation capacity of the building elements; and the strength and character of the ground motion it must resist.

The nonlinear pushover analysis requires development of the capacity curve. The capacity curve is derived from an approximate nonlinear, incremental static analysis for the structure. This capacity curve is simply a plot of the total lateral seismic shear demand, “V,” on the structure, at various increments of loading, against the lateral deflection of the building at the roof level, under that applied lateral force. The slope of a straight line drawn from the origin of the plot for this curve to a point on the curve at any lateral displacement, “d,” represents the secant or “effective” stiffness of the structure when pushed laterally to that displacement.

Two key elements of a performance based design procedure are demand and capacity. Demand is the representation of the earthquake ground motion. Capacity is the representation of the structure’s ability to resist the seismic lateral force. The performance

is dependent on the manner that the capacity is able to handle the demand. In other words, the structure must have the capacity to resist the demands of the earthquake such that the performance of the structure is compatible with the objectives of the design.

Simplified nonlinear analysis procedures using pushover methods, such as the capacity spectrum method and the displacement coefficient method, require determination of three primary elements: capacity, demand (displacement) and performance. Each of these elements is briefly discussed below.

2.4.2 Capacity

The overall capacity of a structure depends on the strength and deformation capacities of the individual components of the structure. In order to determine capacities beyond the elastic limits, some form of nonlinear analysis, such as the pushover procedure, is required. This procedure uses a series of sequential elastic limits, some form of nonlinear analysis, superimposed to approximate a force displacement capacity diagram of the overall structure. The mathematical model of the structure is modified to account for reduced resistance of yielding components. A lateral force distribution is again applied until additional components yield. This process is continued until the structure becomes unstable or until a predetermined limit is reached. The capacity curve approximates how structures behave after exceeding their elastic limit.

2.4.3 Demand (displacement)

Ground motions during an earthquake produce complex horizontal displacement pattern in structures that may vary with time. Tracking this motion at every time-step to determine structural design requirements is judged impractical. Traditional linear analysis methods use lateral forces to represent a design condition. For nonlinear methods it is easier and more direct to use a set of lateral displacements as a design condition. For a given structure and ground motion, the displacement demand is the estimate of the maximum expected response of the building during the ground motion.

2.4.4 Performance

Once a capacity curve and demand displacement is defined, a performance check can be done. A performance check verifies that structural and nonstructural components are not damaged beyond the acceptable limits of the performance objective for the forces and displacement imposed by the displacement demand.

2.4.5 Reduced demand spectra

The capacity of a particular building and the demand imposed upon it by a given earthquake motion are not independent. One source of this mutual dependence is evident from the capacity curve itself. As the demand increases the structure eventually yields and, its stiffness decreases, its period lengthens. Conversion of the capacity curve to spectral ordinates (ADRS) makes this concept easier to visualize. Since the seismic acceleration depends on period, demand also changes as the structure yields. Another source of mutual dependence between capacity and demand is effective damping. As a building yield in response to seismic demand it dissipates energy with hysteretic damping. Building that have large, stable hysteresis loops during cyclic yielding dissipate more energy than those with pinched loops caused by degradation of strength and stiffness.

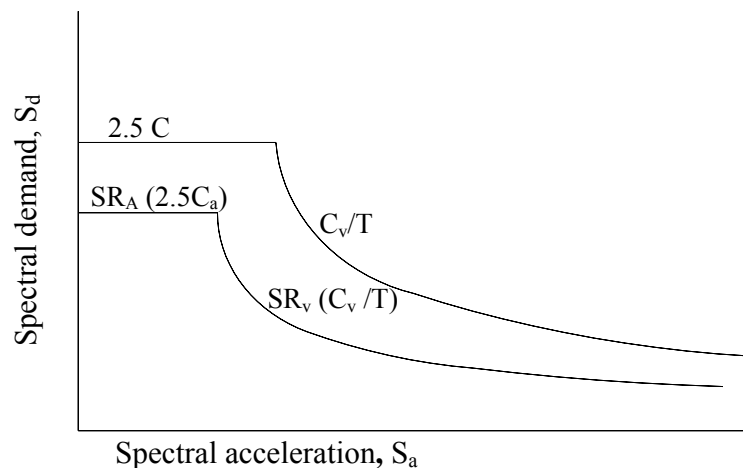


Fig. 2.2 Reduced response spectrum

Since the energy that is dissipated need not be stored in the structure, the effective damping diminishes displacement demand. The reduced displacement demand is shown in Fig.2.2. The equation for the reduced factor SR_A and SR_V are given by:

$$SR_A = \frac{3.21 - 0.681 \ln(\beta_{eff})}{2.12} \geq \text{Value in Table 2.1}$$

$$SR_V = \frac{2.31 - 0.41 \ln(\beta_{eff})}{1.65} \geq \text{Value in Table 2.1}$$

Table 2.1: Minimum allowable SR_A and SR_V values¹ (Adopted from ATC-40)

Structural Behavior Type	SR_A	SR_V
Type A ²	0.33	0.50
Type B	0.44	0.56
Type C.	0.56	0.67

1. Values for SR_A and SR_V shall not be less than those shown in this Table
2. Type A, B and C is taken as defined in ATC 40 (1996)

Severity of earthquakes as classified in ATC-40, 1996 is defined below.

A. The serviceability earthquake (SE)

The serviceability earthquake (SE) is defined probabilistically as the level of ground shaking that has a 50 percent chance of being exceeded in 50-year period. This level of earthquake ground shaking is typically about 0.5 times of the level of ground shaking of the design earthquake. The SE has a mean return period of approximately 75 years. Damage in the nonstructural elements is expected during serviceability earthquake.

B. The design earthquake (DE)

The design earthquake (DE) is defined probabilistically as the level ground shaking that has a 10 percent chance of being exceeded in a 50-year period. The DE represents an infrequent level of ground shaking that can occur during the life of the building. The DE has a mean return period of approximately 500 years. Minor repairable damage in the primary lateral load carrying system is expected during design earthquake. For secondary elements, the damage may be such that they require replacement.

C. The maximum earthquake (ME)

The maximum earthquake (ME) is defined deterministically as the maximum level of earthquake ground shaking which may ever be accepted at the building site within the known geologic frame work. In probabilistic terms, the ME has a return period of about 1,000 years. During maximum earthquake, buildings will be damaged beyond repairable limit but will not collapse.

2.4.6 Development of elastic site response spectra

Elastic response spectra for a site are based on estimate of Seismic Coefficient, C_A which represents the effective peak acceleration (EPA) of the ground and C_V which represents 5 percent damped response of a 1-second system. These coefficients for a particular zone are dependent on the seismicity of the area, the proximity of the site to active seismic sources, and site soil profile characteristics.

2.4.7 Seismic zone

Bangladesh is divided into three seismic zones as per BNBC. The table below shows the values of zone coefficients of Bangladesh.

Table 2.2 Seismic zone factor Z

Zone	1	2	3
Z	0.075	0.15	0.25

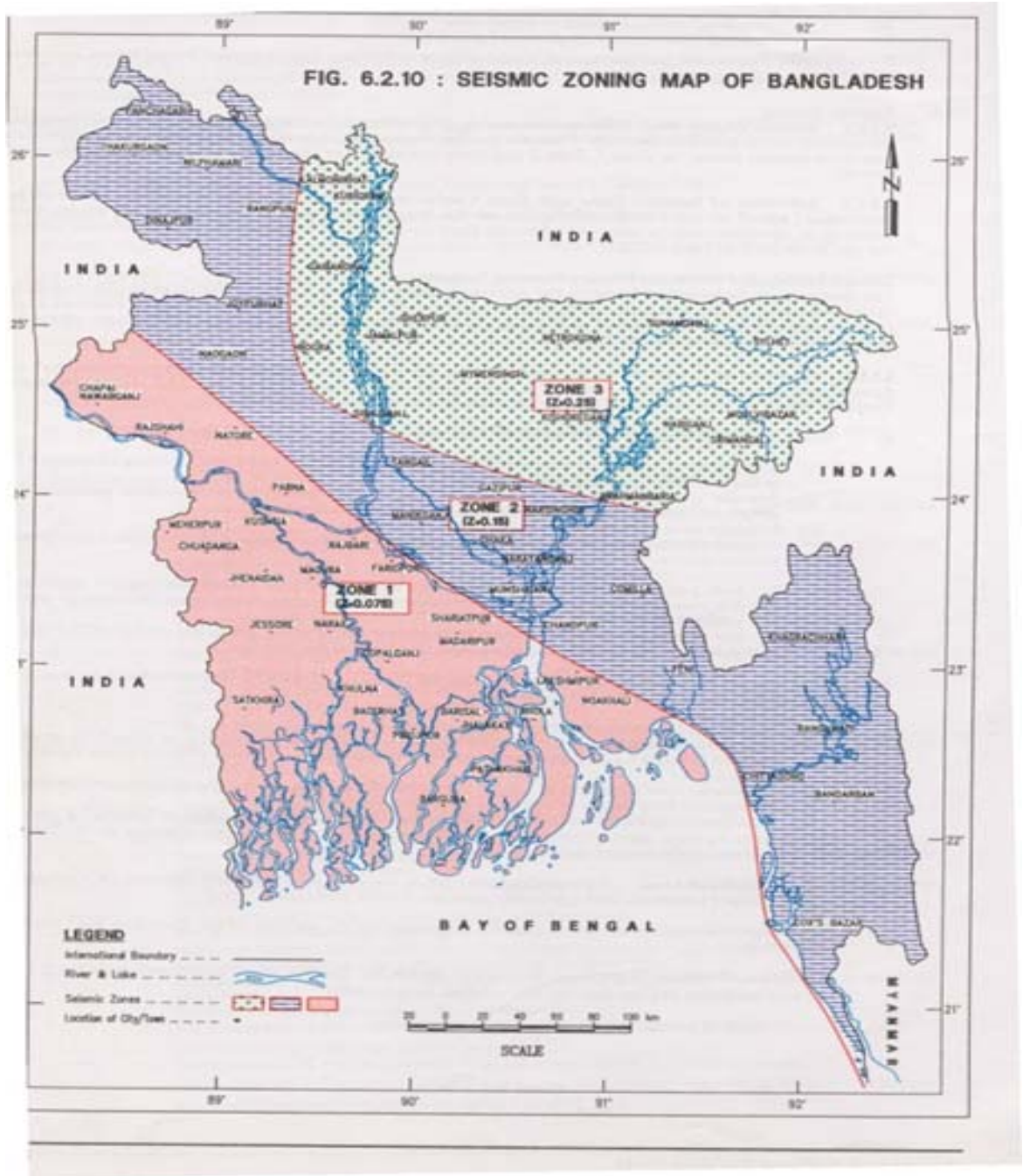


Fig 2.3 Seismic Zoning map of Bangladesh

2.4.8 Seismic source type:

As per ATC-40 (1996), three types of seismic source may be defined as shown in Table 2.3

Table 2.3 Seismic source type as per ATC-40, 1996

Seismic Source Type	Seismic Source Description	Seismic source definition	
		Maximum moment magnitude, M	Slip rate, SR(mm/yr)
A	Faults that are capable to produce large magnitude events and which have a high rate of seismic activity	$M \geq 7.0$	$SR \geq 5$
B	All faults other than types A and C	Not applicable	Not applicable
C	Faults that are not capable to producing large magnitude events and which have a high rate of seismic activity	$M < 6.5$	$SR < 2$

2.4.9 Near source factor

Currently data pertaining to the active faults close to Dhaka city is not available. It is not possible to estimate the seismic source distance from a specific site being considered in this thesis. But it may be safely assumed that all the sources are located at distance more than 15 km and the Table 2.4 (ATC-40, 1996) may be used to consider the Near-Source effects for the present study.

Table 2.4 Seismic source factor

Seismic source type	Closed distance to known seismic source							
	$\leq 2\text{km}$		5 km		10 km		$\geq 15\text{ km}$	
	N_A	N_V	N_A	N_V	N_A	N_V	N_A	N_V
A	1.5	2.0	1.2	1.6	1.0	1.2	1.0	1.0
B	1.3	1.6	1.0	1.2	1.0	1.0	1.0	1.0
C	1.0	1.0	1.0	1.0	1.0	1.0	1.0	1.0

1. The near source factor may be used on the linear interpolation of values for distance other than those shown in the table.

2. The closest distance of the seismic source shall be taken as the minimum distance between the site and the area described by the vertical projecting of source on the surface (i.e., surface projection of fault plane). The surface projecting need not include portions of the source a depths of 10km or greater. The largest value of the near-source factor considering all sources shall be used for design.

2.4.10 Seismic coefficients

For each earthquake hazard level, the structure is assigned a seismic coefficient C_A in accordance Table 2.5 (ATC-40, 1996) and a seismic coefficient C_V in accordance with Table 2.6 (ATC-40, 1996). Seismic coefficient C_A represents the effective peak acceleration (EPA) of the ground. A factor of about 2.5 times C_A represents the average value of peak response of a 5 percent-damped short-period system in the acceleration domain. The seismic coefficient C_V represents 5 percent-damped response of a 1-second system. C_V divided by period (T) defines acceleration response in the velocity domain. These coefficients are dependent on soil profile type and the product of earthquake zoning coefficient-Z, severity of earthquake-E and near source factor-N (ZEN). The soil profile types are classified in Table 2.7.

Table 2.5 Seismic coefficient C_A

Soil profile type	Shaking intensity, ZEN ^{1,2}			
	0.075	0.15	0.20	0.30
S _B	0.08	0.15	0.20	0.30
S _C	0.09	0.18	0.24	0.33
S _D	0.12	0.22	0.28	0.36
S _E	0.19	0.30	0.34	0.36
S _F	Site-specific geo-technical investigation required to determine C_A			

1. The value of E used to determine the product, ZEN, should be taken to be equal to 0.5 for the serviceability earthquake, 1.0 for the design earthquake, and 1.25 for the maximum earthquake.

2. Seismic coefficient C_A should be determined by linear interpolation for values of the product ZEN other than those shown in the table.

Table 2.6 Seismic coefficient C_V (Adopted from ATC-40)

Soil profile type	Shaking intensity, ZEN ^{1,2}			
	0.075	0.15	0.20	0.30
S _B	0.08	0.15	0.20	0.30
S _C	0.13	0.25	0.32	0.45
S _D	0.18	0.32	0.40	0.54
S _E	0.26	0.50	0.64	0.84
S _F	Site-specific geo-technical investigation required to determine C_V			

1. The value of E used to determine the product, ZEN, should be taken to be equal to 0.5 for the serviceability earthquake, 1.0 for the design earthquake, and 1.25 for the maximum earthquake.
2. Seismic coefficient C_V should be determined by linear interpolation for values of the product ZEN other than those shown in the table.

Table 2.7 Soil Profile Types (ATC-40)

Soil Profile Type	Soil profile name/Generic description	Average soil properties for top 100 ft of soil profile		
		Share Wave velocity, V_s (ft/sec)	Standard penetration Test, N or N_{CH} for cohesion less soil layers(blow/ft)	Undrained shear strength, S_u (psf)
S _A ¹	Hard rock	$V_s > 5,000$	Not Applicable	
S _B	Rock	$2,500 < V_s \leq 5,000$	Not Applicable	
S _C	Very dense soil and rock	$1,200 < V_s \leq 2,500$	$N > 50$	$S_u > 2,000$
S _D	Stiff soil profile	$600 < V_s \leq 1,200$	$15 \leq N \leq 50$	$1,000 \leq S_u \leq 2,000$
S _E ²	Soft soil profile	$V_s < 600$	$N < 50$	$S_u < 1,000$
S _F	Soil requiring site-specific evaluation			

Soil profile S_A is not applicable to site in Dhaka.

Soil profile type S_E also include any soil profile with more than 10 feet of soft clay defined as a soil with $PI > 20$, $W_{MC} \geq 40$ and $S_u < 500$ psf..

2.4.11 Development of elastic site response spectra

Elastic response spectra for a site are based on estimate of seismic coefficient, C_A which represents the effective peak acceleration (EPA) of the ground and C_V which represents 5 percent damped response of a 1-second system. These coefficients for a particular zone are dependent on the seismicity of the area, the proximity of the site to active seismic sources, and site soil profile characteristics.

2.4.12 Establishing demand spectra

For the purpose of subsequent analysis to be made in this thesis, it is necessary to establish an earthquake demand spectra against which building performance will be evaluated. The following controlling parameters are considered:

Location of the site : Dhaka City

Soil profile at the site : Soil type S_E as per Table 4.6, soft soil with shear wave velocity $V_s < 600$ ft/sec, $N < 50$ and $S_u < 100$ psf

Earthquake source type : A – considering the events similar to the great Indian Earthquake in Assam in 12 June, 1897

Near Source Factor : > 15 km

Table 2.8: Calculation of C_A

Seismic zone factor, Z	0.15	As per BNBC
Earthquake hazard level, E	1	Design Earthquake
Near source factor, N	1	>15 km, Table 2.4
Shaking intensity, ZEN	0.15	>15 km, Table 2.5
For soil type S_E , C_A	0.3	

Table 2.9: Calculation of C_V

Seismic zone factor, Z	0.15	As per BNBC
Earthquake hazard level, E	1	Design earthquake
Near source factor, N	1	>15km, Table 2.4
Shaking intensity, ZEN	0.15	From Table 2.6
For Soil Type S_E , C_V	0.5	

A typical capacity curve of a hypothetical structure is shown in Fig. 2.4.

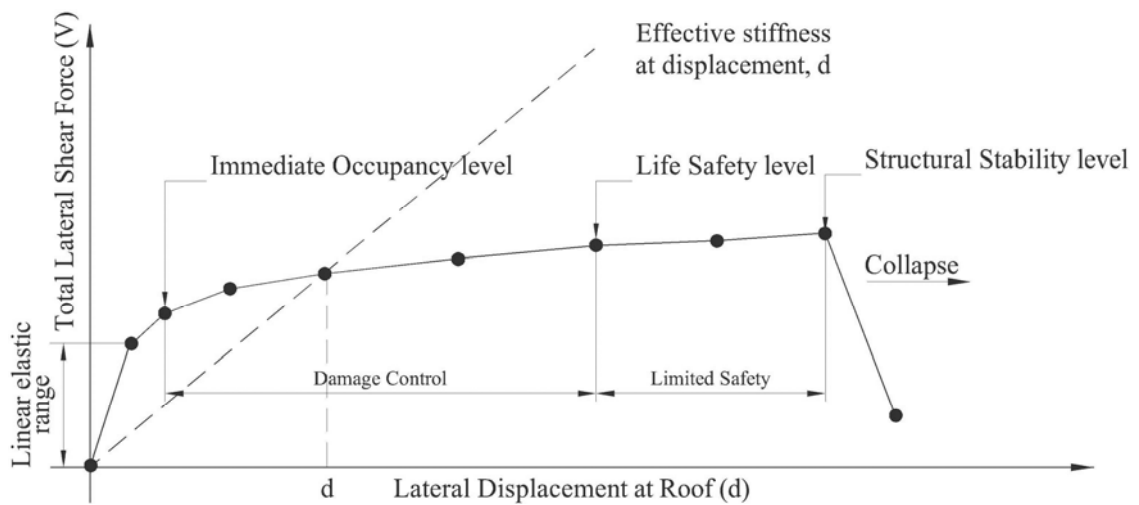


Fig. 2.4 Typical capacity curve

In Fig. 2.4, the discrete points indicated by the symbol ‘•’ represent the occurrence of important events in the lateral response history of the structure. Such an event may be the initiation of yield in a particular structural element or a particular type of damage. Each point is determined by a different analysis sequence. Then, by evaluating the cumulative effects of damage sustained at each of the individual events, and the overall behavior of the structure’s increasing lateral displacements, it is possible to determine and indicate on the capacity curve those total structural lateral displacements that represent limits on the various structural performance levels, as has been done in Fig. 2.4.

The process of defining lateral deformation points on the capacity curve at which specific structural performance levels may be said to have occurred requires the exercise of

considerable judgment on the part of the engineer. For each of the several structural performance levels and global performance levels defined in this chapter. It defines global system response limits as well as acceptance criteria for the individual structural elements. These acceptance criteria generally consist of limiting values of element deformation parameters, such as the plastic chord rotation of a beam or shear angle of a wall. These limiting values have been selected as reasonable approximate estimates of the average deformations at which certain types of element behavior such as cracking, yielding, or crushing, may be expected to occur. As the incremental static nonlinear analyses are performed, the engineer must monitor the cumulative deformations of all important structural elements and evaluate them against the acceptance criteria set before.

The point on the capacity curve at which the first element exceeds the permissible deformation level for a structural performance level does not necessarily represent that the structure as a whole reaches that structural performance level. Most structures contain many elements and have considerable redundancy. Consequently, the onset of unacceptable damage to a small percentage of these elements may not represent an unacceptable condition with regard to the overall performance of the structure. When determining the points along the capacity curve for the structure at which the various structural performance levels may said to be reached, the engineer must view the performance of the structure as whole and consider the importance of damage predicted for the various elements on the overall behavior of the structure.

The methodology described by ATC-40, incorporates the concept of “Primary” and “Secondary” elements to assist the engineer in making these judgments. Primary elements are those that are required as part of the lateral force resisting system for the structure. All other elements are designated as secondary elements. For a given performance level, secondary elements are generally permitted to sustain more damage than primary elements since degradation of secondary elements does not have a significant effect on the lateral load resisting capability of the structure. If in the development of the capacity curve it is determined that a few elements fail to meet the acceptance criteria for a given performance level at an increment of lateral loading and displacement, the engineer has the ability to designate these “nonconforming” elements as secondary, enabling the use of more liberal

acceptance criteria for these few elements. Care is exercised not to designate an excessive number of elements that are effective in resisting lateral forces as secondary.

2.4.13 Capacity spectrum method

The capacity spectrum method, a nonlinear static procedure, provides a graphical representation of the global force-displacement capacity curve of the structure (i.e. pushover curve) and compares it to the response spectra representations of the earthquake demands. This method is a very useful tool in the evaluation and retrofit design of both existing concrete structures. The graphical representation provides a clear picture of how a structure responds to earthquake ground motion, and, as illustrated below, it provides an immediate and clear picture of how various retrofit strategies, such as adding stiffness or strength, will affect the structure response to earthquake demands.

The capacity spectrum curve for the structure is obtained by transforming the capacity curve from lateral force (V) vs. lateral displacement (d) coordinates to spectral acceleration (S_a) vs. spectral displacement (S_d) coordinates using the modal shape vectors, participation factors and modal masses obtained from a modal analysis of the structure. In order to compare the Structure's capacity to the earthquake demand, it is required to plot the response spectrum and the capacity spectrum on the same plot. The conventional response spectrum plotted in spectral acceleration vs. period coordinate has to be changed in to spectral acceleration vs. spectral displacement coordinate. This form of response spectrum is known as acceleration displacement response spectrum (ADRS).

Capacity spectrum method requires plotting the capacity curve in spectral acceleration and spectral displacement domain. This representation of spectral quantities is known as Acceleration displacement response spectra in brief ADRS, which was introduced by Mahaney et al.,(1993). Spectral quantities like spectral acceleration, spectral displacement and spectral velocity is related to each other to a specific structural period T . Building code usually provide response spectrum in spectral acceleration vs. period format which is the conventional format.

Each point on the curve defined in the Fig. 2.5 is related to spectral displacement by

mathematical relation, $S_d = \frac{1}{4\pi^2} S_a T^2$. Converting with this relation response spectrum in ADRS format may be obtained.

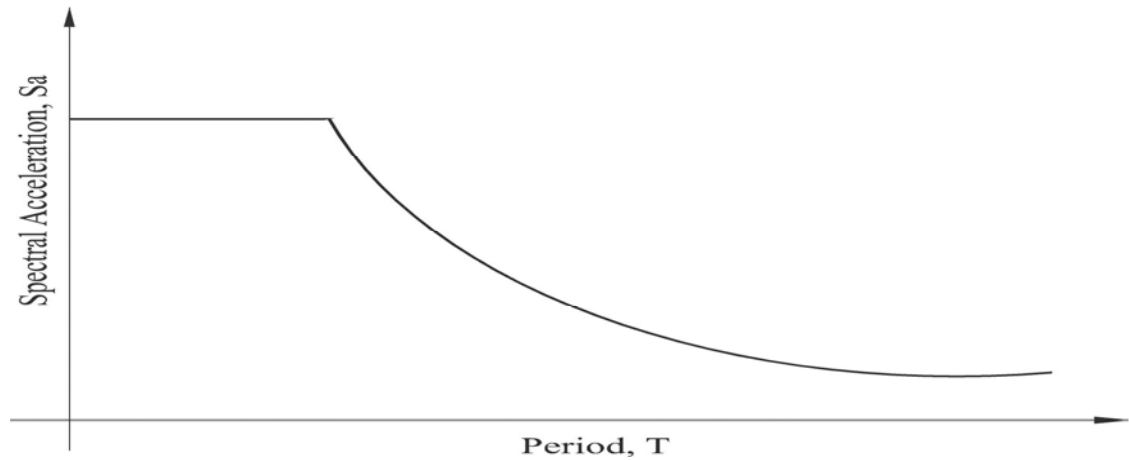


Fig. 2.5 Code specified response spectrum in Spectral acceleration vs. Period.

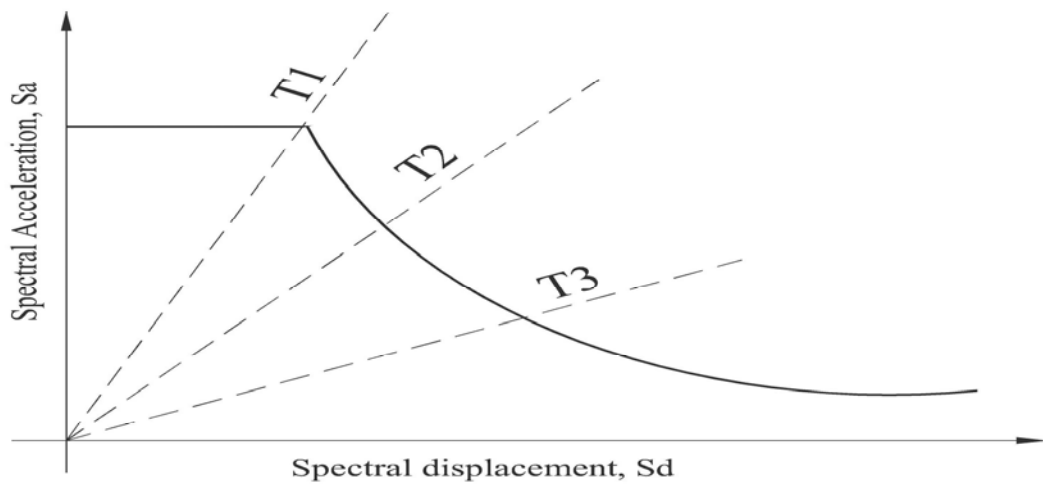


Fig. 2.6 Response spectrum in ADRS format

Any line from the origin of the ADRS format represent a constant period T_i which is related to spectral acceleration and spectral displacement by the mathematical relation,

$$T = 2\pi \sqrt{\frac{S_d}{S_a}}$$

Capacity Spectrum Capacity spectrum is a simple representation of capacity curve in ADRS domain. A capacity curve is the representation of Base Shear (V) to roof displacement (X_d). In order to develop the capacity spectrum from a capacity curve it is necessary to do a point by point conversion to first mode spectral coordinates.

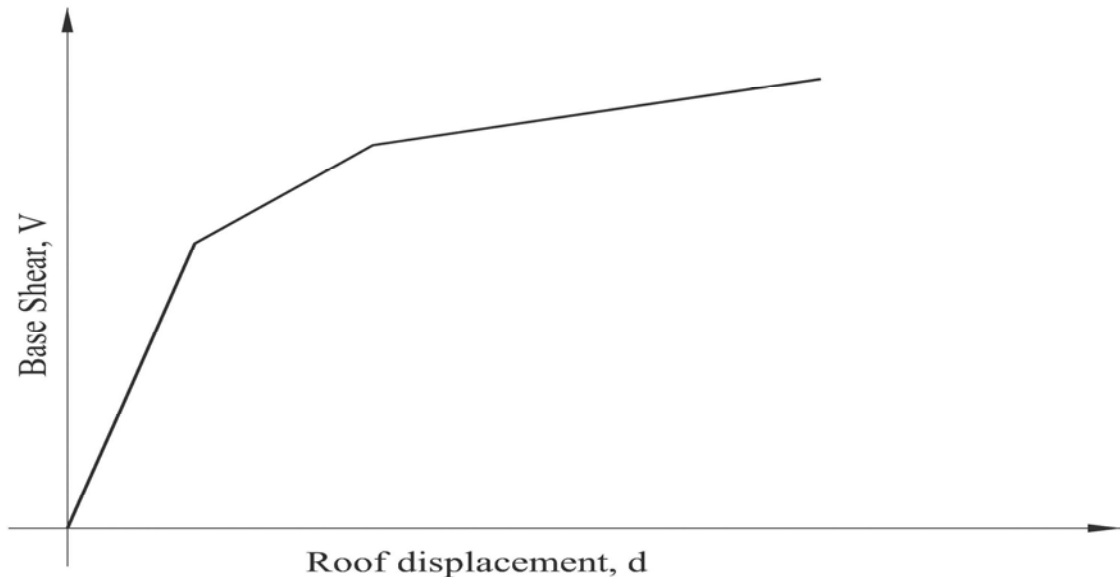


Fig. 2.7 A typical capacity curve

Any point corresponding values of base shear, V_i and roof deflection, Δ_i may be converted to the corresponding point of spectral acceleration, S_{ai} and spectral displacement, S_{di} on the capacity spectrum using relation,

$$S_{ai} = \frac{V_i / W}{\alpha_1} \quad \text{and}$$

$$S_{di} = \frac{\Delta_{Roof}}{PF_1 \times \Phi_{1,Roof}}$$

$$PF_1 = \frac{\left[\sum_1^N (w_i \phi_{i,1}) / g \right]}{\left[\sum_1^N (w_i \phi_{i,1}^2) / g \right]}$$

Modal mass coefficient for the first mode, α_1 is calculated using equation,

$$\alpha_1 = \frac{\left[\sum_1^N (w_i \phi_{i,1}) / g \right]^2}{\left[\sum_1^N w_i / g \right] \left[\sum_1^N (w_i \phi_{i,1}^2) / g \right]}$$

Where:

- PF₁ = modal participation factor for the first natural mode.
- α_1 = modal mass coefficient for the first natural mode
- $\Phi_{1, \text{roof}}$ = roof level amplitude of the first mode.
- w_i/g = mass assigned to level i
- Φ_{i1} = amplitude of mode 1 at level i
- N = level N, the level which is the uppermost in the main portion of the structure
- V = base shear
- W = building dead weight plus likely live loads
- Δ_{roof} = roof displacement
- S_a = spectral acceleration
- S_d = spectral displacement

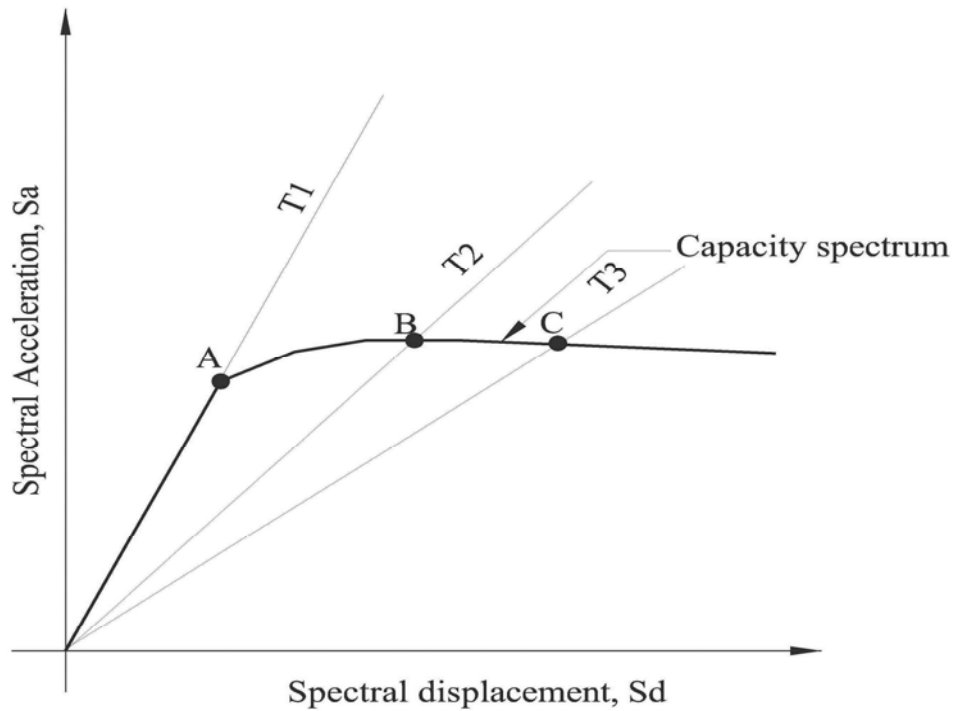


Fig 2.8 Capacity spectrum

Fig. 2.8 shows a typical capacity spectrum converted from capacity curve of Fig. 2.7 of a hypothetical structure. It is seen in the capacity spectrum that up to some displacement corresponding to point A, the period is constant T_1 . That is the structure is behaving elastically. As the structure deflects more to point B, it goes to inelastic deformation and its period lengthens to T_2 .

When the capacity curve is plotted in S_a vs. S_d coordinates, radial lines drawn from the origin of the plot through the curve at various spectral displacements have a slope (ω), where, ω is the radial frequency of the effective (or secant) first-mode response of the structure if pushed by an earthquake to that spectral displacement.

Using the relationship $T=2\pi/\omega$, it is possible to calculate, for each of these radial lines, the effective period of the structure if it is pushed to a given spectral displacements.

Fig. 2.9 is a capacity spectrum plot obtained from the capacity curve of a hypothetical structure shown in Fig. 2.4 and plotted with the effective modal periods shown.

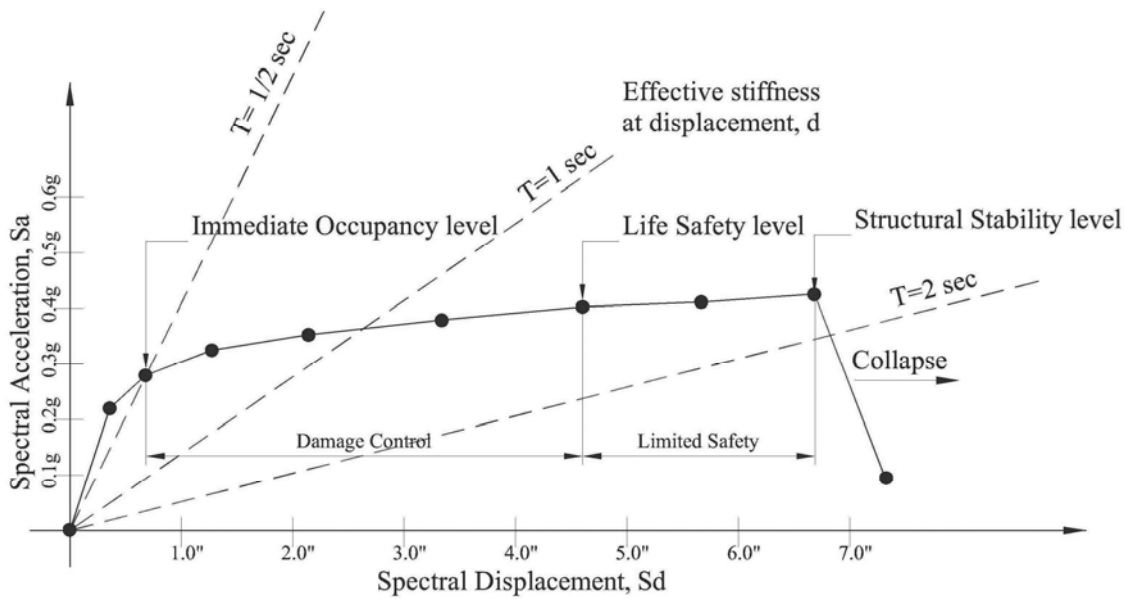


Fig. 2.9 Typical capacity spectrum

The particular structure represented by this plot would have an elastic period of approximately $\frac{1}{2}$ second. As it is pushed progressively further by stronger ground motion, this period lengthens. The building represented in Figs. 2.4 and 2.9 would experience collapse before having its stiffness degraded enough to produce an effective period of 2 seconds.

The capacity of a particular building and the demand imposed upon it by a given earthquake motion are not independent. One source of this mutual dependence is evident from the capacity curve itself. As the demand increases, the structure eventually yields and, as its stiffness decreases, its period lengthens. Conversion of the capacity curve to spectral ordinates (ADRS) makes this concept easier to visualize. Since the seismic accelerations depend on period, demand also changes as the structure yields. Another source of mutual dependence between capacity and demand is effective damping. As a building yield in response to seismic demand it dissipates energy with hysteretic damping.

The capacity spectrum method initially characterizes seismic demand using an elastic response spectrum. This spectrum is plotted in spectral ordinates (ADRS) format showing the spectral acceleration as a function of spectral displacement. This format allows the

demand spectrum to be “overlaid” on the capacity spectrum for the building. The intersection of the demand and capacity spectra, if located in the linear range of the capacity, would define the actual displacement for the structure; however this is not normally the case as most analyses include some inelastic nonlinear behavior. To find the point where demand and capacity are equal, a point on the capacity spectrum need to be selected as an initial estimate. Using the spectral acceleration and displacement defined by this point, reduction factors may be calculated to apply to the 5% elastic spectrum to account for the hysteretic energy dissipation, or effective damping, associated with the specific point. If the reduced demand spectrum intersects the capacity spectrum at or near the initial assumed point, then it is the solution for the unique point where capacity equals demand. If the intersection is not reasonably close to the initial point, then a new point somewhere between may be assumed and repeat the process until a solution is reached. This is the performance point where the capacity of the structure matches the demand or the specific earthquake.

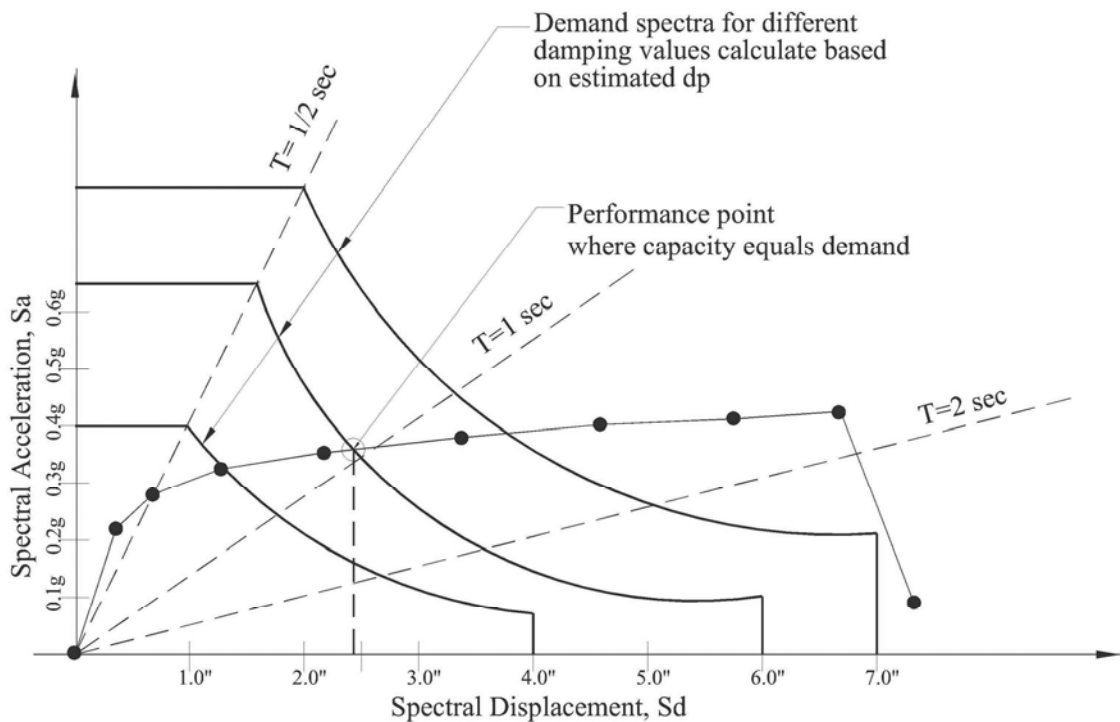


Fig. 2.10 Determination of performance point (Adopted from ATC 40)

Once the performance point has been determined, the acceptability of a rehabilitation design to meet the project performance objectives can be judged by evaluating where the performance point falls on the capacity curve. For the structure and earthquake represented by the overlay indicated in Fig. 2.10, the performance point occurs within the central portion of the damage control performance range as shown in Fig. 2.9, indicating that for this earthquake this structure would have less damage than permitted for the Life Safety level and more than would be permitted for the Immediate Occupancy level. With this information, the performance objective and/or the effectiveness of the particular rehabilitation strategy to achieve the project performance objectives can be judged.

There are three procedures (A, B, C) to find performance point. Which procedure has to be selected for analysis can be judged from the following comparison of three procedures.

Procedure A:

- Clearest, most transparent and direct application of the methodology
- Analytical method
- Conventional for spreadsheet programming
- May be the best method for beginners because it is most direct and easiest to understand.

Procedure B:

- Analytical method
- Simpler than procedure A because of simplifying assumptions (that may not always be valid)
- Most conventional for spreadsheet programming
- Reasonably transparent application of methodology
- Users of this method should fully understand the inherent assumptions

Procedure C:

- Graphical method
- Most convenient method for hand analysis
- Not as convenient for spreadsheet programming
- Least transparent application of methodology

2.4.14 Displacement coefficient method

Another procedure for calculating demand displacement is ‘Displacement Coefficient Method’ which provides a direct numerical process for calculating the displacement demand. Displacement Coefficient Method has not been explored. Performance analysis of the structures under this thesis was made using Capacity Spectrum Method.

2.4.15 Seismic performance evaluation

The essence of virtually all seismic evaluation procedures is a comparison between some measures of the “demand” that earthquake place on structure to a measure of the “capacity” of the building to resist the induced effects. Traditional design procedures characterize demand and capacity as forces. Base shear (total horizontal force at the lowest level of the building) is the normal parameter that is used for this purpose. The base shear demand that would be generated by a given earthquake, or intensity of ground motion is calculated, and compares this to the base shear capacity of the building. If the building were subjected to a force equal to its base shear capacity some deformation and yielding might occur in some structural elements, but the building would not collapse or reach an otherwise undesirable overall level of damage. If the demand generated by the earthquake is less than the capacity then the design is deemed acceptable.

The first formal seismic design procedures recognized that the earthquake accelerations would generate forces proportional to the weight of the building. Over the years, empirical knowledge about the actual behavior of real structures in earthquakes and theoretical understanding of structural dynamics advanced. The basic procedure was modified to reflect the fact that the demand generated by the earthquake accelerations was also a function of the stiffness of the structure.

The inherently better behavior of some buildings over others are also begun to recognize. Consequently, that reduced seismic demand has been assumed for some structure based on the characteristics of the basic structural material and system. The motivation to reduce seismic demand for design came because it could not be rationalized theoretically how structures resisted the forces generated by earthquakes. This was partially the result of the

fundamental assumption that structures resisted loads linearly without yielding or permanent structural deformation.

2.4.16 Nonlinear static procedure for capacity evaluation of structures

Instead of comparing forces, nonlinear static procedures use displacements to compare seismic demand to the capacity of a structure. This approach included consideration of the ductility of the structure on an element by element basis. The inelastic capacity of a building is then a measure of its ability to dissipate earthquake energy. The current trend in seismic analysis is toward these simplified inelastic procedures.

The recommended central methodology is on the formulation of inelastic capacity curve for the structure. This curve is a plot of the horizontal movement of a structure as it is pushed to one side. Initially the plot is a straight line as the structure moves linearly. As the parts of the structure yield the plot begins to curve as the structure softens. This curve is generated by building a model of the entire structure from nonlinear representations of all of its elements and components. Most often this is accomplished with a computer and structural analysis software. The forces and displacement characteristics are specified for each piece of the structure resisting the earthquake demand. These pieces are assembled geometrically to represent the complete lateral load resisting system. The resulting model is subjected to increasing increment of load in a pattern determined by its dynamic properties. The corresponding displacements define the inelastic capacity curve of the building. The generation of the capacity curve defines the capacity of the building uniquely and independently of any specific seismic demand. In this sense it replaces the base shear capacity of conventional procedures. When an earthquake displaces the building laterally, its response is represented by a point on this curve. A point on the curve defines a specific damage state of the building, since the deformation of its entire components can related to the global displacement of the structure.

The capacity of a particular building and the demand imposed upon it by a given earthquake motion are not independent. One source of this mutual dependence is evident from the capacity curve itself. As the demand increases the structure eventually yields and,

as its stiffness decreases, its period lengthens. Since the seismic accelerations depend on period, demand also changes as the structure yields. Another source of mutual dependence between capacity and demand is effective damping. As building yields in response to seismic demand, it dissipates energy with hysteretic damping. Building that have large, stable hysteretic loops during cyclic yielding dissipate more than those with pinched loops cause by degradation of strength and stiffness. Since the energy that is dissipated need not be stored in the structure, the damping has the effect of diminishing displacement demand.

2.4.17 Structural performance levels and ranges

The Performance of a building under any particular event is dependent on a wide range of parameters. These parameters are defined (ATC-40, 1996; FEMA 356, 2000) qualitatively in terms of the safety afforded by the building to the occupants during and after the event; the cost and feasibility of restoring the building to pre-earthquake condition; the length of time the building is removed from service to effect repairs; and economic, architectural, or historic impacts on the larger community. These performance characteristics are directly related to the extent of damage that would be sustained by the building.

The federal emergency management agency in its report 'prestandard and commentary for the seismic rehabilitation of buildings (FEMA-356, 2000) defines the structural performance level of a building to be selected from four discrete structural performance levels and two intermediate structural performance ranges. The discrete Structural Performance Levels are

Immediate Occupancy (S-1), Life Safety (S-3), Collapse Prevention (S-5), and Not Considered (S-6). The intermediate Structural Performance Ranges are the Damage Control Range (S-2) and the Limited Safety Range (S-4)

The definition of these performance ranges are given by FEMA [4]. Acceptance criteria for performance within the damage control structural performance range may be obtained by interpolating the acceptance criteria provided for the Immediate Occupancy (IO) and Life Safety (LS) structural performance Levels. Acceptance criteria for performance within the Limited Safety Structural Performance Range may be obtained by interpolating the acceptance criteria provided for the life safety and collapse prevention structural

performance levels. The performance levels and ranges, as per FEMA are described in the sections that follow.

2.4.17.1 Immediate occupancy structural performance level (S-1)

Structural performance level S-1, immediate occupancy, may be defined as the post-earthquake damage state of a structure that remains safe to occupy, essentially retains the pre-earthquake design strength and stiffness of the structure, and is in compliance with the acceptance criteria specified in this standard for this structural performance levels defined in Table 2-B1 to 2-B3 in the appendix.

Structural performance level S-1, immediate occupancy, means the post-earthquake damage state in which only very limited structural damage has occurred. The basic vertical and lateral-force-resisting systems of the building retain nearly all of their pre-earthquake strength and stiffness. The risk of life-threatening injury as a result of structural damage is very low, and although some minor structural repairs may be appropriate, these would generally not be required prior to re-occupancy.

2.4.17.2 Damage control structural performance range (S-2)

Structural performance range S-2, damage control, may be defined as the continuous range of damage states between the life safety structural performance level (S-3) and the immediate occupancy structural performance level (S-1) defined in Table 2-B1 to 2-B3 in the appendix.

Design for the damage control structural performance range may be desirable to minimize repair time and operation interruption, as a partial means of protecting valuable equipment and contents, or to preserve important historic features when the cost of design for immediate occupancy is excessive.

2.4.17.3 Life safety structural performance level (S-3)

Structural performance level S-3, life safety, may be defined as the post-earthquake damage state that includes damage to structural components but retains a margin against

onset of partial or total collapse in compliance with the acceptance criteria specified in FEMA (FEMA-356, 2000) for this structural performance level defined in Table 2-B1 to 2-B3 in the appendix.

Structural performance level S-3, life safety, means the post-earthquake damage state in which significant damage to the structure has occurred, but some margin against either partial or total structural collapse remains. Some structural elements and components are severely damaged, but this has not resulted in large falling debris hazards, either within or outside the building. Injuries may occur during the earthquake; however, the overall risk of life-threatening injury as a result of structural damage is expected to be low. It should be possible to repair the structure; however, for economic reasons this may not be practical. While the damaged structure is not an imminent collapse risk, it would be prudent to implement structural repairs or install temporary bracing prior to re-occupancy.

2.4.17.4 Limited safety structural performance range (S-4)

Structural performance range S-4, limited safety, may be defined as the continuous range of damage states between the life safety structural performance level (S-3) and the collapse prevention structural performance level (S-5) defined in Table 2-B1 to 2-B3 in the appendix.

2.4.17.5 Collapse prevention structural performance level (S-5)

Structural performance level S-5, collapse prevention, may be defined as the post-earthquake damage state that includes damage to structural components such that the structure continues to support gravity loads but retains no margin against collapse in compliance with the acceptance criteria specified FEMA for this structural performance level defined in Table 2-B1 to 2-B3 in the appendix.

Structural performance level S-5, collapse prevention, means the post-earthquake damage state in which the building is on the verge of partial or total collapse. Substantial damage to the structure has occurred, potentially including significant degradation in the stiffness and strength of the lateral-force resisting system, large permanent lateral deformation of the

structure, and to more limited extent degradation in vertical load carrying capacity. However, all significant components of the gravity load resisting system must continue to carry their gravity load demands. Significant risk of injury due to falling hazards from structural debris may exist. The structure may not be technically practical to repair and is not safe for re-occupancy, as aftershock activity could induce collapse.

2.4.17.6 Target building performance levels

Building performance is a combination of the both structural and nonstructural components. Table 2-B1, 2-B2 and 2-B3 (FEMA-356) describe the approximate limiting levels of structural damage that may be expected of buildings evaluated to the levels defined for a target seismic demand. These tables represent the physical states of mathematical calculation of different performance levels.

2.4.18 Response limit

To determine whether a building meets a specified performance objective, response quantities from a nonlinear analysis are compared with limits given for appropriate performance levels (ATC-40 and FEMA-356). The response limits fall into two categories:

2.4.18.1 Global building acceptability limits

These response limits include requirements for the vertical load capacity, lateral load resistance, and lateral drift. Table 2.10 gives the limiting values for different performance level.

Gravity loads

The gravity load capacity of the building structure must remain intact for acceptable performance at any level. Where an element or component loses capacity to support gravity loads, the structure must be capable to redistributing its load to other elements or components of the existing system.

Lateral loads

Some components types are subjected to degrading over multiple load cycles. If a significant number of components degrade, the overall lateral force resistance of the

building may be affected. The lateral load resistance of the building system, including resistance to the effects of gravity loads acting through lateral displacements, should not degrade by more than 20 percent of the maximum resistance of the structure for the extreme case.

Two effects can lead to loss of lateral load resistance with increasing displacement. The first is gravity loads acting through lateral displacements, known as the P-Δ effect. The P-Δ effect is most prominent for flexible structures with little redundancy and low lateral load strength relative to the structure weight. The second effect is degradation in resistance of individual components of the structure under the action of reversed deformation cycles. When lateral load resistance of the building degrades with increasing displacement, there is a tendency for displacements to accumulate in one direction. This tendency is especially important for long-duration events. The following table presents deformation limits of various performance levels. Maximum total drift is defined as the inter-story drift at the performance point displacement. Maximum inelastic drift is defined as the portion of the maximum total drift beyond the effective yield point. For Structural Stability, the maximum total drift in story i at the performance point should not exceed the quantity $0.33V_i/P_i$, where V_i is the total calculated shear force in story i and P_i is the total gravity load (i.e. dead plus likely live load) at story i (ATC-40).

Table 2.10 Deformation limits (ATC-40)

	Performance Level			
	Immediate occupancy	Damage control	Life safety	Structural stability
Inter story drift limit				
Maximum total drift	0.01	0.01 ~0.02	0.02	$0.33 \frac{V_i}{P_i}$
Maximum inelastic drift	0.005	0.005~0.015	No limit	No limit

2.4.18.2 Element and component acceptability limit

Deformation and force controlled actions

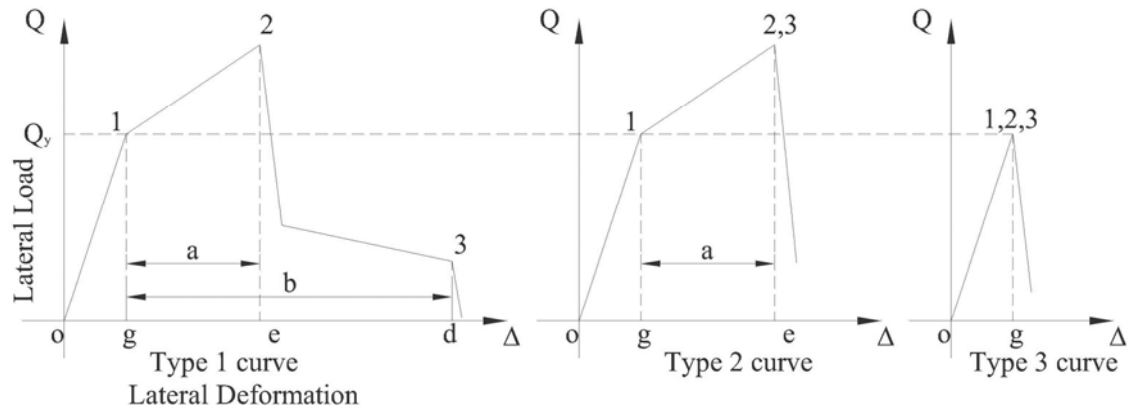


Fig. 2.11 Component force versus deformation curves (FEMA-356)

All structural actions may be classified as either deformation controlled or force-controlled using the component force versus deformation curves shown in Fig. 2.11. The Type 1 curve depicted in Fig. 2.11 is representative of ductile behavior where there is an elastic range (point 0 to point 1 on the curve) followed by a plastic range (points 1 to 3) with non-negligible residual strength and ability to support gravity loads at point 3. The plastic range includes a strain hardening or softening range (points 1 to 2) and a strength-degraded range (points 2 to 3). Primary component actions exhibiting this behavior shall be classified as deformation-controlled if the strain-hardening or strain-softening range is such that $e > 2g$; otherwise, they shall be classified as force controlled. Secondary component actions exhibiting Type 1 behavior shall be classified as deformation-controlled for any e/g ratio. The Type 2 curve depicted in Fig. 2.11 is representative of ductile behavior where there is an elastic range (point 0 to point 1 on the curve) and a plastic range (points 1 to 2) followed by loss of strength and loss of ability to support gravity loads beyond point 2. Primary and secondary component actions exhibiting this type of behavior shall be classified as deformation-controlled if the plastic range is such that $e > 2g$; otherwise, they shall be classified as force controlled. The Type 3 curve depicted in Fig. 2.11 is representative of a brittle or non-ductile behavior where there is an elastic range (point 0 to point 1 on the curve) followed by loss of strength and loss of ability to support gravity loads beyond

point1. Primary and secondary component actions displaying Type 3 behavior shall be classified as force-controlled (FEMA-356).

Deformation controlled and force controlled behavior

Acceptance criteria for primary components that exhibit Type 1 behavior are typically within the elastic or plastic ranges between points 0 and 2, depending on the performance level. Acceptance criteria for secondary elements that exhibit Type 1 behavior can be within any of the performance ranges. Acceptance criteria for primary and secondary components exhibiting Type 2 behavior will be within the elastic or plastic ranges, depending on the performance level. Acceptance criteria for primary and secondary components exhibiting Type 3 behavior will always be within the elastic range. Table 2.11 provides some examples of possible deformation- and force-controlled actions in common framing systems.

Table: 2.11 Examples of possible deformation controlled and force controlled actions (FEMA)

Component	Deformation controlled action	Force controlled action
Moment frames		
Beam	Moment(M)	Shear (V)
Columns	M	Axial load (P), V
Joints	-	V ¹
Shear Walls	M, V	P
Braced Frames		
Braces	P	-
Beams	-	P
Columns	-	P
Shear Link	V	P, M
Connections	P, V, M ³	P, V, M
Diaphragms	M, V ²	P, V, M

2.4.19 Acceptability limit

A given component may have a combination of both force and deformation controlled actions. Each element must be checked to determine whether its individual components satisfy acceptability requirements under performance point forces and deformations. Together with the global requirements, acceptability limits for individual components are the main criteria for assessing the calculated building response.

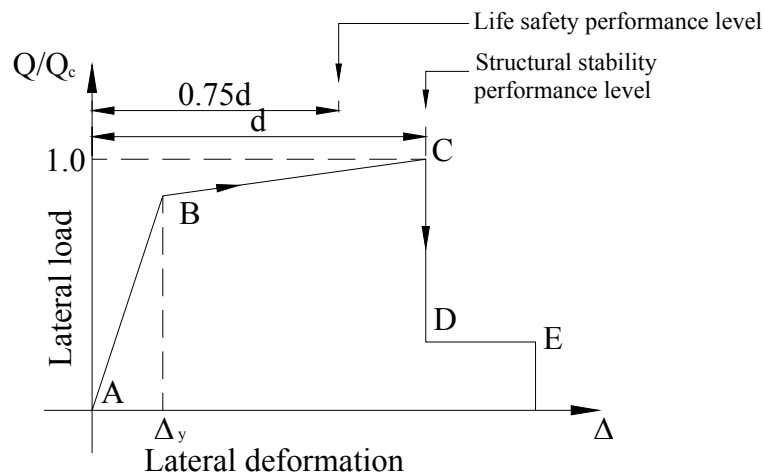


Fig. 2.12 Force deformation action and acceptance criteria (ATC-40)

The Fig. 2.12 shows a generalized load deformation relation appropriate for most concrete components. The relation is described by linear response from A (unloaded component) to an effective yield point B, linear response at reduced stiffness from B to C, sudden reduction in lateral load resistance to D, response at reduced resistance to E, and final loss of resistance thereafter. The following main points relate to the depicted load-deformation relation:

- Point A corresponds to the unloaded condition. The analysis must recognize that gravity loads may induce initial forces and deformations that should be accounted for in the model. Therefore, lateral loading may commence at a point other than the origin of the load-deformation relation.
- Point B has resistance equal to the nominal yield strength. The slope from B to C, ignoring the effects of gravity loads acting through lateral displacements, is usually taken as between 5% and 10% of the initial slope. This strain hardening,

which is observed for most reinforced concrete component, may have an important effect on the redistribution of internal forces among adjacent components.

- c) The abscissa at C corresponding to the deformation at which significant strength degradation begins.
- d) The drop in resistance from C to D represents initial failure of the component.
- e) The residual resistance from D to E may be non-zero in some cases and may be effectively zero in others. Where specific information is not available, the residual resistance usually may be assumed to be equal to 20% of the nominal strength.
- f) Point E is a point defining the maximum deformation capacity. Deformation beyond that limit is not permitted because gravity load can no longer be sustained.

Table 2-C1 to 2-C7 (Appendix) give the acceptance criteria (ATC-40) to be used with Nonlinear Procedures for the acceptance model of individual structural elements of a structure that has been used to evaluated for finding seismic performance of the selected buildings under this thesis.

2.5 Nonlinear time history analysis

Earthquake excitation is time dependent, highly irregular and arbitrary in nature. Usually earthquake excitation in the form of acceleration or displacement or velocity is recorded for a time interval of 0.02 to 0.005 seconds. In this dynamic analysis procedure the response of a structure at every time interval is recorded for the whole earthquake period and the statistical average is represented. Because of its inherent complexities of the procedure and nondeterministic nature of the input ground motion, the analysis procedure has not become popular in the design houses for designing of the structures.

Ground motion time history developed for the specific site shall be representative of the actual earthquake motion for an earthquake. When this procedure is followed an elastic or inelastic dynamic analysis of a structure shall be made using a mathematical model of a structure and applying at its base or any other appropriate level, a ground motion time

history. Time dependent dynamic response of the structure shall be obtained through numerical integration of its equation of motion.

2.5.1 Nonlinear dynamic analysis for earthquake ground motions:

Earthquake causes vibration of the ground which is primarily a horizontal movement, although some vertical movement is also present. The vibrations are time-dependent typically for durations of 10-40 seconds, which increases gradually to the peak amplitude and then decays. The ground vibration is expressed through the temporal variation of ground accelerations which is used in structural analyses. Figs. 4.1 and 4.2 shows the ground accelerations recorded during some of the best known and widely studied earthquakes of the 20th century which are also used in the present study.

The behavior of RC under dynamic loading is not linear when the deformation is large and load is time dependent. The use of linearly elastic analysis procedure is not valid in such cases. In fact there are some situations where the use of such simplified analyses can be misleading and missing in important details. The material and geometric properties which are considered constant in linear analysis do not remain constant in many practical situations. For example severe earthquake vibrations may cause quite large structural deformations and as a result alter the stiffness properties significantly. Moreover, member properties like mass or damping may undergo changes during the dynamic response, while stiffness properties may vary significantly due to the material and geometric nonlinearities caused by significant axial forces. Modal analysis is a commonly used method of linear dynamic analysis, but is not valid for nonlinear systems. The incremental numerical scheme needs to be applied for the dynamic analysis of nonlinear systems like Reinforced Concrete structures.

2.5.2 Linearly elastic and inelastic systems:

For a linearly elastic system, the relationship between the applied force f_s and the resulting deformation u is linear; i.e.,

$$f_s = k u \dots\dots\dots (c)$$

where k is the linear stiffness of the system; its units are force/length. Here the resisting force is directly proportional to the displacement and is a single valued function of u .

This is however not valid when the load-deformation relationship is nonlinear, i.e., when the stiffness itself is not constant but is a function of u . Moreover, structural components undergo cyclic deformation for dynamic problems. The initial loading curve is nonlinear at the amplitudes of deformation; the unloading and reloading curves differ from the initial loading path. This implies that the force f_s corresponding to deformation u is not single-valued and depends on the history of the deformations. It further depends on the rate of change of deformation (i.e., the velocity, particularly on whether it is positive or negative). Thus the resisting force for nonlinear dynamic problems can be expressed as

$$f_s = f_s(u, v) \dots\dots\dots(d)$$

and the system is called inelastic dynamic system.

For RC structures undergoing large deformations due to strong earthquake vibrations, Eq. (d) is more appropriate than Eq. (c). The use of linear elastic dynamic analysis for strong seismic problems can lead to the omission of such important concepts as plasticity, yielding, shifting of equilibrium position, permanent deformation and residual stresses.

2.5.3 Equation of motion for seismic vibration

The governing equation of motion for an inelastic SDOF system subjected to ground motion $u_g(t)$ is given by

$$m \frac{d^2u}{dt^2} + c \frac{du}{dt} + k u = c \frac{du_g}{dt} + k u_g \dots\dots\dots(e)$$

$$\Rightarrow m \frac{d^2u_r}{dt^2} + c \frac{du_r}{dt} + k u_r = -m \frac{d^2u_g}{dt^2} \dots\dots\dots(f)$$

where $u_r = u - u_g$ is the relative displacement of the SDOF system with respect to the ground displacement. Eq. (e) shows that the ground motion appears on the right side of the equation of motion just like a time-dependent load. Therefore, although there is no body-force on the system, it is still subjected to dynamic excitation by the ground displacement.

2.5.4 Solution by incremental time step integration:

For an inelastic SDOF system the equation of motion to be solved numerically is

$$m \frac{d^2u}{dt^2} + c \frac{du}{dt} + f_s(u,v) = f(t) \dots\dots\dots (g)$$

subject to specified initial conditions. In Eq. (g) the system is assumed to have linear viscous damping, but other forms of damping, including nonlinear damping could be considered.

The applied force $f(t)$ is given by a set of discrete values, $f_i = f(t)$, $i = 0 \sim N$. The time interval, $\Delta t_i = t_{i+1} - t_i$ is usually taken to be a constant. The response is determined at the discrete time instants t_i . The displacement, velocity and acceleration of the SDOF system at time t_i are u_i , v_i and a_i and at time t_{i+1} are u_{i+1} , v_{i+1} and a_{i+1} respectively. These values, satisfy Eq. (g) at time t_i and t_{i+1}

$$m a_i + c v_i + (f_s)_i = f_i \dots\dots\dots (h)$$

$$m a_{i+1} + c v_{i+1} + (f_s)_{i+1} = f_{i+1} \dots\dots\dots (i)$$

When applied successively with $i = 0, 1, 2, \dots\dots$ the time stepping procedure gives the desired response at all-time instances $i = 1, 2, 3, \dots\dots$. The known initial conditions provide the information necessary to start the procedure. The difference between Eq. (h) and (i) gives an incremental equilibrium equation

$$m \Delta a_i + c \Delta v_i + (\Delta f_s)_i = \Delta f_i \dots\dots\dots (j)$$

The incremental resisting force, $(\Delta f_s)_i = (k_i)_{sec} \Delta u_i \dots\dots\dots (k)$

where the secant stiffness $(k_i)_{sec}$, as shown in Fig. (d), cannot be determined because u_{i+1} is unknown. On the assumption that the secant stiffness $(k_i)_{sec}$ could be replaced by the tangent stiffness $(k_i)_T$ [as shown in Fig.(d)] over a small time step Δt , Eq. (j) is approximated by

$$(\Delta f_s)_i = (k_i)_T \Delta u_i \dots\dots\dots (l)$$

Dropping the subscript T from $(k_i)_T$ in Eq. (l) and substituting it in Eq. (j) gives

$$m \Delta a_i + c \Delta v_i + k_i \Delta u_i = \Delta f_i \dots\dots\dots (m)$$

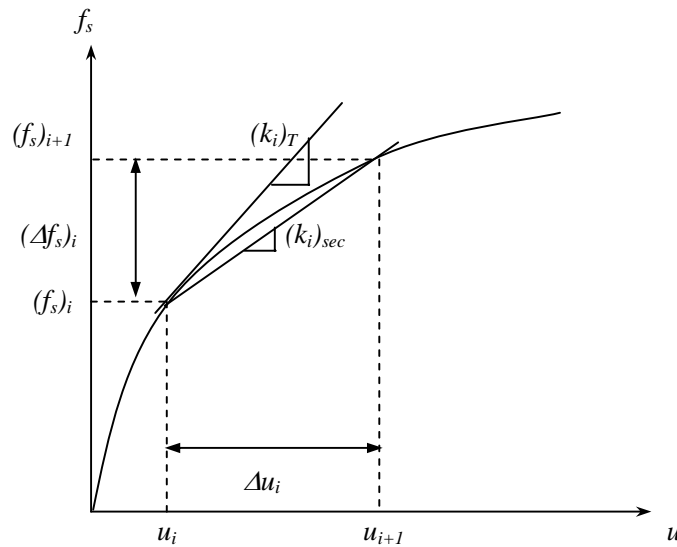


Fig. 2.13 Nonlinear force-displacement relationship

The similarity between this equation and the corresponding equation for linear systems suggests that the non-iterative formulation used for linear systems may also be used in the analysis of nonlinear response. It is necessary only to replace k by the tangent stiffness k_i to be evaluated at the beginning of each time step. In this work, the other properties (like m and c) are assumed constant for each step.

2.5.5 The average acceleration method

Many approximate methods are possible to implement the numerical scheme (described above) efficiently. Convergence, stability and accuracy are the three important requirements for a numerical procedure. The Average Acceleration Method (special case of the Newmark- β method), known for its simplicity and unconditional stability for linear systems, can be used here replacing k by the tangent stiffness k_i to be evaluated at the beginning of each time step.

In the incremental formulation, some adjustments are made to the original formulations for linear dynamic analysis. Using incremental displacement Δu_i ($= u_{i+1} - u_i$) and incremental force Δf_i ($= f_{i+1} - f_i$), the incremental time-step integration shown below can be followed.

The simulation should start with two initial conditions, like the displacement u_0 and velocity v_0 at time $t_0 = 0$. The initial acceleration can be obtained from the equation of motion at time $t_0 = 0$ as

$$a_0 = (f_0 - cv_0 - ku_0)/m$$

The incremental equations used in this formulation are

$$(k_i + 2c/\Delta t + 4m/\Delta t^2) \Delta u_i = \Delta f_i + (2c + 4m/\Delta t) v_i + (2m) a_i$$

$$u_{i+1} = u_i + \Delta u_i$$

$$a_{i+1} = 4 \Delta u_i / \Delta t^2 - 4v_i / \Delta t - a_i$$

$$v_{i+1} = v_i + (a_i + a_{i+1})\Delta t/2$$

Once the incremental displacement Δu_i is obtained from above equation, it can be used to calculate the total displacement (u_{i+1}), acceleration (a_{i+1}) and velocity (v_{i+1}) from above equation.

2.9 Conclusion

In this chapter pushover analysis and earthquake design philosophy have been explained. There are different earthquake analysis methods which have been discussed here. In between those the procedure of finding earthquake force in a structure from BNBC [1] is illustrated. The pushover analysis to find the actual performance of the structure is discussed here in detail. Also dynamic analysis and time history analysis is discussed in this chapter.

Chapter 3

Pushover Analysis

3.1 Introduction

An elastic analysis gives a good indication of the elastic response of structures, but it cannot predict failure mechanisms and account for redistribution of forces during progressive yielding for an earthquake excitation. Inelastic analyses procedures help demonstrate how buildings really work by identifying modes of failure and potential for progressive collapse. The use of inelastic procedures for design and evaluation is an approach to help engineers better understand how structures will behave when subjected to major earthquakes, where it is assumed that the elastic capacity of the structure will be exceeded. Application of this resolves some of the uncertainties associated with code and elastic procedures.

Various analysis methods are available, both linear and nonlinear for evaluation of concrete buildings. The basic inelastic method is nonlinear time history analysis method. This method is too complicated and considered impractical for general use. The central focus of this thesis is to study the simplified nonlinear procedure for the generation of the “pushover” or capacity curve of a structure. This represents the plot of progressive lateral displacement as a function of the increasing level of force applied to the structure. Pushover analysis is a simplified static nonlinear analysis method which uses capacity curve and reduced response spectrum to estimate maximum displacement of a building under a given level of earthquake.

In this chapter three reinforced concrete frames 2, 5, and 12 storied 2D frames are modeled. Two dimensional models of case study frames are prepared using SAP2000 [21], ETABS [20] and SeismoStruct [50] by considering the necessary geometric and strength characteristics of all members that affect the nonlinear seismic response. The structural models are based on centerline dimensions that beams and columns span between the nodes at the intersections of beam and column centerlines. Rigid floor diaphragms are assigned at each story level and the seismic mass of the frames are lumped at the mass center of each story. Gravity loads consisting of dead loads and 25% of live loads are considered in pushover. The dynamic properties of the case study frames are summarized in Table 3.1-3.3. The configuration, member details and dynamic properties of case study frames are presented in this chapter. Both pushover and nonlinear time history analyses are performed using gross section properties and P-Delta effects are considered. Nonlinear member behavior of concrete sections is modeled as discussed below for SAP2000 [21], ETABS [20] and SeismoStruct [50].

In this chapter the procedure for structural performance evaluation in the light of ATC-40[3] and FEMA 356[4] has been described. For the performance evaluation purposes Dhaka is selected as the site and seismic demand for Dhaka has been estimated as per guideline of ATC-40 and the frames are designed as per the provisions of BNBC [1]. Structural performances of three 2D frames with different configuration have been investigated. All structures have regular geometry and stiffness. The performances of the structures as evaluated through pushover analysis have been presented through capacity curves and capacity spectrums described in this chapter.

3.2 Details of pushover analysis in SAP2000 and ETABS

Different software is available for performing nonlinear analysis of concrete structure. In this study ETABS [20] and SAP2000 [21] have been used. In this section, different features and options of ETABS and SAP2000 related to perform pushover analysis is discussed. The structure should be modeled develop according to the architectural design. The concrete and the steel property should be provided according to design criteria. In ETABS and SAP2000 performance based analysis is suitable for frame structure. The two types of loads (gravity and lateral) should be provided according to code provisions. In this regard the loads have to be defined first and then have to be assigned on the structure. In ETABS and SAP2000 superimposed dead loads have to be assigned and it takes buildings own weight from the structure and its property. Live loads should be assigned according its intended use. For seismic load UBC 94 should be used which satisfy BNBC [1].

After running analysis the structure should be designed from concrete frame design options. From this the beam and column sections which are assigned first can also be checked. But the nonlinear analysis takes the column sections which are design first. In defining column sections the reinforcement to be designed option should be provided so that column reinforcement would be checked when structure is designed.

Frame nonlinear hinge properties are used to define nonlinear force displacement and/or moment rotation behavior that can be assigned to discrete locations along the length of frame (line) elements. These nonlinear hinges are only used during static nonlinear (pushover) analysis. The hinge properties are in ETABS and SAP2000 for concrete members and are generally based on in ATC-40[3]. The hinge properties cannot be modified. They also can not be viewed because the default properties are section dependent. The default properties can not be fully defined by the program until the section to which they apply is identified. Thus, to see the effect of the default properties, the

default property should be assigned to a frame element, and then the resulting generated hinge property should be viewed.

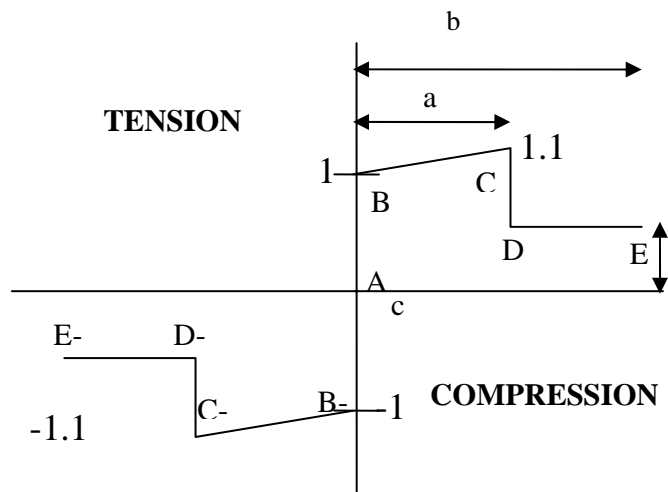


Fig. 3.1: Concrete moment and P-M-M hinge property

Slope between points B and C is taken as 10% total strain hardening for steel. Points C, D and E of M_3 based on Table A4 in appendix. The four conforming transverse reinforcing rows of the table are averaged. M_y based on reinforcement provided, otherwise based on minimum allowable reinforcement. P-M-M curve is for M_3 (major moment) and is taken to be the same as the moment curve in conjunction with the definition of axial–moment interaction curves. Points C, D and E of P-M-M curve based on Table A5 in appendix. The four conforming transverse reinforcing rows of the table are averaged.

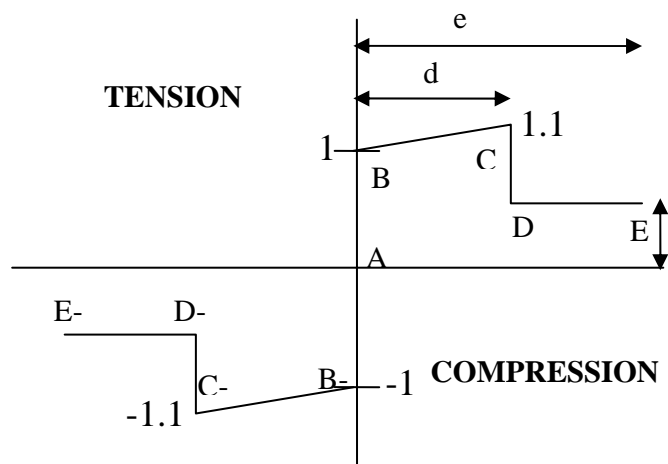


Fig. 3.2 Concrete Shear hinge property

Slope between points B and C is taken as 10% total strain hardening for steel. Points C, D and E based on Table 2 A1-A4 (ATC-40) of Appendix, Item 2, average of the two rows labeled “Conventional longitudinal reinforcement with conforming transverse reinforcement” in appendix.

The acceptance criteria values are deformations (displacements, strains, or rotations) that have been normalized by the same deformation scale factors used to specify the load deformation curve, and are typically located between points B and C and points B' and C' on the curve. They are used to indicate the state of the hinge when viewing the results of the analysis, but they do not affect the behavior of the structure. These acceptance criteria of M3, V2 and P-M-M hinge are taken from Table 2 A1, A2, A3 and A4 of appendix.

Static nonlinear analysis can consist of any number of cases. ETABS and SAP 2000 have been used for the analysis purpose. Each static nonlinear case can have a different distribution of load on the structure. A static nonlinear case may start from zero initial conditions, or it may start from the results at the end of a previous case. Each analysis case may consist of multiple construction stages.

For static nonlinear analysis, displacement controlled is used. The load combination specified in the load pattern area of the form is applied, but its magnitude is increased or decreased as necessary to keep the control displacement increasing in magnitude. This option is useful for applying lateral load to the structure, or for any case where the magnitude of the applied load is not known in advance, or when the structure can be expected to lose strength or become unstable.

The conjugate displacement is a generalized displacement measure that is defined as the work conjugate of the applied Load Pattern. It is a weighted sum of all displacement degrees of freedom in the structure: each displacement component is multiplied by the load applied at that degree of freedom, and the results are summed. The conjugate displacement is usually the most sensitive measure of displacement in the structure under a given specified load. It is usually recommended that to use the conjugate displacement unless one can identify a displacement in the structure that monotonically increases during the analysis. The monitored displacement is a single displacement component at a single point that is monitored during a static nonlinear analysis. When plotting the pushover curve, the program always uses the monitored displacement for the horizontal axis. The monitored displacement is also used to determine when to terminate a displacement controlled analysis.

To start the current cases from the end condition of a previously specified static nonlinear case, select the name of the previous case from the start from previous case drop down list. Typically this option is used for a lateral static nonlinear case to specify that it should start from the end of a gravity static

nonlinear case. To get the positive displacement increments of the pushover curve to be saved, the save positive increments only check box should be checked. In the following example, the solid line represents the pushover curve if the save positive increments only check box is checked (the default) and the dashed line represents the pushover curve if the save positive increments only check box is not checked. Fig. 3.3 showed that positive increment and all increment are saved.

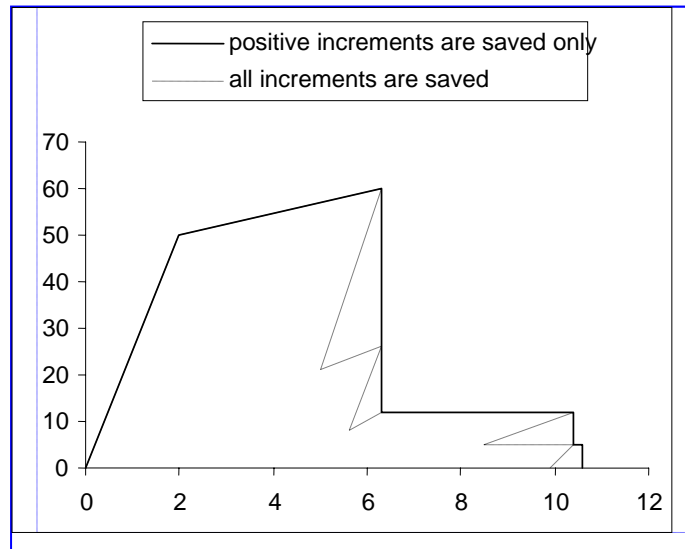


Fig. 3.3 An example to illustrate the option of Save Positive Increments Only

The minimum saved steps restricts the maximum step size used to apply the load in a static nonlinear case. ETABS and SAP2000 automatically creates steps corresponding to events on the hinge stress-strain curves or to significant nonlinear geometric effects. The results of these steps are saved only if they correspond to a significant change in the slope of the pushover curve. The maximum null steps is used, if necessary, to declare failure (i.e., non-convergence) in a run before it reaches the specified force or displacement goal. The program may be unable to converge on a step when catastrophic failure occurs in the structure, or when the load cannot be increased in a load-controlled analysis. There may also be instances where it is unable to converge in a step because of numerical sensitivity in the solution. The maximum total steps limits the total time the analysis will be allowed to run. ETABS and SAP2000 attempts to apply as much of the specified load pattern as possible, but may be restricted by the occurrence of an event, failure to converge within the maximum iterations/step, or a limit on the maximum step size from the minimum number of saved steps. As a result, a typical static nonlinear analysis may consist of a large number of steps. Additional steps may be required by some member unloading methods to redistribute load.

The large displacement option should be used for cable structures undergoing significant deformation; and for buckling analysis, particularly for snap-through buckling and post-buckling behavior. The frame elements and other elements that undergo significant relative rotations within the element should be divided into smaller elements to satisfy the requirement that the strains and rotations within an element are small. For most other structures, the P-delta option is adequate, particularly when material nonlinearity dominates. If reasonable, it is recommended that the analysis be performed first without P-delta (i.e., use none), adding geometric nonlinearity effects later

3.3 Description of case study frames for validation

The effects of lateral load patterns modes on global structural behavior and on the accuracy of pushover predictions have been studied on reinforced concrete moment resisting frames. Three reinforced concrete frames with 2, 5, and 12-stories are model in this chapter. Two dimensional models of case study frames are prepared using SAP2000 [21] and ETABS [20] by considering the necessary geometric and strength characteristics of all members that affect the nonlinear seismic response. The structural modeled are based on centerline dimensions that beams and columns span between the nodes at the intersections of beam and column centerlines and beam column joints are not modeled. Rigid floor diaphragms are assigned at each story level and the seismic mass of the frames are lumped at the mass center of each story. Gravity loads consisting of dead loads and 25% of live loads are considered in pushover analyses. The free vibration analyses of the frames using SAP2000 [21] and ETABS [20] yielded exactly same dynamic properties. The configuration, member details and dynamic properties of case study frames are presented in Table 3.1 to 3.6. The details of shear reinforcement are not considered since controlling behavior of frame members is assumed to be flexure. The pushover analysis is performed using gross section properties and P-Delta effects are neglected. Nonlinear member of concrete sections are modeled as discussed in this chapter for SAP2000 and ETABS.

3.3.1 Two story RC frame

Two story frame is consist two bay moment resisting frame. It is fixed at its support. Typical floor height is 3.962m. The length of each bay is 7.315m. Other structural dimensions and loading properties are given in Table 3.1. Dynamic properties are given in Table 3.2.

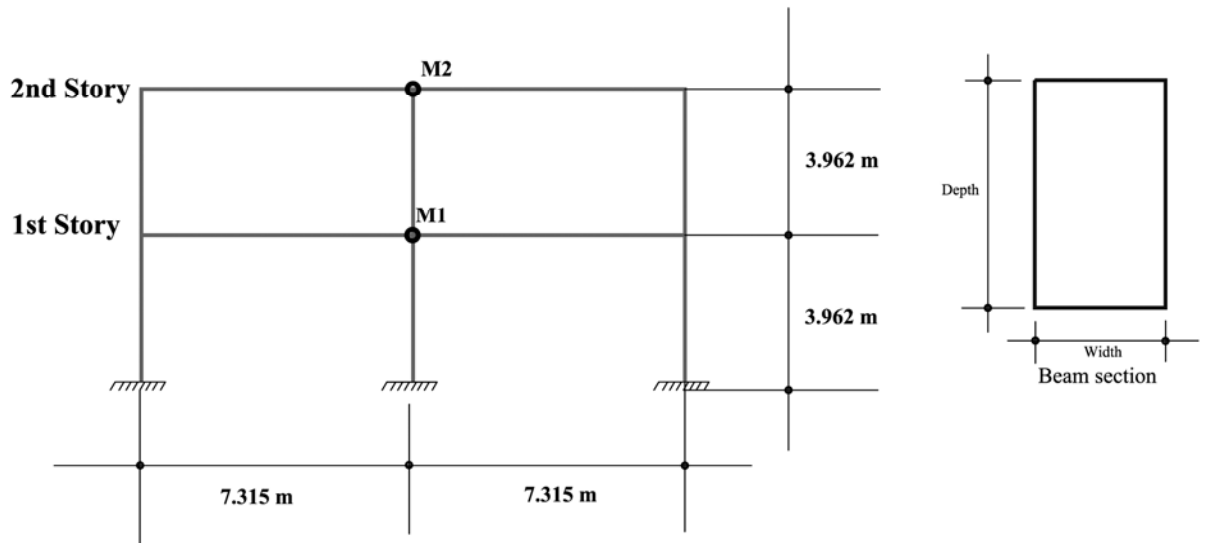


Fig. 3.4 Two story RC Frame

Table 3.1 Cross section and loading properties of two story RC frame

Properties of beam

Story	Beam				Mass (t)	DL (kN/m)	LL (kN/m)
	Dimension (mm)		Reinforcement (sq mm)				
	Depth	Width	Top	Bottom			
1	558	304	1342	3148	178	25.71	1.05
2	508	304	1342	2503	98	19.23	0.98

Properties of column

Story	Column	Dimension (mm)		Number of Bars		Bar Area (sq mm)
		X-dir	Y-dir	X-dir	Y-dir	
1 and 2	Exterior	609.6	609.6	5	5	645.16
	Interior	609.6	609.6	5	5	645.16

Concrete and steel properties of 2-story RC frame

Property	Concrete	Steel
Ultimate strength (MPa)	26	494.4
Modulus of elasticity (MPa)	28730.5	

Table 3.2 Dynamic properties of 2-story RC frame

Modal properties	Mode	
	1	2
Period, T (sec)	0.488	0.148
Modal participation factor	1.336	0.336
Modal mass factor	0.834	0.166

3.3.2 Five story RC frame

Five story frame is consist two bay moment resisting frame. It is fixed at its support. Typical floor height is 3.962m. The length of each bay is 7.315m. Other structural dimensions and loading properties are given in Table 3.3. Dynamic properties are given in Table 3.4.

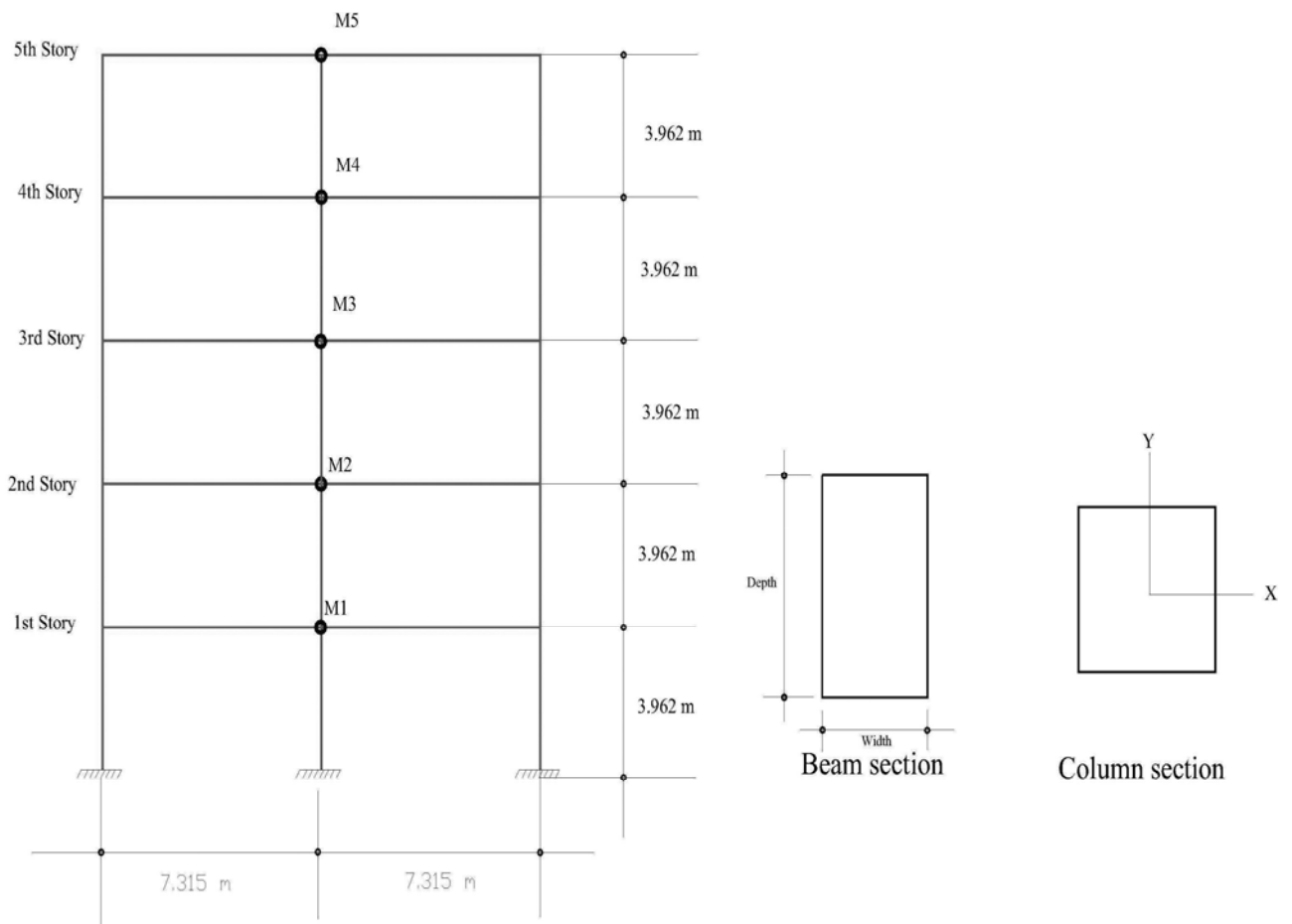


Fig. 3.5 Five story RC frame

Table 3.3 Cross section and loading properties of five story RC frame**Properties of beam**

Story	Beam				Mass (t)	DL (kN/m)	LL (kN/m)
	Dimension (mm)		Reinforcement (sq mm)				
	Depth	Width	Top	Bottom			
1-4	660.4	406.4	5083.86	3148.38	104.025	20.49	1.31
5	508.0	304.8	3793.54	2503.22	77.056	15.64	0.53

Properties of column

Story	Column	Dimension (mm)		Number of Bars		Bar Area (sq mm)
		X-dir	Y-dir	X-dir	Y-dir	
1-5	Exterior	711.2	711.2	6	6	885.8
	Interior	711.2	711.2	6	6	885.8

Concrete and steel properties of 5-story RC frame

Property	Concrete	Steel
Ultimate strength (MPa)	27.6	459.2
Modulus of elasticity (MPa)	27792.8	

Table 3.4 Dynamic properties of 5-story RC frame

Modal properties	Mode		
	1	2	3
Period, T (sec)	0.857	0.272	0.141
Modal participation factor	1.348	0.528	0.258
Modal mass factor	0.794	0.116	0.054

3.3.3 Twelve story RC frame

Twelve story RC frame is consist four bay moment resisting frame. It is fixed at its support. Typical floor height is 3.962m. The length of each bay is 7.315m. Other structural dimensions and loading properties are given in Table 3.5. Dynamic properties are given in Table 3.6.

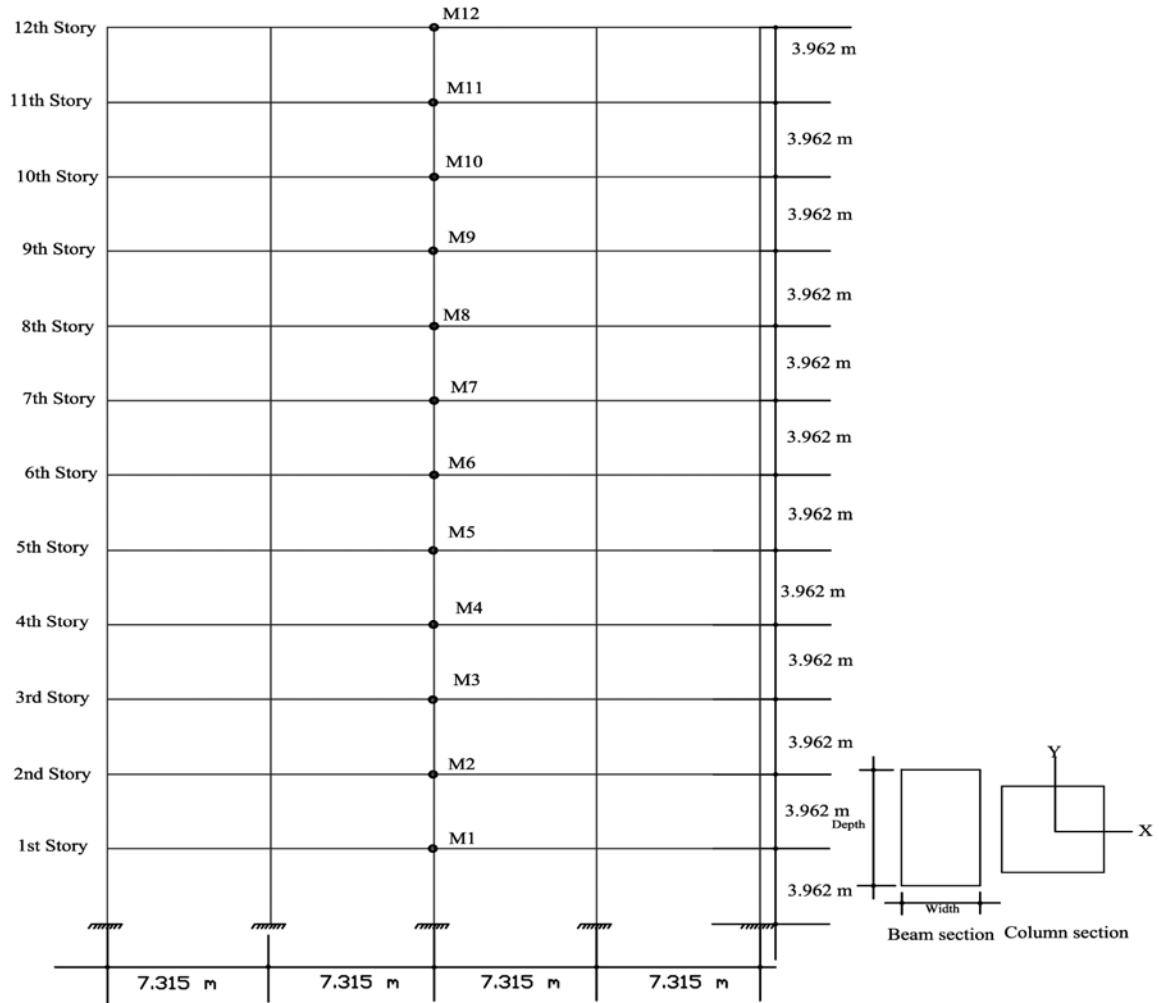


Fig. 3.6 Twelve story RC frame

Table 3.5 Cross Section and Loading properties of twelve story RC frame

Properties of beam

Story	Beam				Mass (t)	DL (kN/m)	LL (kN/m)
	Dimension (mm)		Reinforcement (sq mm)				
	Depth	Width	Top	Bottom			
1-3	1016	508.0	6625.79	6116.12	346.860	16.78	1.1
4-7	914.4	508.0	6625.79	6116.12	346.860	16.78	1.1
8-11	762.0	457.2	5096.76	4077.41	346.860	16.78	1.1
12	609.6	457.2	2038.71	1019.35	294.330	13.45	0.44

Properties of column

Story	Column	Dimension (mm)		Number of Bars		Bar Area (sq mm)
		X-dir	Y-dir	X-dir	Y-dir	
1-3	Exterior	1219.2	1219.2	12	12	509.7
	Interior	1524.0	1524.0	7	7	509.7
4-8	Exterior	1117.6	1117.6	8	8	509.7
	Interior	1447.8	1447.8	6	6	509.7
9-12	Exterior	1016.0	1016.0	7	7	509.7
	Interior	1270.0	609.6	5	5	509.7

Concrete and steel properties of 12-story RC frame

Property	Concrete	Steel
Ultimate strength (MPa)	27.6	459.2
Modulus of elasticity (MPa)	27792.8	

Table 3.6 Dynamic properties of twelve story RC frame

Modal properties	Mode		
	1	2	3
Period, T (sec)	1.610	0.574	0.310
Modal participation factor	1.398	0.615	0.372
Modal mass factor	0.730	0.130	0.052

3.4 Validation of pushover curve for 2D frame

Several types of output have been obtained from the static nonlinear analysis. Base reaction versus monitored displacement has been plotted. Tabulated values of base reaction versus monitored displacement at each point along the pushover curves, along with tabulations of the number of hinges beyond certain control points on their hinge property force displacement curve has been plotted in different figures. Base reaction versus monitored displacement has been plotted in figures. Pushover curves are obtained by performing pushover analyses using SAP2000 [21] and ETABS [20]. The base shear and story displacement data extracted from pushover analysis using SAP2000 [21], ETABS [20] are plotted in Fig. 3.7, 3.8 and 3.9. The base shear and story displacement data extracted from Oguz [13] which are superimposed in Figs. 3.7, 3.8 and 3.9. The superimposed pushover curves are same in elastic part but inelastic part is minor differences. The minor differences between

SAP2000 [21] and ETABS [20] can be attributed to assumption and simplification of modeling. From Fig.3.7, 3.8 and 3.9, it is seen that pushover curves are almost same. So it has been concluded that nonlinear pushover analysis using SAP2000 [21] and ETABS [20] are close to same with results of Oguz [13].

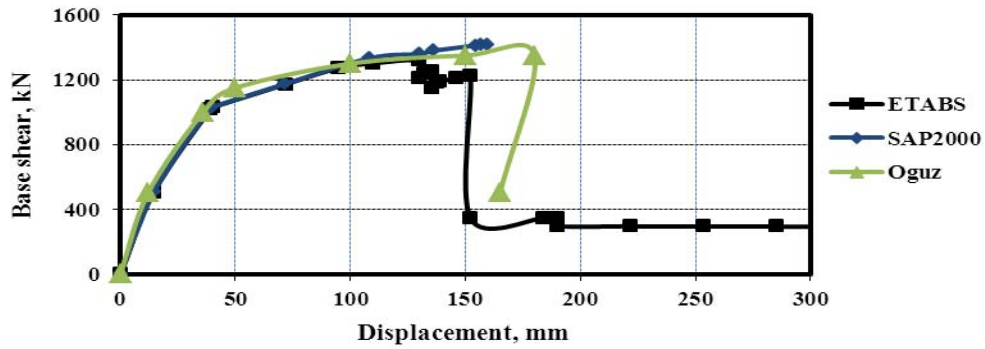


Fig. 3.7 Pushover curve for 2-story 2D frame

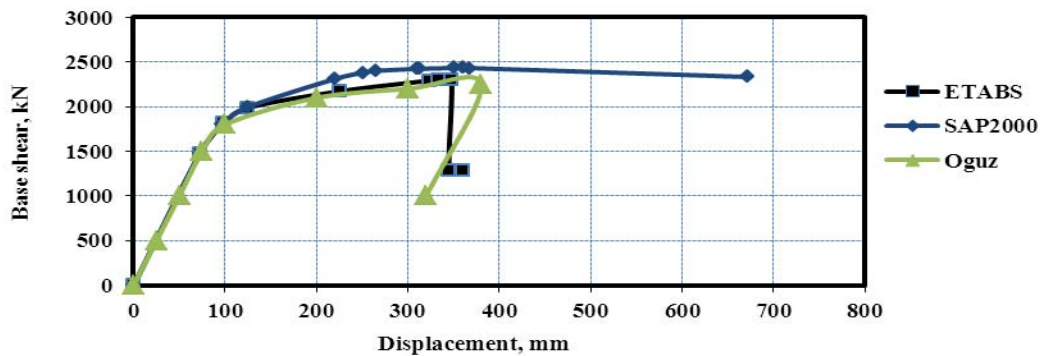


Fig. 3.8 Pushover curve of the 5-story 2D frame

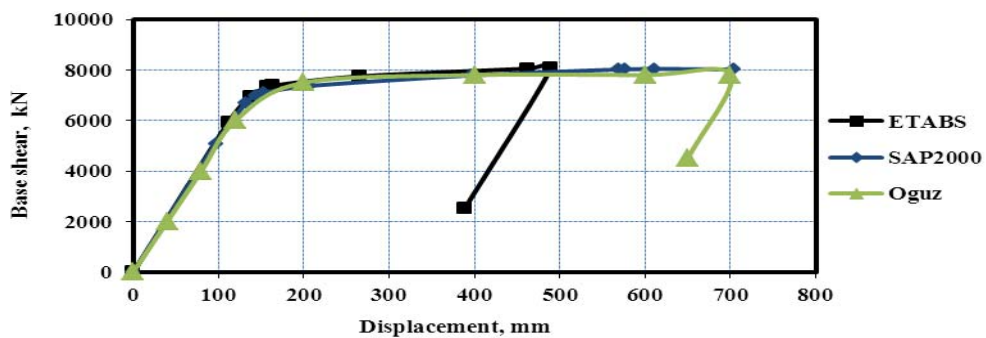


Fig. 3.9 Pushover curve of the 12-story 2D frame

3.5 Comparison of pushover curve for SAP2000 and SeismoStruct

3.5.1 Description of SeismoStruct

SeismoStruct [50] is a finite element package capable of predicting the large displacement behavior of space frames under static or dynamic loading, taking into account both geometric nonlinearities and material inelasticity. Concrete, steel material models are available, together with a large library of 3D elements that may be used with a wide variety of pre-defined steel, concrete and composite section configurations. With the wizard facility the user can create regular/irregular 2D or 3D models and run all types of analyses. The whole process takes no more than a few seconds. Seven different types of analysis are as follows, eigenvalue analysis, static analysis (non-variable load), static pushover analysis, static adaptive pushover analysis, static time history analysis, dynamic time history analysis, incremental dynamic analysis (IDA). conventional (non-adaptive) pushover analysis is frequently utilized to estimate the horizontal capacity of structures featuring a dynamic response that is not significantly affected by the levels of deformation incurred (i.e. the horizontal load pattern, which aims at simulating dynamic response, can be assumed as constant). In static time history analysis, the applied loads (displacement, forces or a combination of both) can vary independently in the pseudo time domain, according to a prescribed load pattern. Dynamic analysis is commonly used to predict the nonlinear inelastic response of a structure subjected to earthquake loading (evidently, linear elastic dynamic response can also be modeled for as long as elastic elements and/or low levels of input excitation are considered). The direct integration of the equations of motion is accomplished using the numerically dissipative integration algorithm, a special case of the former, the well-known Newmark scheme [39], with automatic time step adjustment for optimum accuracy and efficiency (see automatic adjustment of load increment or time step).

The applied loading may consist of constant or variable forces, displacements and accelerations at the nodes. The variable loads can vary proportionally or independently in the pseudo time or time domain. The program accounts for both material inelasticity and geometric nonlinearity. A large variety of reinforced concrete, steel and composite sections are available. In the pushover method the lateral load distribution is not kept constant but is continuously updated, according to the modal shapes and participation factors derived by eigenvalue analysis carried out at the current step. In this way, the stiffness state and the period elongation of the structure at each step, as well as higher mode effects, are accounted for. SeismoStruct possesses the ability to smartly subdivide the loading increment, whenever convergence problems arise. The level of subdivision depends on the

convergence difficulties encountered. When convergence difficulties are overcome, the program automatically increases the loading increment back to its original value. SeismoStruct's processor features real time plotting of displacement curves and deformed shape of the structure, together with the ability of pausing and restarting the analysis. Performance criteria can also be set, allowing the user to identify the instants at which different performance limit states (e.g. non structural damage, structural damage, collapse) are reached. The sequence of cracking, yielding, failure of members throughout the structure can also be, in this manner readily obtained.

Large displacements/rotations and large independent deformations relative to the frame element's chord (also known as P-Delta effects) are taken into account in SeismoStruct. Hence, in SeismoStruct, all analyses (with the obvious exception of eigenvalue procedures) are treated as potentially nonlinear, implying the use of an incremental iterative solution procedure whereby loads are applied in pre-defined increments, equilibrated through an iterative procedure.

Modeling of seismic action is achieved by introducing acceleration loading curves (accelerograms) at the supports, noting that different curves can be introduced at each support, thus allowing for representation of asynchronous ground excitation. In addition, dynamic analysis may also be employed for modeling of pulse loading cases (e.g. blast, impact, etc.), in which case instead of acceleration time histories at the supports, force pulse functions of any given shape (rectangular, triangular, parabolic, and so on), can be employed to describe the transient loading applied to the appropriate nodes. Currently, thirteen material types are available in SeismoStruct. By making use of these material types, the user is able to create an unlimited number of different materials, used to define the cross-sections of structural members. Materials that are to be available within a SeismoStruct project come defined in the materials module, where the name (used to identify the material within the project), type (listed above) and mechanical properties (i.e. strength, modulus of elasticity, strain-hardening, etc.) of each particular material can be defined. Currently, twenty one section types are available in SeismoStruct. These range from simple single material solid sections to more complex reinforced concrete and composite sections. By making use of these section types, the user is able to create up to 500 different cross sections, used to define the different element classes of a structural model. rectangular solid section, rectangular hollow section, circular solid section, circular hollow section, reinforced concrete rectangular section, reinforced concrete circular section etc.

The different elements of the structure are defined in the element connectivity module, where their name, element class and corresponding nodes are identified.

Constrain certain degrees of freedom of slave nodes to a master node, by means of a rigid link. In other words, the rotations of the slave node are equal to the rotations of the master node, whilst the translations of the former are computed assuming a rigid lever arm connection with the latter. Both master and slave nodes need to be defined for this constraint type, and the degrees of freedom to be slaved to the master node (restraining conditions) have to be assigned. The boundary conditions of a model are defined in the restraints module, where all structural nodes are listed and available for selection and restraining against deformation in any of the six degrees of freedom.

There are four load categories in SeismoStruct [50]. These can be applied to any structural model. These comprise all static loads that are permanently applied to the structure. They can be forces (e.g. self-weight) or prescribed displacements (e.g. foundation settlement) applied at nodes. When running an analysis, permanent loads are considered prior to any other type of load, and can be used on all analysis types, with the exception of Eigenvalue analysis, where no loading is present. Note that gravity loads should be applied downwards, for which reason they always feature a negative value.

3.5.2 Description of case study frames

The effects of lateral load patterns on global structural behavior and on the accuracy of pushover predictions are studied on 2-Storeyed and 5-Storeyed 2D reinforced concrete moment resisting frames. Two dimensional models of case study frames are prepared using SAP2000 [21] and SeismoStruct [50] by considering the necessary geometric and strength characteristics of all members that affect the nonlinear seismic response. The structural models are based on centre line dimensions that beams and columns span between the nodes at the intersections of beam and column centerlines and beam-column joints are not modeled. Rigid floor diaphragms are assigned at each story level and the seismic mass of the frames are lumped at the mass center of each story. The dynamic properties of the case study frame are summarized in Table 3.2. The configuration, member details and dynamic properties of case study frame is presented in Table 3.1-3.6. The description of frame is shown in Figs. 3.4, 3.5 and 3.6. Nonlinear member behavior of RC sections is modeled with SAP2000 [21] and SeismoStruct [50].

3.5.3 Analysis and results

Several types of output have been obtained from the static nonlinear analysis. Base reaction versus monitored displacement has been plotted. Tabulated values of base reaction versus monitored

displacement at each point along the pushover curve, force displacement curve have been plotted in Fig.3.13 and 3.14.

3.5.3.1 Two storied 2D frame

Pushover curves are obtained by performing pushover analyses using SeismoStruct [50] and SAP2000 [21] for 2-story 2D frame.. The base reaction is used for plotting the pushover curve. It is the resultant force reaction caused by the load pattern applied in the given static nonlinear case. Story displacements, story pushover curves for any lateral load pattern are extracted from the pushover analysis. The base shear and story displacement data extracted from pushover analysis using SeismoStruct [50] and SAP200 [21] are plotted in Fig. 3.10. The superimposed pushover curves are close to same. The superimposed pushover curves are same in elastic part but inelastic part is quite differences. The differences between SAP2000 [21] and SeismoStruct [50] can be attributed to different approach, assumption and simplification of modeling.

The pushover analyses using uniform lateral load pattern yielded capacity curves are higher than those of the triangular lateral load patterns, for 2-Storied 2D frames considered. This is expected because capacity curve is a function of the point of application of the resultant of lateral load as well as the nonlinear structural characteristics.

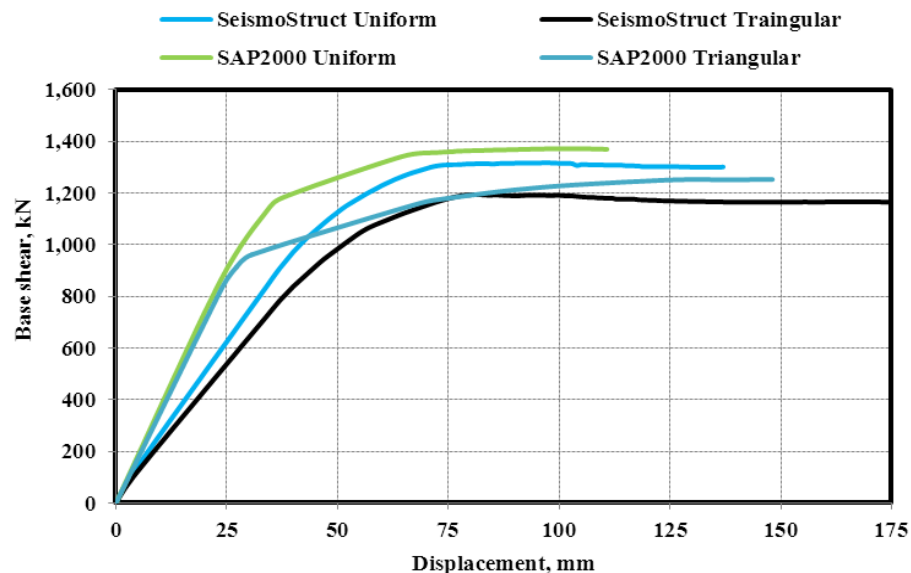


Fig. 3.10 Pushover curve of the 2-story 2D frame for different loading pattern

3.5.3.2 Five storied 2D frame

Pushover curves are obtained by performing pushover analyses using SeismoStruct [50] and SAP2000 [21] for 5-story 2D frame.. The base reaction is used for plotting the pushover curve. It is the resultant force reaction caused by the load pattern applied in the given static nonlinear case. Story displacements, story pushover curves for any lateral load pattern are extracted from the pushover analysis. The base shear and story displacement data extracted from pushover analysis using SeismoStruct [50] and SAP200 [21] are plotted in fig. 3.11. The superimposed pushover curves are almost same. The superimposed pushover curves are same in elastic part but inelastic part is minor differences. The minor differences between SAP2000 [21] and SeismoStruct [50] can be attributed to assumption and simplification of modeling.

The pushover analyses using 'uniform' lateral load pattern yielded capacity curves are higher than those of the triangular lateral load patterns, for 5-Storied 2D frames considered.

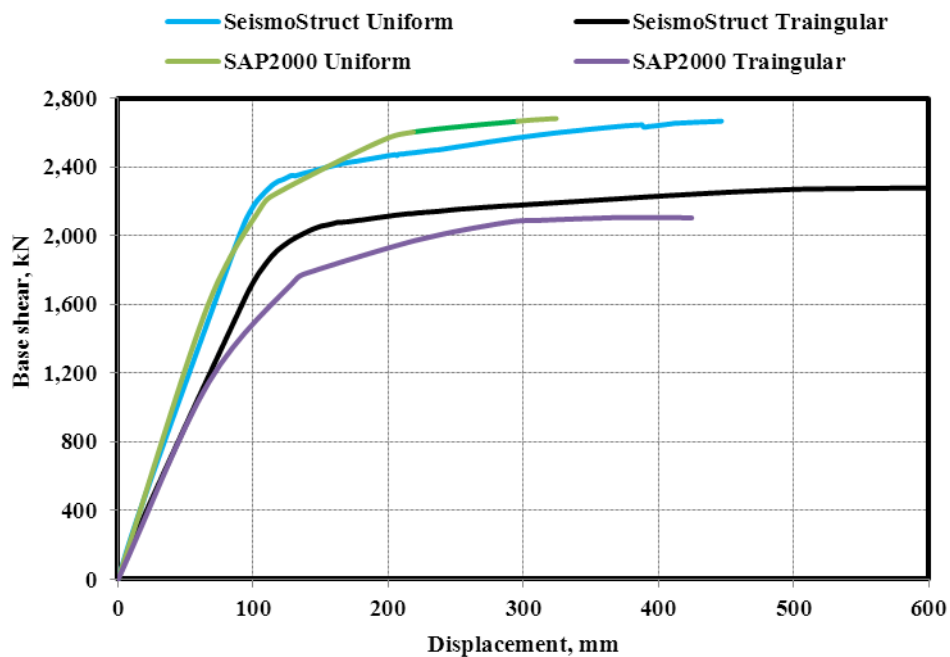


Fig. 3.11 Pushover curve of the 5-story 2D frame for different loading pattern

The results of the analyses for the two programs are superimposed on one plot of the base shear versus roof displacement shown in Fig 3.10 and 3.11. This figure demonstrates that the two responses are almost identical for 2D frame. The differences displayed in the plot have been attributed to errors caused by different approaches to modeling the beam and column elements.

Therefore it can be concluded that nonlinear pushover analysis using SAP2000 [21] and SeismoStruct [50] are almost same and identical. The pushover analyses using uniform lateral load

pattern capacity curves are higher than those of the triangular lateral load patterns for 2D frames with both software. The pushover analyses using 'Uniform' lateral load pattern capacity curves are more accurate with both softwares. Therefore, finally it is concluded that nonlinear pushover analysis run in SeismoStruct is valid and accurate.

3.6 Different loading pattern for pushover curve

The accuracy of invariant lateral load patterns utilized in pushover analysis to predict the behavior imposed on the structure due to nonlinear response are evaluated in this study. For this purpose, global structure behavior, story displacements, inter-story drift ratios, story shears and plastic hinge locations are selected as response parameters.

Pushover curves are obtained by performing pushover analyses using SAP2000 [21] and ETABS [20]. Story displacements, inter story drift ratios, story pushover curves and plastic hinge locations for any lateral load pattern are extracted from the pushover database at the predetermined maximum roof displacement consistent with the deformation level considered and are compared with absolute maximum values of exact response parameters obtained from nonlinear analysis.

Capacity curves (base shear versus roof displacement) are the load-displacement envelopes of the structures and represent the global response of the structures. Capacity curves for case study frames are obtained from the pushover analyses using lateral load patterns and are shown in Fig. 3.12-3.14

3.6.1 Two storied 2D frame

The pushover analyses using 'uniform' lateral load pattern yielded capacity curves are higher than those of the triangular lateral load patterns. This is expected because capacity curve is a function of the point of application of the resultant of lateral load as well as the nonlinear structural characteristics.

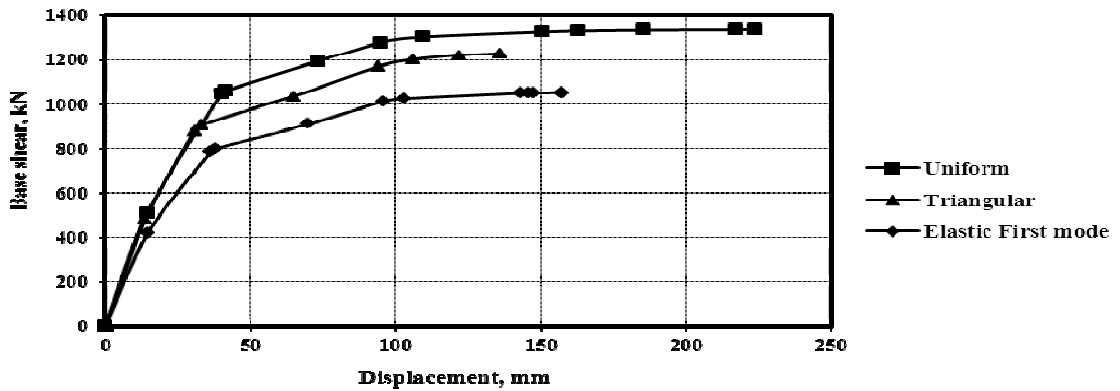


Fig. 3.12 Pushover curve of the 2-story 2D frame for different loading pattern

3.6.2 Five storied 2D frame

The pushover analyses using 'uniform' lateral load pattern yielded capacity curves are higher than those of the triangular lateral load patterns, 'elastic first mode' for 5-storied 2D frames considered. This is expected because capacity curve is a function of the point of application of the resultant of lateral load as well as the nonlinear structural characteristics.

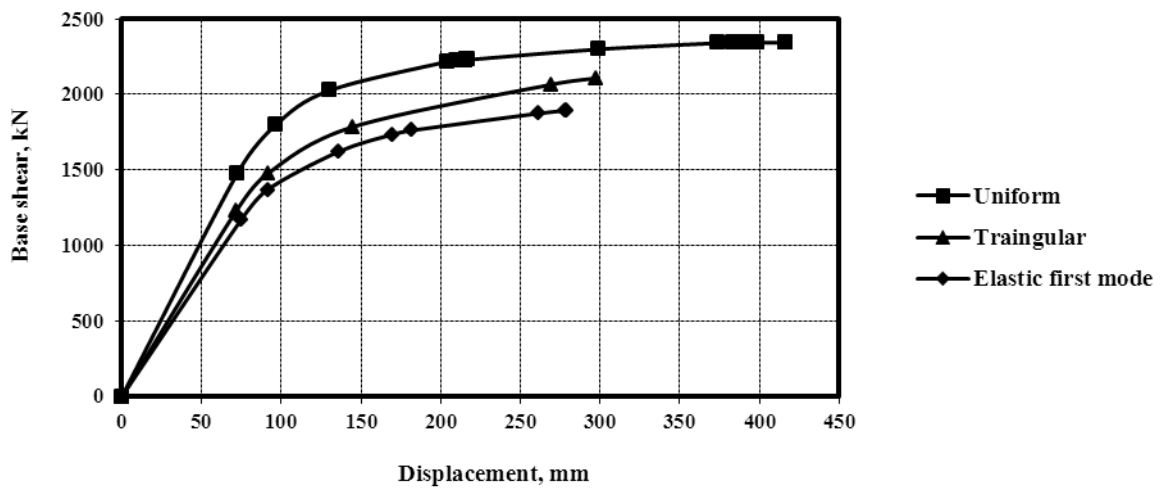


Fig. 3.13 Pushover curve of the 5-story 2D frame for different loading pattern

3.6.3 Twelve storied 2D frame

The pushover analyses using 'uniform' lateral load pattern yielded capacity curves are higher than those of the triangular lateral load patterns, 'elastic first mode' for 12-storied 2D frames considered.

This is expected because capacity curve is a function of the point of application of the resultant of lateral load as well as the nonlinear structural characteristics.

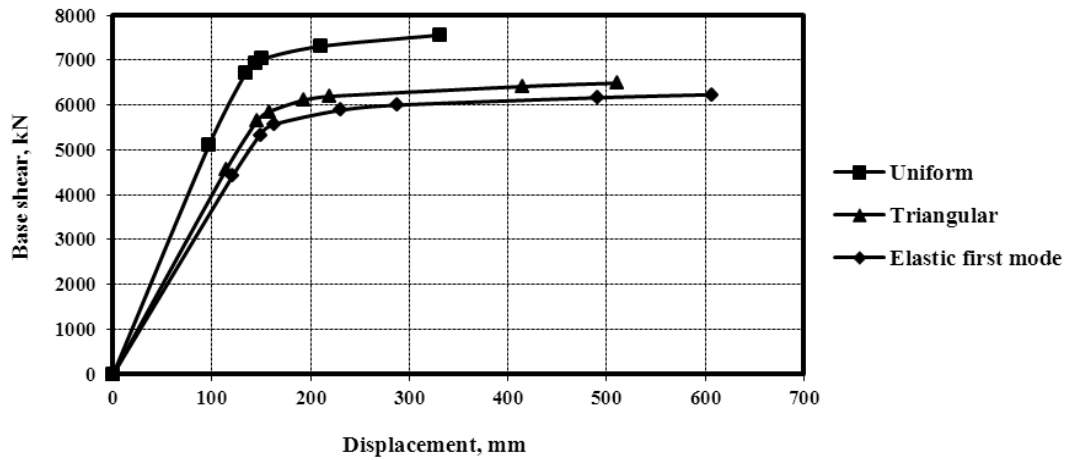


Fig. 3.14 Pushover curve of the 12-story 2D frame for different loading pattern

3.7 Performance evaluation of structure

In this section two reinforced concrete frames 2 and 5 storied 2D frames are modeled. These frames are designed as per the provisions of BNBC [1]. Considering live load 29.19kN/m² and dead load 58.38kN/m² is used floor level. Selfweight of the concrete members are considering unit weight of concrete as 23.56kN/m³. As per BNBC seismic modification factor R=8 (IMRF) has been considered. Performance point of any structure demand curve is required and demand curve can be generated with SAP2000 [21]. But several parameters are required to generate the curves. In this section, those parameters are defined and demand curve is plotted by SAP2000 [21]. The absolute maximum values of roof displacements and base shear are determined for each deformation level to approximate a dynamic capacity curve for the frames. The performance point is determined for serviceability earthquake (SE), design earthquake (DE) and maximum earthquake (ME).

Both the capacity curve and the demand curve are plotted here in the same plotted area in ADRS format. The performance point in spectral acceleration versus spectral displacement coordinates. The effective period and effective damping at the performance point. The shape of the demand spectrum with 5% damping is controlled by the values input in the seismic coefficient C_A and C_V . The parameters are determined as follows.

Establishment demand spectra:

Location of the site: Dhaka city

Soil profile at the site: Soil type S_C as per Table 2.5 when the soil properties are not known in sufficient detail.

Earthquake source type: C, Near Source factor: >15 Km

Table 3.7 Calculation of C_A

Seismic Zone Factor, Z	0.15	As per BNBC/93	0.15	As per BNBC/93	0.15	As per BNBC/93
Earthquake Hazard Level, E	0.5	Design Earthquake	1	Max Earthquake	0.35	Serviceability Earthquake
Factored E (E'X1.4)	0.7		1.4		0.49	
Near-Source Factor	1	>15km, table 2.4	1	>15km, table 2.4	1	>15km, table 2.4
Shaking Intensity, ZEN	0.105		0.21		0.0735	
For Soil Type S_C, C_A	0.126	From Table 2.5	0.249	From Table 2.5	0.088	From Table 2.5

Table 3.8 Calculation of C_V

Seismic Zone Factor, Z	0.15	As per BNBC	0.15	As per BNBC	0.15	As per BNBC
Earthquake Hazard Level, E	0.5	Design Earthquake	1	Max Earthquake	0.35	Serviceability Earthquake
Factored E (E'X1.4)	0.7		1.4		0.49	
Near-Source Factor	1	>15km, table 2.4	1	>15km, table 2.4	1	>15km, table 2.4
Shaking Intensity, ZEN	0.105		0.21		0.0735	
For Soil Type S_C, C_V	0.178	From Table 2.6	0.333	From Table 2.6	0.128	From Table 2.6

3.7.1 Two story 2D frame

From Fig 3.15 it is seen that at the performance point for Procedure A, spectral displacement is 9.40mm and spectral acceleration is 0.22g for SE, spectral displacement is 13.47mm and spectral acceleration is 0.317g for DE and spectral displacement is 24.0mm and spectral acceleration is 0.37g for ME. From Fig 3.16 it is seen that at the performance point for Procedure B, spectral displacement is 9.34mm and spectral acceleration is 0.22g for SE. From Fig 3.17 it is seen that at the performance point spectral displacement is 13.374mm and spectral acceleration is 0.315g for DE. From Fig 3.18 it is seen that at the performance point spectral displacement is 23.84mm and spectral acceleration is 0.377g for ME.

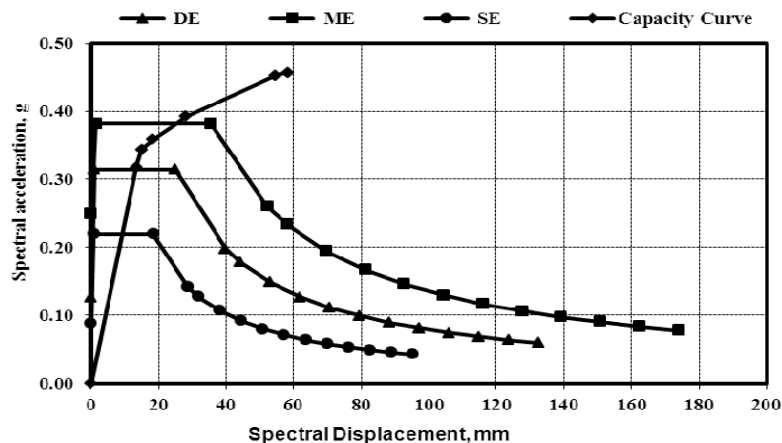


Fig. 3.15 Capacity spectrum of the 2-story 2D frame (Procedure A)

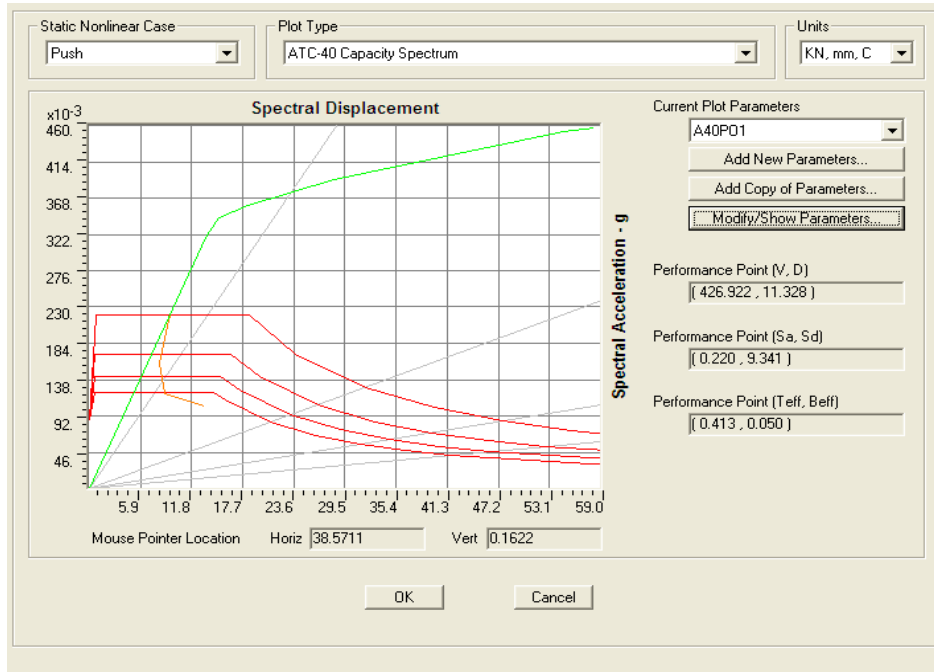


Fig. 3.16 Capacity spectrum of the 2-story frame for SE (Procedure B)

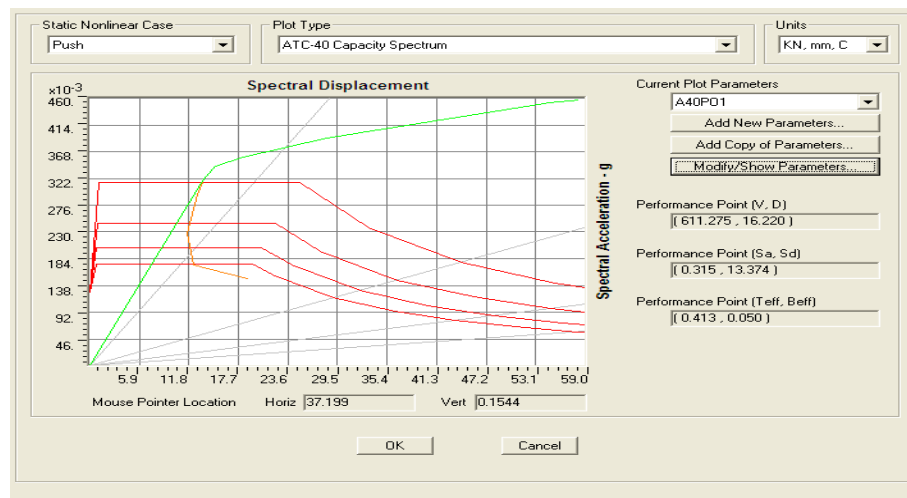


Fig. 3.17 Capacity spectrum of the 2-story frame for DE (Procedure B)

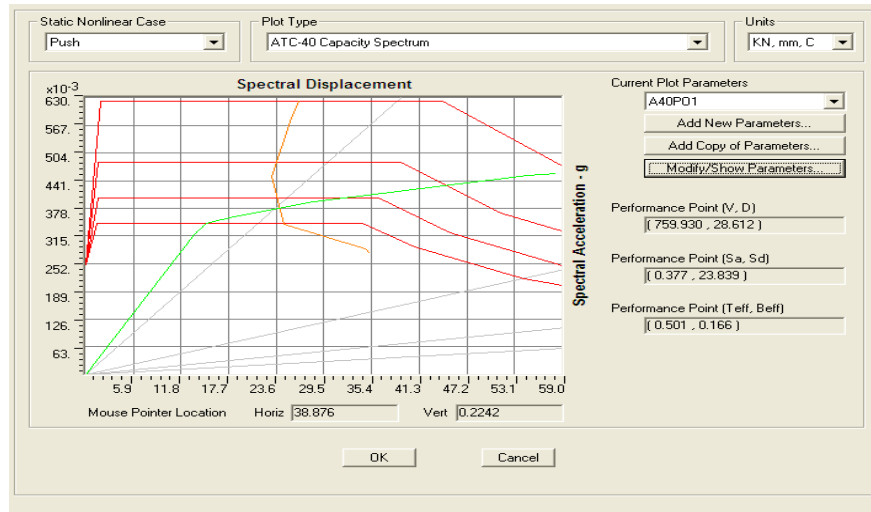


Fig. 3.18 Capacity spectrum of the 2-story frame for ME (Procedure B)

From Procedure A (Fig.3.15) and Procedure B (Figs.3.16 to 3.18), it has seen that performance point spectral displacement and spectral acceleration are close to same. So it has been concluded that capacity spectrum of 2-story frame is close to same for Procedure A and B.

3.7.1.1 Local level performance

The observations have been made from the comparison of plastic hinge locations determined by pushover analyses. Plastic hinges obtained from pushover analyses are generally different for each frame. Hinge curve for 2-Story frame is shown in Figs.3.19 to 3.21. From these Figures at performance point, hinges are in the range of B-IO. For three level of earthquake, no hinge is found to cross the Immediate Occupancy (IO) limits. According ATC-40[3], 2-story frame satisfies local criteria. Therefore it has been said that 2-story frame structure fulfills the performances at local level for serviceability earthquake, design and maximum earthquake.

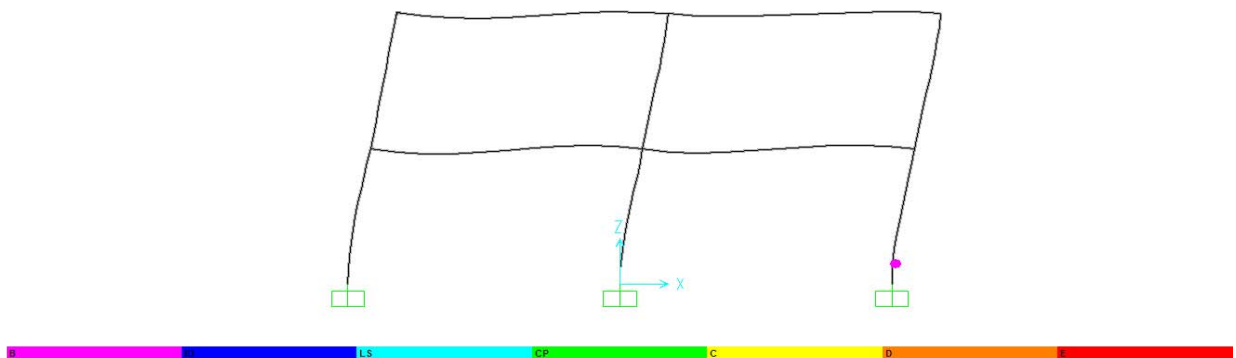


Fig. 3.19 Deformation of the 2-story frame at SE level

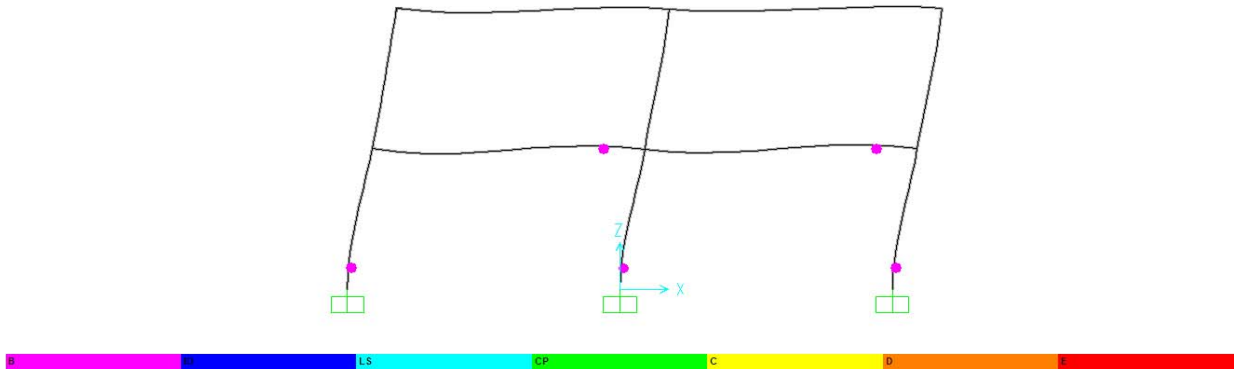


Fig. 3.20 Deformation of the 2-story frame at DE level

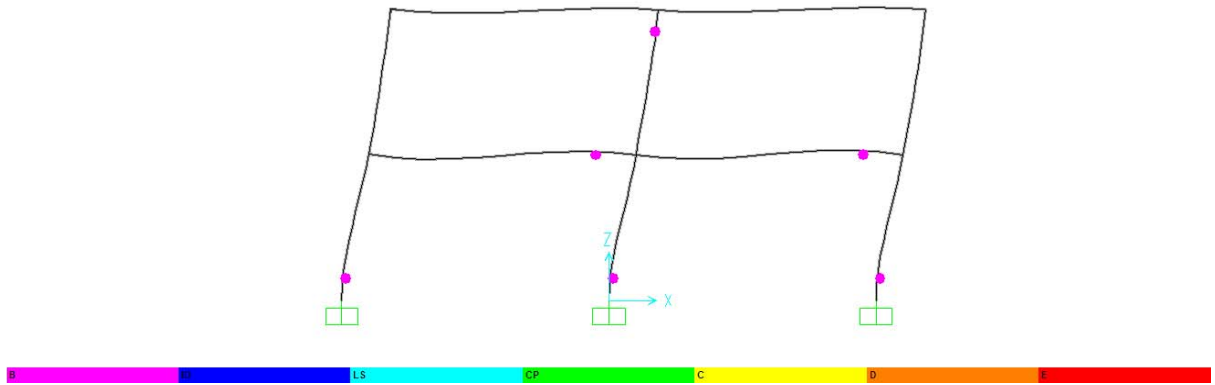


Fig. 3.21 Deformation of the 2-story frame at ME level

3.7.1.2 Global level performance

From the Fig. 3.22, it is seen that the performance point of structure has maximum story drift of 0.0046 at story level 2 for 2-story frame. This is less than allowable IO level 0.01 described in ATC 40[3]. This structure satisfies the requirement of ATC 40[3]. Therefore it has been said that the structure fulfills the performance objective at global level for serviceability earthquake (SE), design earthquake (DE) and maximum earth quake (ME).

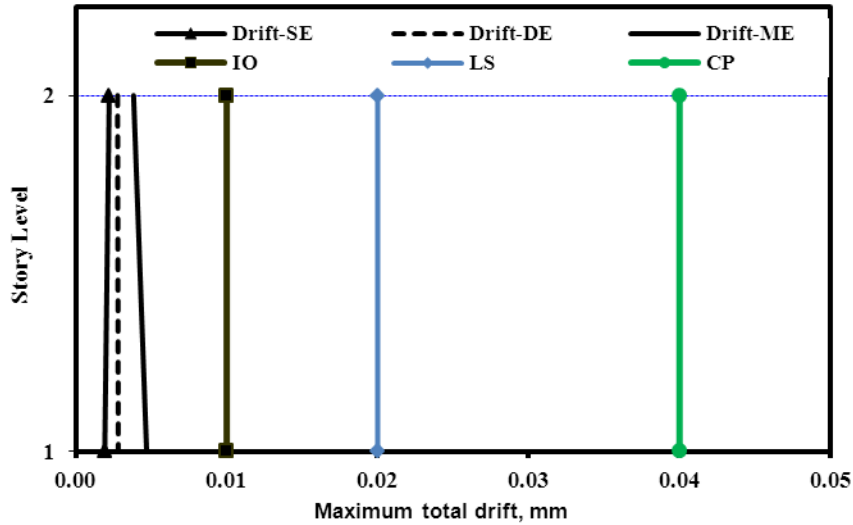


Fig. 3.22 Story drift ratio at performance point of 2-Story 2D frame for different earthquake level

Note: IO=Immediate Occupancy, LS= Life Safety, CP= Collapse Prevention

3.7.2 Five story 2D frame

From Fig. 3.23 it is seen that at the performance point for Procedure A, spectral displacement is 24.0mm and spectral acceleration is 0.14g for SE, spectral displacement is 34.0mm and spectral acceleration is 0.173g for DE and spectral displacement is 61.0mm and spectral acceleration is 0.24g for ME, . From Fig 3.24 it is seen that at the performance point for Procedure B, spectral displacement is 24.73mm and spectral acceleration is 0.141g for SE. From Fig 3.25 it is seen that at the performance point spectral displacement is 33.95mm and spectral acceleration is 0.174g for DE. From Fig 3.26 it is seen that at the performance point spectral displacement is 61.22mm and spectral acceleration is 0.243g for ME.

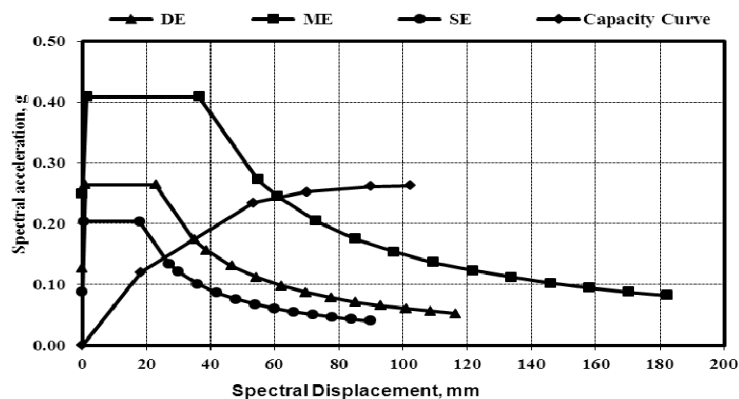


Fig. 3.23 Capacity spectrum of the 5-story 2D frame (Procedure A)

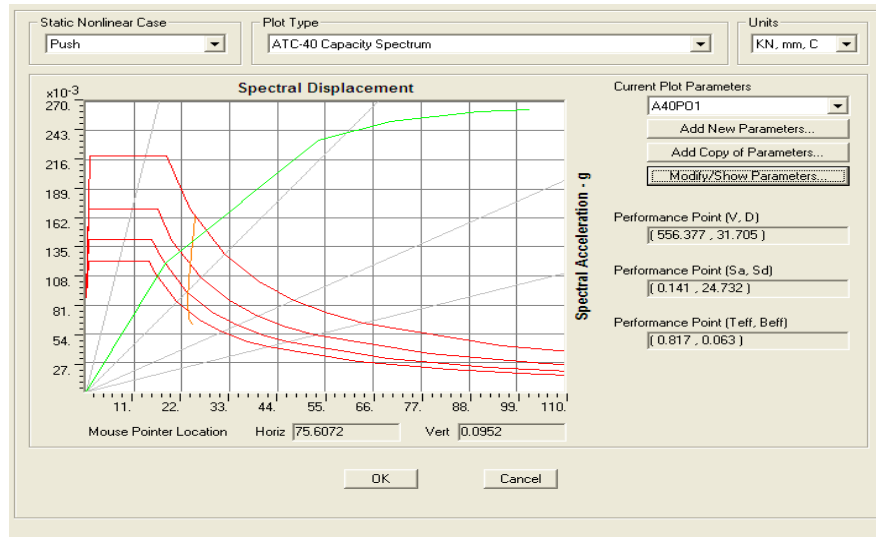


Fig. 3.24 Capacity spectrum of the 5-story frame for SE (Procedure B)

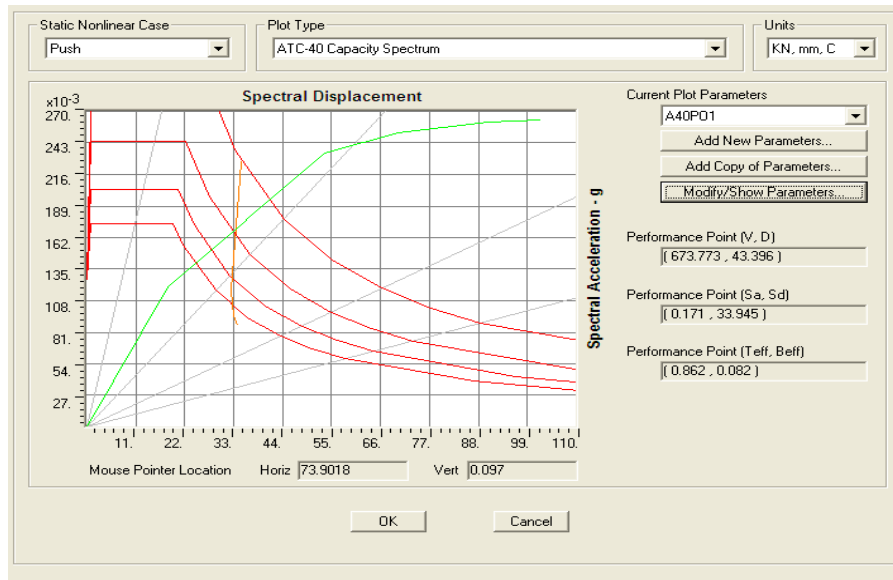


Fig. 3.25 Capacity spectrum of the 5-story frame for DE (Procedure B)

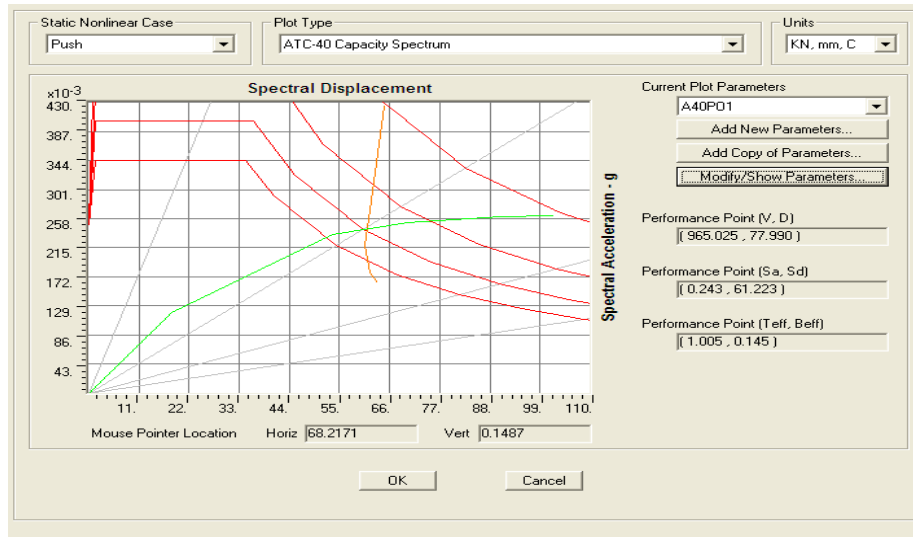


Fig. 3.26 Capacity spectrum of the 5-story frame for ME (Procedure B)

From Procedure A (Fig.3.23) and Procedure B (Figs.3.24to 3.26), it has seen that performance point spectral displacement and spectral acceleration are close to same. So it has been concluded that capacity spectrum of 5-story frame is close to same for Procedure A and B.

3.7.2.1 Local level performance

The observations have been made from the comparison of plastic hinge locations determined by pushover analyses. Plastic hinges obtained from pushover analyses are generally different for each frame. Hinge curve for 5-Story frame is shown in Figs.3.27 to 3.29. From these Figures at performance point, hinges are in the range of B-IO. For three level of earthquake, no hinge is found to cross the Immediate Occupancy (IO) limits. According ATC-40[3], 5-story frame satisfies local criteria. Therefore it has been said that 5-story frame structure fulfills the performance at local level for serviceability, design and maximum earthquake.

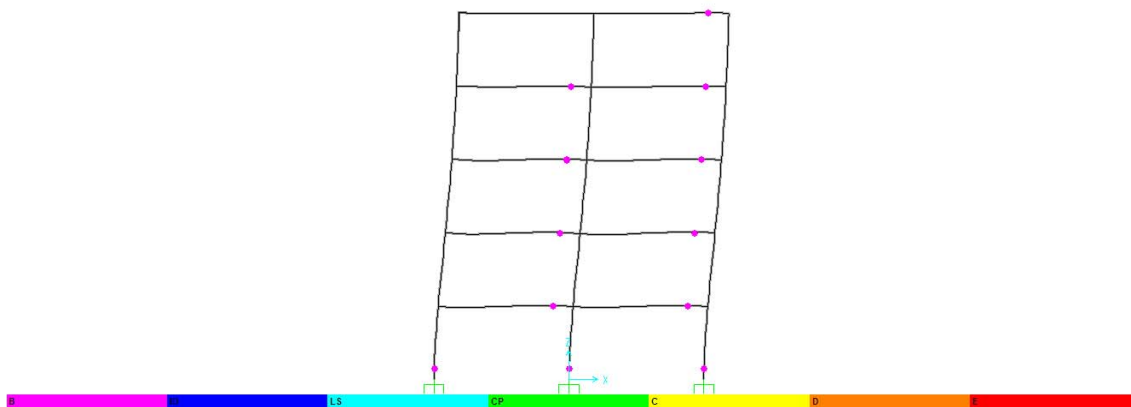


Fig. 3.27 Deformation of the 5-story frame at SE level

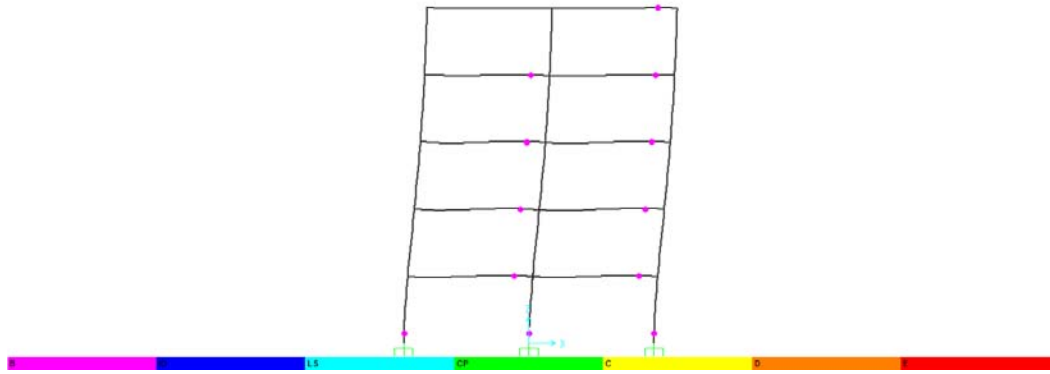


Fig. 3.28 Deformation of the 5-story frame at DE level

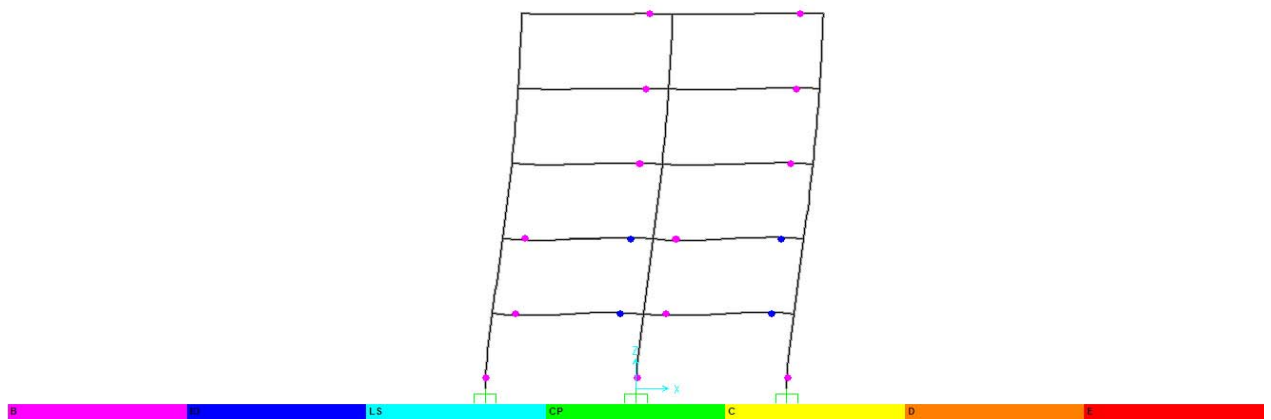


Fig. 3.29 Deformation of the 5-story frame at ME level

3.7.2.2 Global level performance

From the Fig. 3.30, it is seen that the performance point of structure has maximum story drift ratio is 0.006219 for ME at story level 2 for 5-story level. This is less than allowable IO level 0.01 described in ATC 40[3]. So this structure satisfies the requirement of ATC 40[3]. Therefore it has been said that the structure fulfills the performance objective at global level for serviceability earthquake (SE), design earthquake (DE) and maximum earth quake (ME).

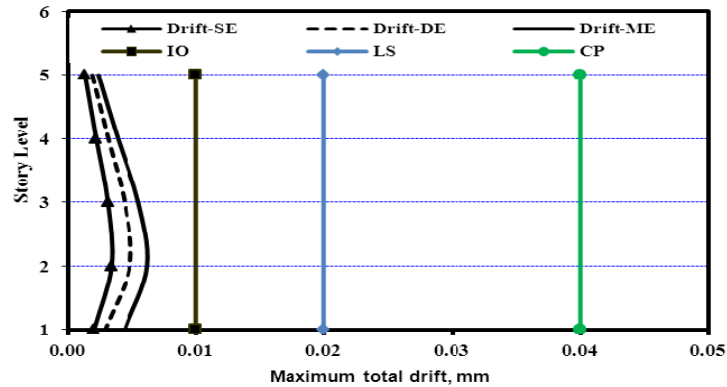


Fig. 3.30 Story drift ratio at performance point of 5-Story 2D frame for different earthquake level

Note: IO=Immediate Occupancy, LS= Life Safety, CP= Collapse Prevention

3.8 Conclusion:

This chapter presented the process of performance based analysis and the way by which the results can be used to predict local and global performance of structure for serviceability, design and maximum earthquakes. SAP2000, ETABS and SeismoStruct softwares have been used in tandem to observe the effect of load pattern on capacity curves. Validation of the simplified nonlinear static analysis i.e. pushover analysis has been confirmed by comparison the capacity curves of 2D frames with published numerical results of Oguz [13]. Building frames design as per the provisions of BNBC has been modeled in SAP2000 to investigate their performances and they have been found to satisfy the local and global performance criteria as per ATC-40 quite easily for three levels of earthquakes. ATC-40 contains two methods of demand evaluation namely Procedure A and Procedure B. ETABS and SAP2000 software include Procedure B in determining the demand. An Excel has been developed incorporating the ATC-40 Procedure A method. The results show that both Procedures A and B yield comparable demand in terms of spectral acceleration and spectral displacement for the 2D frames analyzed.

Chapter 4

Time history analysis

4.1 Introduction

In chapter 3, pushover analysis has been used to check the performance of different RC frames. Nonlinear time history analysis is a more rigorous method of modeling response of a structure and can also be used to determine the performance of structure due to seismic force. The pushover analysis may be more convenient than the nonlinear time history analysis because of computational time. The results shown previous chapter analysis took minutes with the pushover analysis and several hours with the nonlinear time history analysis. For this reason pushover analysis is more practical for use in the design office. But nonlinear time history analysis is more accurate in predicting the building performance than the pushover analysis.

The nonlinear response of structures is very sensitive to the structural modeling and ground motion characteristics. Therefore, two ground motion records that accounts for uncertainties and differences in severity, frequency and duration characteristics has been used to predict the possible deformation modes of the structures for seismic performance evaluation purposes. However, for simplicity, seismic demand prediction is generally performed by pushover analysis which mostly utilizes smoothed response spectra. In this chapter, the accuracy of capacity prediction using pushover analyses for various invariant lateral load patterns is evaluated in comparison with time history capacity obtained using selected ground motion excitations.

In this chapter, the response of case study frames are studied in the elastic and inelastic deformation levels that are represented by peak roof displacements on the capacity (pushover) curve of the frames. For each frame, the ground motion record is gradually scaled to obtain the peak roof displacement versus base shear curve which is comparable to the capacity curve of pushover analysis as shown in Chapter 3. Nonlinear time history analyses are performed by using SAP2000 [21] for the scaled ground motion and maximum absolute values of response parameters such as story displacements, inter-story drift ratios and story shears are determined for each ground motion record. Plastic hinge locations are also identified in nonlinear time history analyses.

4.2 Time history analysis using selected earthquakes

Time history analysis means either an elastic or inelastic dynamic analysis of a structure represented by a mathematical model through applying ground motion acceleration at its base level. The time dependent dynamic response of the structure will be obtained through numerical integration of its equation of motion. Time history analysis has been performed with appropriate horizontal ground-motion time history components that has been selected and scaled from different recorded events. Appropriate time histories have magnitude, fault distance and source mechanism that are consistent with those that control the design basis earthquake. Time history analysis can be of two types, namely elastic time history analysis and nonlinear time history analysis. Nonlinear as well as linear time histories analyses have been carried out and response of RC frames have been obtained for two appropriate ground motions.

The behavior of RC under dynamic loading is not linear when the deformation is large and load is time dependent. The use of linearly elastic analysis procedure is not sufficient to capture the real behavior in such cases. In fact there are some situations where the use of such simplified analyses can be misleading and missing in important details. The material and geometric properties which are considered constant in linear analysis do not remain constant in many practical situations. For example severe earthquake vibrations may cause quite large structural deformations and as a result alter the stiffness properties significantly. Moreover, member properties like mass or damping may undergo changes during the dynamic response, while stiffness properties may vary significantly due to the material and geometric nonlinearities caused by significant axial forces. Modal analysis is a commonly used method of linear dynamic analysis, but is not valid for nonlinear systems. The incremental numerical scheme needs to be applied for the dynamic analysis of nonlinear systems like reinforced concrete structures.

During the last 150 years, seven major earthquakes (with $M > 7.0$) have affected the zone that is now within the geographical borders of Bangladesh. Out of these, three had epicenters within Bangladesh. However, well define peaks and segmented data not available for the country. Earthquake data, especially earthquake induced forces are required for the purpose of structural design, city planning and infrastructure development. From the geological study it is evident that the intensity of earthquake hazard is not same throughout Bangladesh. So the

whole country was divided in the national building code BNBC [1] into three seismic zones; i.e., Zone1, 2 and 3.

Due to unavailability of seismic records, well-recorded available ground motions of El Centro (Imperial Valley, 18 May 1940, NS component) and Kobe earthquake have been selected for the current study. Figures 4.1 and 4.2 show the ground accelerations recorded during some of the best known and widely studied earthquakes of the 20th century. Nonlinear time history analysis of 2, 5 and 12-storied frames are performed by subjecting them to recorded ground motions of El Centro (with ground acceleration ‘zone’ factor $Z = 0.31$) and Kobe earthquake ($Z = 0.55$) using appropriate scaling.

4.2.1 El Centro 1940 Earthquake

The ground motion records used in this study include El Centro (Imperial Valley, 18 May 1940, NS component) earthquake. The N-S component (Peknold Version) recorded at a site in El Centro, California during the Imperial Valley earthquake on 18 May 1940, has become a popular point of reference for dynamic analyses (Han and Billington, 2004; Hueste and Wight, 1999; Liang and Parra-Montesinos 2004; Madan et al. 1997; Chopra, 2003[5]; Ahmed, 1998; and so on). Many versions of this ground motion have been processed from the recorded data. The version from Natural Center for Earthquake Engineering Research (NCEER) is selected for this study. The peak ground accelerations (PGAs) of the selected ground motions is 0.31882g and magnitude is 7.1. The duration of the acceleration time history utilized in this study is 31.18s which is quite long, so provides clear picture of different responses and peaks are also well defined and segmented, which is unique. Detail study of the frames responses are carried out for El Centro 1940 earthquake and presented in this chapter.

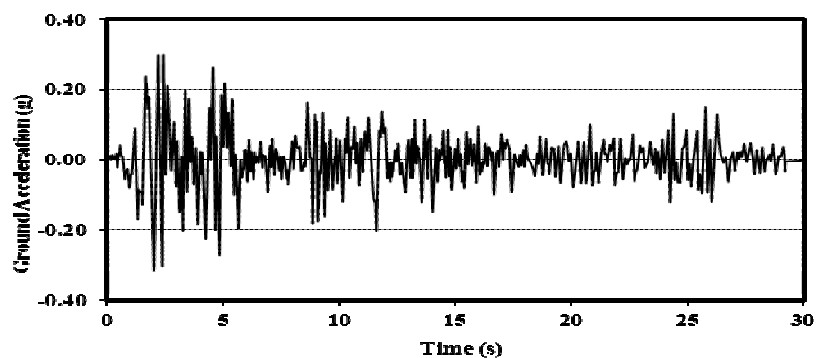


Fig. 4.1 Ground acceleration of El Centro, 1940 earthquake record (N-S), adopted from Chopra [5]

4.2.2 Kobe Earthquake

Time acceleration data of the Kobe earthquake ground motions has also been used to analyze RC plane frames for time history analysis. The peak ground acceleration (PGA) of the selected ground motion is 0.55g. The duration of the acceleration time history utilized in this study is 40.95sec. Figure 4.2 shows the ground acceleration from the Kobe (1995) earthquake, which had caused major destructions in Japan, which is among the ‘best prepared countries’ against earthquake disaster.

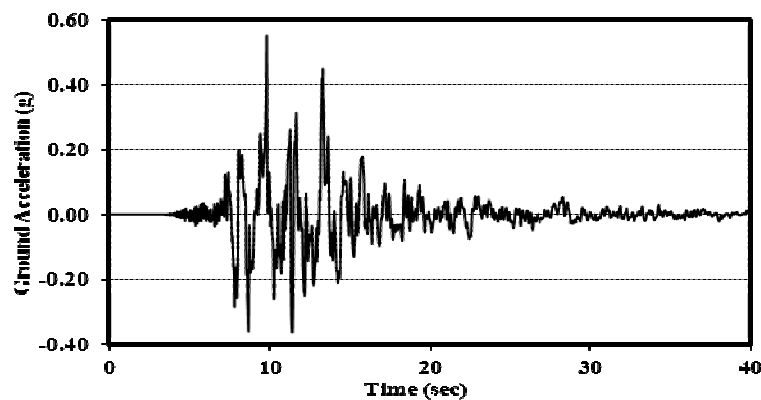


Fig. 4.2 Ground acceleration of Kobe Earthquake

4.3 Validation of linear time history analysis for SDOF system

In this chapter, the response of linear SDOF systems due to earthquake motion has been studied. By definition linear systems are elastic systems and it is also referred as linearly elastic systems to emphasize both properties.

4.3.1 Description of SDOF model

SDOF models of target time periods have suitably been developed by selecting stiffness and mass. To obtain a time period of $T=1.0$ sec, a 12 ft long vertical cantilever with a 4 inch nominal diameter standard steel pipe and supporting a 5200 lbs weight attached at the tip is chosen and is shown in Fig.4.3. The properties of the pipe are: Outside diameter= 4.50 inch, Inside diameter = 4.026 inch, thickness = 0.237 inch and second moment of cross sectional area, $I = 7.23 \text{ in}^4$, elastic modulus $E = 29000 \text{ ksi}$. El Centro ground motion data has been used in the analysis to determine the response of the SDOF system.

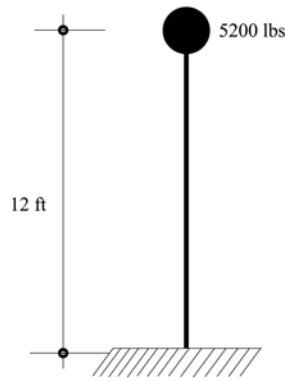


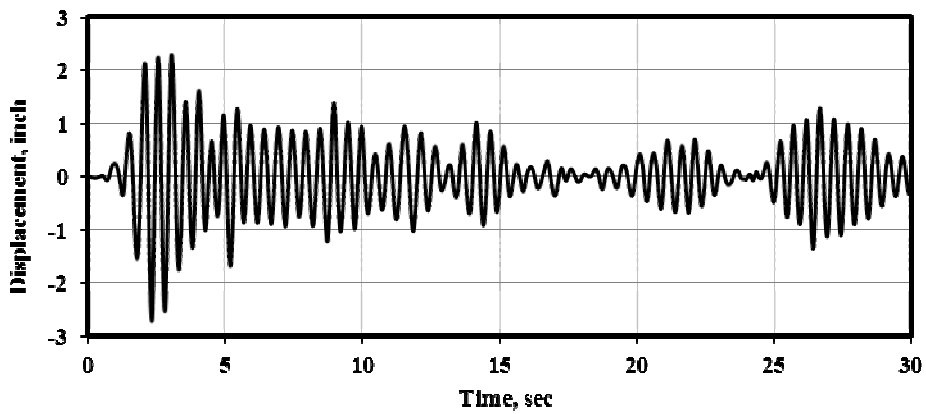
Fig.4.3 SDOF Model

4.3.2 Analysis and Result

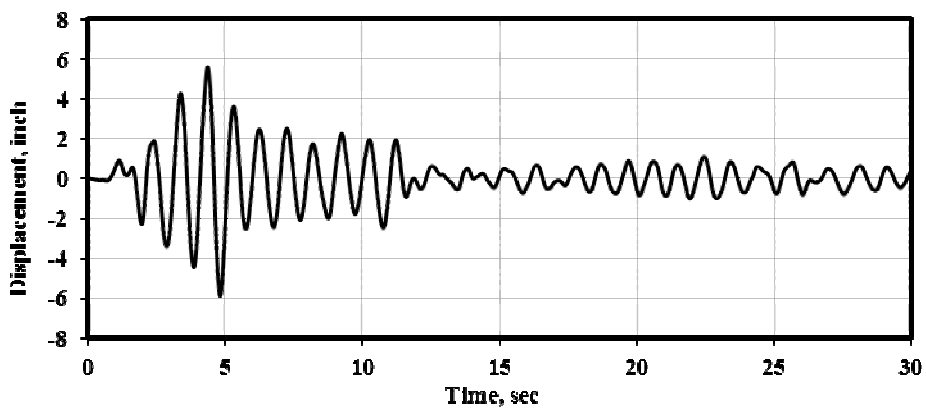
For a given ground motion (El Centro ground motion), the deformation response of an SDOF system depends only on the natural vibration period of the system and its damping ratio. Fig.4.4 shows the deformation response of three different systems due to El Centro ground acceleration. The damping ratio, $\xi=2\%$ is the same for the three systems, so that only the differences in their natural periods are responsible for the large differences in the deformation responses. The damping ratio is the same for the three systems to the same ground motion. It is observed the expected trend that systems with more period respond more deformation. From Fig. 4.4(a) time period $T_n=0.5$ sec and $\xi=2\%$, $d = 2.67$ inch, Fig. 4.4(b) time period $T_n= 1$ sec and $\xi= 2\%$, $d= 5.88$ inch, Fig. 4.4(c) time period $T_n= 2$ sec and $\xi= 2\%$, $d= 7.53$ inch. Fig.4.5 shows these three systems, the longer the vibration period, the greater the peak deformation. It is seen that the expected trend that systems with more damping respond less deformation. From Fig. 4.5(a) time period $T_n =2$ sec and $\xi=0\%$, $d = 9.95$ inch, Fig. 4.5(b) time period $T_n= 2$ sec and $\xi= 2\%$, $d= 7.53$ inch, Fig. 4.5(c) time period $T_n= 2$ sec and $\xi= 5\%$, $d= 5.47$ inch. The comparison of the peak deformations are shown in Table 4.1

Table 4.1 Comparison time history analyses with ETABS of SDOF system and published result from Chopra

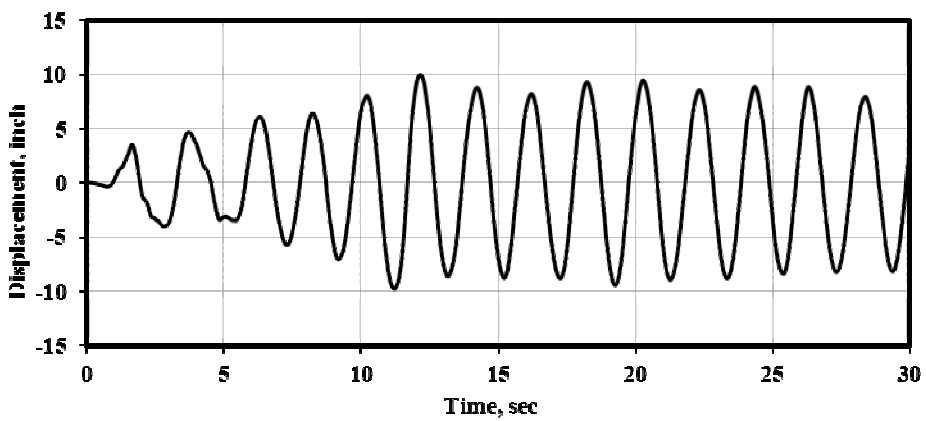
As per Chopra			As per Analysis		
Tn (sec)	Damping ratio	Displacement(in)	Tn (sec)	Damping ratio	Displacement(in)
0.50	0.02	2.67	0.50	0.02	2.69750
1.00	0.02	5.97	1.00	0.02	5.88290
2.00	0.02	7.47	2.00	0.02	7.53498
2.00	0.00	9.91	2.00	0.00	9.95299
2.00	0.02	7.47	2.00	0.02	7.53498
2.00	0.05	5.37	2.00	0.05	5.47091



(a) $T_n = 0.5$ sec, $\xi = 2\%$

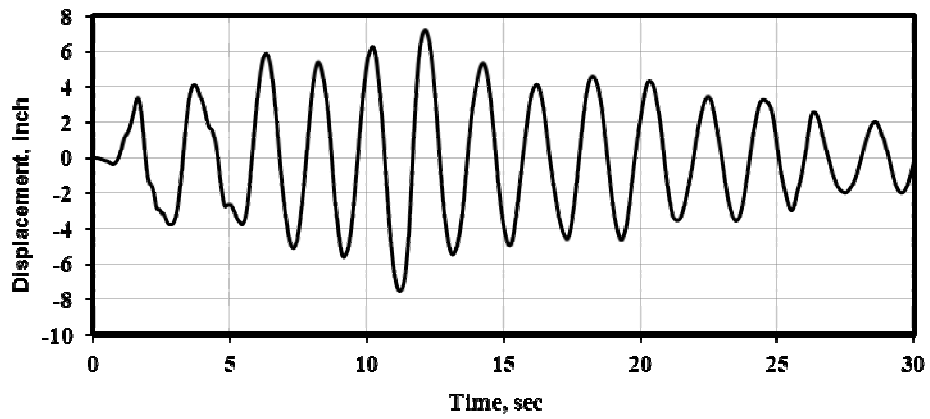


(b) $T_n = 1$ sec, $\xi = 2\%$

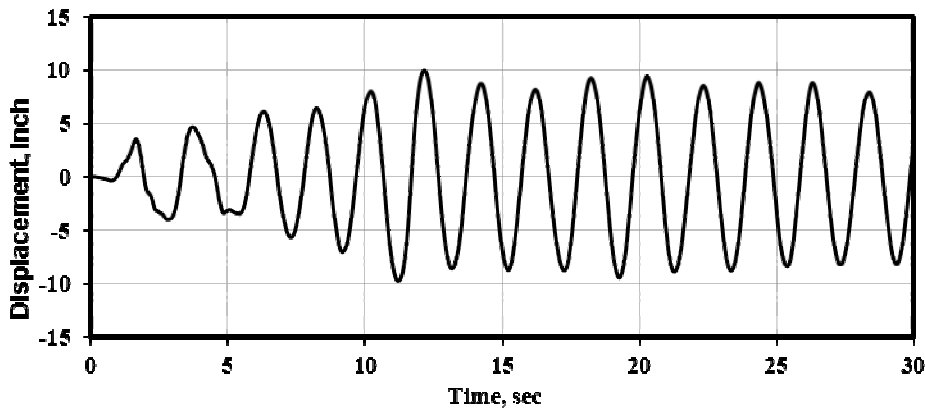


(c) $T_n = 2$ sec, $\xi = 2\%$

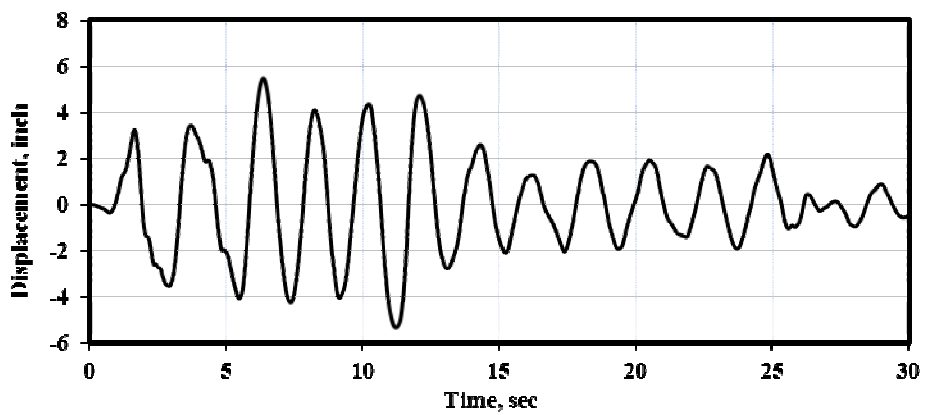
Fig. 4.4 Time history analysis of SDOF system for El Centro ground motion



(a) $T_n = 2$ sec, $\xi = 0\%$



(b) $T_n = 2$ sec, $\xi = 2\%$



(c) $T_n = 2$ sec, $\xi = 5\%$

Fig. 4.5 Time history analysis of SDOF system to El Centro ground motion

Based on the above presented results, it is concluded that deformation responses of the modeled of SDOF system under El Centro ground motion are very close to the published responses of Chopra [5] and thus confirms the validity of the linear time history analysis.

4.4 Nonlinear Time History Analysis

Time history analysis means an elastic or inelastic dynamic analysis of a structure represented by a mathematical model through applying a ground motion time history at its base or any other appropriate level. The time dependent dynamic response of the structure shall be obtained through numerical integration of its equation of motion. Time history analysis shall be performed with appropriate horizontal ground motion time history components that shall be selected and scaled from two recorded events. Appropriate time histories shall have magnitude, fault distance and source mechanism that are consistent with those that control the design basis earthquake (or maximum capable earthquake). The parameters of interest shall be calculated for each time history analysis. If two time history are performed, then the maximum response of the parameters of interest shall be used for design. Time history analysis can be of two types, namely elastic time history analysis and nonlinear time history analysis. Response parameters from elastic time history analysis shall be denoted as elastic response parameters. All elements shall be designed using strength design. Unlike static forces, the amplitude, direction and location of dynamic forces vary significantly with time which causes considerable inertia effects on structures. Whereas the static behavior of structures is solely dependent upon its stiffness characteristics, the behavior of structures under dynamic forces is controlled by their mass, stiffness and damping properties. Due to the large amplitudes caused by dynamic forces, performance of structures depends on both the strength and deformability of constituent members, which is further linked to their internal design forces, the prediction of which in turn depend upon the accuracy of the method employed in their analytical determination. As linear dynamic analysis procedures were developed, the code provisions were found to be inadequate in providing the required structural strength of the building to withstand an intense earthquake. Actual forces calculated by elastic analysis during earthquakes are much higher than the design forces specified in the code. Moreover the behavior of construction materials like reinforced concrete (RC) under dynamic loading is not linear; i.e., stress is not directly proportional to strain which is valid for small deformation and load. In the case of earthquake that produces intense load and large deformations the material properties vary with time and

intensity of load. Hence the time varying and nonlinear characteristics of RC should be well considered in structural analysis. Elastic response parameters may be scaled by using appropriate response modification factor, R. Nonlinear time histories shall developed and results determined for two appropriate ground motions. The maximum inelastic response displacement shall not be reduced and shall comply with story drift limitations.

4.4.1 Validation of Nonlinear Time History Analysis for SDOF system with SeismoStruct

As mentioned earlier the behavior of RC under dynamic loading is not linear when the damage stresses are greater than elastic limit. The use of linearly elastic analysis procedure is not valid in such cases. In fact there are some situations where the use of such simplified analyses can be misleading and missing in important details. The material and geometric properties which are considered constant in linear analysis do not remain constant in many practical situations. For example severe earthquake vibrations may cause quite large structural deformations and as a result alter the stiffness properties significantly. Moreover, member properties like mass or damping may undergo changes during the dynamic response, while stiffness properties may vary significantly due to the material and geometric nonlinearities caused by significant axial forces. The incremental numerical scheme needs to be applied for the dynamic analysis of nonlinear systems like reinforced concrete structures. Nonlinear time history analysis has been carried out using SeismoStruct [50] to predict the response of a full scale blind test of a bridge pier [52] under six levels of ground motion. Detailed information about geometry material properties and input files have been adopted from PEER website [52] and Bianchi [51]. SeismoStruct simulates the response quite reasonably.

4.4.1.1 Description of model

The model of this validation of nonlinear time history is a full scale reinforced concrete bridge pier. The specimen was tested on the NEES Large High Performance Outdoor Shake Table at UCSD's Englekirk Structural Engineering Center under dynamic conditions, as part of a blind prediction contest. Six uniaxial earthquake ground motions as shown in Figs 4.6, 4.7, 4.8, 4.9, 4.10 and 4.11 starting with low intensity shaking are increased so as to bring the pier progressively to near collapse conditions. SeismoStruct is used in this analysis. SeismoStruct[50] is a Finite Element package for structural analysis, capable of predicting the large displacement behavior of space frames under static or dynamic loadings, taking into

account both geometric nonlinearities and material inelasticity. The analytical results obtained with SeismoStruct [50] in terms of displacements at the top of the column and base shear are herein compared Figs.4.14 to 4.16 with the experimental observations. FE model is defined in X-Z plane.

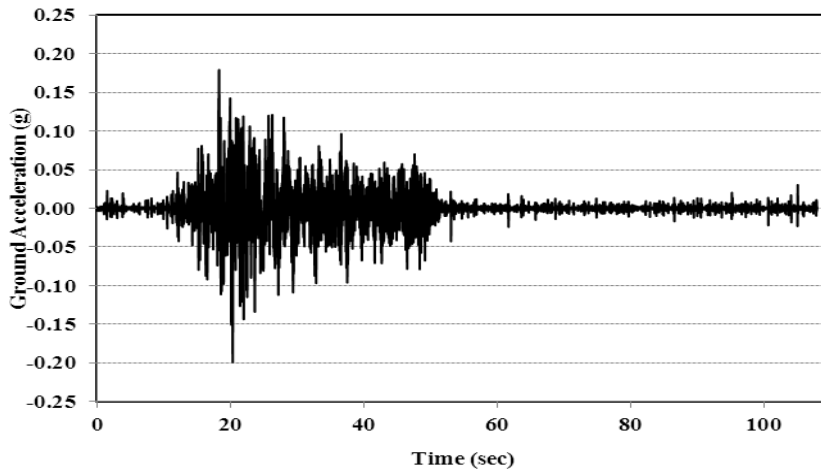


Fig. 4.6 Input Ground motion (EQ1)

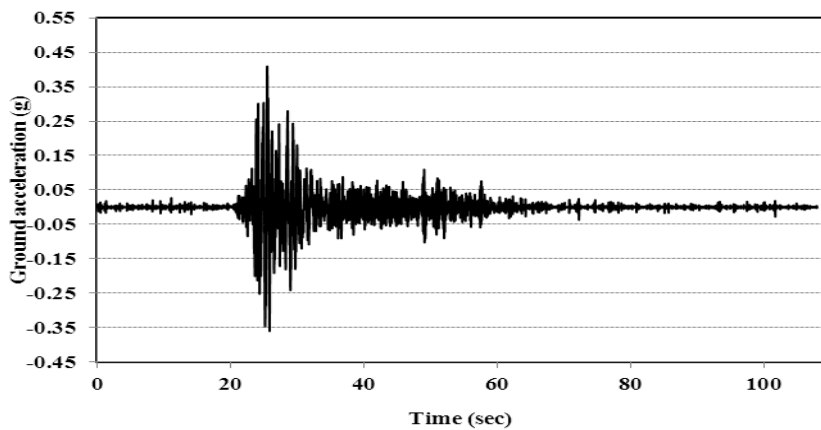


Fig. 4.7 Input Ground motion (EQ2)

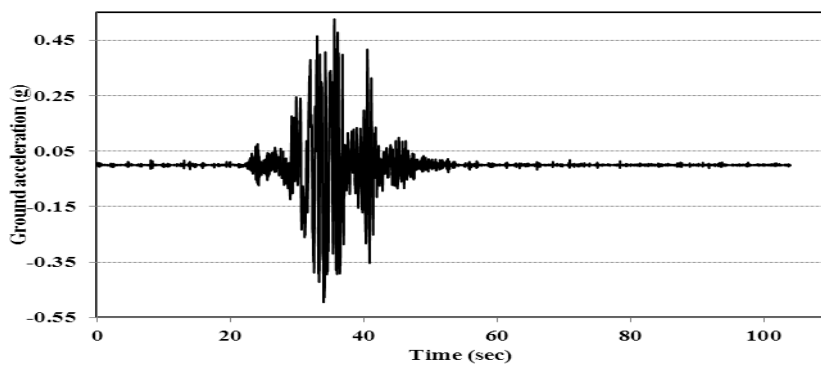


Fig. 4.8 Input Ground motion (EQ3)

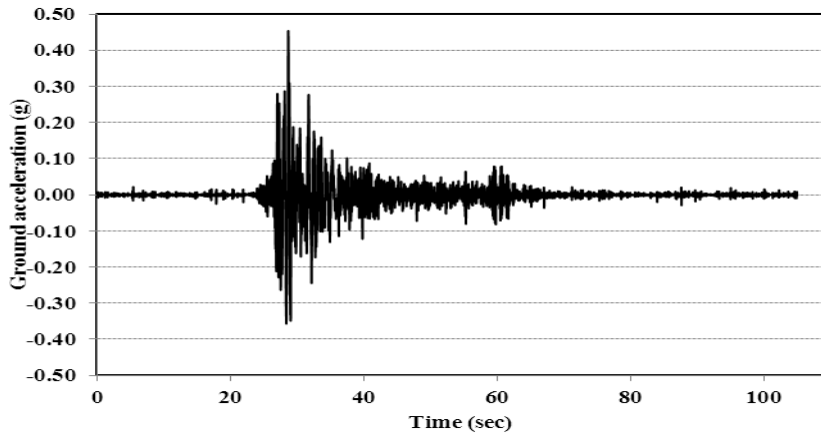


Fig. 4.9 Input Ground motion (EQ4)

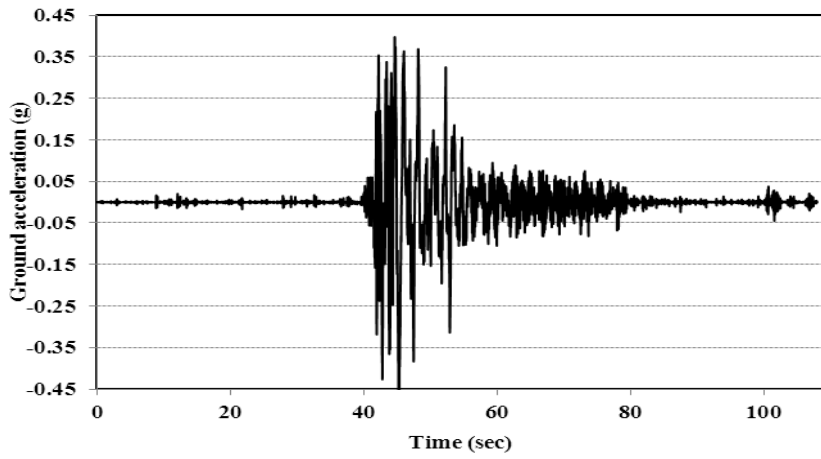


Fig. 4.10 Input Ground motion (EQ5)

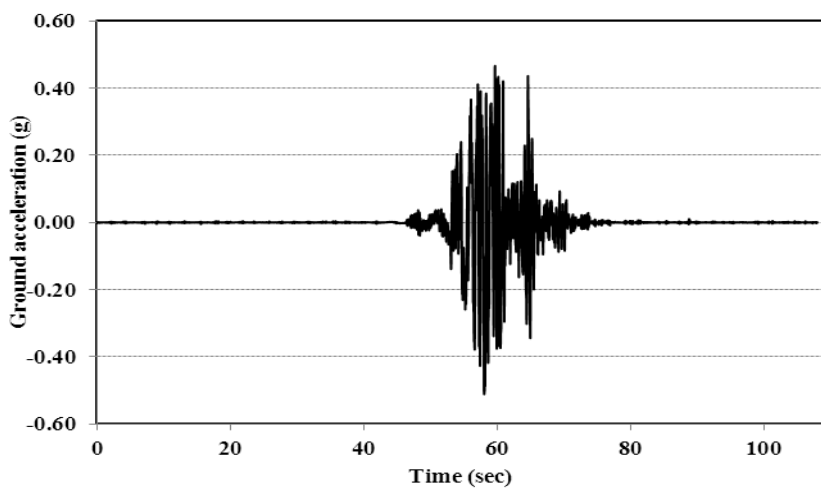


Fig. 4.11 Input Ground motion (EQ6)

4.4.1.2 Structural geometry and properties

The model consists of a 1.22 m diameter cantilevered RC circular column with the properties described hereafter. It is fixed at its support. The height and diameter of column is shown in Fig. 4.12.

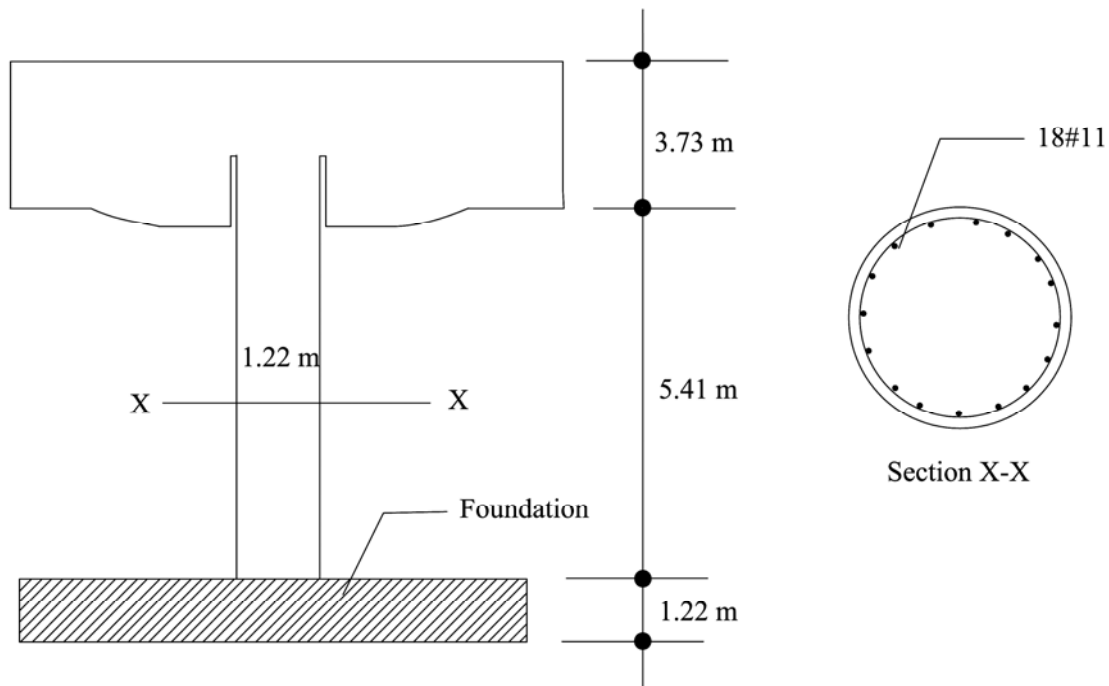


Fig. 4.12 Pier cross section and bridge pier specimen configuration

The concrete model is employed for defining the concrete materials. The characteristic parameters are as follows:

For confined concrete: $f_c' = 41500$ kPa, $f_t = 0$, $\xi_c = 0.0028$ m/m, $k_c = 1.2$, $\gamma = 23.6$ kN/m³

For unconfined concrete: $f_c' = 41500$ kPa, $f_t = 0$, $\xi_c = 0.0028$ m/m, $k_c = 1.0$, $\gamma = 23.6$ kN/m³

For steel: $E_s = 2.000E+008$ kPa, $f_y' = 518500$ kPa, $\mu = 0.008$, $\gamma = 77$ kN/m³

4.4.1.3 Modeling and loading

The column is modeled through a 3D force based inelastic frame element, where the number of fibers used in section equilibrium computations is set to 300. Regarding the applied masses, the effective mass of the pier is considered by assigning the specific weight of the

materials in the ‘materials’ module, whereas a lumped mass of 228 ton is concentrated at the top of the pier.

In order to run a nonlinear dynamic analysis, a time history curve, constituted by six records in series and separated by 10 seconds intervals with no acceleration, is loaded in the “Time history Curve” dialog box. The applied ground motions are shown in Figs. 4.6 to 4.11. The time step for the dynamic analysis is set as 0.00390625 sec. A 1% tangent stiffness proportional damping is applied as global damping in this analysis.

A sketch of the FE model is presented in the following Fig. 4.13.

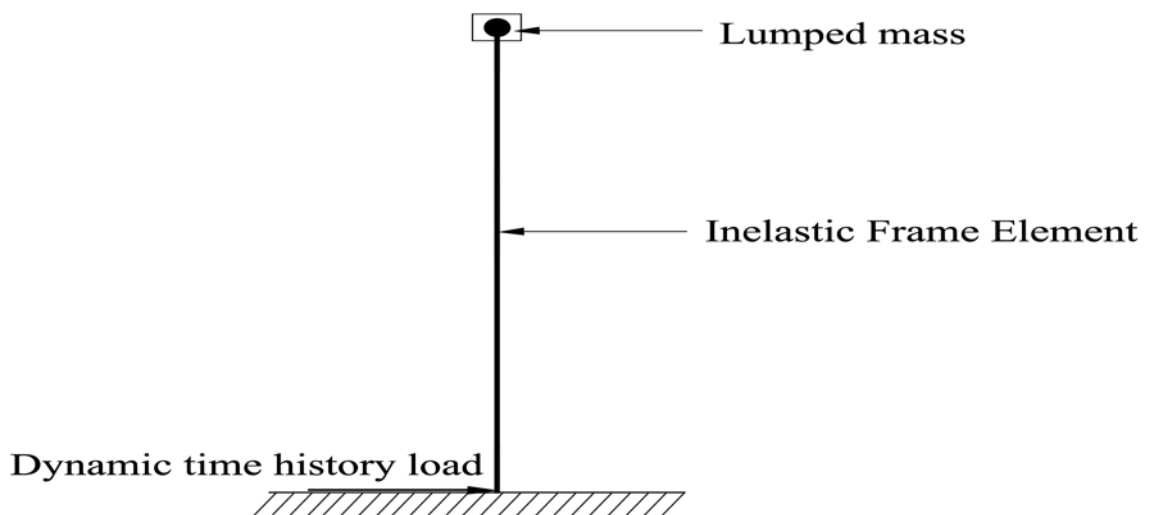


Fig. 4.13 FE model of the bridge column

4.4.1.4 Analysis type

Dynamic analysis is commonly used to predict the nonlinear inelastic response of a structure subjected to earthquake loading (evidently, linear elastic dynamic response can also be modeled for as long as elastic Elements and/or low levels of input excitation are considered). The direct integration of the equations of motion is accomplished using the numerically dissipative α -integration algorithm or a special case of the former, the well known Newmark scheme [39], with automatic time step adjustment for optimum accuracy and efficiency (see Automatic adjustment of load increment or time step). Modeling of seismic action is achieved by introducing acceleration loading curves (accelerograms) at the supports, noting that

different curves can be introduced at each support, thus allowing for representation of asynchronous ground excitation. In addition, dynamic analysis may also be employed for modeling of pulse loading cases, in which case instead of acceleration time histories at the supports, force pulse functions of any given shape (rectangular, triangular, parabolic, and so on), can be employed to describe the transient loading applied to the appropriate nodes. Nonlinear dynamic time history analysis is used in this chapter.

Several types of output can be obtained from the nonlinear dynamic time history analysis:

- (a) Time versus displacement can be plotted,
- (b) Time versus base shear can be plotted and
- (c) Time versus moment can be plotted.

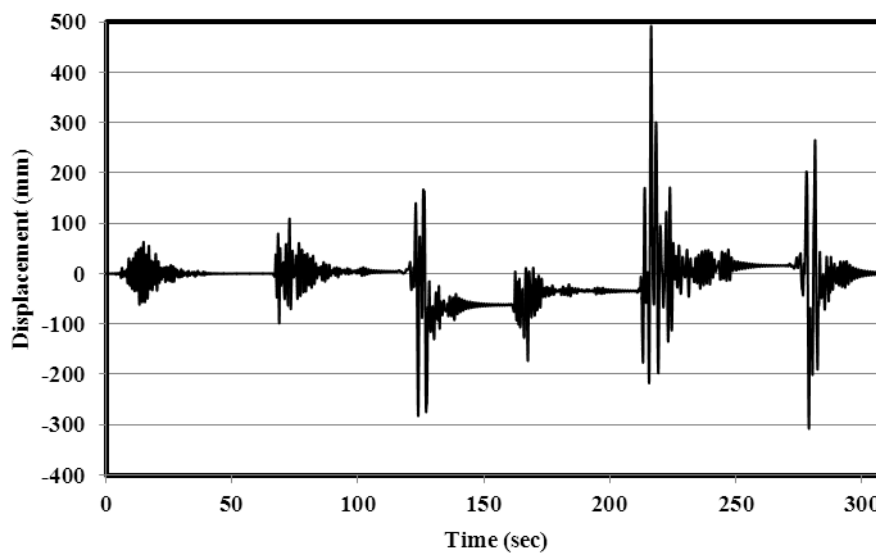


Fig. 4.14 Analytical results at top displacement with time (EQ1 to EQ6)

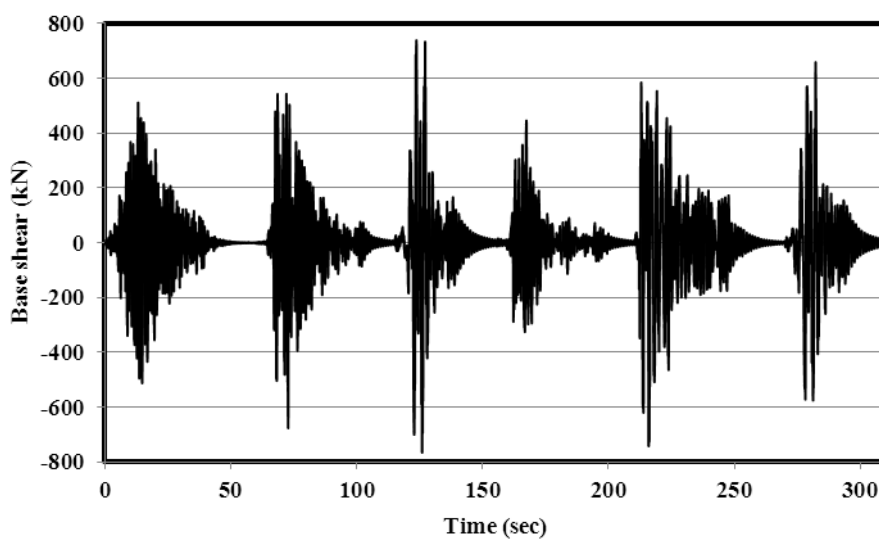


Fig. 4.15 Analytical results at base shear with time (EQ1 to EQ6)

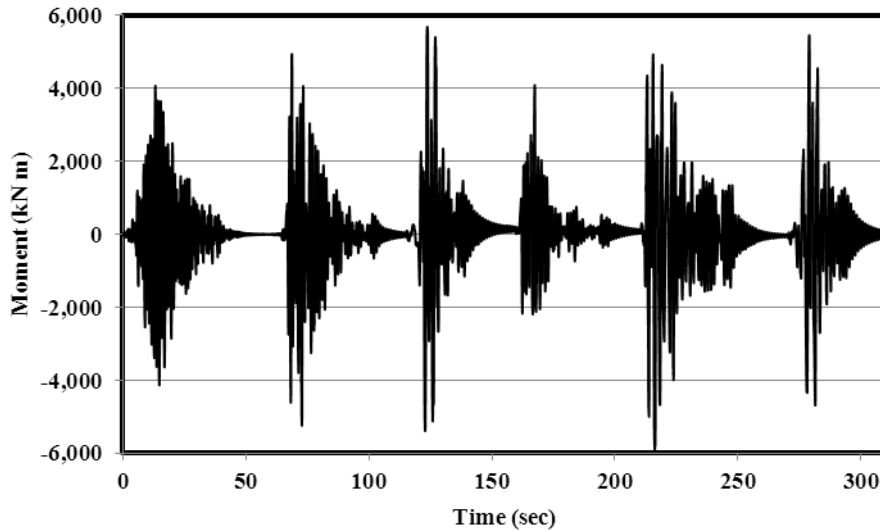


Fig. 4.16 Analytical results at moment with time (EQ1 to EQ6)

4.4.1.5 Comparison of analysis results

The results of the analyses for the EQ1 earthquakes and experimental results are superimposed on one plot of the roof displacement versus time and base shear versus time shown in Figs 4.17, 4.18, 4.19, 4.20, 4.21 and 4.22. These figures demonstrates that the two responses are almost same for most of the time history. The differences displayed in the plot have been attributed to errors caused by different approaches to modeling the column elements. These figures also demonstrates that the analytical displacement responses are very similar to those obtains from experiment. The minor differences between analytical and experimental can be attributed to assumption and simplification of modeling. For the earthquake EQ1 gives a maximum analytical displacement at top of pier is 61.82mm and maximum experimental displacement at top of pier is 62.98mm as shown in Fig.4.17 which is close to same..

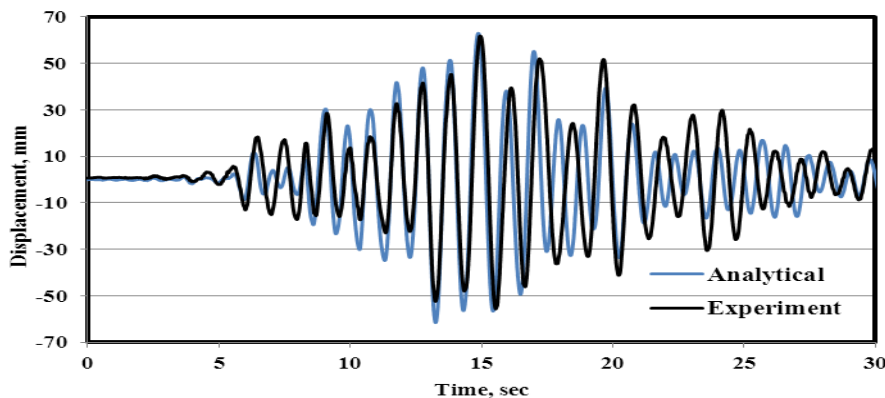


Fig. 4.17 Experiment vs. Analytical results at top displacement time (EQ1)

For the earthquake EQ3 gives a maximum analytical displacement at top level of pier is 185.44mm and maximum experimental displacement at top level of pier is 227.14mm as shown in Fig.4.18 which is close to same..

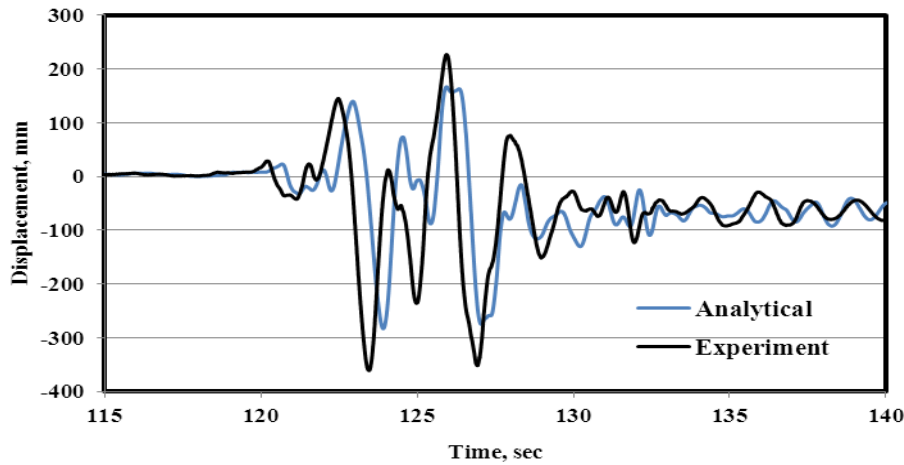


Fig. 4.18 Experiment vs. Analytical results at top displacement time (EQ3)

For the earthquake EQ5 gives a maximum analytical displacement at top level of pier is 495.00mm and maximum experimental displacement at top of pier is 568.97mm as shown in Fig.4.19 which is close to same but last displacements are far differences..

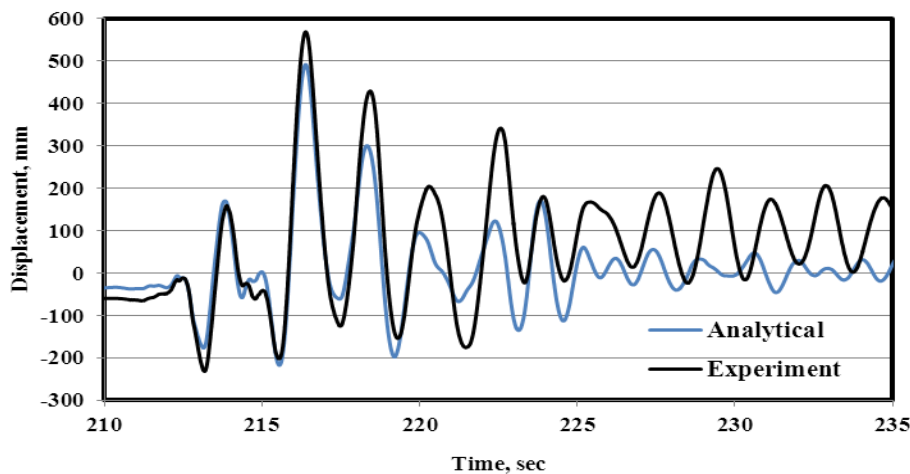


Fig. 4.19 Experiment vs. Analytical results at top displacement time (EQ5)

For the earthquake EQ1 gives a maximum analytical base shear at base level of pier is 511.34kN and maximum experimental base shear at base level of pier is 499.55kN as shown in Fig.4.20 which is close to same..

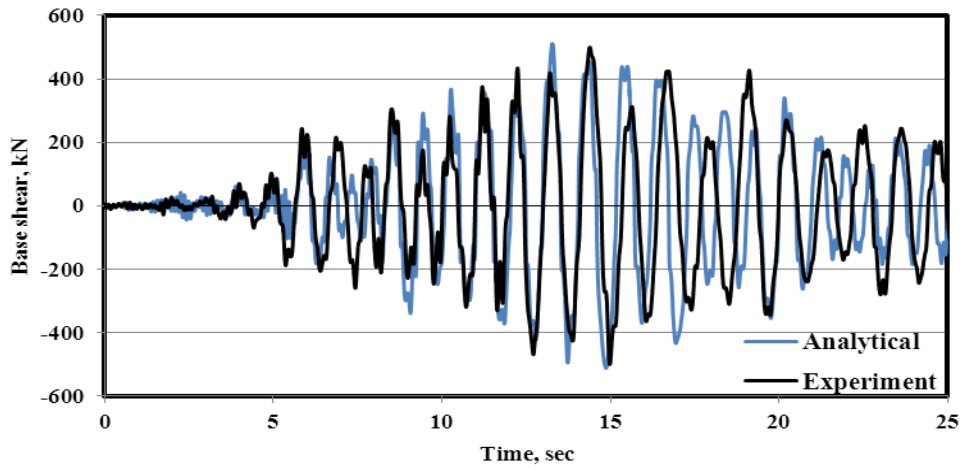


Fig. 4.20 Experiment vs. Analytical results at base shear time (EQ1)

For the earthquake EQ3 gives a maximum analytical base shear at base level of pier is 686.52kN and maximum experimental base shear at base level of pier is 681.45kN as shown in Fig.4.21 which is close to same..

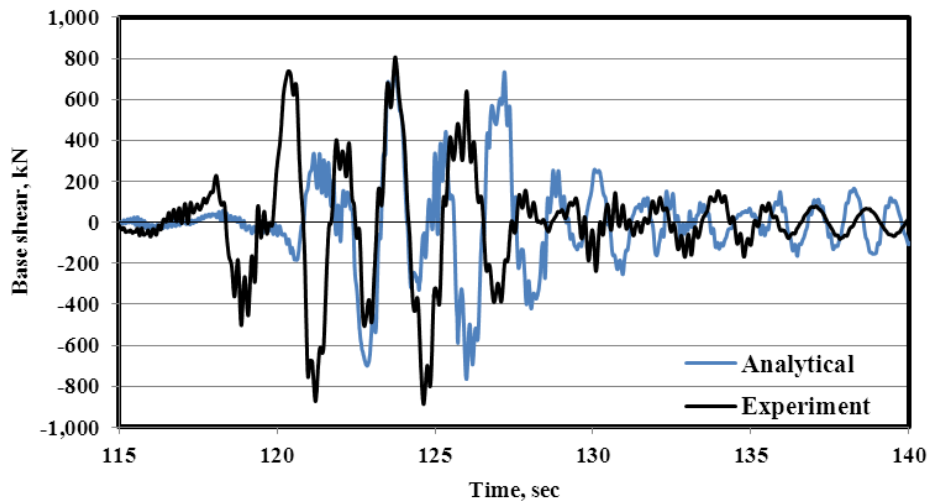


Fig. 4.21 Experiment vs. Analytical results at base shear time (EQ3)

For the earthquake EQ5 gives a maximum analytical base shear at base level of pier is 584.79kN and maximum experimental base shear at base level of pier is 749.26kN as shown in Fig.4.22 which is close to same.

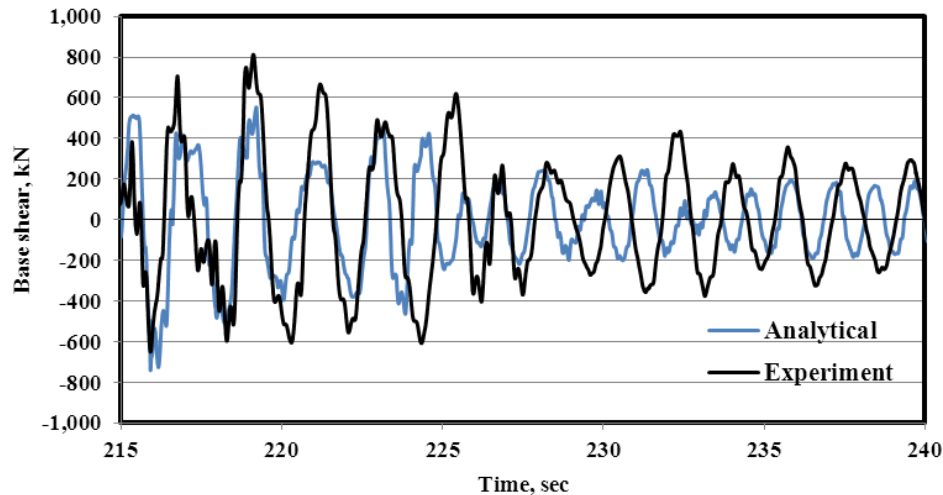


Fig. 4.22 Experiment vs. Analytical results at base shear time (EQ5)

This chapter has done nonlinear dynamic time history analysis of the structure with SeismoStructure [50] software. Base shear and displacements for dynamic load are extracted from the database. Capacity curves (base shear versus roof displacement) are the load-displacement envelopes of the structures and represent the global response of the structures. Time history curves for case study bridge pier is obtained from the dynamic analyses using dynamic load are almost same for blind test. The SDOF system modeled and analyses with SeismoStruct [50] for the blind test pier is capable of simulating the dynamic responses (displacement and base shear) of the actual experiment quite reasonably.

The Validation of the nonlinear dynamic time history analysis for SDOF system using SeismoStruct with experimental results from the blind test [51] is close to same. Therefore, it is concluded that nonlinear dynamic time history analysis run in SeismoStruct is valid and accurate.

From above discussion, different figures we concluded that validation of nonlinear dynamic time history analysis for SDOF system using SeismoStruct [50] is almost same to those of results of blind test results [51].

4.5 Nonlinear time history analysis for 2D frame using SAP2000

The objective of this study is to verify that SAP2000, a relatively new computer program. SAP2000 compared to SeismoStruct to prove the validity of a nonlinear time history analysis. This comparison proved that when the different parameters are chosen carefully, the results

would match for the two programs. SeismoStruct is compared to SAP2000 in order to check the validity of nonlinear pushover analysis. The results of these comparisons showed that nonlinear analysis run in SAP2000 is valid and accurate.

The analysis of the case study model is performed by SAP2000. The results including the displacement, forces and support reactions of the model are recorded. The total number of mode shape used is equal to number of story. In mode shape lateral sway is considered and the time period corresponding to that mode shape is taken.

Frame nonlinear hinge property is used to define nonlinear force displacement and/or moment rotation behavior that can be assigned to discrete locations along the length of frame (line) elements. These nonlinear hinges are only used during static nonlinear (pushover) analysis. The built-in default hinge properties for concrete members are generally based on ATC-40. Default hinge properties cannot be modified. They also can not be viewed because the default properties are section dependent. The default properties cannot be fully defined by the program until the section to which they apply is identified. Moment (M_3) and shear (V_2) hinges is considered at each end of each beam and moment and axial force (P-M-M) is considered at each end of column elements.

4.5.1 Analysis Technique

The step-by-step procedure is a second general approach to dynamic response analysis, and it is well suited to analysis of nonlinear response because it avoids any use of superposition. There are many different step-by-step methods, but in all of them the loading and the response history are divided into a sequence of time intervals or “steps”. The response during each step then is calculated from the initial conditions (displacement and velocity) existing at the beginning of the step and from the history of loading during the step. Thus the response each step is an independent analysis problem, and there is no need to combine response contributions within the step. Nonlinear behavior may be considered easily by this approach merely by assuming that the structural properties remain constant during each step and causing them to change in accordance with any specified form of behavior from one step to the next; hence the nonlinear analysis actually is a sequence of linear analyses of a changing system. Any desired degree of refinement in the nonlinear behavior may be achieved in this procedure by making the time steps short enough; also it can be applied to any type of

nonlinearity, including changes of mass and damping properties as well as the more common nonlinearities due to changes of stiffness.

Step-by-step methods provide the only completely general approach to analysis of nonlinear response; however, the methods are equally valuable in the analysis of linear response because the same algorithms can be applied regardless of whether the structure is behaving linearly or not. Moreover, the procedures used in solving single-degree-of-freedom structures can easily be extended to deal with multi degree system merely replacing scalar quantities of matrices. In fact, these methods are so effective and convenient that time-domain analyses always are done by some form of step-by-step analysis regardless of whether or not the response behavior is linear; the Duhamel method seldom is used in practice.

The response analysis procedures formulated in the time domain or in the frequency domain involve evaluation of many independent response contributions that are combined to obtain the total response. In the time domain procedure (Duhamel integral), the loading $p(t)$ is considered to be a succession of short-duration impulses, and the free-vibration response to each impulse becomes a separate contribution to the total response at any subsequent time. In the frequency-domain method, it is assumed that the loading $p(t)$ is periodic and has been resolved into its discrete harmonic components P_n by Fourier transformation. The corresponding harmonic response components of the structure V_n are then obtained by multiplying these loading components by the frequency response coefficient of the structure H_n , and finally the total response of the structure is obtained by combining the harmonic response components (inverse Fourier transform). Because superposition is applied to obtain the final result in the both procedures, neither of these methods is suited for use in analysis of nonlinear response; therefore judgment must be used in applying them in earthquake engineering where it is expected that a severe earthquake will induce inelastic deformation in a code-designed structure.

4.5.2 Analysis and results

The verification of perform is to validate the accuracy of the nonlinear inelastic time history analysis. The 5-story structure is subjected to the El Centro and Kobe earthquake time history that is previously used and is illustrated in Fig.4.23 and 4.24. The peak acceleration of the loading history is scaled to 0.31g and 0.49g in order to obtain an inelastic response from the structure. It is model inherent natural damping exactly the same in both programs; therefore it

is set to 1%. P-delta effect is also included in this analysis according to the approach described in chapter 3.

The results of the analyses for the two programs are superimposed on one plot of the roof displacement versus time shown in Figs. 4.23 and 4.24. For the El Centro earthquake gives a maximum analytical displacement at top level of 5-story 2D frame is 57.46mm for SAP2000 and 63.31mm for SeismoStruct as shown in Fig.4.23 which is close to same. For the Kobe earthquake gives a maximum analytical displacement at top level of 5-story 2D frame is 82.48mm for SAP2000 and 84.40mm for SeismoStruct as shown in Fig.4.24 which is close to same. These figures demonstrate that the two responses are almost identical for most of the time history. The differences displayed in the plot have been attributed to errors caused by different approaches to modeling the beam and column elements. Therefore, it is concluded that nonlinear dynamic time history analysis run in SAP2000 and SeismoStruct is valid and accurate.

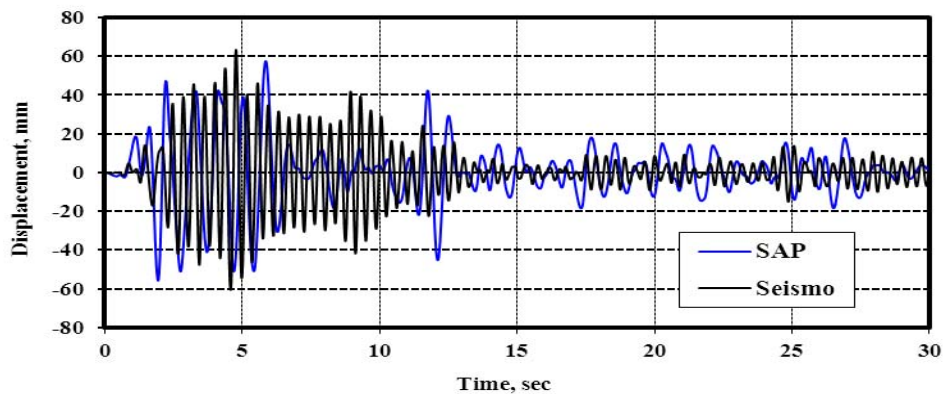


Fig. 4.23 Time History Analysis for 5-Story 2D Frame (El Centro earthquake)

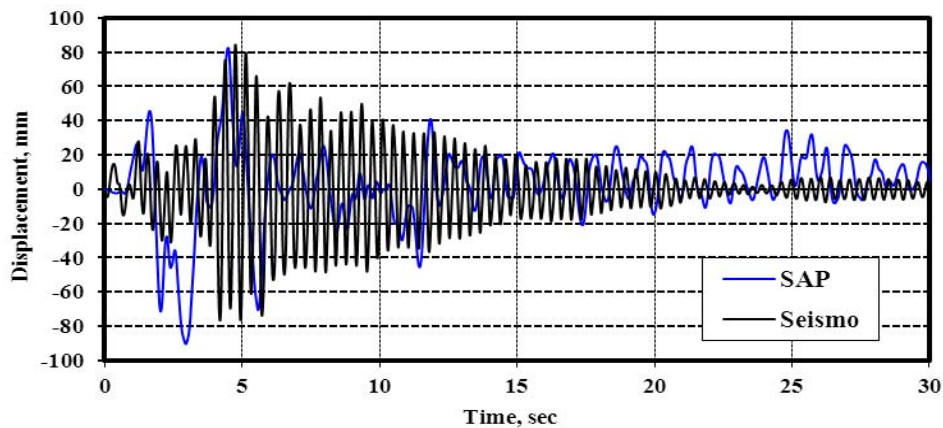


Fig. 4.24 Time History Analysis for 5-Story 2D Frame (Kobe earthquake)

4.6 Comparison of Linear and Nonlinear Time History Analysis

The linear and nonlinear time history analysis is used to estimate maximum seismic displacement demands of 2, 5 and 12-story reinforced concrete frames under El Centro and Kobe earthquakes. The displacements are compared obtained from linear and nonlinear time history analysis and shown in Figs. 4.25, 4.26 and 4.27. SAP2000 [21] is used to perform linear and nonlinear time history analyses. Nonlinear time history analyses of 2D frame structures to determine displacements are performed by SAP2000 [21]. Target displacements estimated using each procedure, values determined from nonlinear time history analyses for all frames and ground motions are given in figures. The comparison of displacements obtained from linear and nonlinear time history analyses could not reveal a clear particular trend because structural response is affected by the variations in ground motion characteristics and structural properties that each frame under each ground motion should be considered as a case. However, the overall interpretation of results shows that the estimation of approximate procedures yield different target displacement values than the exact results for almost all cases. The accuracy of the predictions depends on ground motion characteristics and structural properties as well as the inherent limitations of the procedures.

For the two story frame, the linear time history analysis gives a maximum dynamic displacement at the roof of 70.48mm (2.56sec), minimum displacement 77.26mm (2.32sec) and nonlinear time history analysis gives maximum dynamic displacement at the roof of 49.69mm (4.7sec), minimum displacement 50.65mm (4.9sec) as shown in Fig. 4.25.

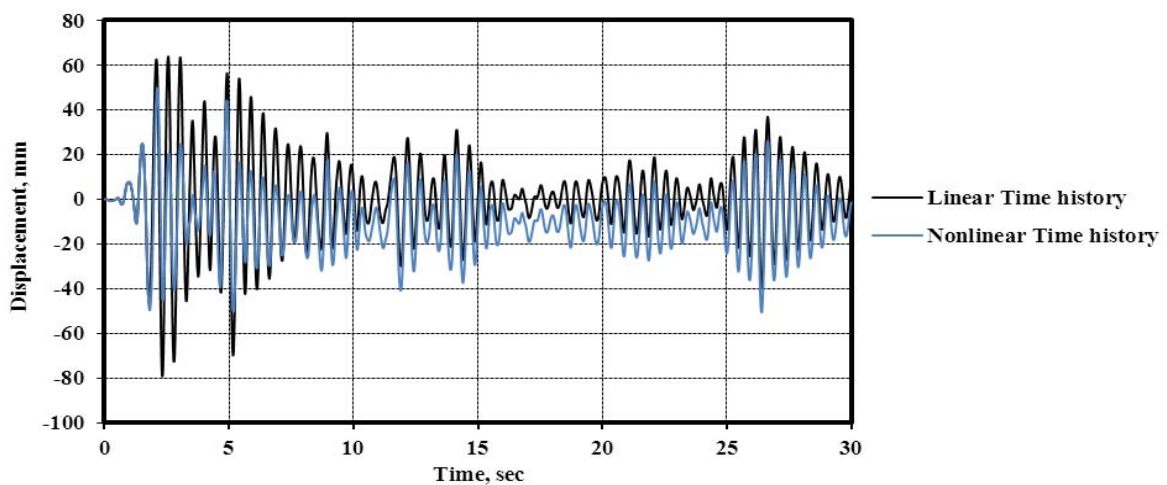


Fig. 4.25 Comparison of linear and nonlinear time history analysis for 2-Story frame (El Centro Earthquake)

For Kobe earthquake, the two story frame, the linear time history analysis gives a maximum dynamic displacement at the roof of 70.48mm (12sec), minimum displacement 77.67mm (11.74sec) and nonlinear time history analysis gives maximum dynamic displacement at the roof of 45.31mm (11.52sec), minimum displacement 90.91mm (13.42sec) as shown in Fig.4.26. From this figure it is seen that deformation is around 50 mm.

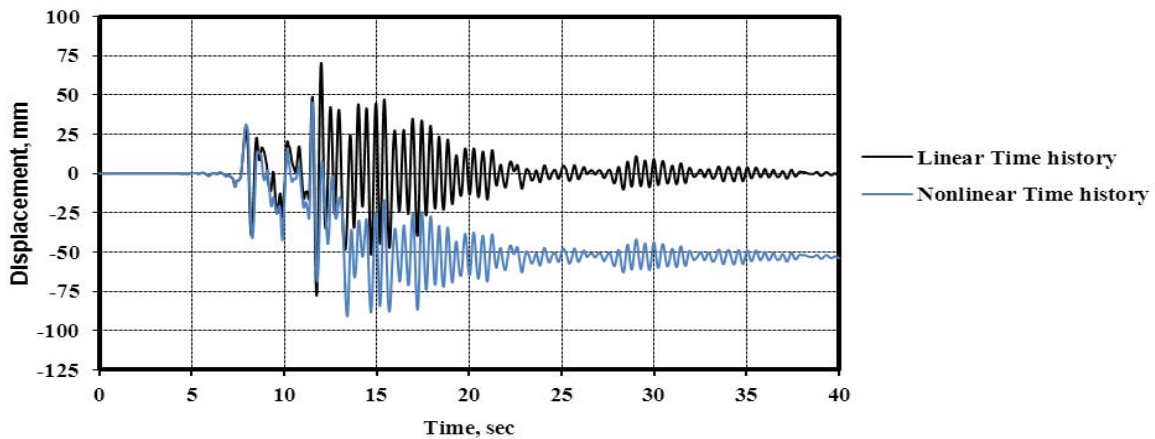


Fig. 4.26 Comparison of linear and nonlinear time history analysis for 2-Story frame (Kobe Earthquake)

For the five story frame, the linear time history analysis gives a maximum dynamic displacement at the roof of 146.87mm (5.82sec), minimum displacement 124.74mm (5.82sec) and nonlinear time history analysis gives maximum dynamic displacement at the roof of 99.65mm (5.84sec), minimum displacement 103.62mm (5.46sec) as shown in Fig. 4.27.

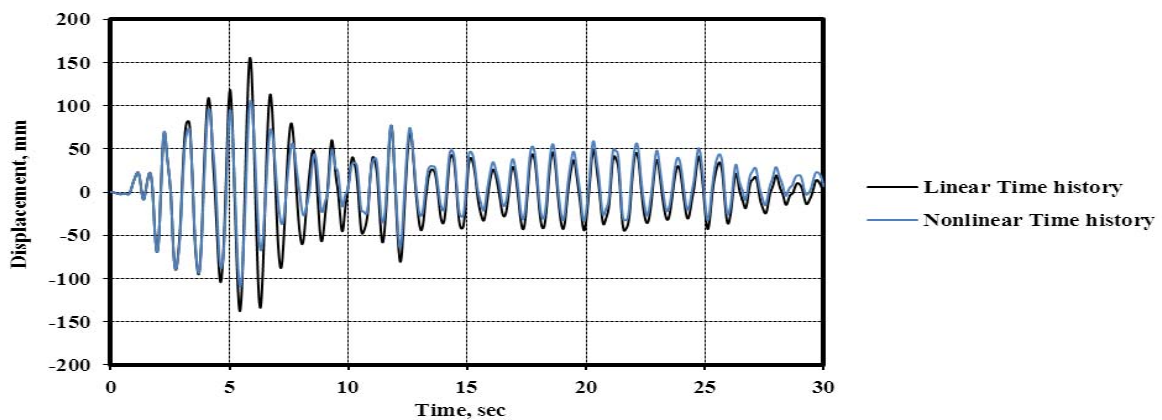


Fig. 4.27 Comparison of linear and nonlinear time history analysis for 5-Story frame (El Centro Earthquake)

For Kobe earthquake, the 5-story frame, the linear time history analysis gives a maximum dynamic displacement at the roof of 217.48mm (14sec), minimum displacement 232.25mm (13.54sec) and nonlinear time history analysis gives maximum dynamic displacement at the roof of 82.48mm (4.48sec), minimum displacement 90.32mm (2.96sec) as shown in Fig. 4.28.

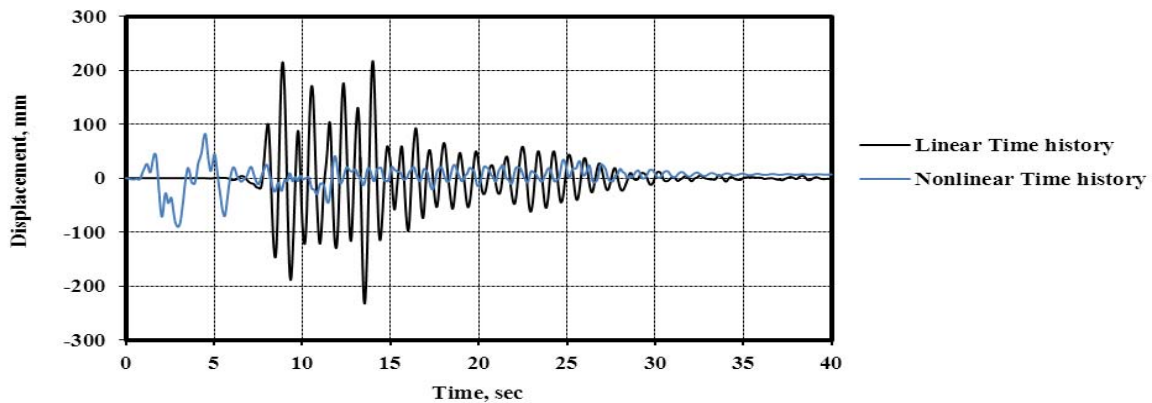


Fig. 4.28 Comparison of linear and nonlinear time history analysis for 5-Story frame (Kobe Earthquake)

For the twelve story frame, the linear time history analysis gives a maximum dynamic displacement at the roof of 137.65mm (6.12sec), minimum displacement 117.88mm (5.38sec) and nonlinear time history analysis gives maximum dynamic displacement at the roof of 84.16(6.12sec), minimum displacement 146.88mm (5.4sec) as shown in Fig. 4.29.

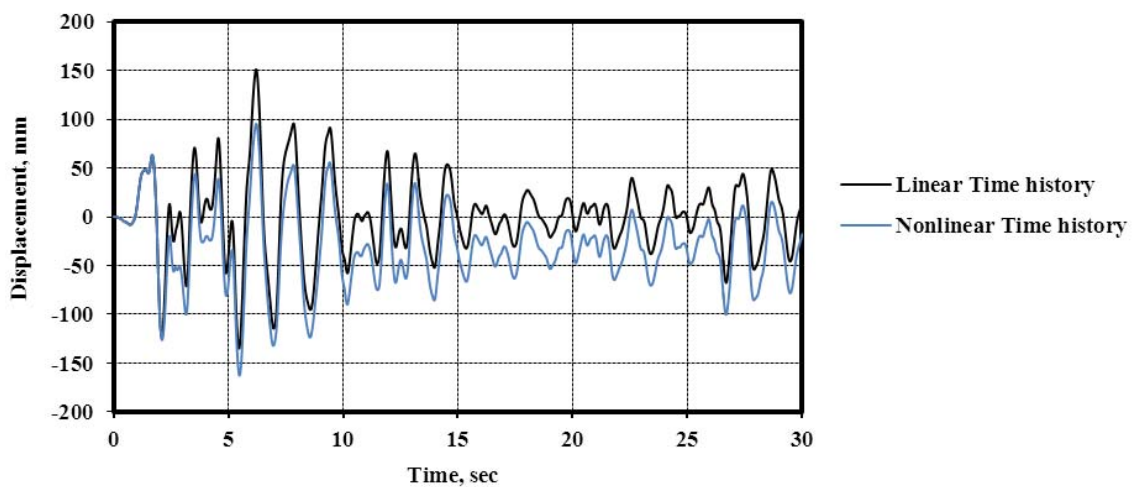


Fig. 4.29 Comparison of linear and nonlinear time history analysis for 12-Story frame (El Centro Earthquake)

For Kobe earthquake, the 12-story frame, the linear time history analysis gives a maximum dynamic displacement at the roof of 498.98mm (10.8sec), minimum displacement 481.56mm (11.54sec) and nonlinear time history analysis gives maximum dynamic displacement at the roof of 583.8mm (9.66sec), minimum displacement 239.53mm (10.62sec) as shown in Fig. 4.30. From this figure it is seen that deformation is around 200 mm.

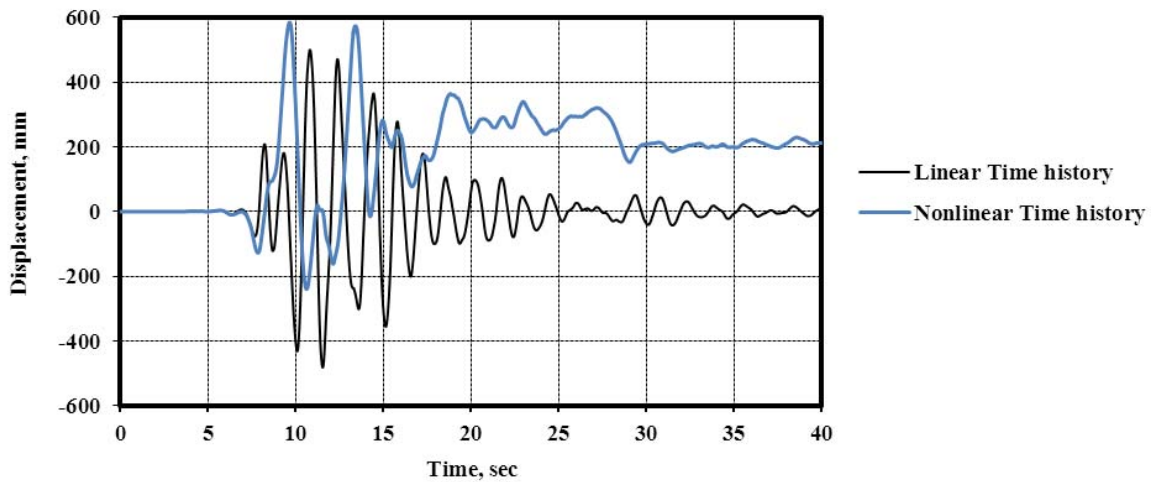


Fig. 4.30 Comparison of linear and nonlinear time history analysis for 12-Story frame (Kobe Earthquake)

4.7 Comparison of capacity curves of pushover and nonlinear time history analysis

Most of the simplified nonlinear analysis procedures utilized for seismic performance evaluation make use of pushover analysis and/or equivalent SDOF representation of actual structure. However, pushover analysis involves certain approximations that the reliability and the accuracy of the procedure should be identified. For this purpose, researchers investigated various aspects of pushover analysis to identify the limitations and weaknesses of the procedure and proposed improved pushover procedures that consider the effects of loading patterns, higher modes, failure mechanisms, etc.

The nonlinear response of structures is very sensitive to the structural modeling and ground motion characteristics. Therefore, different ground motion records that accounts for uncertainties and differences in severity, frequency and duration characteristics has to be used to predict the possible deformation modes of the structures for seismic performance evaluation purposes. However, for simplicity, seismic demand prediction is generally performed by pushover analysis which mostly utilizes smoothed response spectra. In this

study, the accuracy of demand prediction of pushover analyses for various loading patterns is evaluated for the response obtained from selected ground motion data. In this study, the response of case study frames are studied in the elastic and inelastic deformation levels that are represented by peak roof displacements on the capacity (pushover) curve of the frames. For each frame and each ground motion record is scaled to obtain the predetermined peak roof displacement for the frame considered. The ground motion scale factors used to obtain the predetermined peak roof displacements corresponding to the considered deformation levels and the predetermined peak roof displacements are presented for reinforced concrete frames in chapter 3. Nonlinear time history analyses are performed by using SAP2000 [21] for the scaled ground motion records and maximum absolute values of response parameters such as story displacements, inter-story drift ratios and story shears are determined at the considered deformation for each ground motion record. It is also mentioning that the maximum values of any response parameter over the height of the frames generally occurred at different instants of time. Also, plastic hinge locations are identified in nonlinear time history analyses. In pushover analyses, five different loading patterns are used in this study.

4.7.1 Description of case studies model

The pushover and nonlinear dynamic analysis are performed on moment resisting frames of two displacement obtained from the pushover analysis can then be compared with the maximum and minimum roof displacements induced by the dynamic analyses. The dimensions of each frame are shown in Figs. 3.4, 3.5, 3.6 and also the fundamental, second, third periods of each frame are shown in the Tables 3.2, 3.4 and 3.6.

The building frames are located in Dhaka area, on stiff soil, 5% structural damping, and were designed for an earthquake with a 10% probability 50 years (Life safety). For the dynamic load, the 1940 EI Centro ground motions are considered. Since a comparison is to be made between dynamic and pushover responses, the ground motion should represent the same conditions as the response spectrum. The 1940 EI Centro ground motions are selected for the analyses.

4.7.2 Analysis and Result

The effects and the accuracy of invariant lateral load patterns utilized in pushover analysis to predict the behavior imposed on the structure due to selected individual ground motions

causing elastic and various levels of nonlinear response are evaluated in this study. For this purpose, global structure behavior, story displacements, inter story drift ratios, story shears and plastic hinge locations are selected as response parameters. Pushover curves are obtained by performing pushover analyses using SAP2000[21], story displacements, inter-story drift ratios, story pushover curves and plastic hinge locations for any lateral load pattern are extracted from the pushover analysis at the predetermined maximum roof displacement consistent with the different level considered and are compared with absolute maximum values of response parameters obtained from nonlinear time history analyses for each scale factor for each ground motion. It should be mentioned that maximum story displacements and inter story drift ratios for any story level generally occurred at different times in nonlinear time history analyses. Also, story displacements; inter story drift ratios and plastic hinge locations are estimated by performing pushover analysis on case study frames. Story displacement, inter story drift ratio and corresponding error profiles for case study frames for each pushover method at each scale factor for all ground motions are illustrated in this chapter.

Location of weak points and potential failure modes that structure shall experience in case of a seismic event is expected to be identified by pushover analyses. The accuracy of various lateral load patterns utilized in traditional pushover analyses to predict the plastic hinges similar to those predicted by nonlinear time history analyses is evaluated in this study. The location of plastic hinges for case study R/C frames are predicted by pushover analyses performed considering the lateral load patterns used in this study at roof displacements corresponding to the nonlinear time history analysis by different scale factor. These deformation levels represent low levels of nonlinear behavior, global yield and high levels of nonlinear behavior. The pushover and nonlinear time history hinge patterns are compared. The plastic hinge locations are also estimated for R/C frames by modal pushover analysis.

The ground motion scale factors used to obtain the peak roof displacements. Nonlinear time history analysis are performed by SAP2000[21] for the scale ground motion records and maximum absolute values of response parameters such as story displacements and base shear are determined for El Centro ground motion record. It is also mentioning that the maximum values of any response over the height of the frames generally occurred at different instance of time. Capacity curve for 2-Story, 5-story and 12-Story frames are shown in Figs.4.31, 4.32 and 4.33. The base shear/weight (%) and story displacement/ height (%) data extracted from thesis paper of Ogus [13] which are superimposed in Figs. 4.31, 4.32 and 4.33. From

Fig.4.31, 4.32 and 4.33, we have seen that capacity curves are close to same with different loading pattern and nonlinear time history curve. Nonlinear time history analysis are performed by SeismoStruct[50] for the scale ground motion records and maximum absolute values of response parameters such as story displacements and base shear are determined for El Centro ground motion record. It is also mentioning that the maximum values of any response over the height of the frames generally occurred at different instance of time. Capacity curve for 2-Story, 5-story and 12-story frames are shown in Figs.4.31, 4.32 and 4.33 which are close to SAP2000.

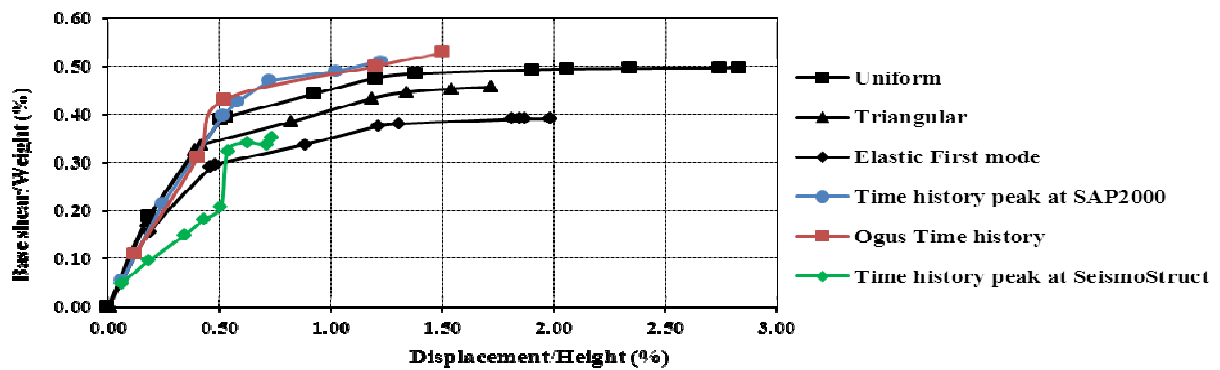


Fig. 4.31 Capacity Curve for 2-Story Frame (El Centro earthquake)

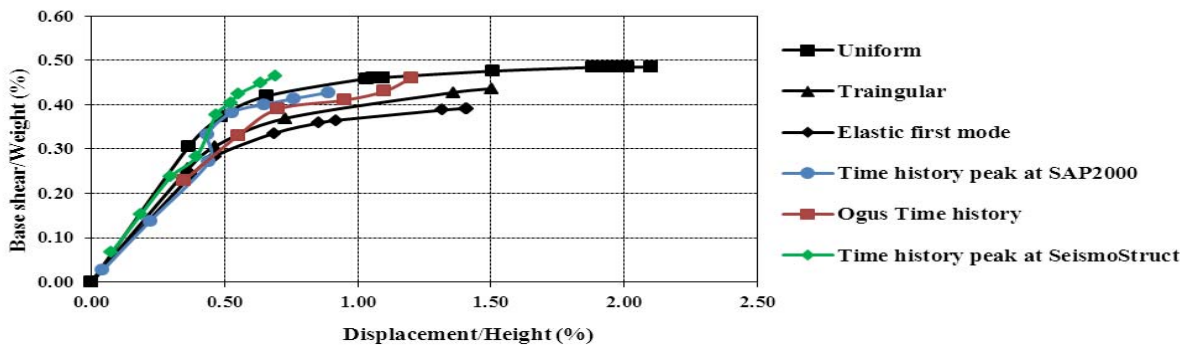


Fig. 4.32 Capacity Curve for 5-Story Frame (El Centro earthquake)

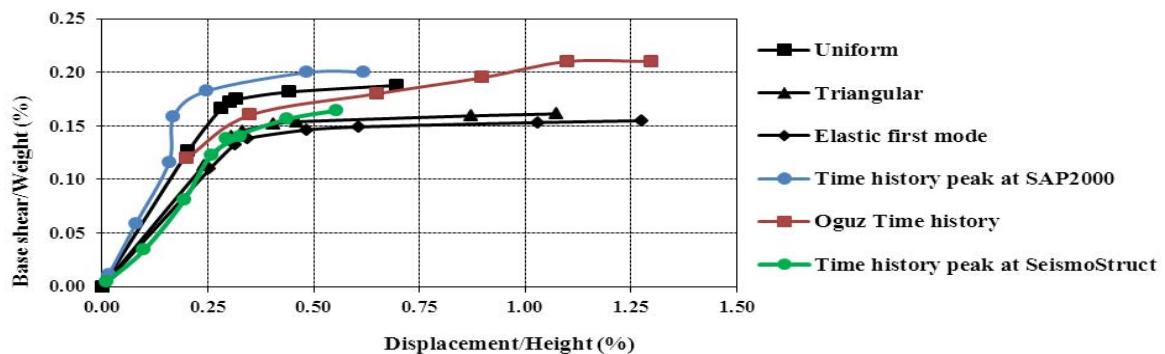


Fig. 4.33 Capacity Curve for 12-Story Frame (El Centro earthquake)

4.8 Performance Evaluation of the Structure using time history

The observations have been made from the comparison of plastic hinge locations determined by pushover analyses and nonlinear time history analyses are locations of plastic hinges obtained from nonlinear time history analyses are generally different for each ground motion for each frame. None of the lateral load patterns could capture adequately the exact plastic hinge locations obtained from nonlinear time history analyses at any considered deformation level. Pushover analyses could not predict the plastic hinging in same sequence with nonlinear time history analyses predictions. In this section two reinforced concrete frames 2 and 5 storied 2D frames are modeled. These frames are designed as per the provisions of BNBC [1]. Considering live load 29.19kN/m² and dead load 58.38kN/m² is used floor level. Self weight of the concrete members considering unit weight of concrete as 23.56kN/m³, As per BNBC seismic modification factor R=8 (IMRF) has been considered.

Performance point of any structure demand curve is required and demand curve can be generated with SAP2000 [21]. But several parameters are required to generate the curves. In this section, those parameters are defined and demand curve is plotted by SAP2000 [21]. The performance point is determined for serviceability earthquake (SE), design earthquake (DE) and maximum earthquake (ME).

4.8.1 Local level performance

Hinge curve for 2-Story frame for El Centro earthquake are shown in Fig.4.34 and for Kobe earthquake are shown in Fig. 4.35. From Fig. 4.34 at performance point there is no hinge form for ME level. From Fig. 4.35 at performance point there are 2 hinges for ME level which are in the range of B-IO. There is no hinge form for SE and DE level. For three level of earthquake, no hinge is found to cross the Immediate Occupancy (IO) limits. According ATC-40[3], 2-story frame satisfies local criteria. Therefore it has been said that 2-story frame structure fulfills the performance at local level for both earthquake.

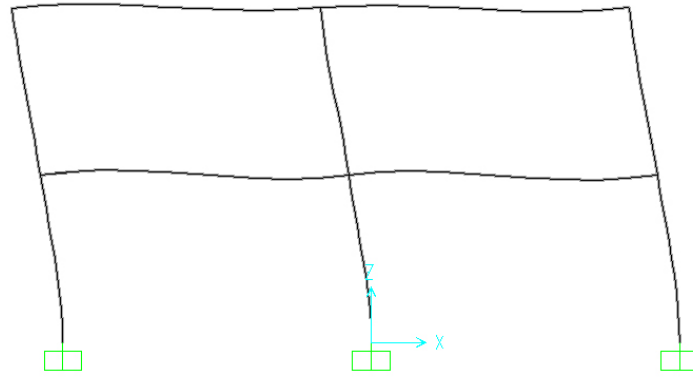


Fig. 4.34 Deformation of the 2-Story 2D frame for ME (El Centro earthquake)

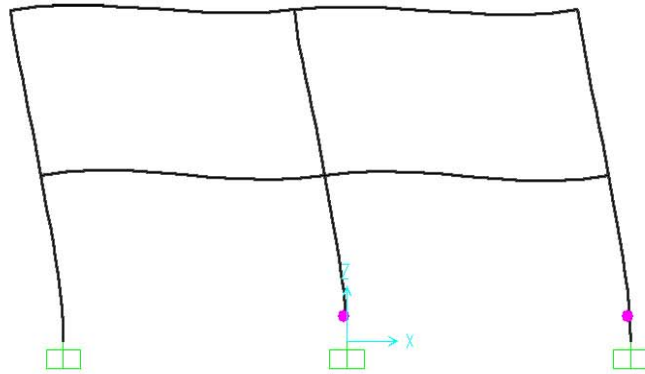


Fig. 4.35 Deformation of the 2-Story 2D frame for ME (Kobe earthquake)

Hinge curve for 5-Story frame for El Centro earthquake is shown in Fig.4.36 and for Kobe earthquake is shown in Fig. 4.37. From Fig. 4.36 at performance point there are 10 hinges which are in the range of B- IO. There is no hinge form for SE level. For three level of earthquake, no hinge is found to cross the Immediate Occupancy (IO) limits. This 5-story frame satisfies local criteria specified in ATC-40[3]. Therefore it has been said that 5-story frame structure fulfills the performance at local level for El Centro earthquake and Kobe earthquake.

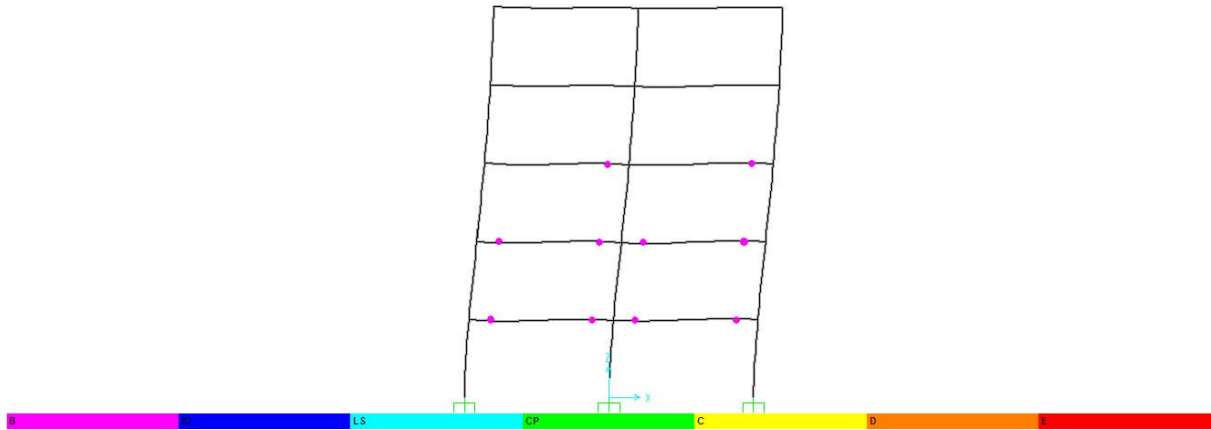


Fig. 4.36 Deformation of the 5-Story 2D frame for ME (El Centro earthquake)

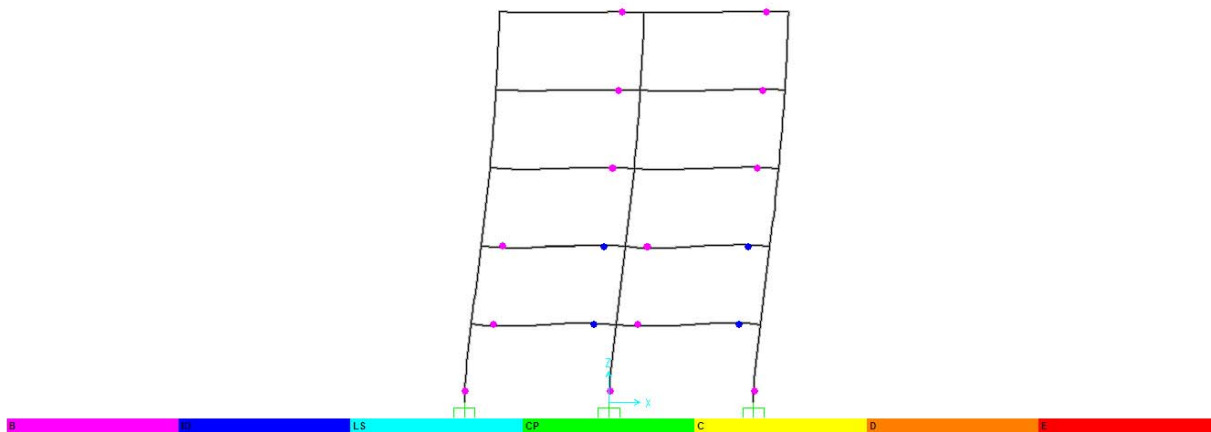


Fig. 4.37 Deformation of the 5-Story 2D frame for ME (Kobe earthquake)

4.8.2 Global level performance

From the Figs. 4.38 and 4.39 it is seen that the performance point of 2-story frame structure has maximum story drift of 0.0017 at story level 2 for El Centro earthquake and 0.0022 at story level 2 for Kobe earthquake. These are less than allowable IO level 0.01 described in ATC 40[3]. So this structure satisfies the requirement of ATC 40[3]. Therefore it has been said that 2-story frame structure fulfills the performance objective at global level in serviceability earthquake (SE), design earthquake(DE) and maximum earthquake(ME).

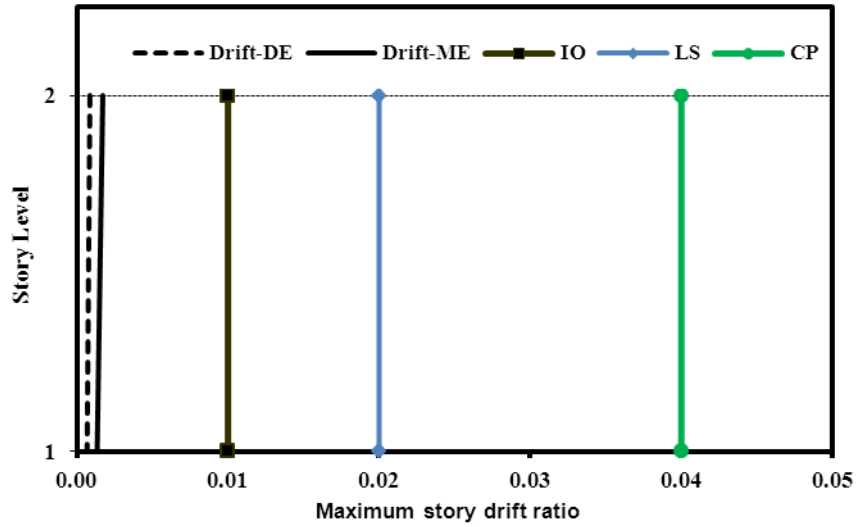


Fig. 4.38 Maximum story drift at performance point of 2-Story 2D frame for different earthquake level (El Centro earthquake)

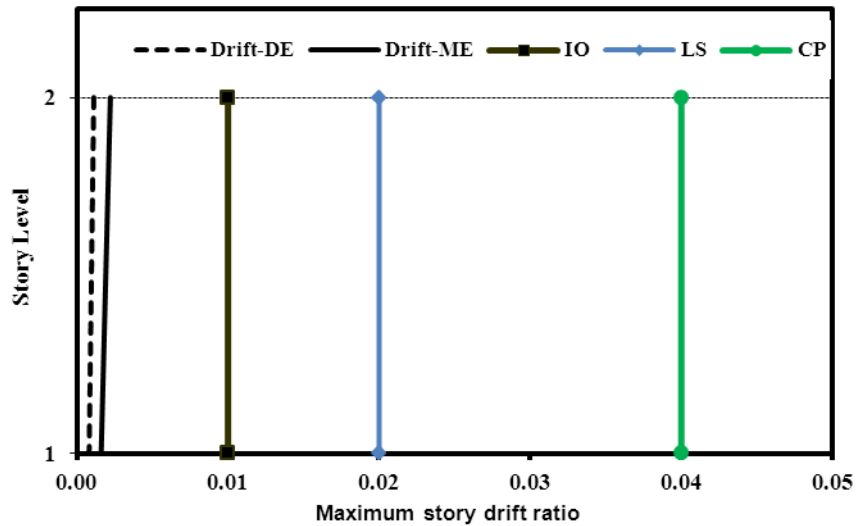


Fig. 4.39 Maximum story drift at performance point of 2-Story 2D frame for different earthquake level (Kobe earthquake)

Note: IO=Immediate Occupancy, LS= Life Safety, CP= Collapse Prevention

From the Figs. 4.40 and 4.41 it is seen that the performance point of 5-story frame structure has maximum story drift of 0.002024 at story level 2 for El Centro earthquake (ME) and 0.003006 at story level 2 for Kobe earthquake (ME). These are less than allowable IO level 0.01 described in ATC 40[3]. So this structure satisfies the requirement of ATC 40[3]. Therefore it has been said that 5-story frame structure fulfills the performance objective at

global level in serviceability earthquake (SE), design earthquake(DE) and maximum earthquake(ME).

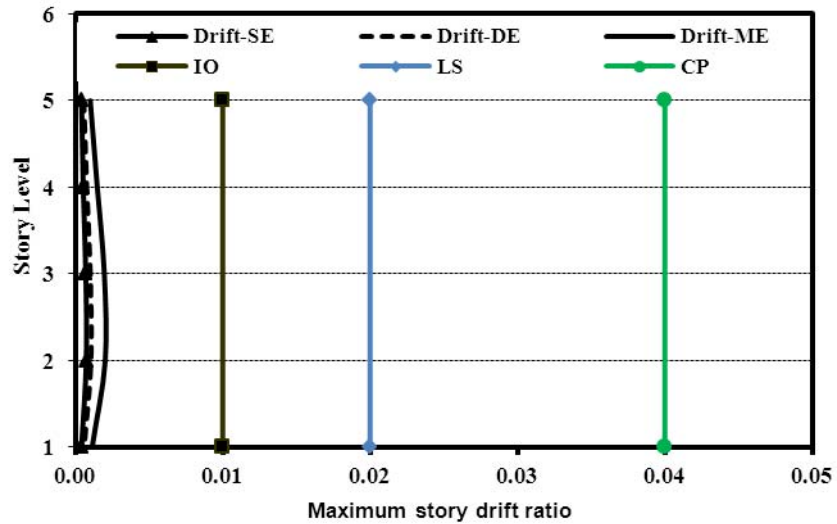


Fig. 4.40 Maximum story drift at performance point of 5-Story 2D frame for different earthquake level (El Centro earthquake)

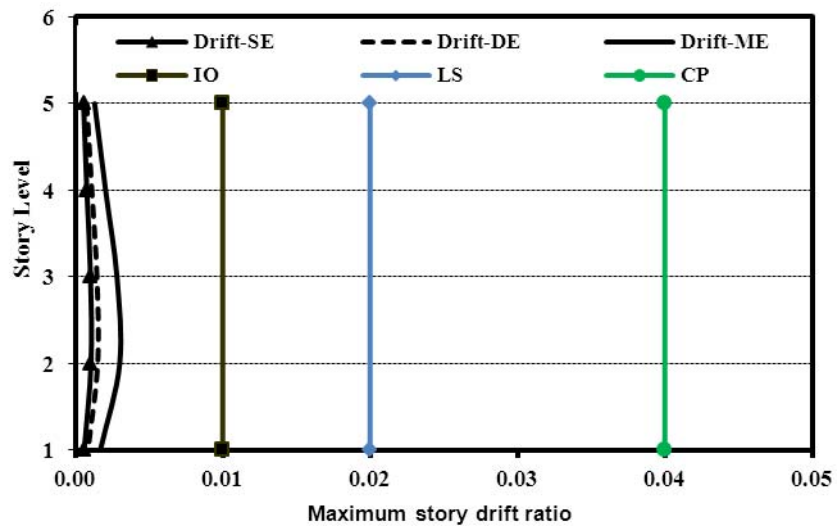


Fig. 4.41 Maximum story drift at performance point of 5-Story 2D frame for different earthquake level (Kobe earthquake)

Note: IO=Immediate Occupancy, LS= Life Safety, CP= Collapse Prevention

From above discussion, different figures, it has been concluded that the performance point of structure has maximum story drift ratio for 2-story frame and 5-story frames are less than IO

level in maximum earthquake level. These two frame satisfy local and global criteria specified in ATC-40[3]. Therefore it has been said that both the structure fulfills the performance objective at global level in serviceability earthquake (SE), design earthquake(DE) and maximum earthquake(ME).

4.9 Conclusion

Pushover analysis is a simplified nonlinear analysis to develop capacity curves of a structure and determine their performance. However, the correctness of using this analysis is sometimes questionable; particularly the load pattern used in pushover analysis to push the structure to failure is an important issue and should be able to model the real response under a seismic load. On the other hand, a nonlinear time history analysis (NLTHA) is capable of modeling the real seismic response under a real earthquake ground motion, although the method is time consuming and complicated. An important part of this current work is to compare capacity curves of pushover analysis with different load patterns and compare them with NLTHA.

In this chapter, linear time history analysis (LTHA) has been validated against published results of Chopra for a SDOF system. A nonlinear time history analysis (NLTHA) using SeismoStruct has also been tried to simulate an experiment where a bridge pier had been subjected to six different levels of ground motion and the results are comparable with the experiment. NLTHA was also carried out using SAP2000 [21] and the results were found to compare well with those of Seismostruct. A comparative study was done to observe the effect of damage in a NLTHA if used instead of linear analysis. NLTHA were extensively carried out on three frames to develop capacity curves and compare them with those obtained from pushover analysis with different load pattern e.g. triangular, elastic first mode and uniform. These analyses show that pushover analysis with uniform load pattern compares well with that of NLTHA. The analysis also showed that current pushover curves were similar to some published results. A performance evaluation of RC frames were carried out using NLTHA and showed that frames designed by BNBC for Dhaka city can easily satisfy the local and global performance requirements.

Chapter 5

Performance based analysis of RC frame building

5.1 Introduction

In Chapter 3, pushover analysis method has been validated by comparing capacity curves of 2D frames with published results. Demand curves are also checked by comparing procedures A and B. Performances of 2D frames designed by BNBC [1] has been found to satisfy required local and global performance levels. More rigorous nonlinear time history analysis has been studied in Chapter 4 where it has been validated against published result. Performance of 2D frames have also been checked by nonlinear time history analysis and BNBC designed frames have been found to satisfy the requirements. Loading patterns used in pushover analysis has been studied by comparing the capacity curves with those of nonlinear time history analysis to determine the more suitable pattern. Nonlinear time history analysis is more correct and rigorous method, however, use of nonlinear time history analysis is not suitable for everyday design office use and pushover analysis method can be a simpler alternative. In this chapter, pushover analysis is carried out on 3D buildings designed by BNBC [1] to check their performance adequacies for local and global cases.

A six storied building with RC moment resisting frames has been analyzed and design as per the provisions of BNBC [1] and pushover analysis is carried out to find the capacity curve. Local and global performances are investigated for three levels of earthquake demand for Dhaka city.

5.2 Performance requirements

To determine whether a building meets a specified performance objective, response quantities from a nonlinear static are compared with limits for appropriate performance levels. This chapter presents those structural response limits, which constitute acceptance criteria for the building structure. The response limits falls into two categories:

- a) Global acceptable limits: These response limits include requirements for the vertical load capacity, lateral load resistance and lateral drift.

- b) Element and component acceptability limits: Each element (frame, wall, diaphragm, or foundation) must be checked to determine if its components respond within acceptable limits.

Building performance objectives are checked against some predefined seismic demand. Seismic demand for a structure is totally site depended. For analysis development of site dependent elastic response spectrum is needed. The Federal Emergency Management Agency (FEMA-356) has recommended standard procedure to establish seismic demand at a site.

5.3 Description of 6-story reinforced concrete frame structure building

The structure is a six story residential building. The building is a 4x3 bay immediate moment resisting frame of grid 6m in both sides. It is fixed at its support at 2.0m below the existing ground level. Typical floor height is 3.0m except 4.0m at the ground floor for parking. Other structural dimensions are given in Table 5.1.

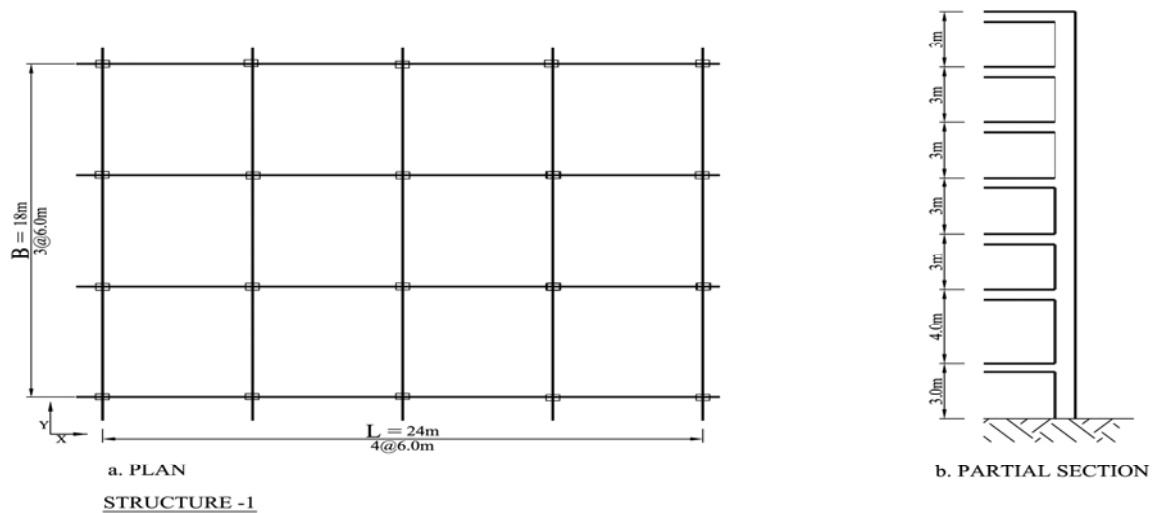


Fig. 5.1 Layout of the 6-story building

Table 5.1 Structural dimension of 6-story building

Element		Above ground	Below ground	Clear cover to re-bar center
COLUMN	Exterior	300x450mm	375x525mm	50.0 mm above ground and 75.0 mm below ground
	Interior	300x550mm	375x625mm	
BEAM	Grade Beam	325x455mm		75.0 mm all sides
	Floor Beam	250x450mm		50.0 mm all sides
SLAB	All Floor	140mm		

Default concrete material was used in the design of RC beam column having the following property:

28 days Cylinder strength of Concrete, $f'_c = 25$ MPa

Yield strength of Steel, $f_y = 410$ MPa

Modulus of elasticity, $E_c = 24821$ Mpa

Standard steel bar is used as reinforcing material.

Load used in design:

The Self weight of the structure is calculated automatically by the program. In addition to floor finish 1 kN/m² distributed on the floors including roof, live load 2 kN/m² are considered as dead load in typical floor level including roof. Self weight of the concrete members considering unit weight of concrete as 24 kN/m³, 250mm Brick work on the exterior beams and 125 mm brick work on the interior beams. Though there are no wall in the parking floor (ground Floor), 125 mm B/W assumed on the grade beams. Parapet on the roof considered as 125 mm brick work of height 1.50 m. Unit wt. of brick work considered as 23 kN/m³. Here site location is Dhaka. As per BNBC [1] seismic modification factor $R=8$ (IMRF) has been considered. Other co-efficient used as

Seismic zone coefficient, $Z=0.15$ for Zone 2, Structure importance coefficient, $I= 1.00$

Site coefficient, $S=1.5$

Assumption for pushover Analysis

ETABS is used here for the pushover analysis. The assumptions that are considered for the analysis by this software are as follows:

- 1) Moment (M3) and shear (V2) hinge is considered at each end of each beam and moment and axial (P-M-M) is considered at each end of column elements.
- 2) Three nonlinear cases are defined here. (a) Pushover analysis has been done using load pattern of equivalent static earthquake load calculated by program.
(b) Dead load was considered as the previous pushover cases for each analysis.
(c) Unload entire structure is selected for distribution of loads when local hinges fail.
(d) Geometric non-linearity (P- Δ effect) is considered with full dead load.
(e) Unload entire structure is considered for member unloading method.
(f) Horizontal displacement of topmost corner node has been selected for performance monitoring of roof displacement.
- 3) Special seismic design data are not included here.

4) In analysis option P- Δ effect and dynamic analysis option are considered.

5.3.1 Performance evaluation of a structure design as per BNBC

In Bangladesh, buildings are designed according to BNBC [1]. In this section, a structure, designed for gravity load and earthquake loads are analyzed to assess its performance. The geometry and other structural details are mention in the previous section 5.3. The design followed as BNBC [1] including earthquake and gravity loads. Performance point of the structure is evaluated for serviceability, design and maximum earthquake.

Performance point of any structure, demand curve is required and demand curve has been generated with ETABS [20]. But several parameters are required to generate the curves. In this section, those parameters are defined and demand curve is plotted by ETABS [20]. Capacity curves (base shear versus roof displacement) are the load-displacement envelopes of the structures and represent the global response of the structures. The maximum values of roof displacements and base shear are determined for deformation level to approximate a dynamic capacity curve for the building frame. The performance point is determined and compared for different level of earthquakes.

Establishment Demand Spectra: Location of the site: Dhaka city

Soil profile at the site: Soil type S_C as per Table 2.5 and 2.6 when the soil properties are not known in sufficient detail.

Table 5.2 Calculation of C_A

Seismic Zone Factor, Z	0.15	As per BNBC/93	0.15	As per BNBC/93	0.15	As per BNBC/93
Earthquake Hazard Level, E	0.5	Design Earthquake	1	Max Earthquake	0.35	Serviceability Earthquake
Factored E (E' \times 1.4)	0.7		1.4		0.49	
Near-Source Factor	1	>15km, table 2.4	1	>15km, table 2.4	1	>15km, table 2.4
Shaking Intensity, ZEN	0.105		0.21		0.0735	
For Soil Type S_C, C_A	0.126	From Table 2.5	0.249	From Table 2.5	0.088	From Table 2.5

Table 5.3 Calculation of C_V

Seismic Zone Factor, Z	0.15	as per BNBC/93	0.15	as per BNBC/93	0.15	as per BNBC/93
Earthquake Hazard Level, E	0.5	Design Earthquake	1	Max Earthquake	0.35	Serviceability Earthquake
Factored E (E' \times 1.4)	0.7		1.4		0.49	
Near-Source Factor	1	>15km, table 2.4	1	>15km, table 2.4	1	>15km, table 2.4
Shaking Intensity, ZEN	0.105		0.21		0.0735	
For Soil Type S_C, C_V	0.178	From Table 2.6	0.333	From Table 2.6	0.128	From Table 2.6

Table 5.4: Calculation of reduction factor

	Design Earthquake		Max Earthquake		Serviceability Earthquake	
	X-dir	Y-dir	X-dir	Y-dir	X-dir	Y-dir
Effective damping, β_{eff}	12.10	10.70	22.10	25.40	7.60	6.20
Spectral acceleration reduction factor, SR_A	0.71	0.75	0.52	0.48	0.86	0.93
Spectral velocity reduction factor, SR_V	0.78	0.81	0.63	0.60	0.90	0.95
Effective peak ground acceleration (EPA)	0.126g	0.126g	0.249g	0.249g	0.088g	0.088g
Average value of peak response	0.225g	0.237g	0.324g	0.297g	0.190g	0.204g
T_A	0.123 sec	0.122 sec	0.129 sec	0.134 sec	0.121 sec	0.119 sec
T_s	0.617 sec	0.608 sec	0.647 sec	0.669 sec	0.604 sec	0.593 sec

The capacity curve is superimposed on the response spectrum curve in ADRS format. It is seen from the analysis that the capacity curve intersects the demand curve. Performance point is the intersection point.

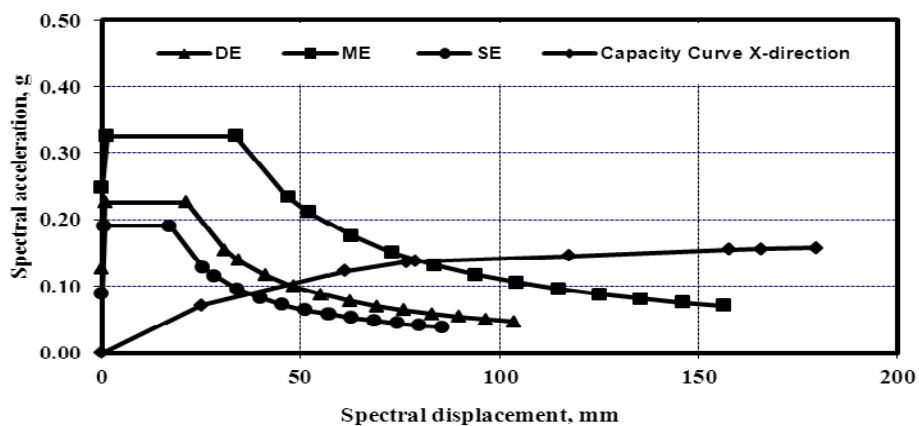


Fig. 5.2 Capacity spectrum of the six-story frame structure building in x-direction (Procedure A)

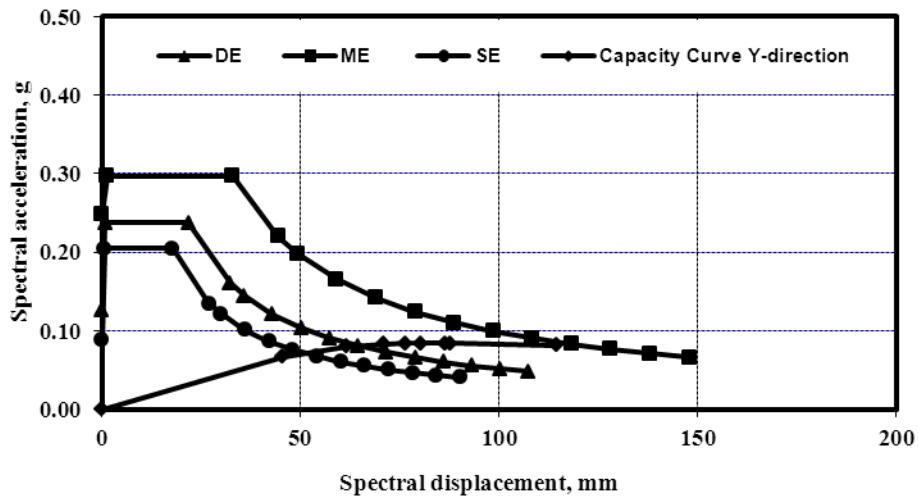


Fig. 5.3 Capacity spectrum of the six-story frame structure building in y-direction (Procedure A)

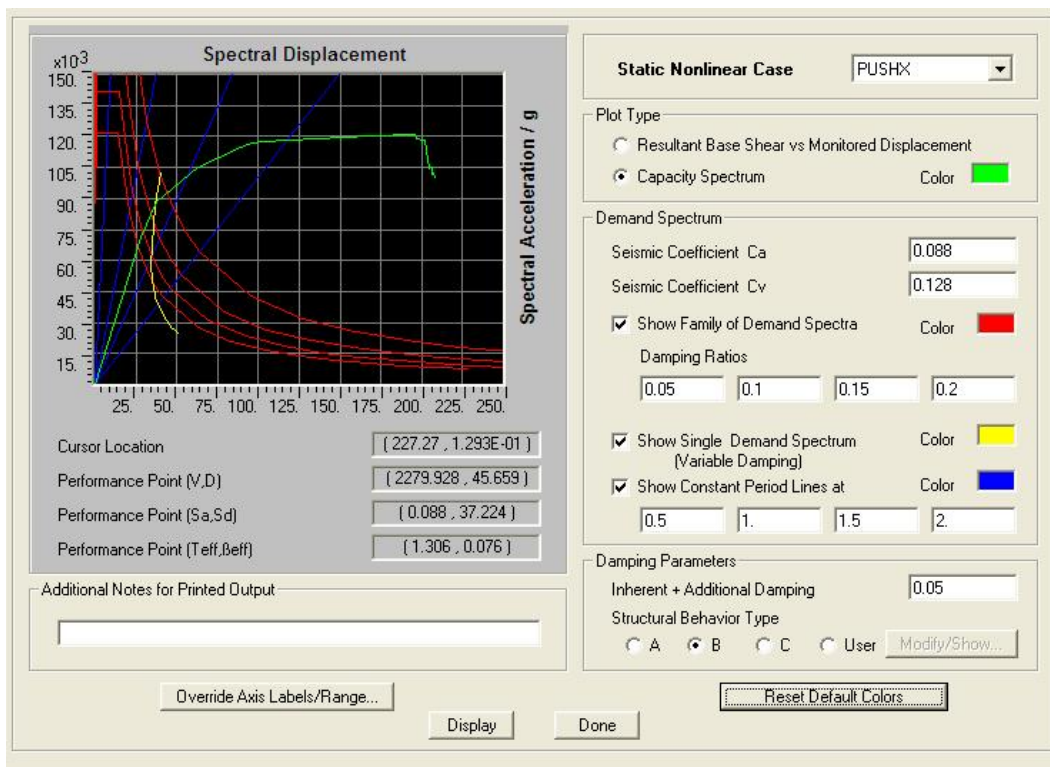
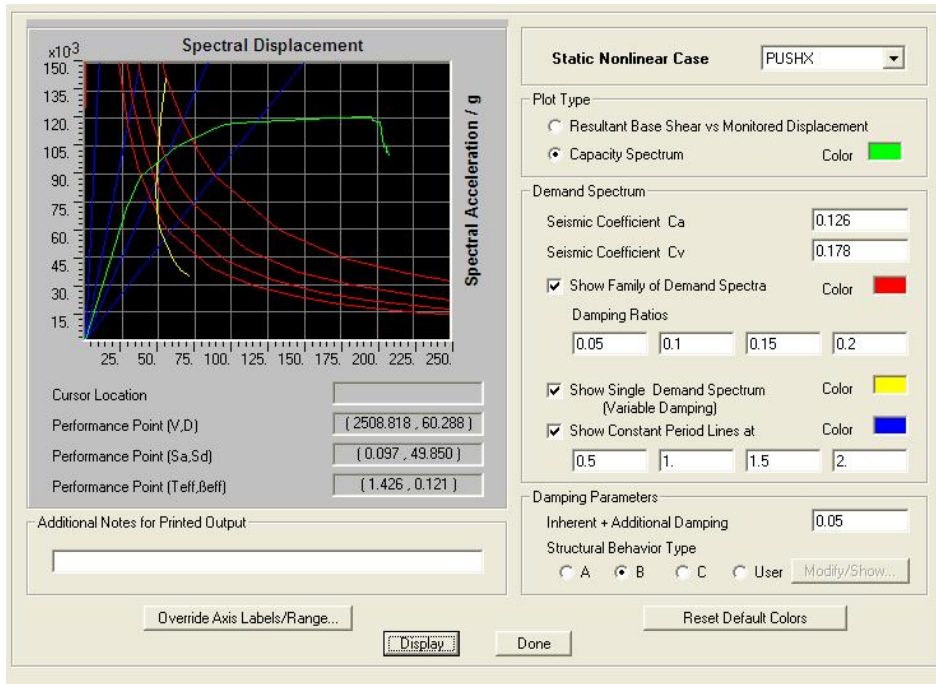
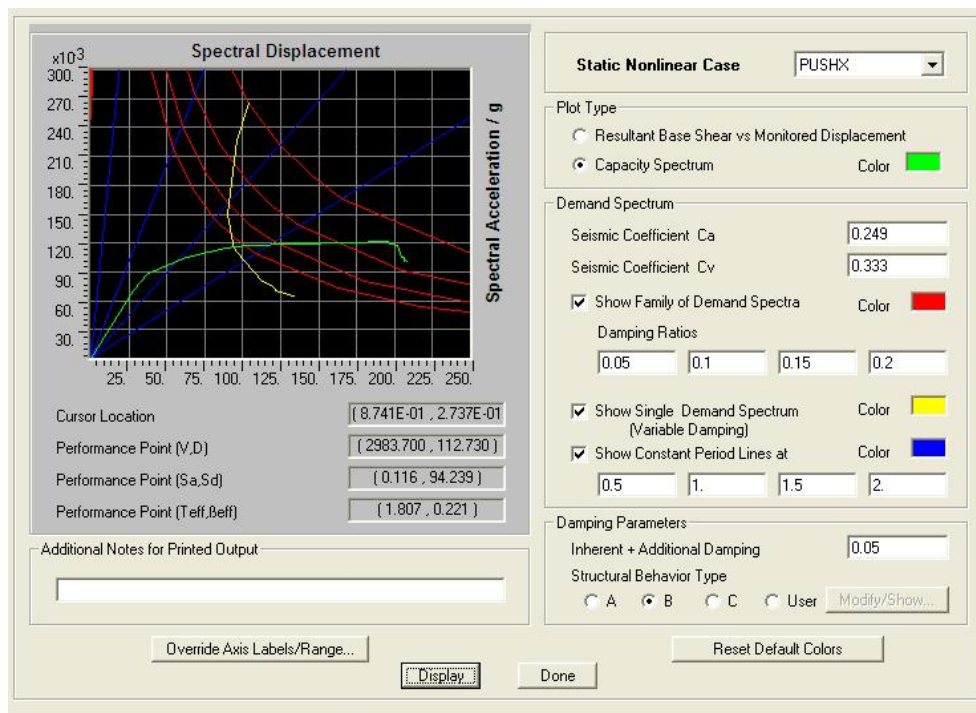


Fig. 5.4 Capacity spectrum of the six-story frame structure building in x-direction (SE) (Procedure B)



**Fig. 5.5 Capacity spectrum of the six-story frame structure building in x-direction (DE)
(Procedure B)**



**Fig. 5.6 Capacity spectrum of the six-story frame structure building in x-direction (ME)
(Procedure B)**

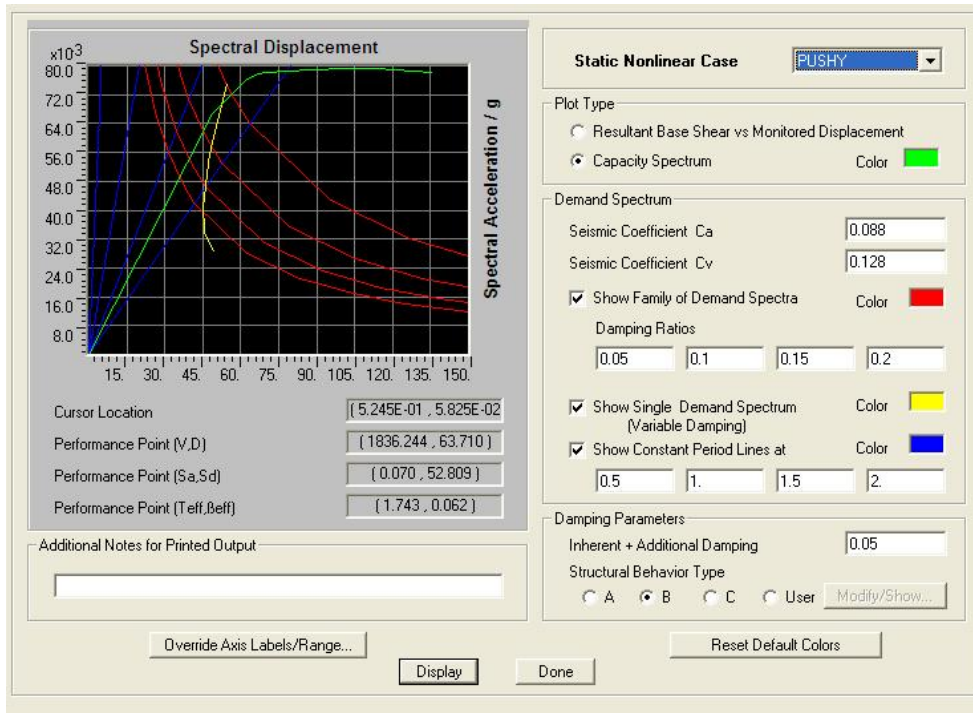


**Fig. 5.7 Capacity spectrum of the six-story frame structure building in y-direction (SE)
(Procedure B)**

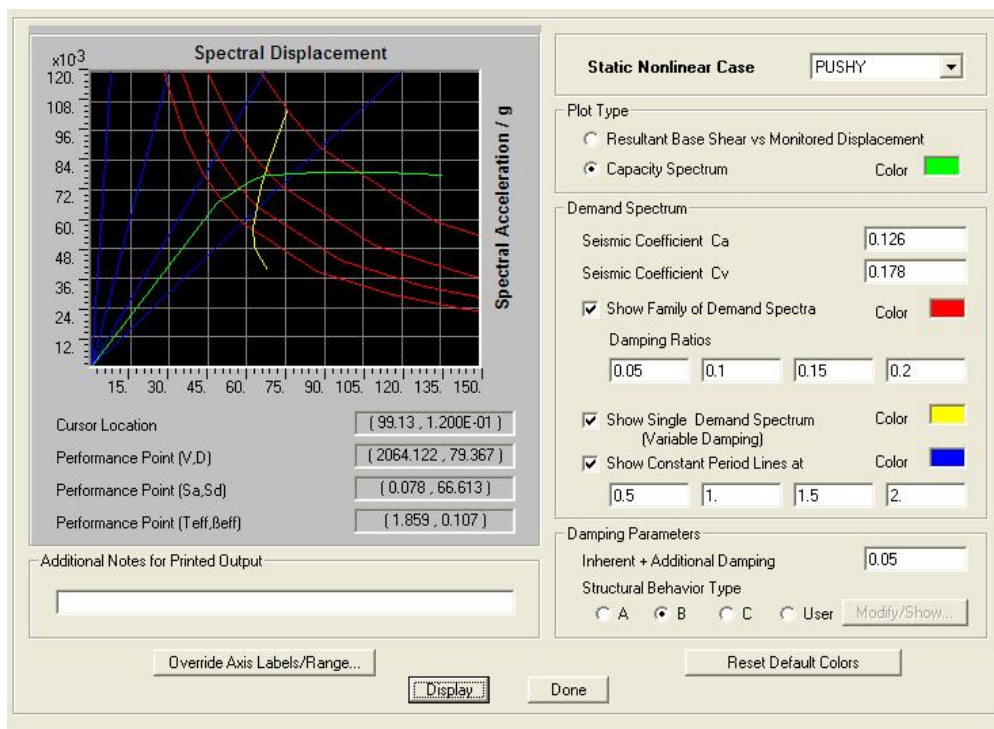


**Fig. 5.8 Capacity spectrum of the six-story frame structure building in y-direction (DE)
(Procedure B)**

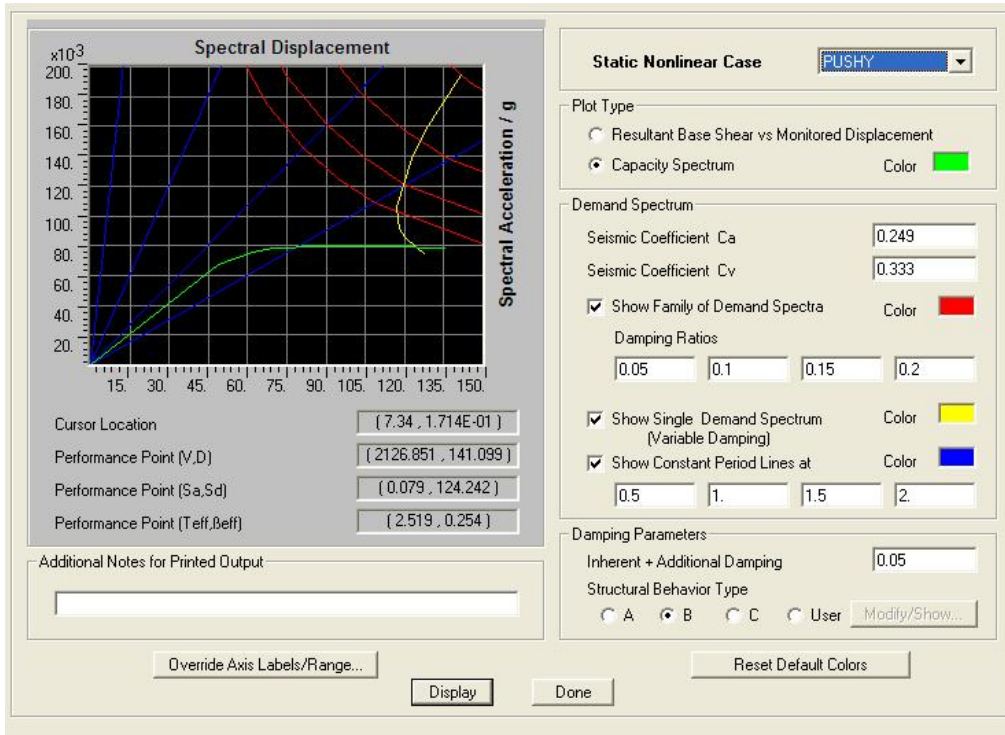


**Fig. 5.9 Capacity spectrum of the six-story frame structure building in y-direction (ME)
(Procedure B)**

From procedure A and B capacity curve illustrated in Figs 5.2 to 5.9. The performance point spectral displacement and spectral acceleration data for different earthquake are in Table 5.5.

Table 5.5 Capacity spectrum of the six story building (Procedure A and B)

	X-direction				Y-direction			
	Spectral acceleration		Spectral displacement, mm		Spectral acceleration		Spectral displacement, mm	
	Procedure A	Procedure B	Procedure A	Procedure B	Procedure A	Procedure B	Procedure A	Procedure B
Serviceability earthquake	0.085	0.088	38.00	37.22	0.075	0.070	51.00	52.80
Design earthquake	0.098	0.097	49.96	49.85	0.080	0.078	65.51	66.61
Maximum earthquake	0.126	0.116	78.63	94.24	0.081	0.079	118.20	124.24

From procedure A and B (Table 5.5) and Figs.5.4 to 5.9, it has seen that performance point spectral displacement and spectral acceleration are close to same. So it has been concluded that capacity spectrum of six story frame structure building is close to same for Procedure A and B.

5.3.1.1 Local level performance

For serviceability earthquake, number of hinges formed in x and y direction does not cross the Immediate Occupancy (IO) limit (Table 5.6). So it can be concluded that the local criteria as per ATC-40 [3] is satisfied for serviceability earthquake.

For design earthquake, number of hinges formed in x and y direction does not cross the Life Safety (LS) limit (Table 5.6). So it can be concluded that the local criteria as per ATC-40 [3] is satisfied for design earthquake.

For maximum earthquake, number of hinges formed in x and y direction does not cross the Collapse prevention (CP) limits (Table 5.6). So it can be concluded that the local criteria as per ATC-40 [3] is satisfied for maximum earthquake.

Therefore it has been said that the structure fulfills the performance objective at local level and performance of building frames designed as per BNBC has been evaluated against targeted performance levels for serviceability, design and maximum earthquakes.

Table 5.6 Number of hinges formed in the 6-storied frame structure building in x and y-direction

	A-B	B-IO	IO-LS	LS-CP	CP-C	C-D	D-E	>E	TOTAL
X-direction									
Serviceability earthquake	592	122	0	0	0	0	0	0	714
Design earthquake	558	96	60	0	0	0	0	0	714
Maximum earthquake	538	112	64	0	0	0	0	0	714
Y-direction									
Serviceability earthquake	639	71	4	0	0	0	0	0	714
Design earthquake	629	78	7	0	0	0	0	0	714
Maximum earthquake	584	65	35	18	0	2	3	7	714

Note: IO=Immediate Occupancy, LS= Life Safety, CP= Collapse Prevention

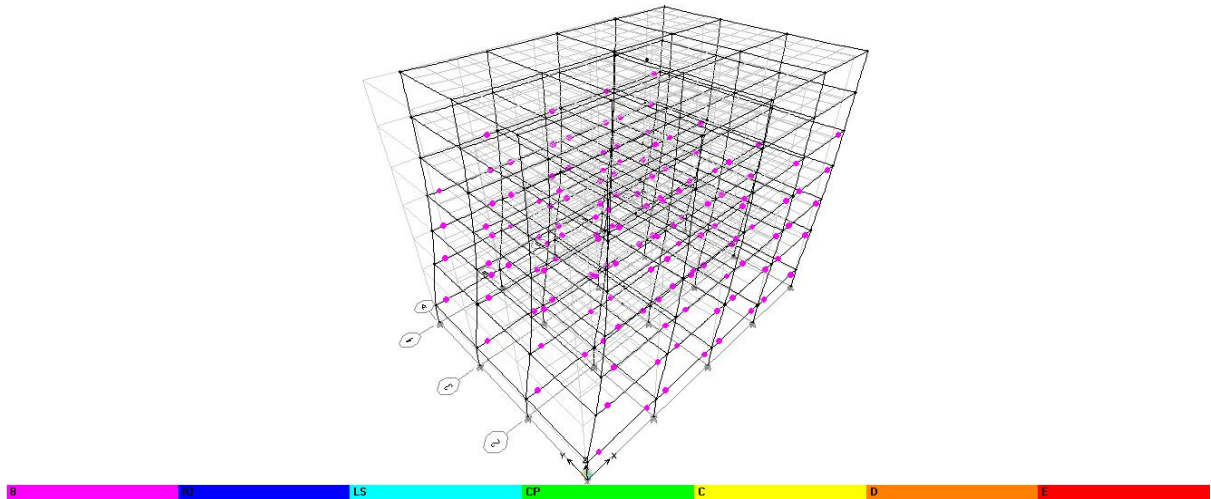


Fig. 5.10 Deformation of the building at performance point in x-direction for SE

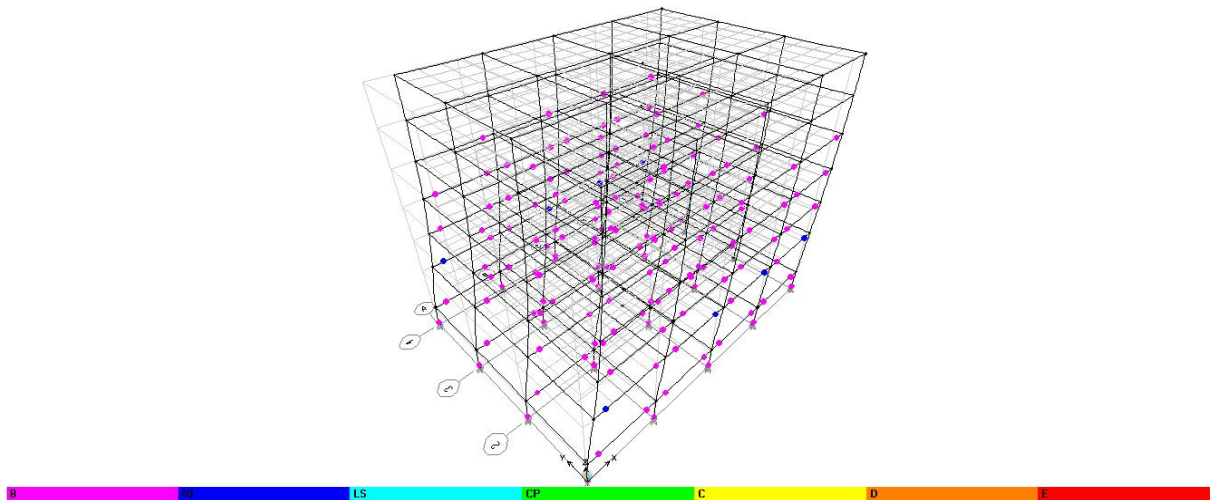


Fig. 5.11 Deformation of the building at performance point in x-direction for DE

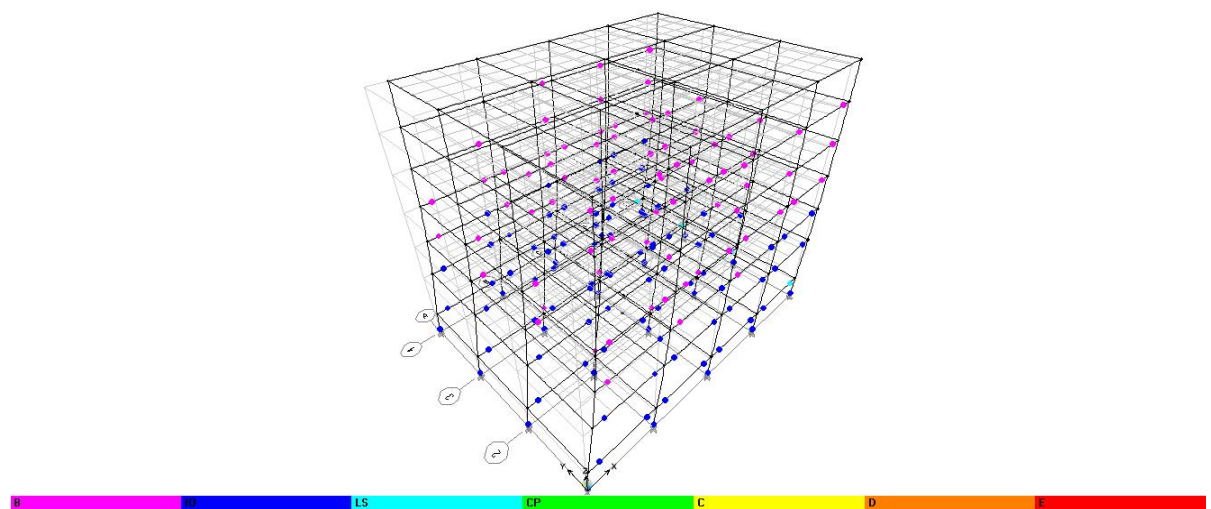


Fig. 5.12 Deformation of the building at performance point in x-direction for ME

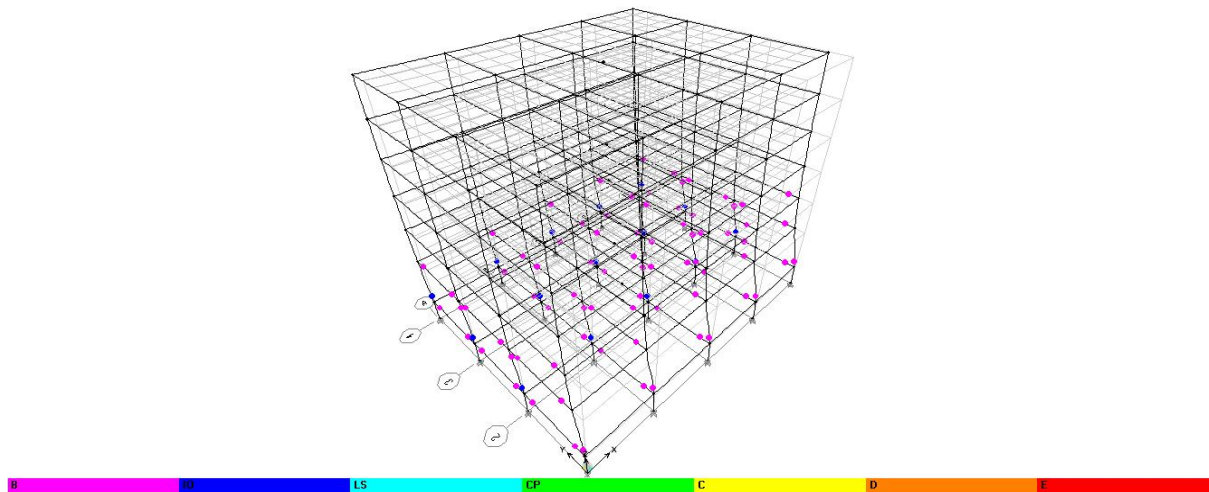


Fig. 5.13 Deformation of the building at performance point in y-direction for SE

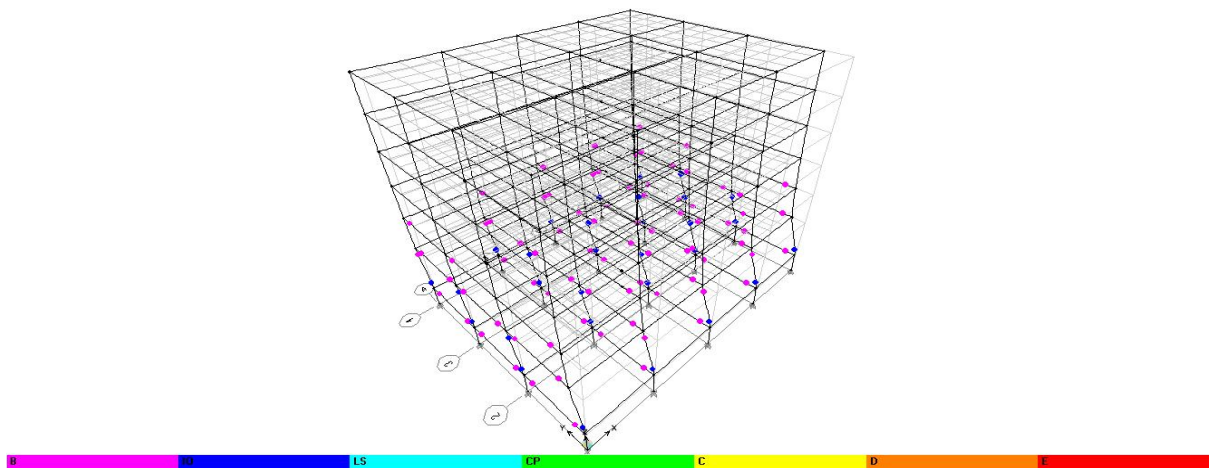


Fig. 5.14 Deformation of the building at performance point in y-direction DE

5.3.1.2 Global level performance

In this section, a structure, designed for gravity load and earthquake as per BNBC [1] is analyzed to assess its performance. The geometry and other structural details are same as mention in the previous section 5.3. The design followed as BNBC including earthquake and gravity loads. Performance point of the structure is evaluated for serviceability, design and maximum earthquake.

For serviceability earthquake, from Figs. 5.15 and 5.16, it is seen that story drift ratio does cross the Immediate Occupancy (IO) limits. So it can be concluded that structure is designed for earthquake and gravity load as per BNBC [1] satisfy at small earthquake.

For design earthquake, from Figs. 5.15 and 5.16, it is seen that story drift ratio does not cross the Life Safety (LS) limits. So it can be concluded that the global criteria as per ATC-40 [3] is satisfied for design earthquake.

For maximum earthquake, From Figs. 5.15 and 5.16, it is seen that story drift ratio does not cross the Life Safety (LS) limits. So it can be concluded that the global criteria as per ATC-40 [3] is satisfied for maximum earthquake.

Therefore it has been said that the structure fulfills the performance objective at global level and performance of building frames designed as per BNBC has been evaluated against targeted performance levels for serviceability, design and maximum earthquakes.

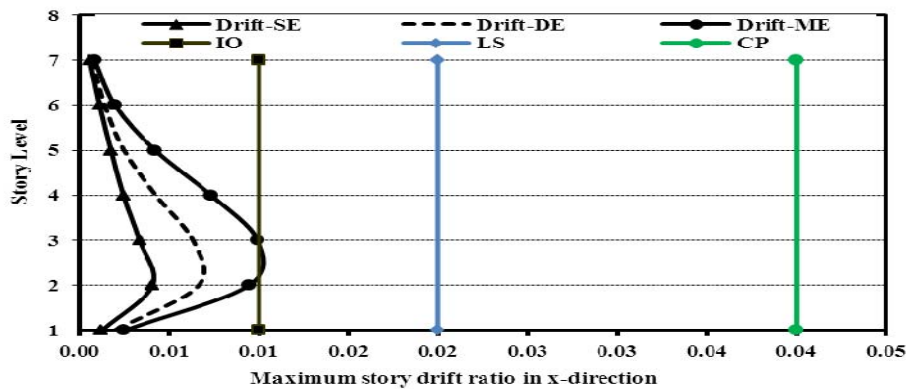


Fig. 5.15 Maximum story drift ratio at performance point for different earthquake level in X-direction

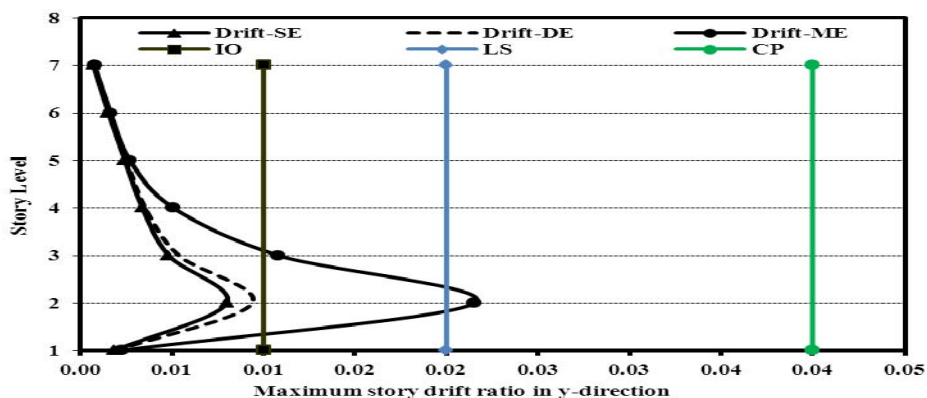


Fig. 5.16 Maximum story drift ratio at performance point for different earthquake level in Y-direction

Note: IO=Immediate Occupancy, LS= Life Safety, CP= Collapse Prevention

5.4 Performance of 6-story RC narrow building

In section 5.3 a 4X3 bay building, designed as per BNBC, has been analyzed to check its performance. In this current section, a somewhat narrow building is considered to observe whether it can satisfy the performance requirements as before. The geometry and other structural details are mentioned in the previous section 5.3. The building is a 4x2 bay immediate moment resisting frame of grid 6m in X-direction and 6m in Y-direction. It is fixed at its support at 2.0m below the existing ground level. Typical floor height is 3.0m except 4.0m at the ground floor for parking. Other structural dimensions are given in Table 5.7.

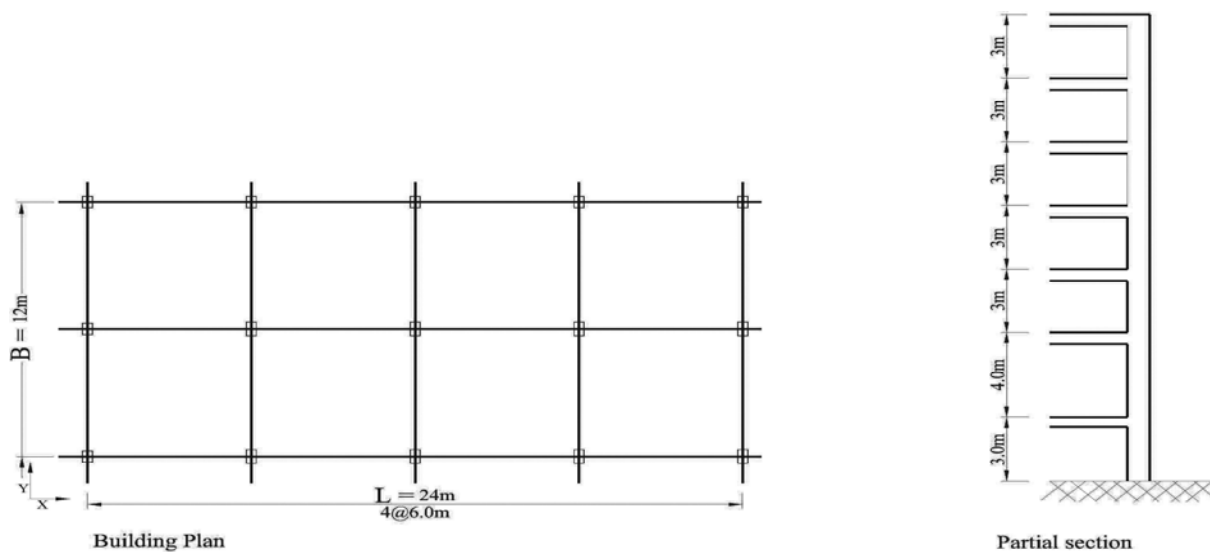


Fig. 5.17 Layout of the 6-story building

Table 5.7 Structural dimension of 6-story building

Element		Above ground	Below ground	Clear cover to re-bar center
COLUMN	Exterior	304x558mm	381x635mm	50.0 mm above ground and 75.0 mm below ground
	Interior	381x635mm	381x812mm	
BEAM	Grade Beam	325x455mm		75.0 mm all sides
	Floor Beam	250x450mm		50.0 mm all sides
SLAB	All Floor	140mm		

Materials properties are same as mention in the previous section 5.3. Load used in design are same as mention in the previous section 5.3.

5.4.1 Performance evaluation of a structure design as per BNBC

In Bangladesh, buildings are designed according to BNBC [1]. In this section, a structure, designed for gravity load and earthquake loads are analyzed to assess its performance. The geometry and other structural details are mention in the previous section 5.3. The design followed as BNBC [1] including earthquake and gravity loads. Performance point of the structure is evaluated for serviceability, design and maximum earthquake.

Performance point of any structure, demand curve is required and demand curve has been generated with ETABS [20]. But several parameters are required to generate the curves. In this section, those parameters are defined and demand curve is plotted by ETABS [20]. Capacity curves (base shear versus roof displacement) are the load-displacement envelopes of the structures and represent the global response of the structures. The maximum values of roof displacements and base shear are determined for deformation level to approximate a dynamic capacity curve for the building frame. The performance point is determined and compared for different level of earthquakes.

Establishment Demand Spectra: Location of the site: Dhaka city

Soil profile at the site: Soil type S_C as per Table 2.5 and 2.6 when the soil properties are not known in sufficient detail.

Table 5.8 Calculation of reduction factor

	Design Earthquake		Max Earthquake		Serviceability Earthquake	
	X-dir	Y-dir	X-dir	Y-dir	X-dir	Y-dir
Effective damping, β_{eff}	13.10	10.50	22.10	23.50	8.10	6.50
Spectral acceleration reduction factor, SR_A	0.69	0.76	0.52	0.50	0.84	0.91
Spectral velocity reduction factor, SR_V	0.76	0.82	0.63	0.62	0.88	0.93
Effective peak ground acceleration (EPA)	0.126g	0.126g	0.249g	0.249g	0.088g	0.088g
Average value of peak response	0.217g	0.230g	0.324g	0.312g	0.185g	0.201g
T_A	0.125 sec	0.121 sec	0.129 sec	0.131 sec	0.121 sec	0.119 sec
T_s	0.624 sec	0.607 sec	0.647 sec	0.657 sec	0.605 sec	0.595 sec

The capacity curve is superimposed on the response spectrum curve in ADRS format. It is seen from the analysis that the capacity curve intersects the demand curve. Performance point is the intersection point.

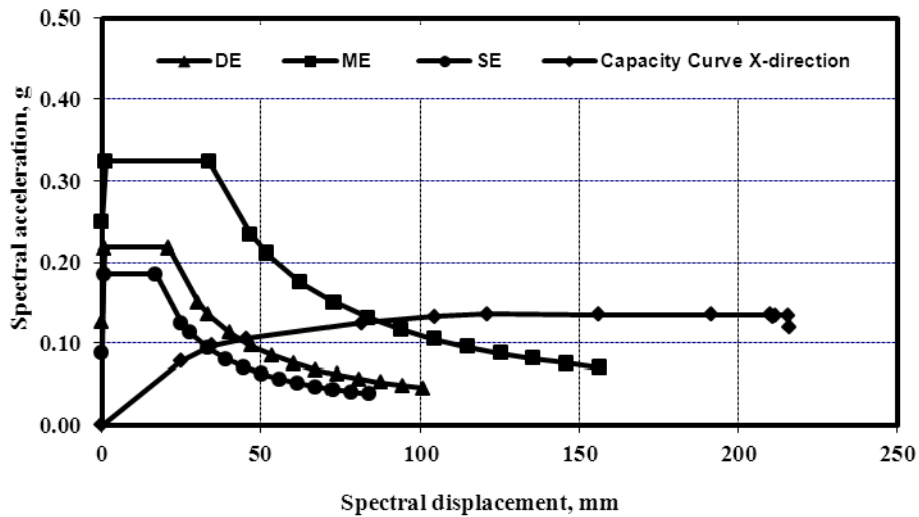


Fig. 5.18 Capacity spectrum of the six-story frame structure building in x-direction (Procedure A)

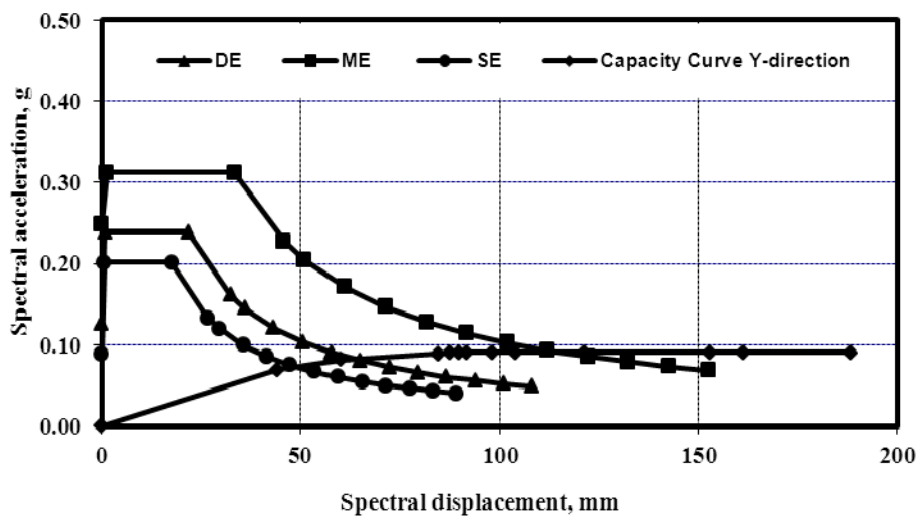


Fig. 5.19 Capacity spectrum of the six-story frame structure building in y-direction (Procedure A)

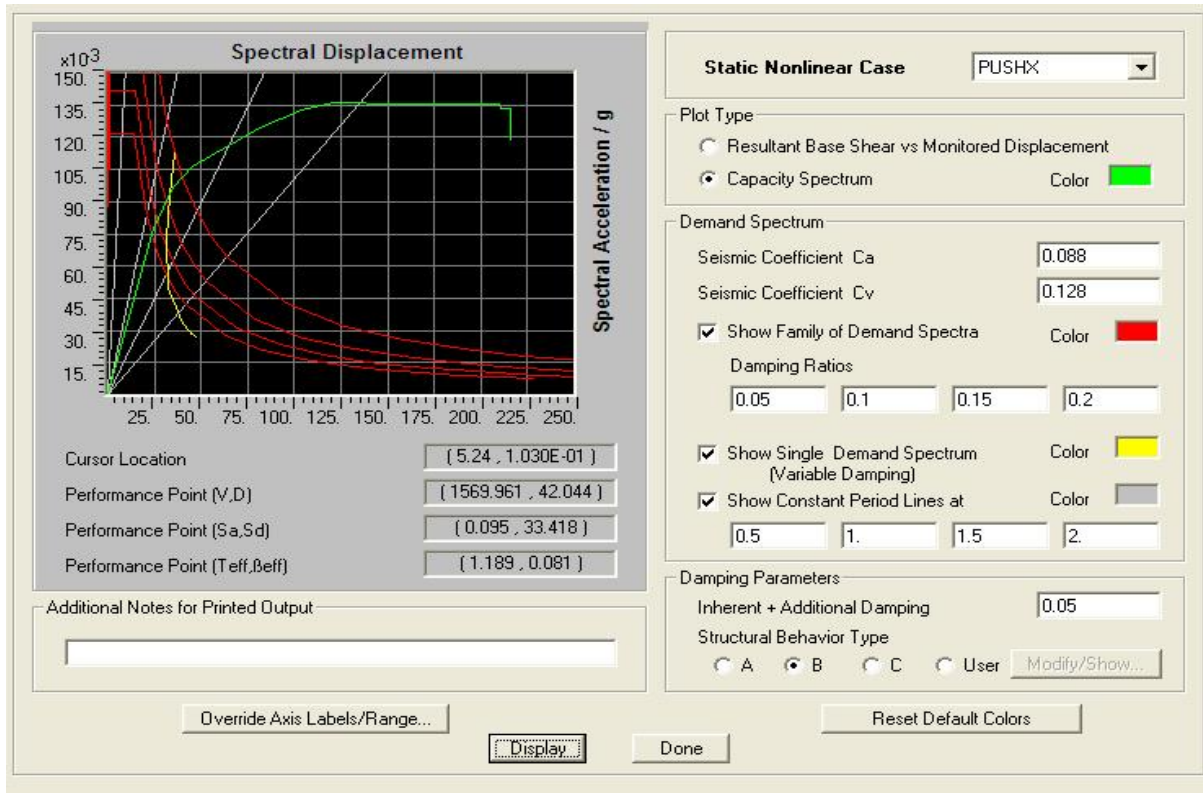


Fig. 5.20 Capacity spectrum of the six-story frame structure building in x-direction (SE) (Procedure B)

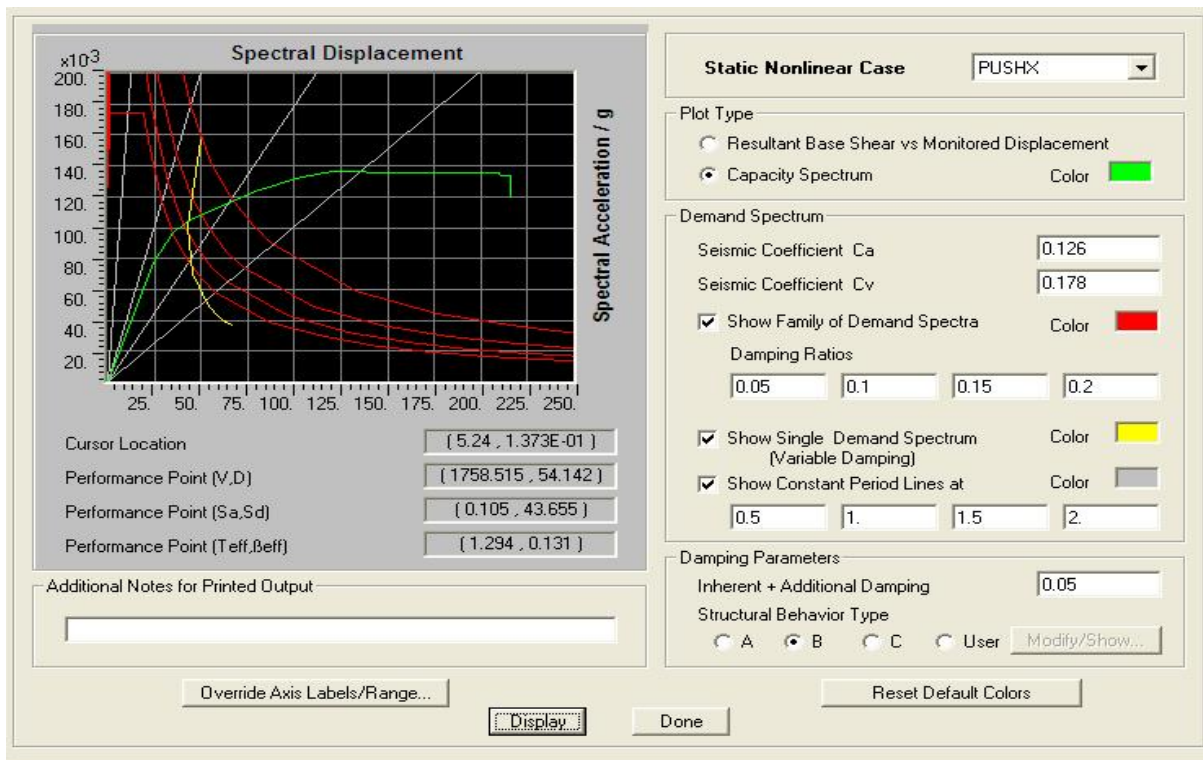


Fig. 5.21 Capacity spectrum of the six-story frame structure building in x-direction (DE) (Procedure B)

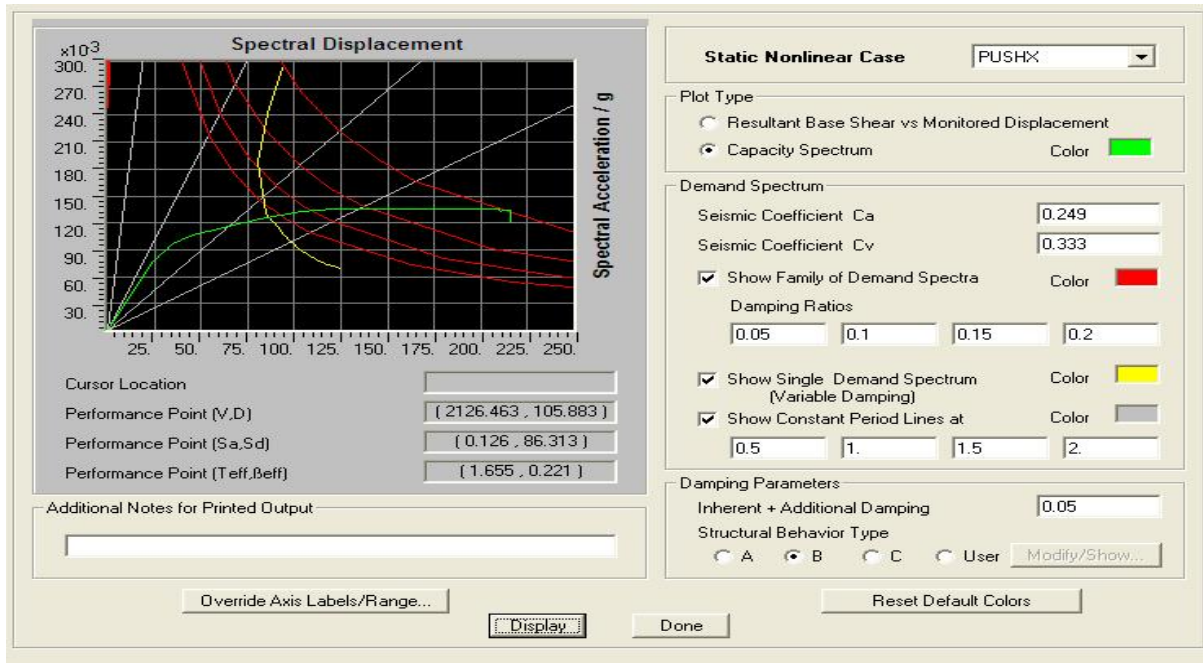


Fig. 5.22 Capacity spectrum of the six-story frame structure building in x-direction (ME) (Procedure B)

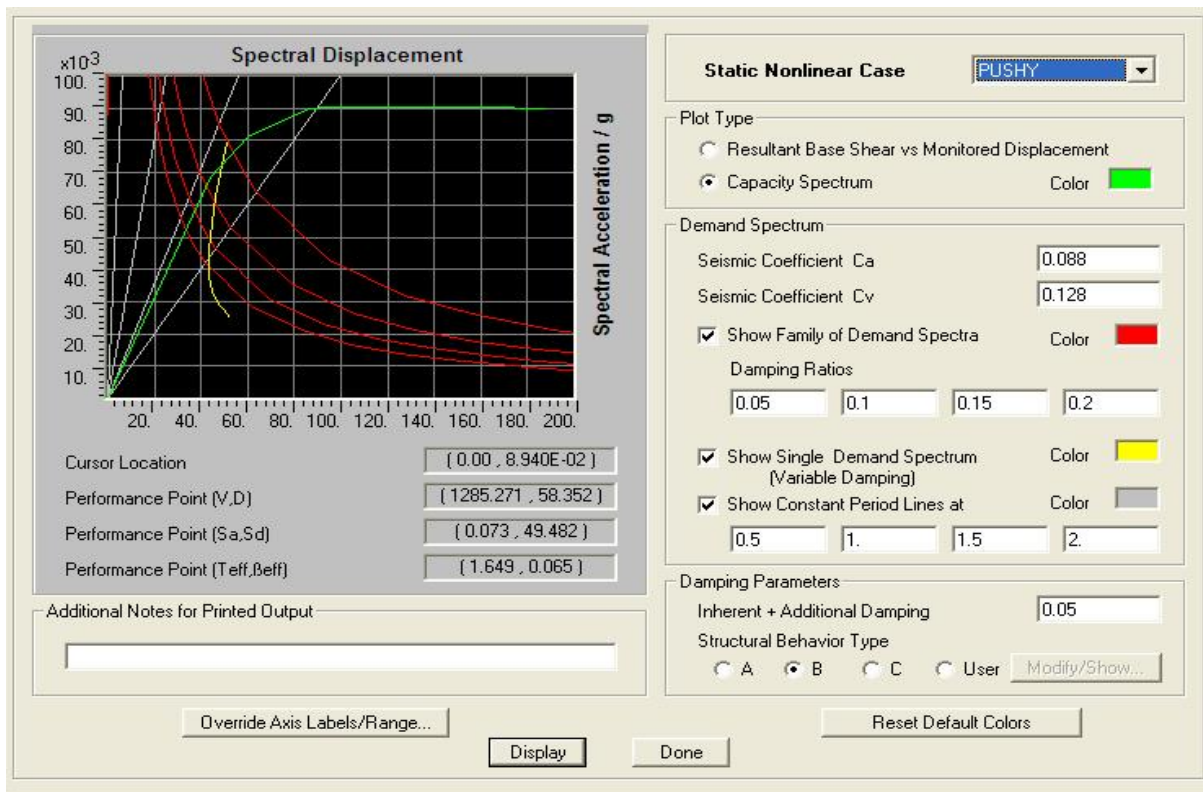


Fig. 5.23 Capacity spectrum of the six-story frame structure building in y-direction (SE) (Procedure B)

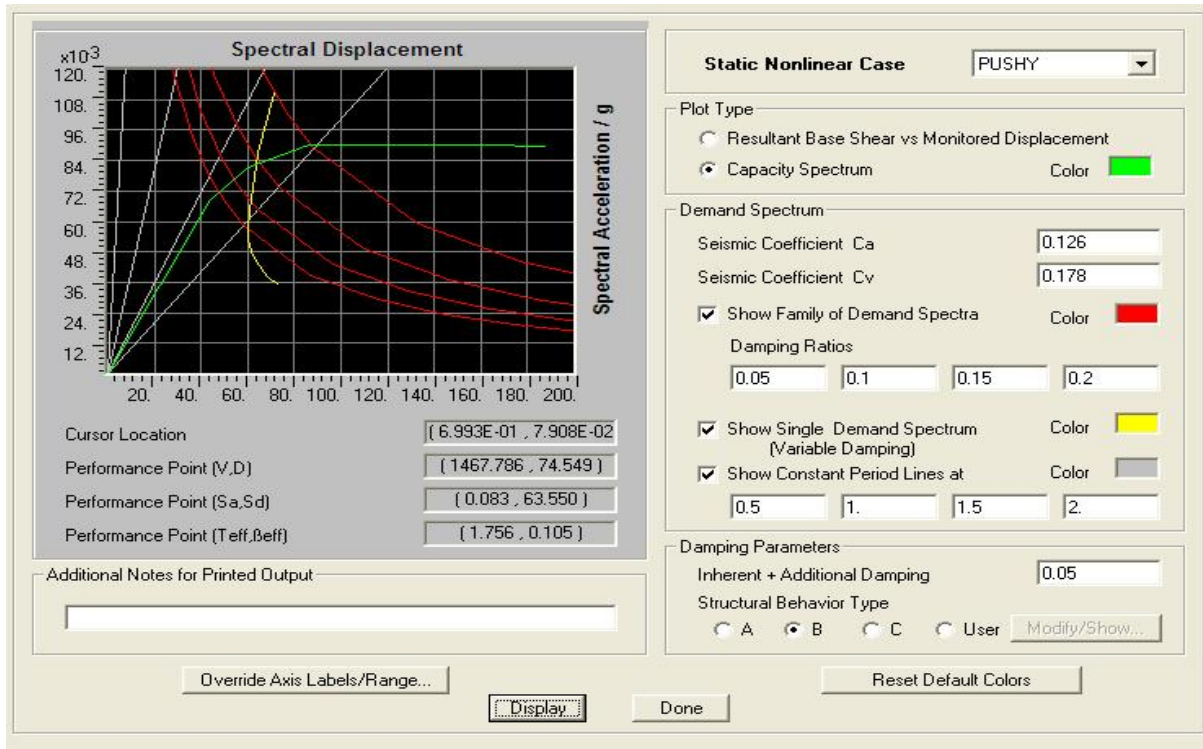


Fig. 5.24 Capacity spectrum of the six-story frame structure building in y-direction (DE) (Procedure B)

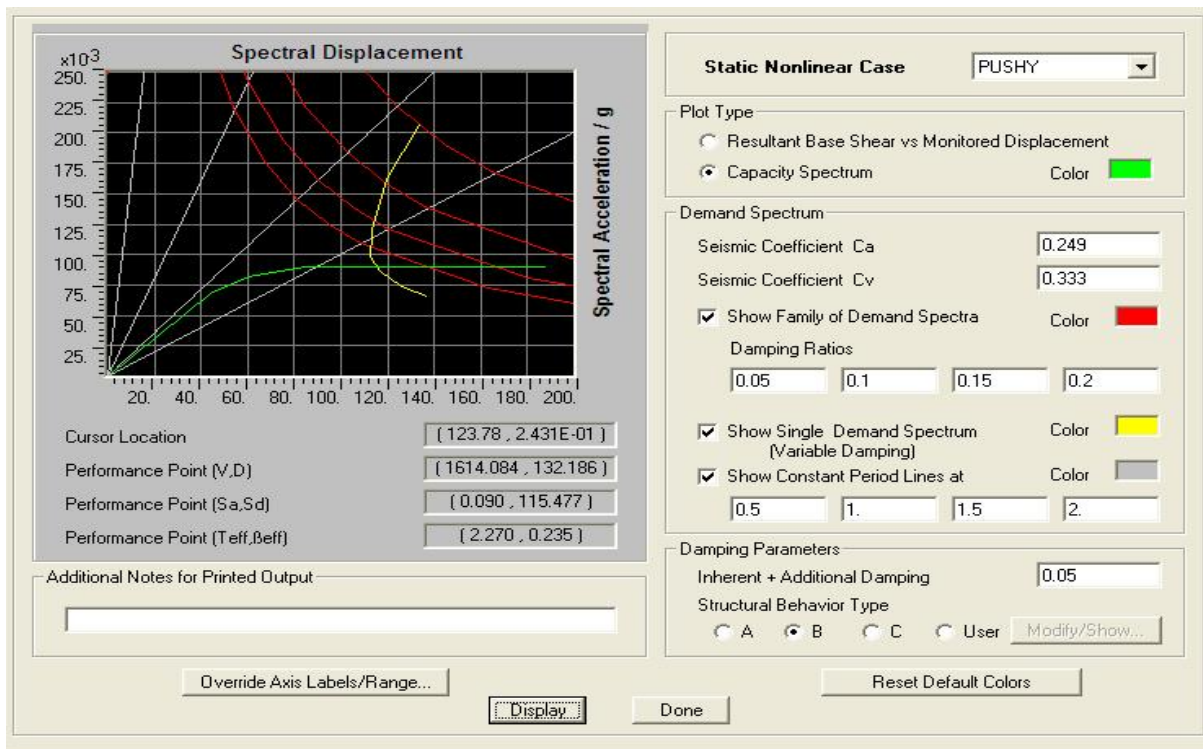


Fig. 5.25 Capacity spectrum of the six-story frame structure building in y-direction (ME) (Procedure B)

From procedure A and B capacity curve illustrated in Figs 5.18 to 5.25. The performance point spectral displacement and spectral acceleration data for different earthquake are in Table 5.9.

Table 5.9 Capacity spectrum of the six story building (Procedure A and B)

	X-direction				Y-direction			
	Spectral acceleration		Spectral displacement, mm		Spectral acceleration		Spectral displacement, mm	
	Procedure A	Procedure B	Procedure A	Procedure B	Procedure A	Procedure B	Procedure A	Procedure B
Serviceability earthquake	0.097	0.095	34.54	33.42	0.081	0.073	45.17	49.48
Design earthquake	0.106	0.105	45.58	43.65	0.089	0.083	64.88	63.55
Maximum earthquake	0.125	0.126	84.32	86.31	0.09	0.09	125.44	115.48

From procedure A and B (Table 5.9) and Figs.5.20 to 5.25, it has seen that performance point spectral displacement and spectral acceleration are close to same. So it has been concluded that capacity spectrum of six story frame structure building is close to same for Procedure A and B.

5.4.1.1 Local level performance

For serviceability earthquake, number of hinges formed in x and y direction does not cross the Immediate Occupancy (IO) limit (Table 5.10). For design earthquake, number of hinges formed in x and y direction does not cross the Life Safety (LS) limit (Table 5.10). For maximum earthquake, number of hinges formed in x and y direction does not cross the Collapse prevention (CP) limits (Table 5.10). So it can be concluded that the local criteria as per ATC-40 [3] is satisfied for serviceability, design and maximum earthquake.

Therefore it has been said that the structure fulfills the performance objective at local level and performance of building frames designed as per BNBC has been evaluated against targeted performance levels for serviceability, design and maximum earthquakes.

Table 5.10 Number of hinges formed in the 6-storied frame structure building in x and y-direction

	A-B	B-IO	IO-LS	LS-CP	CP-C	C-D	D-E	>E	TOTAL
X-direction									
Serviceability earthquake	434	84	0	0	0	0	0	0	518
Design earthquake	405	71	42	0	0	0	0	0	518
Maximum earthquake	359	87	57	15	0	0	0	0	518
Y-direction									
Serviceability earthquake	451	57	10	0	0	0	0	0	518
Design earthquake	444	64	10	0	0	0	0	0	518
Maximum earthquake	423	40	20	35	0	0	0	0	518

Note: IO=Immediate Occupancy, LS= Life Safety, CP= Collapse Prevention

5.4.1.2 Global level performance

In this section, a structure, designed for gravity load and earthquake as per BNBC [1] is analyzed to assess its performance. The geometry and other structural details are same as mention in the previous section 5.3. The design followed as BNBC including earthquake and gravity loads. Performance point of the structure is evaluated for serviceability, design and maximum earthquake.

For serviceability earthquake, from Figs. 5.26 and 5.27, it is seen that story drift ratio does cross the Immediate Occupancy (IO) limits. For design earthquake, from Figs. 5.26 and 5.27, it is seen that story drift ratio does not cross the Life Safety (LS) limits. For maximum earthquake, from Figs. 5.26 and 5.27, it is seen that story drift ratio does not cross the Life Safety (LS) limits. So it can be concluded that the global criteria as per ATC-40 [3] is satisfied for serviceability, design and maximum earthquake.

Therefore it has been said that the structure fulfills the performance objective at global level and performance of building frames designed as per BNBC has been evaluated against targeted performance levels for serviceability, design and maximum earthquakes.

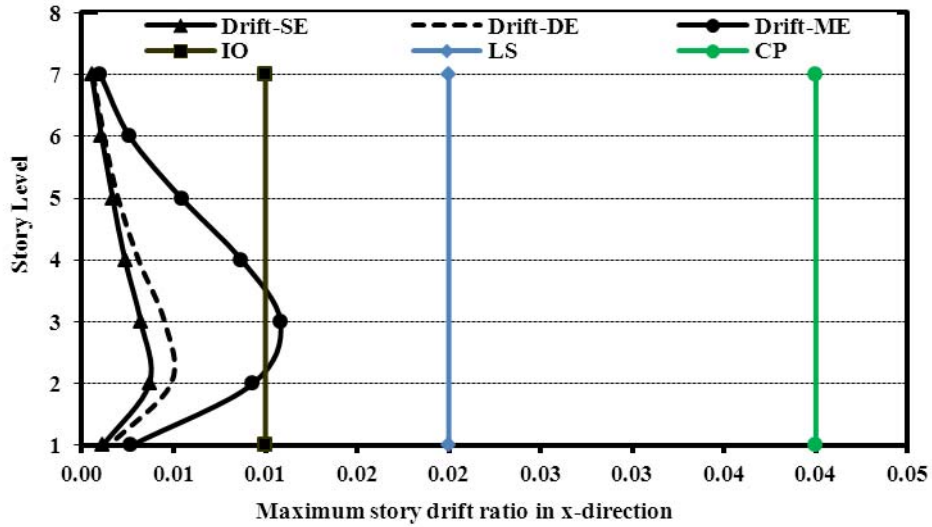


Fig. 5.26 Maximum story drift ratio at performance point for different earthquake level in X-direction

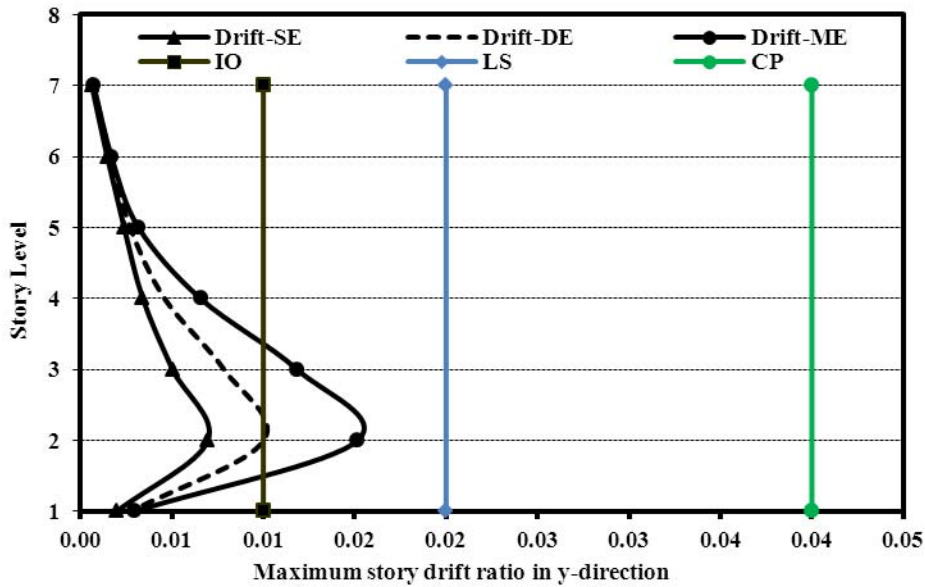


Fig. 5.27 Maximum story drift ratio at performance point for different earthquake level in Y-direction

Note: IO=Immediate Occupancy, LS= Life Safety, CP= Collapse Prevention

A typical 6-story building with aspect ratio of 0.5, situated in Dhaka city (Zone 2) was analyzed using finite element methodology developed in this study. The results obtained from the analysis are studied and seismic performances are checked against ATC-40[3] local and global requirements. It has been seen that the story drifts for maximum, design, and serviceability

earthquakes are within specified limits. It has also been found that number of hinges formed in the structure does not cross the specified limits for three levels of earthquakes.

5.5 Performance of 12-story RC frame building

In sections 5.3 and 5.4, 6-storied buildings have been considered to check their seismic performances. In the current section, the structure chosen for analysis is a 12-story residential building. The building is a 4x3 bay immediate moment resisting frame of grid 6m in both sides. It is fixed at its support at 2.0m below the existing ground level. Typical floor height is 3.0m except 4.0m at the ground floor for parking. Other structural dimensions are given in Table 5.11.

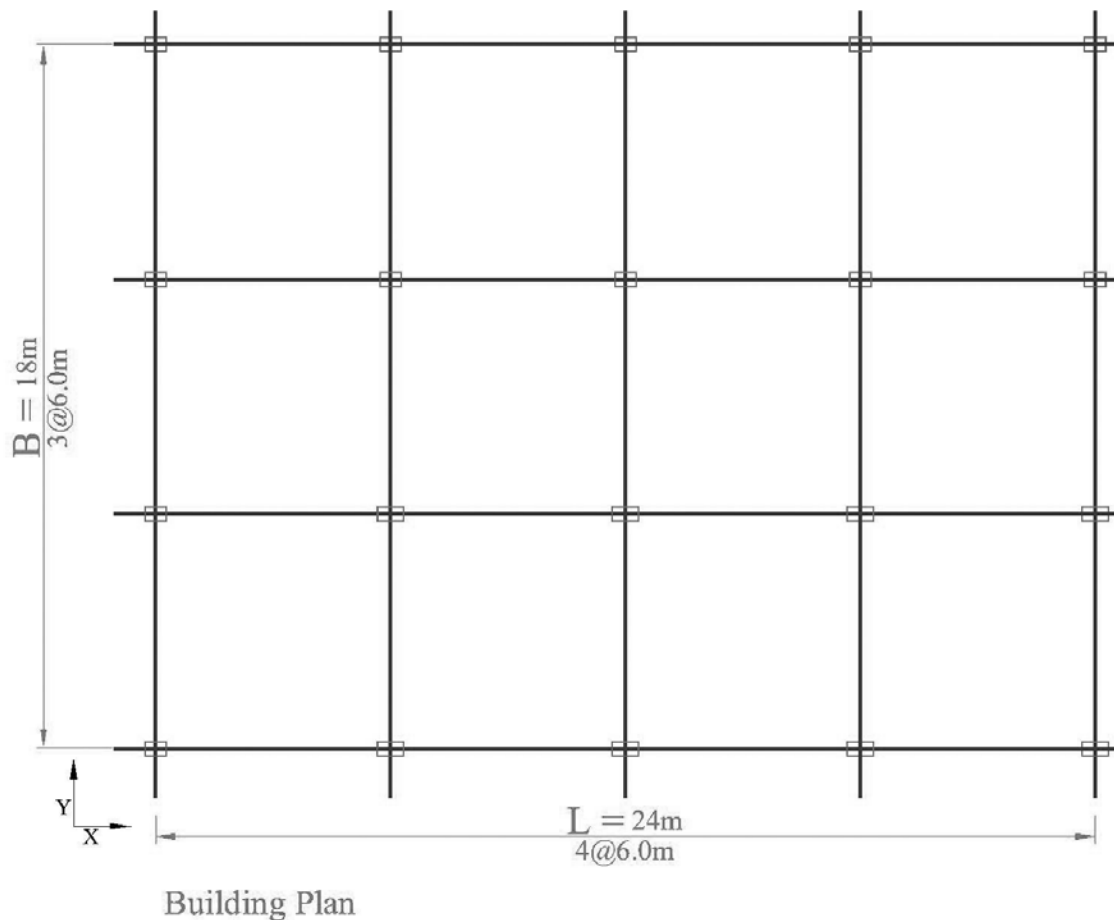


Fig. 5.28 Layout of 12-story building

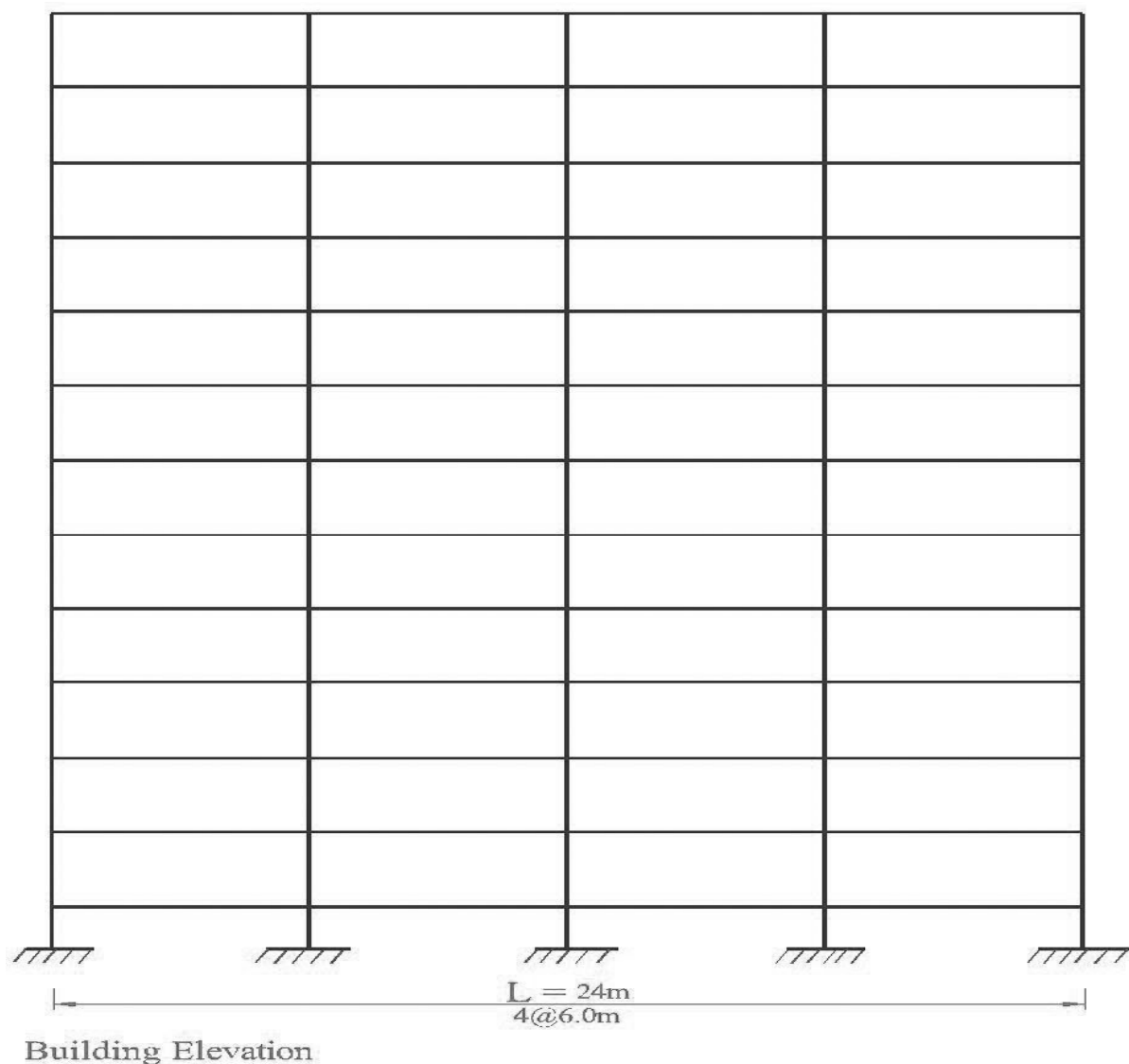


Fig. 5.29 Elevation of 12-story building

Table 5.11 Structural dimension of 12-story building

Element		Above ground	Below ground	Clear cover to re-bar center
COLUMN	Exterior	381x635mm	381x635mm	50.0 mm above ground and 75.0 mm below ground
	Interior	381x635mm	381x762mm	
BEAM	Grade Beam	325x455mm		75.0 mm all sides
	Floor Beam	250x450mm		50.0 mm all sides
SLAB	All Floor	140mm		

Materials properties are same as mention in the previous section 5.3. Load used in design are same as mention in the previous section 5.3.

5.5.1 Performance evaluation of a structure design as per BNBC

In Bangladesh, buildings are designed according to BNBC [1]. In this section, a structure, designed for gravity load and earthquake loads are analyzed to assess its performance. The geometry and other structural details are mention in the previous section 5.3. The design followed as BNBC [1] including earthquake and gravity loads. Performance point of the structure is evaluated for serviceability, design and maximum earthquake.

Performance point of any structure, demand curve is required and demand curve has been generated with ETABS [20]. But several parameters are required to generate the curves. In this section, those parameters are defined and demand curve is plotted by ETABS [20]. Capacity curves (base shear versus roof displacement) are the load-displacement envelopes of the structures and represent the global response of the structures. The maximum values of roof displacements and base shear are determined for deformation level to approximate a dynamic capacity curve for the building frame. The performance point is determined and compared for different level of earthquakes.

Establishment Demand Spectra: Location of the site: Dhaka city

Soil profile at the site: Soil type S_C as per Table 2.5 and 2.6 when the soil properties are not known in sufficient detail.

Table 5.12 Calculation of reduction factor

	Design Earthquake		Max Earthquake		Serviceability Earthquake	
	X-dir	Y-dir	X-dir	Y-dir	X-dir	Y-dir
Effective damping, β_{eff}	11.80	10.70	22.90	24.70	6.70	5.90
Spectral acceleration reduction factor, SR_A	0.72	0.75	0.51	0.49	0.90	0.94
Spectral velocity reduction factor, SR_V	0.79	0.81	0.62	0.60	0.93	0.96
Effective peak ground acceleration (EPA)	0.126g	0.178g	0.249g	0.333g	0.088g	0.128g
Average value of peak response	0.228g	0.237g	0.317g	0.303g	0.199g	0.208g
T_A	0.123 sec	0.122 sec	0.131 sec	0.133 sec	0.119 sec	0.118 sec
T_s	0.615 sec	0.608 sec	0.653 sec	0.665 sec	0.597 sec	0.591 sec

The capacity curve is superimposed on the response spectrum curve in ADRS format. It is seen from the analysis that the capacity curve intersects the demand curve. Performance point is the intersection point.

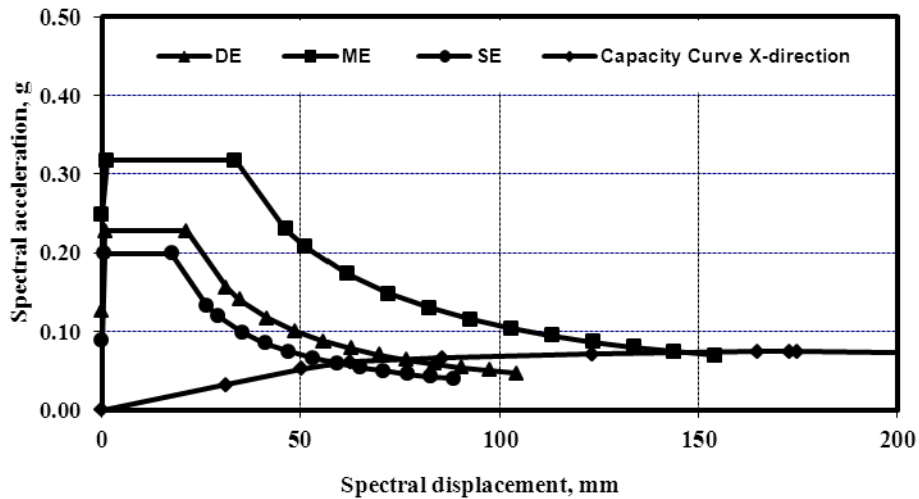


Fig. 5.30 Capacity spectrum of the 12-story frame structure building in x-direction (Procedure A)

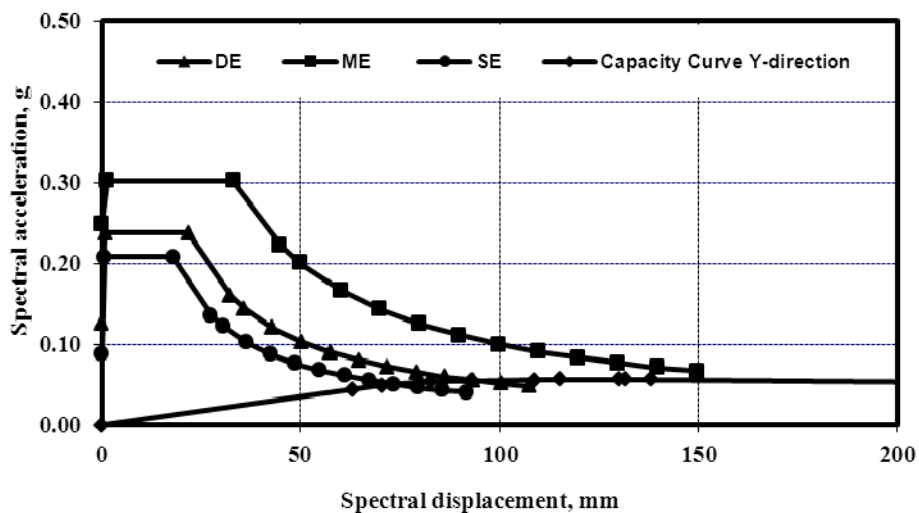


Fig. 5.31 Capacity spectrum of the 12-story frame structure building in y-direction (Procedure A)

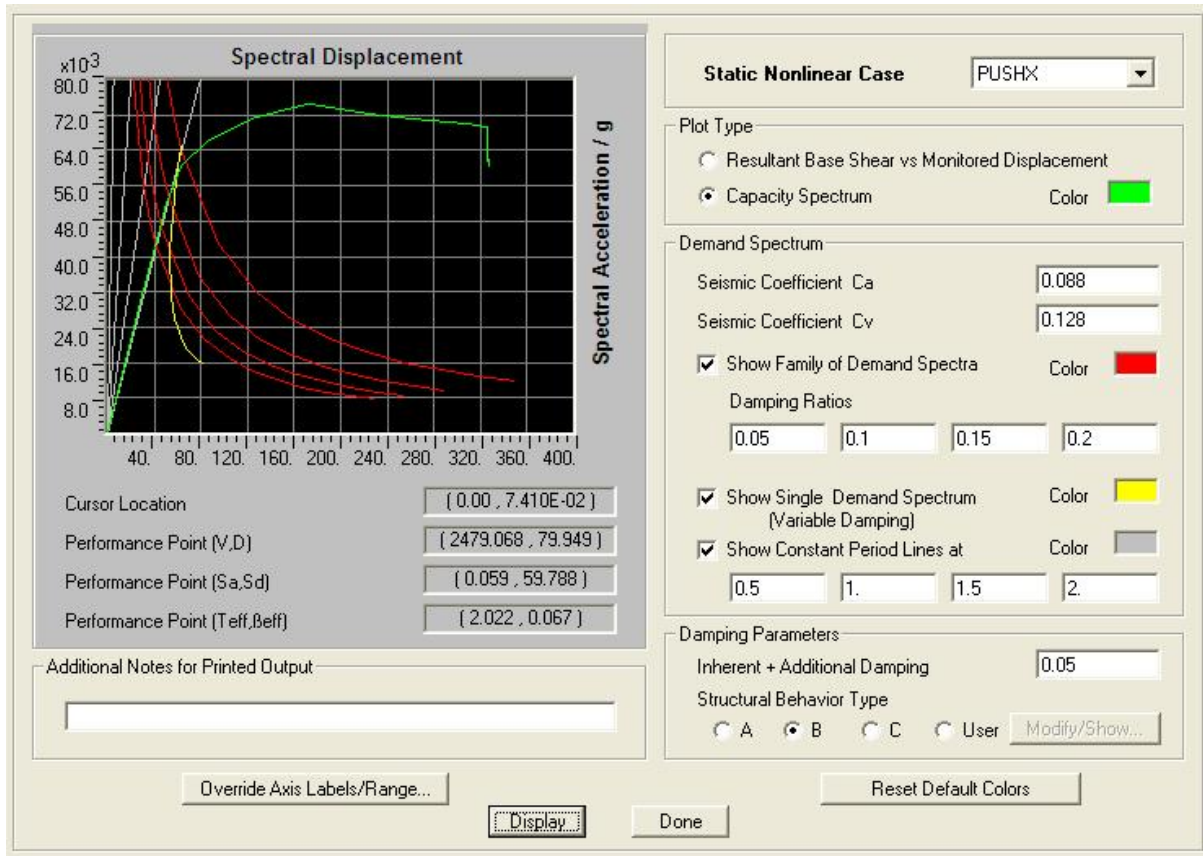


Fig. 5.32 Capacity spectrum of the 12-story frame structure building in x-direction (SE) (Procedure B)

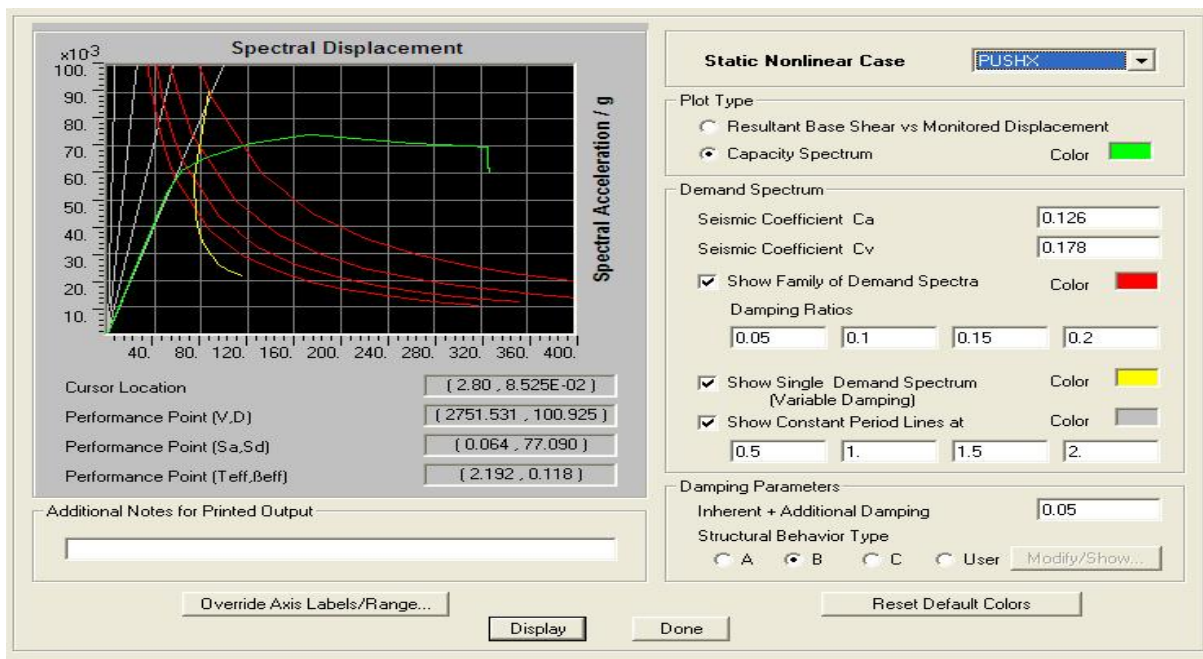


Fig. 5.33 Capacity spectrum of the 12-story frame structure building in x-direction (DE) (Procedure B)

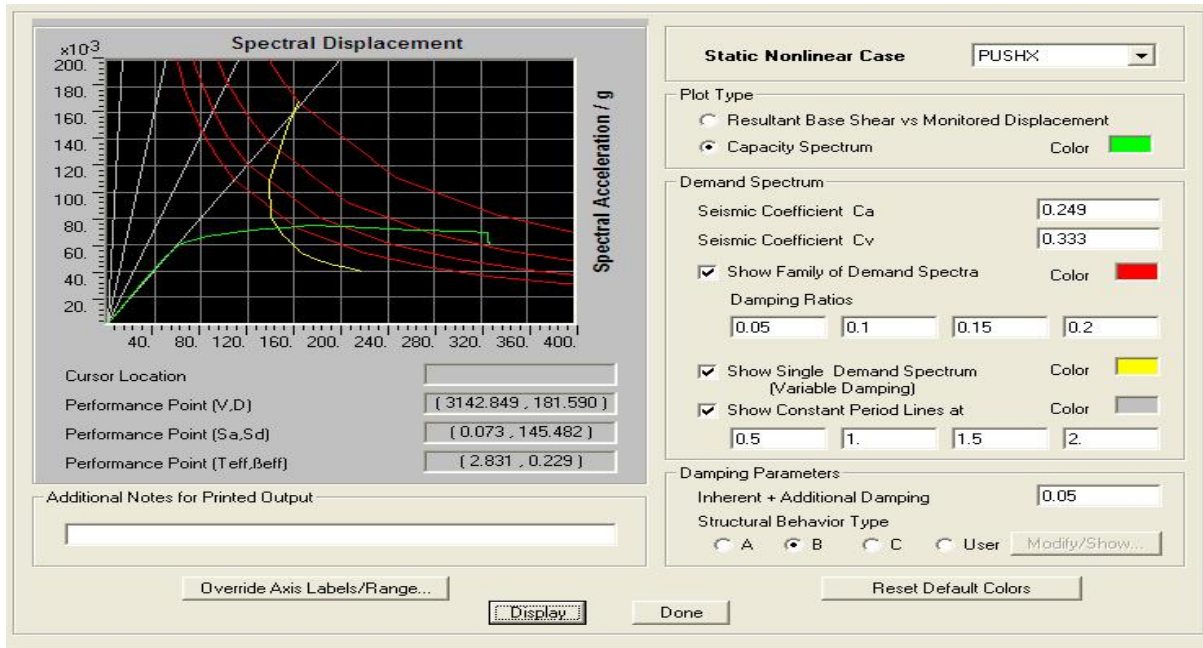


Fig. 5.34 Capacity spectrum of the 12-story frame structure building in x-direction (ME) (Procedure B)

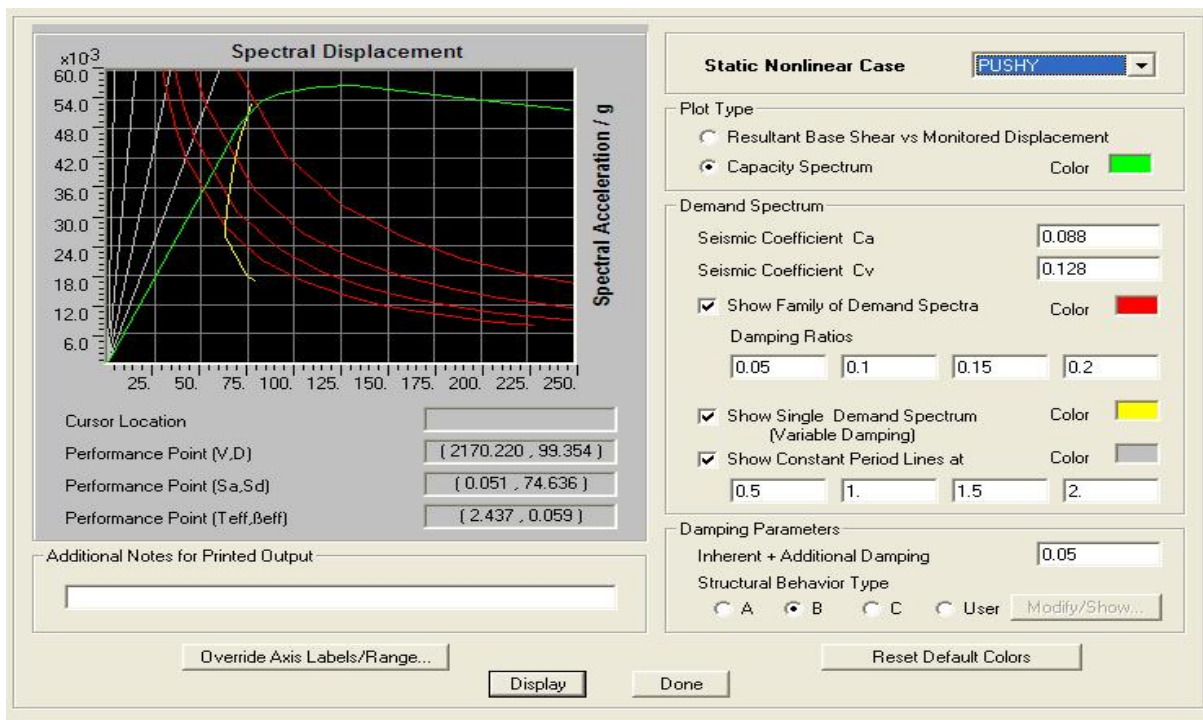


Fig. 5.35 Capacity spectrum of the 12-story frame structure building in y-direction (SE) (Procedure B)

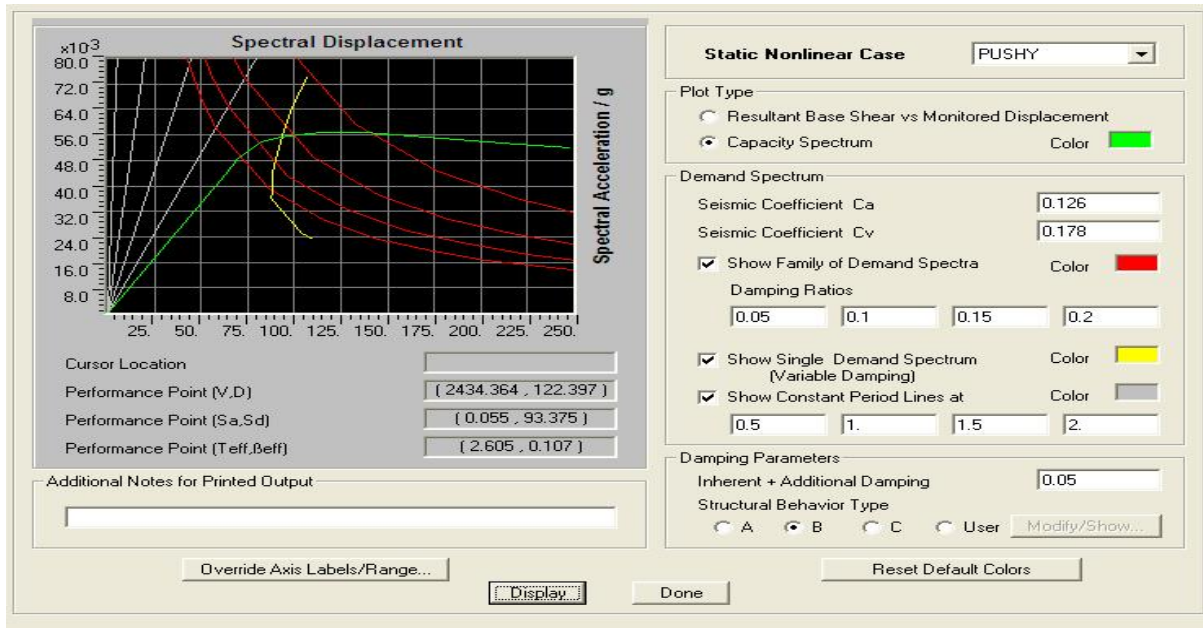


Fig. 5.36 Capacity spectrum of the 12-story frame structure building in y-direction (DE) (Procedure B)

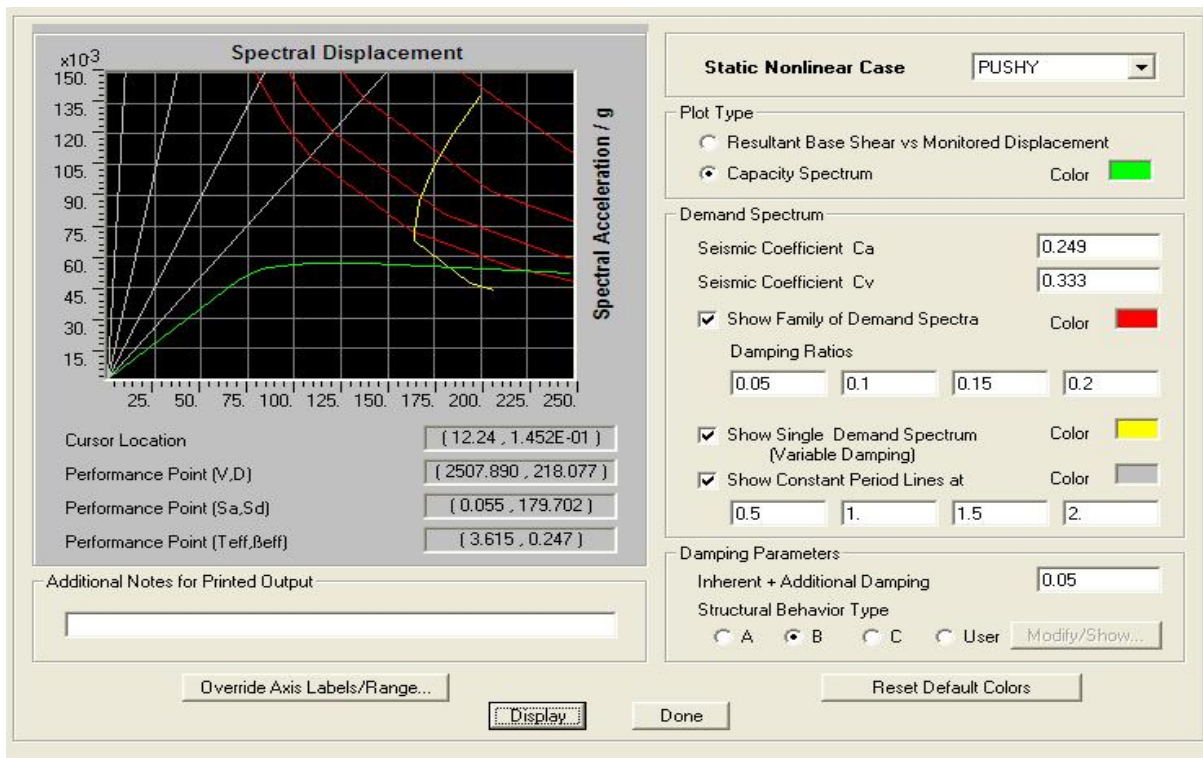


Fig. 5.37 Capacity spectrum of the 12-story frame structure building in y-direction (ME) (Procedure B)

From procedure A and B capacity curve illustrated in Figs 5.30 to 5.37. The performance point spectral displacement and spectral acceleration data for different earthquake are in Table 5.13.

Table 5.13 Capacity spectrum of the 12 story building (Procedure A and B)

	X-direction				Y-direction			
	Spectral acceleration		Spectral displacement, mm		Spectral acceleration		Spectral displacement, mm	
	Procedure A	Procedure B	Procedure A	Procedure B	Procedure A	Procedure B	Procedure A	Procedure B
Serviceability earthquake	0.061	0.059	62.30	59.79	0.054	0.051	79.22	74.64
Design earthquake	0.066	0.064	80.00	77.09	0.055	0.055	92.77	93.38
Maximum earthquake	0.069	0.073	148.00	145.48	0.067	0.055	150.00	179.70

From procedure A and B (Table 5.13) and Figs.5.30 to 5.37, it has seen that performance point spectral displacement and spectral acceleration are close to same. So it has been concluded that capacity spectrum of 12-story frame structure building is close to same for Procedure A and B.

5.5.1.1 Local level performance

For serviceability earthquake, number of hinges formed in x and y direction does not cross the Immediate Occupancy (IO) limit (Table 5.14). For design earthquake, number of hinges formed in x and y direction does not cross the Life Safety (LS) limit (Table 5.14). For maximum earthquake, number of hinges formed in x and y direction does not cross the Collapse prevention (CP) limits (Table 5.14). So it can be concluded that the local criteria as per ATC-40 [3] is satisfied for serviceability, design and maximum earthquake.

Therefore it has been said that the structure fulfills the performance objective at local level and performance of building frames designed as per BNBC has been evaluated against targeted performance levels for serviceability, design and maximum earthquakes.

Table 5.14 Number of hinges formed in the 12-storied frame structure building in x and y-direction

	A-B	B-IO	IO-LS	LS-CP	CP-C	C-D	D-E	>E	TOTAL
X-direction									
Serviceability earthquake	1174	152	0	0	0	0	0	0	1326
Design earthquake	1116	146	64	0	0	0	0	0	1326
Maximum earthquake	1058	140	128	0	0	0	0	0	1326
Y-direction									
Serviceability earthquake	1236	90	0	0	0	0	0	0	1326
Design earthquake	1208	118	0	0	0	0	0	0	1326
Maximum earthquake	1144	72	30	80	0	0	0	0	1326

Note: IO=Immediate Occupancy, LS= Life Safety, CP= Collapse Prevention

5.5.1.2 Global level performance

In this section, a structure, designed for gravity load and earthquake as per BNBC [1] is analyzed to assess its performance. The geometry and other structural details are same as mention in the previous section 5.3. The design followed as BNBC including earthquake and gravity loads. Performance point of the structure is evaluated for serviceability, design and maximum earthquake.

For serviceability earthquake, From Figs. 5.38 and 5.39, it is seen that story drift ratio does cross the Immediate Occupancy (IO) limits. So it has been said that structure is designed for earthquake and gravity load as per BNBC [1] satisfy at small earthquake. For design earthquake, From Figs. 5.38 and 5.39, it is seen that story drift ratio does not cross the Life Safety (LS) limits. For maximum earthquake, From Figs. 5.38 and 5.39, it is seen that story drift ratio does not cross the Life Safety (LS) limits. So it can be concluded that the global criteria as per ATC-40 [3] is satisfied for serviceability, design and maximum earthquake.

Therefore it has been said that the structure fulfills the performance objective at global level and performance of building frames designed as per BNBC has been evaluated against targeted performance levels for serviceability, design and maximum earthquakes.

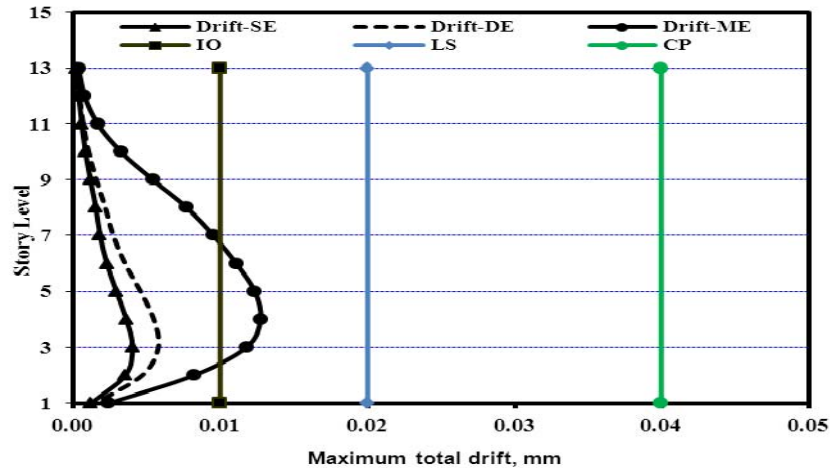


Fig. 5.38 Maximum story drift ratio at performance point for different earthquake level in X-direction

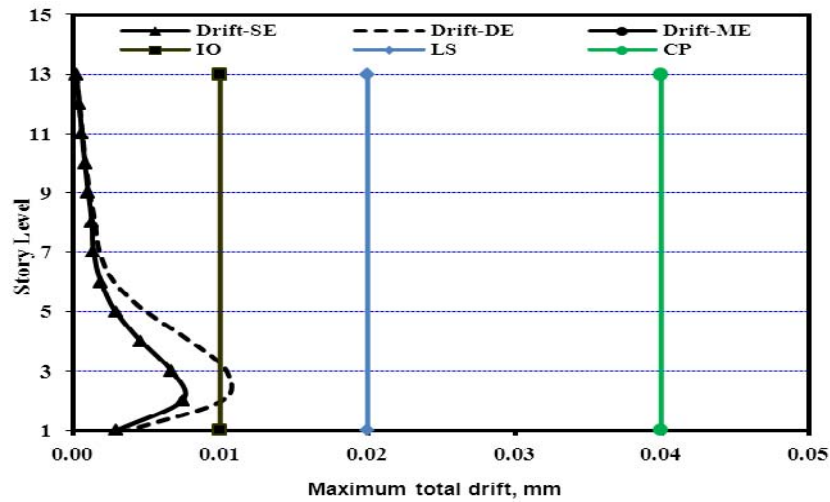


Fig. 5.39 Maximum story drift ratio at performance point for different earthquake level in Y-direction

Note: IO=Immediate Occupancy, LS= Life Safety, CP= Collapse Prevention

A typical 12-story building situated in Dhaka city (Zone 2) was analyzed using finite element methodology developed in this study. The results obtained from the analysis are studied and seismic performances are checked against ATC-40[3] local and global requirements. It has been seen that the story drifts for maximum, design, and serviceability earthquakes are within specified limits. It has also been found that number of hinges formed in the structure does not cross the specified limits for three levels of earthquakes.

5.6 Performance evaluation of structure for gravity loads only

In this section, a structure, designed only for gravity load is analyzed to assess its performance. The geometry and other structural details are same as mention in the previous section 5.3. The design followed as BNBC [1] excluding earthquake and wind loads. Performance point of the structure is evaluated for serviceability, design and maximum earthquake.

For serviceability earthquake, number of hinges formed in x and y direction cross the Immediate Occupancy (IO) limits (Table 5.15). From Figs. 5.40 and 5.41, it is seen that story drift ratio cross the Immediate Occupancy (IO) limits. So it can be concluded that structure designed only for gravity load as per BNBC [1] fails even at small earthquake.

For design earthquake, number of hinges formed in x and y direction does not cross the Life Safety (LS) limits (Table 5.15). From Figs. 5.40 and 5.41, it is seen that story drift ratio does not cross the Life Safety (LS) limits. So it can be concluded that the local and global criteria as per ATC-40 [3] is satisfied for design earthquake.

For maximum earthquake, performance point for this structure is not found. From table 5.15, number of hinges formed in x and y direction cross the Collapse prevention (CP) limits (Table 5.15). So it can be concluded that structure designed only for gravity load as per BNBC [1] fails at maximum earthquake level.

Table 5.15 Number of hinges for different level of earthquakes

	A-B	B-IO	IO-LS	LS-CP	CP-C	C-D	D-E	>E	TOTAL
X-direction									
Serviceability earthquake	546	82	62	24	0	0	0	0	714
Design earthquake	514	72	88	40	0	0	0	0	714
Maximum earthquake*	512	38	52	108	0	4	0	0	714
Y-direction									
Serviceability earthquake	579	50	60	25	0	0	0	0	714
Design earthquake	576	48	62	28	0	0	0	0	714
Maximum earthquake*	535	64	61	50	0	2	2	0	714

Note: IO=Immediate Occupancy, LS= Life Safety, CP= Collapse Prevention

*Corresponding to last step of pushover curve

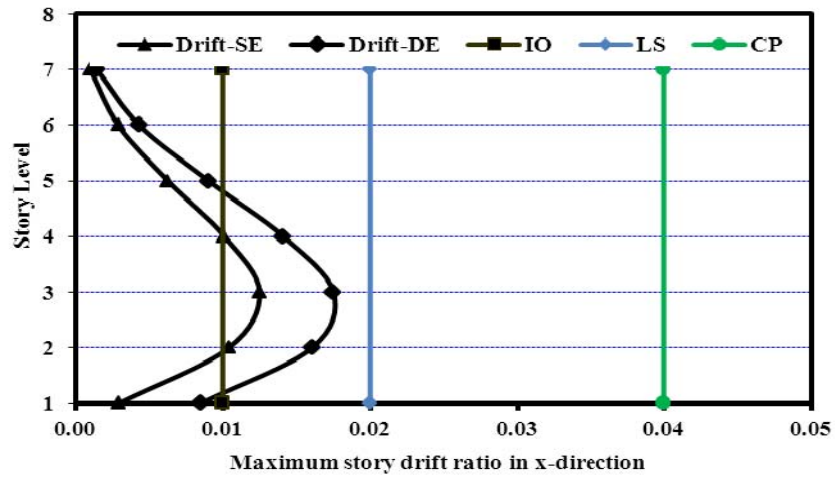


Fig. 5.40 Maximum story drift ratio at performance point for different earthquake level in x-direction

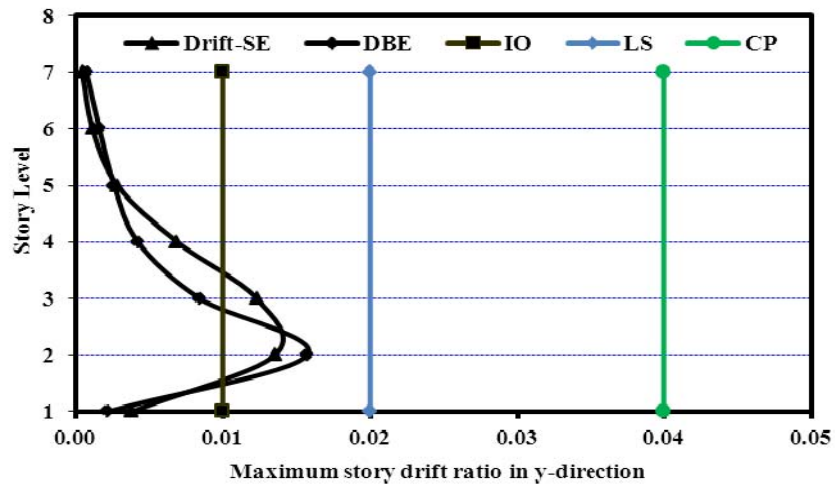


Fig. 5.41 Maximum story drift ratio at performance point for different earthquake level in y-direction

Note: IO=Immediate Occupancy, LS= Life Safety, CP= Collapse Prevention
 Performance point for ME has not been achieved

5.7 Conclusion

In this chapter, performance based analysis of different 3D RC buildings, designed as per BNBC [1] have been carried out. Typical buildings situated in Dhaka city (Zone 2) with different aspect ratio and story heights were analyzed using finite element methodology developed in this study. The results obtained from the analyses are studied and seismic performances are checked against ATC-40[3] local and global requirements. It has been seen that the story drifts for maximum, design, and serviceability earthquakes are within specified limits for all cases considered. It has also been found that number of hinges formed in the structure does not cross the specified limits for three levels of earthquakes. The buildings designed following seismic provisions of BNBC [1] would behave rather conservatively during an earthquake.

It has been seen that spectral displacement and spectral acceleration of performance points are almost same for procedure A and B. It can be concluded that demand requirements of 3D frame structures are same for procedure A and B and either method can be used.

The chapter also shows the importance of considering seismic force in design. A building designed only for gravity load ignoring the seismic forces has been found to fail in satisfying the performance requirement levels particularly those for the serviceability and maximum earthquakes.

Chapter 6

Conclusions and Recommendations

6.1 Introduction

In this thesis, an attempt has been made to demonstrate the validity and efficiency of pushover analysis method of ATC-40[3] as incorporated in ETABS [20], SAP2000 [21] and SeismoStruct [50]. The work also studied the effectiveness of pushover analysis in comparison to more rigorous nonlinear time history analysis with particular emphasis on the load pattern employed in pushover analysis. Finally performance of building frames designed as per BNBC has been evaluated against targeted performance levels for serviceability, design and maximum earthquakes.

In Chapter 2, provisions of BNBC [1] for seismic design have been discussed in detail. Fundamentals of pushover analysis as proposed by ATC-40[3] have also been presented. Pushover is a simplified nonlinear analysis to determine the performance of a structure for a given level of earthquake. ATC-40[3] gives provisions to obtain capacity and demand curves; also it specifies local and global requirements for different levels of earthquake. A brief description of nonlinear time history analysis has been presented in Chapter 2. In Chapter 3, Pushover analysis method as incorporated in ETABS [20] and SAP2000 [21] has been validated by comparing the capacity curves of 2D frames with published results. Pushover analyses have been carried out on 2D frames designed according to BNBC and their performances have been found to be satisfactory as per the requirements of ATC-40[3]. Different load pattern have been used in the pushover analysis to demonstrate their effect on capacity curve.

Chapter 4 presents linear and nonlinear time history analysis using SAP2000 [21] and SeismoStruct [50]. Both linear and nonlinear time history analyses have been validated against published results. Nonlinear time history analysis, although complicated and time consuming, is a more rigorous method for modeling seismic response of a structure. Different load patterns i.e. triangular, uniform, elastic first modes have been used in pushover analysis to identify the most suitable one that compares well with nonlinear time history analysis. Performances have been evaluated for 2D frames designed according to BNBC [1] using nonlinear time history. Well known earthquake i.e. El Centro and Kobe earthquakes have suitably scaled as per required Z value for use in the analysis. A comparison of linear and

nonlinear time history analyses have been carried out to demonstrate that damage caused during an earthquake. In Chapter 5, similar pushover analyses have been carried out for 3D buildings designed according to BNBC [1] to determine their performance under three levels of earthquakes. A building which is designed only for gravity load has also been studied to see whether it is capable of satisfying the requirements of ATC-40 [3].

6.2 Findings of the study

The findings of the study regarding the effectiveness of pushover and time history analyses as implemented in finite element method can be summarized as follows:

- 1) Capacity curves of pushover analysis as obtained by ETABS and SAP2000 have been validated with published numerical result of Oguz [13]. The curves obtained by SAP2000 [21] and ETABS [20] are almost identical in elastic range and compares well in the inelastic range.
- 2) Performance based analysis of the structure with SeismoStruct [50] software has also been carried out. Capacity curve of pushover analysis using SeismoStruct has been compared to that of SAP2000[21] and two software, even though different in their formulation, yield comparable results.
- 3) Linear time history analysis of ETABS [20] has been validated for SDOF system by comparing the response with published results of Chopra [5].
- 4) Nonlinear time history analysis has been carried out using SeismoStruct [50] to predict the response of a full scale blind test of a bridge pier [52] under six levels of ground motion. SeismoStruct simulates the response quite reasonably.
- 5) Effectiveness of pushover analysis depends significantly on the load pattern used in finding the capacity curve. Different loading patterns have been compared with the results of nonlinear time history analysis and uniform loading pattern have been found to compare better.
- 6) A comparative study was done to observe the effect of damage under seismic loading by analyzing using both nonlinear time history and linear time history analysis.
- 7) Two methods of ATC-40 [3], i.e. Procedure A and Procedure B, have been compared to find the demand curve of pushover analysis. It has been seen that spectral displacement and spectral acceleration corresponding to performance point are almost same for procedure A and B.

Typical buildings situated in Dhaka city (Zone 2) with different aspect ratio and story heights were analyzed using finite element methodology developed in this study. It has been found that the buildings designed following seismic provisions of BNBC [1] would behave quite conservatively during an earthquake. The major findings related to seismic performance of building designed according to BNBC [1] can be summarized as follows:

- 1) Performance of building frames designed as per BNBC [1] has been evaluated using pushover analysis, against targeted performance levels for serviceability, design and maximum earthquakes and found to satisfy the ATC-40[3] local and global requirements.
- 2) Performance evaluations of 2D RC frames were carried out using nonlinear time history analysis and showed that frames designed by BNBC [1] for Dhaka city can easily satisfy the local and global performance requirements.
- 3) Different RC buildings with varying story number, aspect ratio have been designed as per BNBC [1]. Performances of these buildings have been carried out using 3D pushover analysis. The building easily satisfies the seismic requirements of ATC-40[3].
- 4) To demonstrate the importance of considering seismic load in design, a 3D building has been designed without earthquake load and its performance has been checked by pushover analysis. The building has been found to be inadequate for serviceability and maximum earthquakes.

6.3 Recommendation for future study

This study employed a few number of reinforced concrete moment resisting frames and a limited number of ground motion excitations. An extensive study containing a larger number of frames and a set of representative ground motion records for Bangladesh would enhance the results obtained in the accuracy of capacity of structure and seismic demand prediction of pushover procedures.

This work may be extended in future to include the following:

- 1) More representative earthquake data should be considered for analyzing the structures and to compare the resulting structural responses.

- 2) Three dimensional models of case study frames should be used for time history analysis by considering the necessary geometric and strength characteristics of all members that affect the nonlinear seismic response.
- 3) Experimental works should be carried out to verify the numerical results of 3D frames.
- 4) Nonlinear time history analysis of RC 3D frames with soft story should be carried out as it is an important issue in local residential areas.
- 5) Nonlinear behavior of RC structure with vertical irregularity should be studied to assess their performance under a seismic event.
- 6) Different pushover analysis methods, i.e. adaptive pushover, modal pushover should be studied in detail.

References

- [1] House Building Research Institute, Bangladesh National Building Code (BNBC), 1993.
- [2] UBC, Uniform Building Code, 1991.
- [3] Applied Technology Council, ATC-40, Seismic Evaluation and Retrofit of Concrete Buildings, Volume 1-2, Redwood City, California. 1996,
- [4] FEMA 356, Pre-standard and Commentary for the Seismic Rehabilitation of Buildings, Prepared by American Society of Civil Engineers, Reston, Virginia. 2000.
- [5] Chopra, A.K. Dynamics of Structures-Theory and Application to Earthquake Engineering, Prentice Hall, New Jersey. 1995.
- [6] Comartin, C.G., Niewiarowski, R.W., Freeman, S.A. and Turner, F.M., “Seismic Evaluation and Retrofit of Concrete Buildings: A practical overview of the ATC40 document” Earthquake Spectra, Vol.16, No1, pp241-261, 2000.
- [7] Fajfar P. and Fischinger M., “Nonlinear seismic analysis of R/C buildings: implications of a case study”, European Earthquake Engineering, 31-43. 1987.
- [8] Krawinkler H. and Seneviratna G.D.P.K., “Pros and cons of a pushover analysis of seismic performance evaluation”, Engineering Structures, Vol.20, 452- 464, 1998.
- [9] Ýnel M., Tjhin T. and Aschheim A.M., “The Significance of Lateral Load Pattern in Pushover Analysis”, Istanbul Fifth National Conference on Earthquake Engineering, Paper No: AE-009, Istanbul, Turkey. 2003.
- [10] Chintanapakdee C. and Chopra A.K., Evaluation of Modal Pushover Analysis Using Generic Frames, Earthquake Engineering and Structural Dynamics, Vol. 32,

417-442, 2003..

[11] Sasaki F., Freeman S. and Paret T., “Multi-mode pushover procedure (MMP)- a method to identify the effect of higher modes in a pushover analysis”, Proc. of 6th U.S. National Conference on Earthquake Engineering, Seattle, EERI, Oakland, 1998.

[12] Kalkan, E. and Chopra, A.K., “Modal-Pushover-based Ground Motion Scaling Procedure”, Journal of Structural Engineering Special Issue, 2010.

[13] Oguz, S., Evaluation of pushover analysis procedures for frame structures, MSc thesis, Graduate School of Natural and Applied Sciences, Middle East Technical University, 2005.

[14] Rashid, M.A., Evaluation of seismic design deficiencies of midrise apartment building and remedies, MEng Thesis, BUET, 2007.

[15] Rahman, M.M., Pushover analysis of 2-D frames with stiffness irregularity in vertical direction, MSc Engg Thesis, BUET, 2008.

[16] Mondal, S.S., Remedial measures for reduction of seismic vulnerability in buildings with soft ground storey, MSc Engg Thesis, BUET, 2009.

[17] Bhuiyan, M.S.I, Nonlinear time history analysis of RC frames with brick masonry fill, MSc Engg Thesis, BUET, 2007.

[18] Hossen, M.M. and Anam, I. “Seismic performance of concrete flat slabs”, Proceedings of the 3rd International Earthquake Symposium, Dhaka, March, 2010.

[19] Abdullah, A.K. M. , Awal, M.A., Anam, I. and Mahbub, A. al., “Seismic detailing and behavior of RC frames”, Proceedings of the 3rd International Earthquake Symposium, Dhaka, March, 2010.

- [20] Computers and Structures Inc. (CSI), ETABS: Three Dimensional Analysis of Building Systems, Berkeley, California. 2010.
- [21] Computers and Structures Inc. (CSI), SAP2000 Three Dimensional Static and Dynamic Finite Element Analysis and Design of Structures, Berkeley, California, 2010.
- [22] ACI Committee 318, Building Code Requirement for Structural Concrete, American Concrete Institute, Detroit, 2002.
- [23] Nilson, A.H., Darwin, D., and Dolan, C.W. Design of Concrete Structure (Thirteenth edition), Mc Graw Hill, New York, USA, 2003.
- [24] Building Seismic Safety Council. NEHRP Guidelines for the Seismic Rehabilitation of Buildings, FEMA-273, Federal Emergency Management Agency, Washington, D.C., 1997.
- [25] American Society of Civil Engineers. Pre-standard and Commentary for the Seismic Rehabilitation of Buildings, FEMA-356, Federal Emergency Management Agency, Washington, D.C., 2000.
- [26] Jan T.S., Liu M.W. and Kao Y.C., An Upper-Bound Pushover Analysis Procedure for Estimating the Seismic Demands of High-Rise Buildings, Engineering Structures, Vol. 26, 117-128, 2004.
- [27] Kim B, D'Amore E. "Pushover analysis procedure in earthquake engineering." Earthquake Spectra, 13(2):417-434, 1999.
- [28] Elnashai AS. "Advanced inelastic static (pushover) analysis for earthquake applications." Structural Engineering and Mechanics, 12(1):51-69, 2001.

- [29] Fajfar P. "Structural analysis in earthquake engineering a breakthrough of simplified non-linear method." Proceedings of the 12th European Conference on Earthquake Engineering, London, Paper Reference 843.
- [30] Rosenblueth E. and Herrera I., On a Kind of Hysteretic Damping, Journal of Engineering Mechanics Division, ASCE, Vol. 90, 37-48, 1964.
- [31] Bracci JM, Kunnath SK, Reinhorn AM. "Seismic performance and retrofit evaluation for reinforced concrete structures." ASCE, Journal of Structural Engineering, 123:3-10, 1997.
- [32] Gupta B., Enhanced Pushover Procedure and Inelastic Demand Estimation for Performance-Based Seismic Evaluation of Buildings, Ph.D. Dissertation, University of Central Florida, Orlando, FL, 1999.
- [33] Moghadam A.S., A Pushover Procedure for Tall Buildings, 12th European Conference on Earthquake Engineering, Paper Reference 395.
- [34] Chopra AK, Goel RK. "A modal pushover analysis procedure for estimating seismic demands for buildings." Earthquake Engineering and Structural Dynamics 31:561-582, 2002.
- [35] Takeda T., Sözen M.A. and Nielson N.N., Reinforced Concrete Response to Simulated Earthquakes, Journal of Structural Division, ASCE, Vol. 96, 2557-2573, 1970.
- [36] Gulkan P. and Sozen M.A., Inelastic Response of Reinforced Concrete Structures to Earthquake Ground Motions, Journal of the American Concrete Institute, Vol. 71, 601-609, 1974.
- [37] Miranda E., Inelastic Displacement Ratios for Structures on Firm Sites, Journal of Structural Engineering, Vol. 126, 1150-1159, 2000.
- [38] Miranda E. and Ruiz-García J., Evaluation of Approximate Methods to

Estimate Maximum Inelastic Displacement Demands, *Earthquake Engineering and Structural Dynamics*, Vol. 31, 539-560, 2002.

[39] Newmark N.M. and Hall W.J., *Earthquake Spectra and Design*, Earthquake Engineering Research Institute, Berkeley, CA, 1982.

[40] Chopra. AK, Goel, RK. "Evaluation of NSP to estimate seismic deformation: SDF Systems." *ASCE, Journal of Structural Engineering*, 26:482-490, 2000.

[41] Chopra AK, Goel RK. "Capacity-demand-diagram methods based on inelastic design spectrum." *Earthquake Spectra*, 15:637-656, 1999.

[42] Veletsos AS, Newmark NM. "Effect of inelastic behavior on the response of simple systems to earthquake motions." *Proceedings of the 2nd World Conference on Earthquake Engineering*, Vol. II, Tokyo, Japan, 895–912, 1960.

[43] Chopra AK, Goel R. "A modal pushover analysis procedure to estimate seismic demands for unsymmetrical plan buildings." *Earthquake Engineering and Structural Dynamics*, to appear in 2004.

[44] BSSC, "NEHRP Guidelines for Seismic Rehabilitation of Buildings," Report No. FEMA-273, Federal Emergency Management Agency, Washington, D.C., 1997.

[45] BSSC, "1997 Edition: NEHRP Recommended Provisions for Seismic Regulations for New Buildings and Other Structures, Part 1 - Provisions." Report No. FEMA-302, Federal Emergency Management Agency, Washington, D.C., 1998.

[46] BSSC, "1997 Edition: NEHRP Recommended Provisions for Seismic Regulations for New Buildings and Other Structures, Part 2 – Commentary." Report No. FEMA 303, Federal Emergency Management Agency, Washington, D.C. 1998.

[47] Hamburger, R. O. "Performance-Based Seismic Engineering: The Next Generation of Structural Engineering Practice." EQE Summary Report, 1996.

[48] Freeman, S.A. The capacity spectrum method for determining the demand displacement. ACI Spring Convention, 1994.

[49] Valles, R.E., A.M. Reinhorn, and R. Barrón. Seismic evaluation of a low-rise building in the vicinity of the New Madrid seismic zone. Technical Report NCEER-96, State University of New York at Buffalo, 1996.

[50] SeismoStruct's, Seismosoft Ltd. Seismosoft Ltd. Via Boezio, 10, 27100, Pavia (PV), Italy. E-mail: info@seismosoft.com, website: www.seismosoft.com 2002-2012.

[51] Bianchi F., Sousa R., Pinho R. "Blind prediction of a full-scale RC bridge column tested under dynamic conditions", Proceedings of 3rd International Conference on Computational Methods in Structural Dynamics and Earthquake Engineering (COMPDYN 2011), Paper no. 294, Corfu, Greece, 2011.

[52] PEER, "Concrete Column Blind Prediction Contest 2010", http://nisee2.berkeley.edu/peer/prediction_contest/, University of California, Berkeley, 2010.

Appendix A

Table 2-A1 Modeling Parameters for Nonlinear Procedures – Reinforced Concrete Beams (ATC-40)

			Modeling Parameters ³		
			Plastic Rotation Angle, rad		Residual Strength Ratio
Component Type			a	b	c
1. Beam Controlled by Flexure¹					
$\frac{\rho - \rho'}{\rho_{bal}}$	Transverse Reinforcement ²	$\frac{V}{b_w d \sqrt{f'_c}}$ ⁴			
≤0.0	C	≤3	0.025	0.05	0.2
≤0.0	C	≥6	0.02	0.04	0.2
≥0.5	C	≤3	0.02	0.03	0.2
≥0.5	C	≥6	0.015	0.02	0.2
≤0.0	NC	≤3	0.02	0.03	0.2
≤0.0	NC	≥6	0.01	0.01 5	0.2
≥0.5	NC	≤3	0.01	0.01 5	0.2
≥0.5	NC	≥6	0.005	0.01	0.2
2. Beams controlled by shear¹					
Stirrup spacing ≤d/2			0.0	0.02	0.2
Stirrup spacing > d/2			0.0	0.01	0.2
3. Beams controlled by inadequate development or splicing along the span¹					
Stirrup spacing ≤d/2			0.0	0.02	0.0
Stirrup spacing >d/2			0.0	0.01	0.0
4. Beams controlled by inadequate embedment into beam-column joint¹					
			0.015	0.03	0.2

1. When more than one of the conditions 1,2,3 and 4 occur for a given component, use the minimum appropriate numerical value from the table.
2. Under the heading “transverse reinforcement,” ‘C’ and ‘NC’ are abbreviations for conforming and non-conforming details, respectively. A component is conforming if within the flexural plastic region: (1) closed stirrup are spaced at ≤d/3 and 2) for components of moderate and high ductility demand the strength provided by the stirrup (Vs) is at least three-fourths of the design shear. Otherwise, the component is considered non-conforming.
3. Linear interpolation between values listed in the table is permitted
4. V = design shear force

Table 2-A2 Modeling Parameters for Nonlinear Procedures – Reinforced Concrete Column (ATC-40)

			Modeling Parameters ⁴		
			Plastic Rotation Angle, rad		Residual Strength Ratio
Component Type			a	b	c
1. Columns Controlled by Flexure ¹					
$\frac{P}{A_g f'_c}$ ⁵	Transverse Reinforcement ²	$\frac{V}{b_w d \sqrt{f'_c}}$ ⁶			
≤0.1	C	≤3	0.02	0.03	0.2
≤0.1	C	≥6	0.015	0.025	0.2
≥0.4	C	≤3	0.015	0.025	0.2
≥0.4	C	≥6	0.01	0.015	0.2
≤0.1	NC	≤3	0.01	0.015	0.2
≤0.1	NC	≥6	0.005	0.005	-
≥0.4	NC	≤3	0.005	0.005	-
≥0.4	NC	≥6	0.0	0.0	-
2. Columns controlled by shear ¹					
Hoop spacing ≤ d/2 or $\frac{P}{A_g f'_c} \leq 0.1$			0.0	0.015	0.2
Other cases			0.0	0.0	0.0
3. Columns controlled by inadequate development or splicing along the clear height ^{1,3}					
Hoop spacing ≤ d/2			0.01	0.02	0.4
Hoop spacing > d/2			0.0	0.01	0.2
4. Column with axial loads exceeding 0.40 P ₀ ^{1,3}					
Conforming reinforcement over the entire length			0.015	0.025	0.02
All other cases			0.0	0.0	0.0

- When more than one of the conditions 1,2,3 and 4 occur for a given component, use the minimum appropriate numerical value from the table.
- Under the heading “transverse reinforcement,” ‘C’ and ‘NC’ are abbreviations for conforming and non-conforming details, respectively. A component is conforming if within the flexural plastic hinge region: (1) closed hoops are spaced at ≤d/3 and 2) for components of moderate and high ductility demand the strength provided by the stirrup (Vs) is at least three-fourths of the design shear. Otherwise, the component is considered non-conforming.
- To quality, (1) hoops must not be lap spliced in the cover concrete, and (2) hoops must have hooks embedded in the core or must have other details to ensure that hoops will be adequately anchored following spalling of cover concrete.
- Linear interpolation between values listed in the table is permitted.
- P = Design axial load
- V = design shear force

Table 2-A3 Modeling Parameters for Concrete Axial Hinge (FEMA-356, 2000)

	Modeling Parameters ¹		
	Plastic Deformation		Residual Strength Ratio
Component Type	a	b	c
1. Braces in Tension (except EBF braces)	$11\Delta_T$	$14\Delta_T$	0.8

¹ Δ_T is the axial deformation at expected tensile yielding load.

Table 2-A4 Modeling Parameters for Nonlinear Procedures-Coupling Beams (ATC-40)

		Modeling Parameters ³		
		Chord Rotation, rad		Residual Strength Ratio
Component Type		d	e	c
1. Coupling beams controlled by flexure				
Longitudinal reinforcement and transverse reinforcement ¹	$\frac{V}{b_w d \sqrt{f'_c}}$ ²			
Conventional longitudinal reinforcement with	≤ 3	0.025	0.040	0.75
Conforming transverse reinforcement	≥ 6	0.015	0.030	0.50
Conventional longitudinal reinforcement with non-	≤ 3	0.020	0.035	0.50
Conforming transverse reinforcement	≥ 6	0.010	0.025	0.25
Diagonal reinforcement	N/A	0.030	0.050	0.80
2. Coupling beams controlled by shear				
Longitudinal reinforcement and transverse reinforcement ¹	$\frac{V}{b_w d \sqrt{f'_c}}$ ²			
Conventional longitudinal reinforcement with	≤ 3	0.018	0.030	0.60
Conforming transverse reinforcement	≥ 6	0.012	0.020	0.30
Conventional longitudinal reinforcement with non-	≤ 3	0.012	0.025	0.40
Conforming transverse reinforcement	≥ 6	0.008	0.014	0.20

1. Conventional longitudinal steel consists of top and bottom steel parallel to the longitudinal axis of the beam. The requirements for conforming transverse reinforcement are: (1) closed stirrups are to be provided over the entire length of the beam at spacing not exceeding $d/3$; and (2) the strength provided by the stirrups (V_s) should be at least three-fourths of the design shear.
2. V = the design shear force on the coupling beam in pounds, b_w = the web width of the beam, d = the effective depth of the beam and f'_c = concrete compressive strength in psi.
3. Linear interpolation between values listed in the table is permitted.

Appendix B

Table 2-B1 Damage Control and Building Performance Levels (FEMA-356)

	Target Building Performance Levels			
	Collapse Prevention Performance Level	Life Safety Performance Level	Immediate Occupancy Performance Level	Operational Performance Level
Overall Damage	Severe	Moderate	Light	Very Light
General	Little residual stiffness and strength, but load-bearing columns and walls function. Large permanent drifts. Some exits blocked. Infills and unbraced parapets failed or at incipient failure. Building is near collapse	Some residual strength and stiffness left in all stories. Gravity-load-bearing elements function. No out-of-plane failure of walls or tipping of parapets. Some permanent drift. Damage to partitions. Building may be beyond economical repair.	No permanent drift. Structure substantially retains original strength and stiffness. Minor cracking of facades, partitions, and ceilings as well as structural elements. Elevators can be restarted. Fire protection operable.	No permanent drift. Structure substantially retains original strength and stiffness. Minor cracking of facades, partitions, and ceilings as well as structural elements. All systems important to normal operation are functional.
Nonstructural components	Extensive damage	Falling hazards mitigated but many architectural, mechanical and electrical systems are damaged.	Equipment and contents are generally secure, but may not operate due to mechanical failure or lack of utilities.	Negligible damage occurs. Power and other utilities as available, possibly from standby sources.
Comparison with performance intended for buildings designed under the NEHRP Provisions, for the Design Earthquake	Significantly more damage and greater risk.	Somewhat more damage and slightly higher risk.	Less damage and lower risk.	Much less damage and lower risk.

Table 2-B2 Structural Performance Levels and Damage^{1,2,3} – Vertical Elements (FEMA-356)

Structural Performance Levels				
		Collapse Prevention	Life Safety	Immediate Occupancy
Elements	Type	S-5	S-3	S-1
Concrete Frames	Primary	Extensive cracking and hinge formation in ductile elements. Limited cracking and/or splice failure in some non-ductile columns. Severe damage in short columns	Extensive damage to beams. Spalling of cover and shear cracking (<1/8" width) for ductile columns. Minor spalling in non-ductile columns. Joint cracks <1/8" wide.	Minor hairline cracking. Limited yielding possible at a few locations. No crushing (strains below 0.003).
	Secondary	Extensive spalling in columns (limited shortening) and beams. Severe joint damage. Some reinforcing buckled	Extensive cracking and hinge formation in ductile elements. Limited cracking and/or splice failure in some nonductile columns. Severe damage in short columns	Minor spalling in non-ductile columns and beams. Flexural cracking in beams and columns. Shear cracking in Joint <1/6" width.
	Drift	4% transient or permanent	2% transient; 1% permanent	1% transient; negligible permanent
Steel Moment Frames	Primary	Extensive distortion of beams and column panels. Many fractures at moment connections, but shear connections remain intact	Hinges form. Local buckling of some beam elements. Severe joint distortion; isolated moment connection fractures, but shear connections remain intact. A few elements may intact. A few elements may experience partial fracture.	Minor or local yielding at a few places. No fractures. Minor buckling or observable permanent distortion of members.
	Secondary	Same as primary	Extensive distortion of beams and column panels. Many fractures at moment connections, but shear connections remain intact	Same as primary
	Drift	5% transient or permanent	2.5% transient; 1% permanent	0.7% transient; negligible permanent
Braced Steel Frames	Primary	Extensive yielding and buckling of braces. Many braces and their connections may fail.	Many braces yield or buckle but do not totally fail. Many connections may fail	Minor yielding or buckling of braces.

Structural Performance Levels				
		Collapse Prevention	Life Safety	Immediate Occupancy
Elements	Type	S-5	S-3	S-1
	Secondary	Same as primary	Same as primary	Same as primary
	Drift	2% transient or permanent	1.5% transient; 0.5% permanent	0.5% transient; negligible permanent
Concrete Walls	Primary	Major flexural and shear cracks and voids. Sliding at joints. Extensive crushing and buckling of reinforcement. Failure around openings. Severe boundary element damage. Coupling beams shattered and virtually disintegrated.	Some boundary element stress, including limited buckling of reinforcement. Some sliding at joints. Damage around openings. Some crushing and flexural cracking. Coupling beams: extensive shear and flexural cracks; some crushing, but concrete generally remains in place.	Minor hairline cracking of walls, <1/16" wide. Coupling beams experience cracking <1/8" width.
	Secondary	Panels shattered and virtually disintegrated	Major flexural and shear cracks. Sliding at joints. Extensive crushing. failure around openings. Severe boundary element damage. Coupling beams shattered and virtually disintegrated.	Minor hairline cracking of walls. Some evidence of sliding at construction joints. Coupling beams experience cracks <1/8" width. Minor spalling.
	Drift	2% transient or permanent	1% transient; 0.5% permanent	0.5% transient; negligible permanent
Un-reinforced Masonry Infill Walls	Primary	Extensive cracking and crushing; portions of face course shed	Extensive cracking and some crushing but wall remains in place. No falling units. Extensive crushing and spalling of veneers at corners of openings.	Minor (<1/8" width) cracking of masonry infill and veneers. Minor spalling in veneers at a few corner openings.
	Secondary	Extensive crushing and shattering; some walls dislodge.	Same as primary	Same as primary
	Drift	0.6% transient or permanent	0.5% transient; 0.3% permanent	0.1% transient; negligible permanent
Un-reinforced	Primary	Extensive cracking; face course and veneer	Extensive cracking. Noticeable in-plane	Minor (<1/8" width) cracking of veneers.

Structural Performance Levels				
		Collapse Prevention	Life Safety	Immediate Occupancy
Elements	Type	S-5	S-3	S-1
Masonry (Non infill) Walls		may peel off. Noticeable in plane and out-of-plane offsets	offsets of masonry and minor out-of-plane offsets	Minor spalling in veneers at a few corner openings. No observable out-of-plane offsets.
	Secondary	Nonbearing panels dislodge	Same as primary	Same as primary
	Drift	1% transient or permanent	0.6% transient; 0.6% permanent	0.3% transient; 0.3% permanent
Reinforced Masonry Walls	Primary	Crushing; extensive cracking. Damage around openings and at corners. Some fallen units	Extensive cracking (<1/4") distributed throughout wall. Some isolated crushing	Minor (<1/8" width) cracking. No out-of-plane offsets.
	Secondary	Panels shattered and virtually disintegrated	Crushing; extensive cracking. Damage around openings and at corners. Some fallen units	Same as primary
	Drift	1.5% transient or permanent	0.6% transient; 0.6% permanent	0.2% transient; 0.2% permanent
Wood Stud Walls	Primary	Connections loose. Nails partially withdrawn. Some splitting of members and panels. Veneers dislodged	Moderate loosening of connections and minor splitting of members	Distributed minor hairline cracking of gypsum and plaster veneers.
	Secondary	Sheathing sheared off. Let in braces fractured and buckled. Framing split and fractured	Connections loose. Nails partially withdrawn. Some splitting of members and panels.	Same as primary
	Drift	3% transient or permanent	2% transient; 1% permanent	1% transient; 0.25% permanent
Precast Concrete Connections	Primary	Some connection failures but no elements dislodged	Local crushing and spalling at connections, but no gross failure of connections.	Minor working at connections; cracks <1/16" width at connections.
	Secondary	Same as primary	Some connection failures but no elements dislodged	Minor crushing and spalling at connections
Foundations	General	Major settlement and tilting	Total settlements <6" and differential settlements <1/2" in 30ft.	Minor settlement and negligible tilting.

1. Damage states indicated in this table are provided to allow an understanding of the severity of damage that may be sustained by various structural elements when present in structures meeting the definitions of the Structural Performance Levels. These damage states are not intended for use in post-earthquake evaluation of damage or for judging the safety of, or required level of repair to, a structure following an earthquake.
2. Drift values, differential settlements, crack widths, and similar quantities indicated in these tables are not intended to be used as acceptance criteria for evaluating the acceptability of a rehabilitation design in accordance with the analysis procedures provided in this standard; rather, they are indicative of the range of drift that typical structures containing the indicated structural elements may undergo when responding within the various Structural Performance Levels. Drift control of a rehabilitated structure may often be governed by the requirements to protect nonstructural components. Acceptable levels of foundation settlement or movement are highly dependent on the construction of the superstructure. The values indicated are intended to be qualitative descriptions of the approximate behavior of structures meeting the indicated levels.
3. For limiting damage to frame elements of infilled frames, refer to the rows for concrete or steel frames.

Table 2-B3 Structural Performance Levels and Damage^{1,2} – Horizontal Elements (FEMA-356)

	Structural Performance Levels		
	Collapse Prevention	Life Safety	Immediate Occupancy
Elements	S-5	S-3	S-1
Metal Deck Diaphragms	Large distortion with buckling of some units and tearing of many welds and seam attachments	Some localized failure of welded connections of deck to framing and between panels. Minor local buckling of deck	Connections between deck units and framing intact. Minor distortions.
Wood Diaphragms	Large permanent distortion with partial withdrawal of nails and extensive splitting of elements	Some splitting at connections. Loosening of sheathing. Observable withdrawal of fasteners. Splitting of framing and sheathing.	No observable loosening or withdrawal of fasteners. No splitting of sheathing or framing.
Concrete Diaphragms	Extensive crushing and observable offset across many cracks.	Extensive cracking (<1/4" width). Local crushing and spalling	Distributed hairline cracking. Some minor cracks of larger size (<1/8" width).
Precast Diaphragms	Connections between units fail. Units shift relative to each other. Crushing and spalling at joints.	Extensive cracking (<1/4" width). Local crushing and spalling.	Some minor cracking along joints.

1. Damage states indicated in this table are provided to allow an understanding of the severity of damage that may be sustained by various structural elements when present in structures meeting the definitions of the Structural Performance Levels. These damage states are not intended for use in post-earthquake evaluation of damage or for judging the safety of, or required level of repair to, a structure following an earthquake.
2. Drift values, differential settlements, crack widths, and similar quantities indicated in these tables are not intended to be used as acceptance criteria for evaluating the acceptability of a rehabilitation design in accordance with the analysis procedures provided in this standard; rather, they are indicative of the range of drift that typical structures containing the indicated structural elements may undergo when responding within the various Structural Performance Levels. Drift control of a rehabilitated structure may often be governed by the requirements to protect nonstructural components. Acceptable levels of foundation settlement or movement are highly dependent on the construction of the superstructure. The values indicated are intended to be qualitative descriptions of the approximate behavior of structures meeting the indicated levels.

Appendix C

Table 2-C1 Numerical Acceptance Criteria for Plastic Hinge Rotations in Reinforced Concrete Beams, in radians (ATC-40)

			Performance Level ³				
			Primary			Secondary	
Component Type			IO	LS	SS	LS	SS
1. Beams Controlled by Flexure¹							
$\frac{\rho - \rho'}{\rho_{bal}}$	Transverse Reinforcement ²	$\frac{V}{b_w d \sqrt{f'_c}}$					
≤0.0	C	≤3	0.005	0.020	0.025	0.020	0.050
≤0.0	C	≥6	0.005	0.010	0.020	0.020	0.040
≥0.5	C	≤3	0.005	0.010	0.020	0.020	0.030
≥0.5	C	≥6	0.005	0.005	0.015	0.015	0.020
≤0.0	NC	≤3	0.005	0.010	0.020	0.020	0.030
≤0.0	NC	≥6	0.000	0.005	0.010	0.010	0.015
≥0.5	NC	≤3	0.005	0.010	0.010	0.010	0.015
≥0.5	NC	≥6	0.000	0.005	0.005	0.005	0.010
2. Beams controlled by shear¹							
Stirrup spacing ≤ d/2			0.0	0.0	0.0	0.010	0.020
Stirrup spacing > d/2			0.0	0.0	0.0	0.005	0.010
3. Beams controlled by inadequate development or splicing along the span¹							
Stirrup spacing ≤ d/2			0.0	0.0	0.0	0.010	0.020
Stirrup spacing > d/2			0.0	0.0	0.0	0.005	0.010
4. Beams controlled by inadequate embedment into beam-column joint¹							
			0.0	0.01	0.015	0.020	0.030

1. When more than one of the conditions 1,2,3 and 4 occur for a given component, use the minimum appropriate numerical value from the table.
2. Under the heading “transverse reinforcement,” ‘C’ and ‘NC’ are abbreviations for conforming and non-conforming details, respectively. A component is conforming if within the flexural plastic region: (1) closed stirrup are spaced at ≤d/3 and 2) for components of moderate and high ductility demand the strength provided by the stirrup (V_s) is at least three-fourths of the design shear. Otherwise, the component is considered non-conforming.
3. Linear interpolation between values listed in the table is permitted.
 IO = Immediate Occupancy
 LS = Life Safety
 SS = Structural Stability
4. V = Design Shear

Table 2-C2 Numerical Acceptance Criteria for Plastic Hinge Rotations in Reinforced Concrete Columns, in radians (ATC-40)

			Performance Level ⁴				
			Primary			Secondary	
Component Type			IO	LS	SS	LS	SS
1. Columns Controlled by Flexure¹							
$\frac{P}{A_g f'_c}$ ⁵	Transverse Reinforcement ²	$\frac{V}{b_w d \sqrt{f'_c}}$ ⁶					
≤0.1	C	≤3	0.005	0.010	0.020	0.015	0.030
≤0.1	C	≥6	0.005	0.010	0.015	0.010	0.025
≥0.4	C	≤3	0.000	0.005	0.015	0.010	0.025
≥0.4	C	≥6	0.000	0.005	0.010	0.010	0.015
≤0.1	NC	≤3	0.005	0.005	0.010	0.005	0.015
≤0.1	NC	≥6	0.005	0.005	0.005	0.005	0.005
≥0.4	NC	≤3	0.000	0.000	0.005	0.000	0.005
≥0.4	NC	≥6	0.000	0.000	0.000	0.000	0.000
2. Columns controlled by shear^{1,3}							
Hoop spacing ≤d/2, or $\frac{P}{A_g f'_c} \leq 0.1$			0.000	0.000	0.000	0.010	0.015
Other cases			0.000	0.000	0.000	0.000	0.000
3. Columns controlled by inadequate development or splicing along the clear height^{1,3}							
Hoop spacing ≤d/2			0.0	0.0	0.0	0.010	0.020
Hoop spacing >d/2			0.0	0.0	0.0	0.005	0.010
4. Columns with axial loads exceeding 0.70^{1,3}							
Conforming reinforcement over the entire length			0.0	0.0	0.005	0.005	0.010
All other cases			0.0	0.0	0.0	0.0	0.0

1. When more than one of the conditions 1, 2, 3 and 4 occur for a given component, use the minimum appropriate numerical value from the table. See Chapter 9 for symbol definitions.
2. Under the heading “transverse reinforcement,” ‘C’ and ‘NC’ are abbreviations for conforming and non-conforming details, respectively. A component is conforming if within the flexural plastic hinge region: (1) closed hoops are spaced at ≤d/3 and 2) for components of moderate and high ductility demand

the strength provided by the stirrup (V_s) is at least three-fourths of the design shear. Otherwise, the component is considered non-conforming.

3. To qualify, (1) hoops must not be lap spliced in the cover concrete, and (2) hoops must have hooks embedded in the core or must have other details to ensure that hoops will be adequately anchored following spalling of cover concrete.
4. Linear interpolation between values listed in the table is permitted.
IO = Immediate Occupancy
LS = Life Safety
SS = Structural Stability
5. P = Design axial load
6. V = Design shear force

Table 2-C3 Numerical Acceptance Criteria for Chord Rotations for Reinforced Concrete Coupling Beams

		Performance Level ³				
		Primary			Secondary	
Component Type		IO	LS	SS	LS	SS
1. Coupling beams controlled by flexure						
Longitudinal reinforcement and transverse reinforcement ¹	$\frac{V}{b_w d \sqrt{f'_c}}$ ²					
Conventional longitudinal reinforcement with conforming transverse reinforcement	≤3	0.006	0.015	0.025	0.025	0.040
Conventional longitudinal reinforcement with conforming transverse reinforcement	≥6	0.005	0.010	0.015	0.015	0.030
Conventional longitudinal reinforcement with non-conforming transverse reinforcement	≤3	0.006	0.012	0.020	0.020	0.035
Conventional longitudinal reinforcement with non-conforming transverse reinforcement	≥6	0.005	0.008	0.010	0.010	0.025
Diagonal reinforcement	N/A	0.006	0.018	0.030	0.030	0.050
2. Coupling beams controlled by shear						
Longitudinal reinforcement and transverse reinforcement ¹	$\frac{V}{b_w d \sqrt{f'_c}}$ ²					
Conventional longitudinal reinforcement with conforming transverse reinforcement	≤3	0.006	0.012	0.015	0.015	0.024
Conventional longitudinal reinforcement with conforming transverse reinforcement	≥6	0.004	0.008	0.010	0.010	0.016
Conventional longitudinal reinforcement with non-conforming transverse reinforcement	≤3	0.006	0.008	0.010	0.010	0.020
Conventional longitudinal reinforcement with non-conforming transverse reinforcement	≥6	0.004	0.006	0.007	0.007	0.012

- Conventional longitudinal steel consists of top and bottom steel parallel to the longitudinal axis of the beam. The requirements for conforming transverse reinforcement are: (1) closed stirrups are to be provided over the entire length of the beam at spacing not exceeding d/3; and (2) the strength provided by the stirrups (Vs) should be at least three-fourths of the design shear.
- V = the design shear force on the coupling beam in pounds, b_w = the web width of the beam, d = the effective depth of the beam and f'_c = concrete compressive strength in psi.
- Linear interpolation between values listed in the table is permitted.
 IO = Immediate occupancy
 LS = Life Safety
 SS = Structural Stability

Table 2-C4 Numerical Acceptance Criteria for Reinforced Concrete Column Axial Hinge (FEMA-356)

Component Type	Plastic Deformation ¹				
	Primary			Secondary	
	IO	LS	SS	LS	SS
1. Braces in Tension (except EBF braces)	$7\Delta_T$	$9\Delta_T$	$11\Delta_T$	$11\Delta_T$	$13\Delta_T$

¹ Δ_T is the axial deformation at expected tensile yielding load.

Table 2-C5 Numerical Acceptance Criteria for Total Shear Angle in Reinforced Concrete Beam-Columns Joints, in radians (ATC-40, 1996)

			Performance Level ⁴				
			Primary ⁶			Secondary	
Component Type			IO	LS	SS	LS	SS
1. Interior joints							
$\frac{P}{A_g f'_c}$ ²	Transverse Reinforcement ¹	$\frac{V}{V_n}$ ³					
≤0.1	C	≤1.2	0.0	0.0	0.0	0.020	0.030
≤0.1	C	≥1.5	0.0	0.0	0.0	0.015	0.020
≥0.4	C	≤1.2	0.0	0.0	0.0	0.015	0.025
≥0.4	C	≥1.5	0.0	0.0	0.0	0.015	0.020
≤0.1	NC	≤1.2	0.0	0.0	0.0	0.015	0.020
≤0.1	NC	≥1.5	0.0	0.0	0.0	0.010	0.015
≥0.4	NC	≤1.2	0.0	0.0	0.0	0.010	0.015
≥0.4	NC	≥1.5	0.0	0.0	0.0	0.010	0.015
2. Other joints							
$\frac{P}{A_g f'_c}$ ²	Transverse Reinforcement ¹	$\frac{V}{V_n}$ ³					
≤0.1	C	≤1.2	0.0	0.0	0.0	0.015	0.020
≤0.1	C	≥1.5	0.0	0.0	0.0	0.010	0.015
≥0.4	C	≤1.2	0.0	0.0	0.0	0.015	0.020
≥0.4	C	≥1.5	0.0	0.0	0.0	0.010	0.015
≤0.1	NC	≤1.2	0.0	0.0	0.0	0.005	0.010
≤0.1	NC	≥1.5	0.0	0.0	0.0	0.005	0.010
≥0.4	NC	≤1.2	0.0	0.0	0.0	0.000	0.000
≥0.4	NC	≥1.5	0.0	0.0	0.0	0.000	0.000

- Under the heading “transverse reinforcement,” ‘C’ and ‘NC’ are abbreviations for conforming and non-conforming details, respectively. A joint is conforming if closed hoops are spaced at $\leq h_c/3$ within the joint. Otherwise, the component is considered non-conforming. Also, to qualify as conforming details under condition 2, (1) closed hoops must not be lap spliced in the cover concrete, and (2) hoops must have hooks embedded in the core or must have other details to ensure that hoops will be adequately anchored following spalling of cover concrete.
- The ratio $\frac{P}{A_g f'_c}$ is the ratio of the design axial force on the column above the joint to the product of the gross cross-sectional and lateral forces.
- The ratio V/V_n is the ratio of the design shear force to the shear strength for the joint.
- Linear interpolation between values listed in the table is permitted.
 IO = Immediate Occupancy
 LS = Life Safety
 SS = Structural Stability
- No inelastic deformation is permitted since joint yielding is not allowed in a conforming building.

Table 2-C6 Numerical Acceptance Criteria for Plastic Hinge Rotation in Reinforced Concrete Two-way Slabs and Slab-Column Connections, in radians (ATC-40)

		Performance Level ⁴				
		Primary			Secondary	
Component Type		IO	LS	SS	LS	SS
1. Slabs controlled by flexure and slab column connections¹						
$\frac{V_g}{V_o}$ ²	Continuity Reinforcement ³					
≤0.2	Yes	0.01	0.015	0.02	0.030	0.05
≥0.4	Yes	0.00	0.000	0.00	0.030	0.04
≤0.2	No	0.01	0.015	0.02	0.015	0.02
≥0.4	No	0.00	0.000	0.00	0.000	0.00
2. Slabs controlled by inadequate development or splicing along the span¹						
		0.00	0.00	0.000	0.01	0.02
3. Slabs controlled by inadequate embedment into slab-column joint¹						
		0.01	0.01	0.015	0.02	0.03

1. When more than one of the conditions 1, 2, 3 and 4 occur for a given component, use the minimum appropriate numerical value from the table.
2. V_g = the gravity shear acting on the slab critical section as defined by ACI 318, V_o = the direct punching shear strength as defined by ACI 318.
3. Under the heading “Continuity reinforcement” assume ‘Yes’ where at least one of the main bottom bars in each direction is effectively continuous through the column cage. Where the slab is post-tensioned, assume “Yes” where at least one of the post-tensioning tendons in each direction passes through the column cage. Otherwise, assume “No.”
4. Linear interpolation between values listed in the table is permitted.
 IO = Immediate Occupancy
 LS = Life Safety
 SS = Structural Stability

Table 2-C7 Numerical Acceptance Criteria for Plastic Hinge Rotations in Reinforced Concrete Walls and Wall Segments Controlled by Flexure, in radians (ATC-40)

Component Type	Performance Level ⁴						
	Primary			Secondary			
	IO	LS	SS	LS	SS		
1. Walls and wall segments controlled by flexure							
$\frac{(A_s - A_s')f_y + P}{t_w l_w f_c}$ ¹	$\frac{V}{t_w l_w \sqrt{f_c}}$ ²	Boundary Element ³					
≤0.1	≤3	C	0.005	0.010	0.015	0.015	0.020
≤0.1	≥6	C	0.004	0.008	0.010	0.010	0.015
≥0.25	≤3	C	0.003	0.006	0.009	0.009	0.012
≥0.25	≥6	C	0.001	0.003	0.005	0.005	0.010
≤0.1	≤3	NC	0.002	0.004	0.008	0.008	0.015
≤0.1	≥6	NC	0.002	0.004	0.006	0.006	0.010
≥0.25	≤3	NC	0.001	0.002	0.003	0.003	0.005
≥0.25	≥6	NC	0.001	0.001	0.002	0.002	0.004

1. A_s = the cross-sectional area of longitudinal reinforcement in tension, A_s' = the cross-sectional area of longitudinal reinforcement in compression, f_y = yield stress of longitudinal reinforcement, P = axial force acting on the wall considering design load combinations, t_w = wall web thickness, l_w = wall length, and f_c = concrete compressive strength.
2. V = the design shear force acting on the wall, and other variables are as defined above.
3. The term “C” indicates the boundary reinforcement effectively satisfies requirements of ACI 318. The term “NC” indicates the boundary requirements do not satisfy requirements of ACI 318.
4. Linear interpolation between values listed in the table is permitted.

IO = Immediate Occupancy

LS = Life Safety

SS = Structural Stability